The aryl hydrocarbon receptor nuclear translocator (ARNT) transcriptional co-regulator complex: Effects on estrogen and hypoxia signaling

by

Mark Labrecque

B.Sc., University of British Columbia, 2007

Thesis Submitted in Partial Fulfillment of the
Requirements for the Degree of
Doctor of Philosophy

in the
Doctor of Philosophy Program
Faculty of Health Sciences

SIMON FRASER UNIVERSITY

Summer 2016

Approval

Name: **Mark Labrecque**

Degree: **Doctor of Philosophy**

Title: ***The aryl hydrocarbon receptor nuclear translocator (ARNT) transcriptional co-regulator complex: Effects on estrogen and hypoxia signaling***

Examining Committee: **Chair:** Dr. Tim Takaro
Professor

Dr. Timothy Beischlag
Senior Supervisor
Associate Professor

Dr. Frank Lee
Supervisor
Associate Professor

Dr. Gratien Prefontaine
Supervisor
Associate Professor

Dr. Christopher Beh
Internal Examiner
Associate Professor
Department of Molecular Biology and Biochemistry

Dr. Judy Wong
External Examiner
Associate Professor
Faculty of Pharmaceutical Sciences
University of British Columbia

Date Defended/Approved: August 11, 2016

Abstract

The basic Helix-Loop-Helix/PER-ARNT-SIM (bHLH-PAS) domain family of proteins mediates cellular responses to a variety of stimuli. The bHLH-PAS proteins are heterodimeric transcription factors that are further sub-classified into sensory and aryl hydrocarbon receptor nuclear translocator (ARNT) proteins. The ARNT protein is constitutively expressed and heterodimerizes with hypoxia-inducible factors (HIFs) to mediate oxygen-sensing mechanisms and heterodimerizes with the aryl hydrocarbon receptor (AHR) to combat environmental contaminant exposure. Firstly, a reciprocal disruption relationship exists between AHR ligands, like 2,3,7,8-tetrachlorodibenzo-p-dioxin (TCDD) and estrogen receptor (ER) ligands, like 17β-estradiol (E2). Ligand-bound ER tethers to the AHR/ARNT transcription factor complex and represses TCDD-inducible gene transcription. However, the tethering paradigm and molecular mechanisms employed by AHR and ARNT at ER-regulated genes remains to be determined. Secondly, thyroid hormone receptor/retinoblastoma-interacting protein 230 (TRIP230) interacts with ARNT and is a coactivator required for hypoxia-regulated transcription. The retinoblastoma protein (Rb) is a negative regulator of the cell cycle and also negatively regulates TRIP230 coactivator potential. Thus, Rb may influence ARNT transcription factor functions via TRIP230. Rb-loss in many solid tumours directly precedes the activation of HIF-regulated genes and correlates with increased angiogenesis and metastasis. As most solid tumours contain regions of hypoxia and only correlative data between HIF/ARNT activity and Rb-loss has been gathered, we have identified a need to rigorously examine the role of Rb-loss in concert with hypoxia in breast and prostate cancer models. In this thesis, I used siRNA technology to knockdown ARNT and AHR expression and found that TCDD-mediated disruption of ER-signalling is AHR-dependent and that ARNT is a coactivator in MCF7 cells and a corepressor in ECC1 cells. Additionally, I used siRNAs and shRNA technology in concert with microarray analysis in LNCaP prostate cancer cells and MCF7 breast cancer cells to delineate the role of the ARNT-TRIP230-Rb transcriptional complex in hypoxia-regulated transcription. I found that Rb-depletion in conjunction with hypoxia exacerbates HIF1-mediated transcription and promotes a more invasive and late stage phenotype in both breast and prostate cancer models. The molecular mechanisms and gene pathways described herein should prove useful for developing chemotherapies for late stage breast and prostate cancers.

Keywords: ARNT; AHR; ER; TRIP230, Retinoblastoma protein; HIF1

For my wife, Alexa, and our son, Lincoln,

Thank you for all the love and support and for always bringing a smile to my face

Acknowledgements

My journey at SFU has been long, interesting and slightly unexpected and it would not have been possible without the support and guidance from several key individuals. I would like to thank my senior supervisor, Dr. Timothy Beischlag, for giving me the opportunity to develop as a scientist and for sparking a curiosity that has led to both personal and intellectual growth. I am grateful for his mentorship, leadership and encouragement; my time as a graduate student under his guidance has profoundly changed my life. I am indebted to my supervisory committee, Dr. Gratien Prefontaine and Dr. Frank Lee, for their valuable feedback over the years and for helping me stay on track. I would also like to extend my thanks to my internal examiner, Dr. Christopher Beh, and my external examiner, Dr Judy Wong, for taking the time to read my thesis and for sitting on my examining committee.

To all the past and present members of the Beischlag Lab, thank you for making the lab an enjoyable and productive environment. Kevin Tam, Julienne Jagdeo, Mandeep Takhar, Lillian Wong, Alex Reers, Stephanie Santacruz and Rebecca Nason, thank you for your support and for all the hardwork that has made several of our publications a reality. To Shabnam Massah and Sam Khakshour, thank you for your friendship and for allowing me to collaborate with you on interesting research projects that have enriched my time as a graduate student at SFU.

To Dr. Michael Cox and his team at the Vancouver Prostate Centre, and to Dr. Kevin Bennewith and his team at the BC Cancer Research Centre, thank you for all your research insights, for being so generous with your time and for the mentorship and learning opportunities that were provided. I will forever cherish my graduate student experiences at your world-class organizations.

Lastly but most importantly, thank you to my family. My graduate student journey would not have been possible without the steadfast support of my wife, mom, dad, brother and sister. You inspire me to be a better man and to reach for the stars.

This work was supported in part by graduate fellowships from Simon Fraser University and by a graduate studentship award from Prostate Cancer Canada.

Table of Contents

List of Tables

List of Figures

List of Acronyms

AHR	Aryl hydrocarbon receptor
AHRC	Aryl hydrocarbon receptor complex
AR	Androgen receptor
ARNT	Aryl hydrocarbon receptor nuclear translocator
bHLH-PAS	Basic helix-loop-helix – Per ARNT SIM domain
CDK	Cyclin dependent kinase
cDNA	Complementary deoxyribonucleic acid
ChIP	Chromatin immunoprecipitation
CO_2	Carbon dioxide
CRPC	Castration resistant prostate cancer
CXCR4	Chemokine (C-X-C Motif) Receptor 4
CYP1A1	Cytochrome P450 1A1
DHT	Dihydrotestosterone
DMEM	Dulbecco's modified eagle medium
DNA	Deoxyribonucleic acid
E2	17β-estradiol
ECC-1	Endometrial cancer cell -1
EDC	Endocrine disrupting chemical
ENO2	Enolase 2
EPO	Erythropoietin
ER	Estrogen receptor
ERE	Estrogen response element
FBS	Fetal bovine serum
FIH	Factor inhibiting hif
HDAC	Histone deacetylase
HIF1	Hypoxia inducible factor complex
HIF1,2,3α	Hypoxia inducible factor 1-3α
HRE	Hypoxia response element
HSP90	Heat-shock protein 90
HTR5A	5-hydroxytryptamine receptor 5A

In vitro	“in glass”
In vivo	“in life”
IPA	Ingenuity Pathway Assist
KISS1R	Kisspeptin receptor 1
LNCaP	Lymph node carcinoma of the prostate
MCF7	Michigan cancer foundation 7
NCOR1	Nuclear receptor corepressor-1
NDRG1	N-myc downstream regulated 1
NE	Neuroendocrine
NED	Neuroendocrine differentiation
NEPC	Neuroendocrine prostate cancer
NFκB	Nuclear factor-κ-B
O_2	Oxygen
PBS	Phosphate buffered saline
PHD	Prolyl hydroxylase
PLOD2	procollagen-lysine, 2-oxoglutarate 5-dioxygenase 2
PR	Progesterone receptor
pS2	Trefoil factor
RNA	Ribonucleic acid
SCX	Scrambled
shRNA	Short hairpin ribonucleic acid
siRNA	Short interfering ribonucleic acid
TCDD	2,3,7,8 – tetrachlorodibenzo-p-dioxin
TRIP230	Thyroid hormone receptor/retinoblastoma-interacting protein 230
VEGF	Vascular endothelial growth factor
XAP2	Hepatitis B virus X-associated protein
XRE	Xenobiotic response element

Chapter 1. Introduction

Deoxyribonucleic acid (DNA) carries the genetic information of almost all living organisms and is the primary component of chromosomes. In 1962, Francis Crick, James Watson and Maurice Wilkins shared the Nobel Prize in Physiology and Medicine for determining that DNA has a double helix structure composed of two complimentary polynucleotide chains with sugar-phosphate backbones and cytosine-guanine or thymine-adenine base pairs holding the chains together [1]. Although they made groundbreaking observations that identified the molecular structure of DNA and postulated how traits may be passed on from generation to generation, the mechanisms of heredity and gene expression remained elusive. Subsequently, it was determined that the basic unit of the genetic code is the codon (a triplet sequence of nucleotides) and that codons are degenerate, do not overlap, and are read from a specific starting point [2]. In addition, Jacob and Monod produced mechanistic insight of DNA regulation through studies involving the *lac* operon in E. coli. They showed that enzyme protein expression could be either repressed or induced via DNA-interacting proteins and that a transient molecule was required to facilitate ribosome-mediated protein synthesis from DNA templates [3]. This work was one of the first to recognize messenger ribonucleic acid (mRNA) and amassed compelling evidence for the DNA-RNA-Protein paradigm.

Eukaryotic systems were more difficult to study; however, the identification of RNA polymerase II [4], the isolation of the general transcription factors for RNA polymerase II (TFIIB, D, E, F and H) [5] and the establishment of DNA promoter and enhancer sequences [6,7] inspired Roger Kornberg, who detailed the mechanisms of eukaryotic transcription using Baker's yeast as a model system. Importantly, he outlined the roles of RNA polymerase II in eukaryotic systems and determined that the mediator complex links gene-specific, DNA-binding transcription factors to RNA polymerase II and the general transcription factors [8-10]. Together, these seminal works laid the foundation for investigating the molecular control of eukaryotic transcription and opened

new avenues of research examining gene- and transcription factor-specific regulatory mechanisms.

The general basic premise of this thesis is to elaborate on the ability of transcription factors to not only act by DNA-binding interactions but to also differentially regulate other transcription factors by protein-protein interactions. In the following sections of this chapter, I provide background information on the aryl hydrocarbon receptor nuclear translocator (ARNT) protein and discuss its roles in the transcriptional control of hypoxia and dioxin-mediated disruption of estrogen signaling. Additionally, I describe the retinoblastoma (Rb) protein and the thyroid hormone receptor/retinoblastoma-interacting protein-230 (TRIP230) protein and how they relate to ARNT transcription factor functions. Finally, I introduce prostate and breast cancer as our research models and outline the rationales, hypotheses and objectives of this thesis. Sections 1.1, 1.2, 1.2.2, 1.5, and 1.6 and Table 1-1 have been modified to fit this thesis but resemble sections presented in:

Labrecque, MP, Prefontaine, GG, and Beischlag, TV (2013). The aryl hydrocarbon receptor nuclear translocator (ARNT) family of proteins: transcriptional modifiers with multi-functional protein interfaces. Curr Mol Med 13: 1047-1065.

1.1. The aryl hydrocarbon receptor nuclear translocator (ARNT) family of proteins

The PER-ARNT-SIM (PAS) family of transcription factors act as environmental sensors and are key regulators of growth, development and cellular homeostasis. The discovery of the circadian rhythm regulator period (per) in Drosophila melanogaster [11] was a catalyst for a plethora of research aimed at understanding mechanisms governing gene regulation and protein interactions. The per locus was first cloned and characterized by Michael Young, Jeffrey Hall and Michael Rosbash in 1984 [12-14]. A comprehensive analysis of the per locus identified a 0.9 kb RNA transcript that was crucial for normal circadian rhythmicity [14]. Elucidation of molecular mechanisms in the dioxin-signaling pathway and in regulation of development and neurogenesis in flies, revealed 250-300 amino acid sequences of homology to PER between the human aryl

hydrocarbon receptor nuclear translocator (ARNT) and the fly single-minded (sim) transcript [15,16]. This approximately 270 amino acid sequence was termed the PAS sequence and contains tandem ~70 amino acid repeat regions known as the PAS-A and PAS-B domains [17,18]. The hallmarks of the PAS domain are that it represents a dimerization motif that allows interactions between PAS [19] and non-PAS domain containing proteins [20]. The subject of this thesis, the ARNT protein, also referred to as hypoxia-inducible factor-1β (HIF1β), is the dimerization partner for a large number of these structurally related transcription factors.

Another structural feature common to ARNT and its dimerization partners is the basic Helix-Loop-Helix (bHLH) domain (Figure 1.1A). This region is defined by an N-terminal basic region that is required for DNA binding adjacent to a hydrophobic C-terminal region with two amphipathic α-helices separated by a variable loop region required for dimerization [21]. The archetypical DNA binding sequence for bHLH proteins is known as an E-Box, which has the sequence CANNTG and contains either CG or GC dinucleotides at the variable positions [22]. Typical bHLH-PAS proteins operate as DNA-binding heterodimeric protein complexes with the most conventional pairing composed of one constitutively expressed protein and the other protein whose expression relies on tissue specificity, time or the presence of activating agents [23] (Figure 1.1B). The ARNT protein and related ARNT2 (also named HIF2β), ARNT-like protein 1 (ARNTL, also named BMAL1, MOP3 or ARNT3) [24-26] and ARNT-like protein 2 (ARNTL2, also named BMAL2, MOP9 or CLIF) [27-29] proteins are some of the most broadly expressed bHLH-PAS proteins in eukaryotic systems and are involved in three major biological pathways; i) oxygen sensing through dimerization with hypoxia inducible factors (HIFs) [30]; ii) circadian rhythm regulation through dimerization with CLOCK [31]; and iii) metabolic responses to environmental contaminant exposure through dimerization with the aryl hydrocarbon receptor (AHR) [16]. Pathways that are not as well understood but have implicated the ARNT family of proteins as transcriptional modifiers include embryogenesis and neurogenesis through dimerization with SIM1 or SIM2 [32,33], neurogenesis through dimerization with NPAS1 [34], NPAS3 [35], or NPAS4 [36] and heme binding and carbon monoxide sensing [37] (Table 1-1).

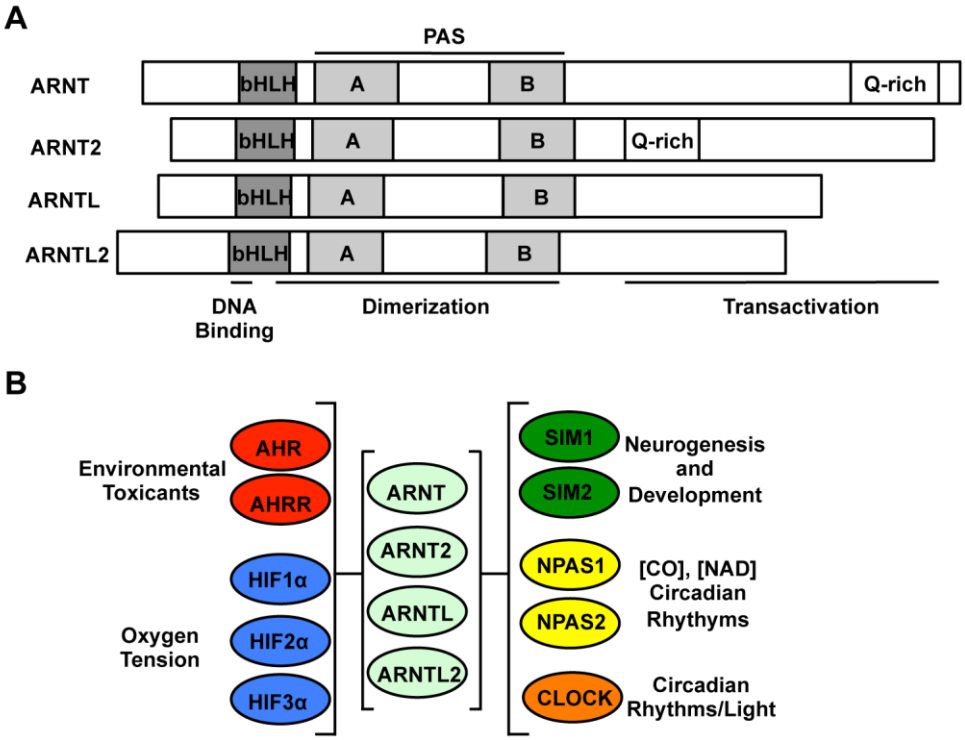

Figure 1.1. The ARNT family of proteins

(A) A schematic depicting the molecular domains of the ARNT family of proteins, bHLH = basic Helix-Loop-Helix domain, PAS = PER-ARNT-SIM domain, Q-rich = glutamine rich domain. **(B)** A summary of the bHLH-PAS transcription factors associated with the ARNT family of proteins.

Table 1.1. Summary of bHLH-PAS transcription factors and associated signaling pathways.

Gene Name	Full Name	Alternative Name(s)	Binding Partner(s)	Pathways
AHR	Aryl hydrocarbon receptor	Dioxin Receptor	ARNT, ARNT2	Environmental contaminant metabolism, immune system
AHRR	Aryl hydrocarbon receptor repressor		ARNT	Represses AHRC signaling
CLOCK			ARNTL, ARNTL2	Circadian rhythm regulation
NPAS2	Neuronal PAS domain protein 2	MOP4	ARNTL	Circadian rhythm regulation CO sensing
HIF-1α	Hypoxia inducible factor 1α	MOP1	ARNT, ARNT2	Hypoxia response
EPAS1	Endothelial PAS domain-containing protein 1	HIF-2α, MOP2	ARNT, ARNT2	Hypoxia response
			ARNTL	Bone development

Gene Name	Full Name	Alternative Name(s)	Binding Partner(s)	Pathways
HIF-3α	Hypoxia inducible factor 3α	MOP7	ARNT	Hypoxia response
NPAS1	Neuronal PAS domain protein 1	MOP5	ARNT, ARNT2	Neurogenesis
NPAS3	Neuronal PAS domain protein 3	MOP6	ARNT	
NPAS4	Neuronal PAS domain protein 4	NXF	ARNT, ARNT2 ARNTL	
SIM1	Single-minded homolog 1		ARNT ARNT2	Embryogenesis and Neurogenesis
SIM2	Single-minded homolog 2		ARNT	
ARNT	Aryl hydrocarbon receptor nuclear translocator	HIF-1β	AHR, AHRR HIF-1/2/3α NPAS1,NPAS3 NPAS4, SIM1, SIM2,	
ARNT2	Aryl hydrocarbon receptor nuclear translocator 2	HIF-2β	AHR HIF-1α, HIF-2α NPAS4	
ARNTL	Aryl hydrocarbon receptor nuclear translocator- like	BMAL1, MOP3, ARNT3	CLOCK HIF-2α NPAS2, NPAS4	
ARNTL2	Aryl hydrocarbon receptor nuclear translocator- like 2	BMAL2, MOP9, CLIF	CLOCK	

*Modified from Labrecque, MP *et al*. Current Molecular Medicine, 2013. [38]

1.2. The aryl hydrocarbon receptor (AHR)

The aryl hydrocarbon receptor (AHR) is a ligand activated bHLH-PAS transcription factor [39] that activates transcription of several genes upon association with polycyclic aromatic hydrocarbons and halogenated aromatic hydrocarbons, including its most potent activator 2,3,7,8-tetrachlorodibenzo-p-dioxin (dioxin, TCDD) [40,41]. Several AHR target genes are involved in environmental contaminant

metabolism, such as Cytochromes P450 1A1, 1A2 and 1B1 (CYP1A1, CYP1A2 and CYP1B1). AHR is also required for development, homeostasis and certain functions of the immune response [42]. Until recently, no known endogenous activators of AHR had been identified that work at biologically relevant concentrations. However, the tryptophan catabolite kynurenine was recently identified as a bona fide AHR ligand that promotes tumor cell survival and suppresses anti-tumor immune responses [43]. Further examination of the relationship between kynurenine and AHR will likely increase our knowledge of the true physiological role of AHR.

Unliganded AHR exists in the cytoplasm as part of a multimeric complex including two molecules of HSP90, the HSP90 co-chaperone p23, and a 36-kDa protein termed hepatitis B virus X-associated protein 2 (XAP2) [44-47]. Once activated through ligand binding, AHR moves to the nucleus where it associates with ARNT to form a functional transcription factor complex that recruits coactivators, such as the SRC/p160 family of coactivators, to initiate transcription [48,49] (Figure 1.2). The interaction domains essential for AHR and ARNT dimerization have been the subjects of numerous *in vitro* and *in vivo* assays with conflicting results. The first and second α-helices in the mouse ARNT bHLH domain are essential for dimerization with AHR [50] whereas the ARNT PAS domains appear to be important for dimer stabilization [51] but are not required [50]. Intriguingly, a murine AHR deletion mutant termed DRΔLBD, that lacks the PAS-B domain cannot associate with ARNT or induce transcription of a xenobiotic response element (XRE) driven reporter construct [52]. However, a constitutively active form of AHR (CA-AHR/DRΔPASB) lacking the minimal PAS-B ligand binding and HSP90 interaction motifs, is able to heterodimerize with ARNT and activate transcription of reporter constructs and endogenous AHR target genes [52,53].

Although the canonical AHR signaling pathway involves AHR:ARNT heterodimerization, *in vitro* studies looking at ARNT2 showed that ARNT2 could heterodimerize with AHR and induce transcription of a catalase-reporter construct driven by the CYP1A1 promoter sequence [54]. However, Sekine and colleagues used Hepa1-c4 cells, which are deficient in ARNT protein, and determined that ectopically expressed ARNT2 and 3MC-activated AHR could not induce transcription of XRE-driven reporter constructs [54]. Additionally, Dougherty and Pollenz also used Hepa1-c4 cells and

showed that expression of ectopic ARNT and TCDD-activated AHR induced expression of CYP1A1 protein but expression of ectopic ARNT2 and TCDD-activated AHR could not induce CYP1A1 protein expression [55]. Thus, ARNT2 may heterodimerize with AHR *in vitro* but it is not involved in the activation of endogenous AHR-target genes.

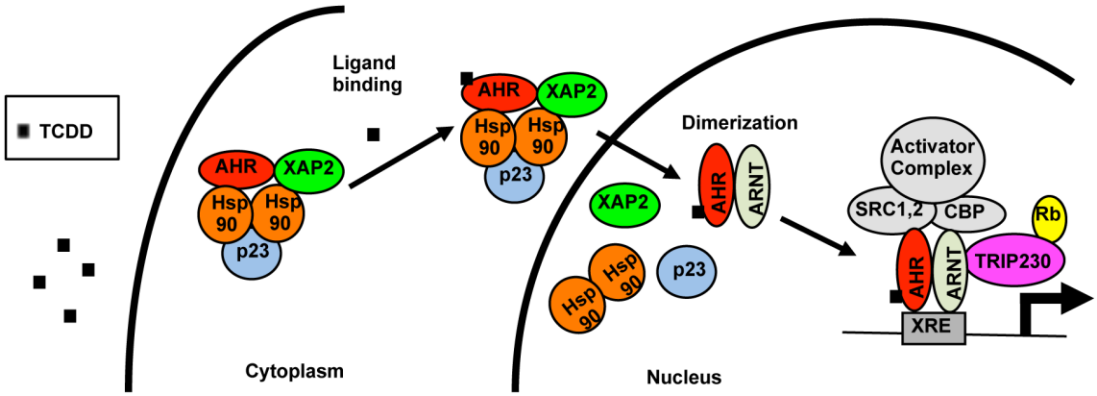

Figure 1.2. Schematic of AHR signal transduction
AHR is kept inactivated in the cytoplasm by chaperone proteins heatshock protein 90 (Hsp90), p23 and hepatitis B virus x-associated protein (XAP2). TCDD enters the cell and binds the chaperoned AHR complex. The ligand-bound receptor complex translocates into the nucleus and discards the chaperone proteins. AHR dimerizes with ARNT and the activated transcription factor complex then binds xenobiotic response elements (XREs) within the genome. Recruitment of transcriptional coactivators (SRC1,2, CBP) leads to transcriptional activation of target genes.

1.2.1. Endocrine disruption and the estrogen receptor (ER)

The production of chemicals and their release into the environment has exponentially increased due to industrialization. Several of these exogenous chemicals are able to interfere with endogenous hormone signaling pathways and thus have become known as endocrine disrupting chemicals (EDCs). Endocrine disruption may occur through direct or indirect mechanisms. EDCs with direct mechanisms may mimic an endogenous hormone or antagonize a receptor while examples of indirect mechanisms include blocking hormone synthesis or interfering with receptor turnover or transport [56]. The most established endocrine disrupting pathways involve hormone receptors from the nuclear receptor family of transcription factors, such as the estrogen receptor (ER).

The nuclear receptors (NRs) are ligand-binding transcription factors activated by lipid-soluble compounds that freely traverse the plasma membrane, such as steroid

hormones and vitamins [57]. In humans, the superfamily is composed of 48 NRs that are further sub-classified according to sequence homology [58]. The catalysts for nuclear receptor research occurred over 30-years ago when the glucocorticoid receptor (GR) and the estrogen receptor were first isolated and characterized [59,60]. Comparison of cDNA sequences revealed several structural features common to the majority of NRs, including an N-terminal domain containing activation function-1 (AF-1), a highly conserved DNA-binding domain (DBD), a hinge domain, and a ligand-binding domain (LBD) containing activation function-2 (AF-2) [57,61] (Figure 1.3A). The ligand-dependent AF-2 domain found near the carboxy-terminus is strictly conserved throughout the NR family and recruits p160 coactivator proteins required for transcriptional activation through LXXLL-motifs [62,63]. The ligand-independent AF-1 domain is the most variable region between family members in both size and sequence homology. However, the AF-1 domain also interacts with p160 coactivator proteins and synergizes with AF-2 functions, but does so through an LXXLL-independent mechanism [64,65].

ERα/β are from the steroid receptor subfamily of NRs and bind 17β-estradiol (E2) to regulate genes involved in reproduction and cellular growth and proliferation [66]. Like most nuclear receptor family members, two classical models describe transcriptional activation of ER (Figure 1.3B). The first model is similar to activation of AHR in that in the absence of an agonist, ER is associated with chaperone proteins and kept inactivated in the cytoplasm. Upon ligand binding, ER homo- or heterodimerizes, translocates to the nucleus and binds estrogen response elements (EREs) in target gene promoters to initiate transcription [66,67]. The second model suggests that ERs are continuously bound to their cognate response elements in the DNA of target genes and that inactivated ERs are associated with corepressors, such as nuclear receptor corepressor 1 (NCOR1) and histone deacetylases (HDACs), which leaves them transcriptionally repressed. Ligand binding causes a conformational change that facilitates the exchange of corepressors for coactivators, such as CBP/p300 and steroid receptor coactivator 1 (SRC1), and this leads to transcriptional activation [68].

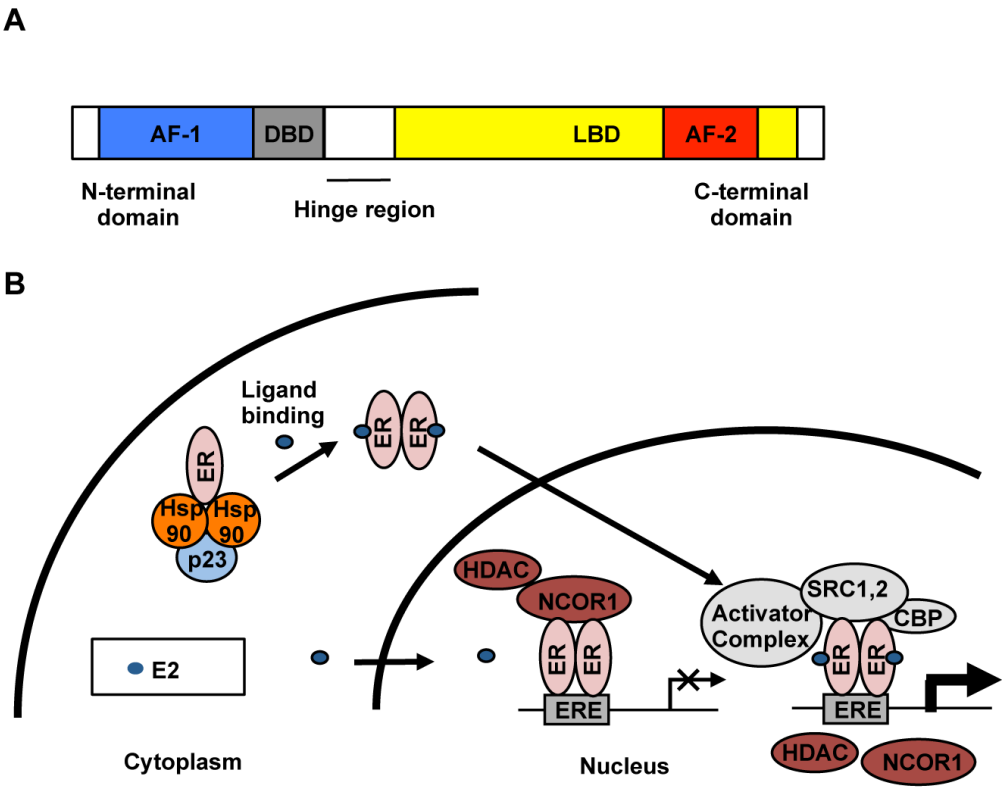

Figure 1.3. Nuclear receptor structure and ER signal transduction.
(**A**) Linear schematic of a nuclear receptor and classical structural domains; activation function-1 (AF-1); DNA binding domain (DBD); ligand binding domain (LBD), activation function-2 (AF-2). (**B**) In the absence of an agonist, ER is associated with chaperone proteins and kept inactivated in the cytoplasm. Upon ligand binding, ER homo- or heterodimerizes, translocates to the nucleus and binds estrogen response elements (EREs) in target gene promoters to initiate transcription. A second mechanism of signal transduction includes inactive ER constantly bound to estrogen response elements (EREs) within the genome and associated with transcriptional corepressors (NCOR, HDAC). Ligand binding causes a conformational change that facilitates the exchange of corepressors for coactivators, which in turn activates transcription.

1.2.2. AHR, ER and ARNT crosstalk

The observation that glucocorticoid receptor (GR) null mutations are lethal in mice [69] juxtaposed to the subsequent finding that DNA-binding/dimerization deficient GR mutant mice are viable [70] suggests the intriguing possibility that protein-protein interactions and not DNA binding properties of GR are essential for survival [70]. Similarly, several studies over the last decade suggest that AHR may mediate off-target or DNA-binding independent transcription factor function. The most compelling evidence for this is provided by the ability of diverse classes of AHR ligands to disrupt ER-regulated signaling. Interestingly, there is a ligand-dependent reciprocal disruption

between ER and AHR signaling [71-73]. TCDD inhibits the expression of several E2-inducible genes, including pS2 [74], cathepsin D [75,76] and c-fos [77] while E2 inhibits expression of the TCDD inducible gene CYP1A1 [73,78,79]. One explanation for TCDD-induced disruption of ER signaling included a TCDD-dependent increase in aryl hydrocarbon-hydroxylase enzymatic activity which mediated rapid metabolism of E2 [80]. Subsequent studies supported a transcriptional down-regulation of ER-target genes through upstream inhibitory dioxin response elements [71] and AHR-mediated activation of a proteasome complex that degrades ER proteins essential for E2-induced transcription [81]. Furthermore, AHR has been identified as a ligand-dependent E3-ubiquitin ligase and part of a CUL4B proteosome complex which targets sex steroid receptors for degradation [82].

Another possible mode of AHR-dependent disruption of ER signaling is through direct protein-protein interactions [72]. However, experiments using 3-methylcholanthrene (3MC) as an AHR ligand produced some perplexing results because 3MC can also serve as an ER agonist and drive ERE-driven reporter assays [83]. Nevertheless, chromatin immunoprecipitation (ChIP) assays have confirmed that ligand co-treatments recruit ERs to XREs at CYP1A1 and AHR and ARNT to EREs at ER-regulated genes [73,84-86] and sequential ChIPs showed a direct or extremely close ER-AHR association [73]. In addition, GST-pull-down assays and *in vivo* co-immunoprecipitation assays have demonstrated a direct interaction between ARNT and ER [73,84] or AHR and ER [72,73]. Furthermore, E2-activated ERα dampens AHR transcriptional activity at CYP1A1 through direct protein-protein interactions in MCF7 breast cancer cells [73]. Thus, a reciprocal protein-protein interaction at ER-regulated genes seems probable. Interestingly, ER-mediated disruption of CYP1A1 and CYP1B1 transcription can occur through either ERα or ERβ depending on the tissue or type of ER or AHR activating agents [87,88]. For example, resveratrol is a putative cardioprotective and chemopreventive phytoalexin found in red wine [89] and low doses (100 nM) decreases AHR-mediated CYP1A1 mRNA accumulation through ERα in MCF7 and BEAS-2b breast cancer cells but attenuates CYP1A1 accumulation through both ERα and ERβ in Caco-2 colon cancer cells [88]. However, resveratrol used at higher doses (10 μM) inhibits AHR-dependent transcription independent of ERα in certain breast cancer cell lines [90]. This suggests that multiple mechanisms are responsible for

resveratrol-mediated repression of AHR signaling and a more in-depth analysis of the transcriptional machinery involved during low and high dose exposures is warranted.

Distinguishing individual protein partners recruited by AHR or ARNT to modulate estrogen signaling has revealed a more complex crosstalk model than previously thought. ARNT physically interacts with ligand activated ERα and ERβ and displays coactivator properties independent of AHR ligands [84]. Follow-up studies using ERE-driven reporter constructs and siRNAs directed towards endogenous ARNT in murine and human cancer cell lines, support ARNT coactivator function during ER-mediated transcription but highlight a significantly greater effect during ERβ signaling [91]. Although endogenous ER-mediated gene activation was not rigorously tested, it was proposed that AHR-mediated disruption of ER-transcriptional activities occurs through AHR and ER competition for ARNT as a transcriptional coactivator and the lack of ARNT availability reciprocally disrupts AHR- and ER-mediated transcription [91].

1.3. Carcinogenesis

Cancer, also known as malignant neoplasia, is defined as the uncontrolled growth of cells in a particular area of the body. Cancerous cells rapidly divide to form tissue masses known as tumours and these cells have the potential to spread or invade to other parts of the body through a process called metastasis. Benign tumours are a collection of neoplastic cells without metastatic capabilities, and are thus non-cancerous, but may develop cancerous characteristics through tumour progression [92]. In the 1970's, two important classes of genes were discovered that related to cancer initiation and progression: oncogenes and tumour-suppressor genes. Oncogenes induce tumourgenesis and acquire mutations that either confer constitutive activity or promote aberrant protein expression patterns. Oncoprotein perturbations may arise through gene duplications, retroviral transduction or integration, chromosomal translocations or intragenic mutations that affect crucial post-translational modification residues or protein-protein interaction interfaces [93]. In addition, oncogenes typically require only one mutated allele to confer oncogenic activity and are thus considered dominant. Classical examples of oncogenic pathways include; Receptor tyrosine kinase (RTK)/RAS/RAF/MAPK proteins and maintenance of mitogenic growth signals [93,94];

PI3K/AKT/CREBB proteins and stimulation of cellular proliferation and survival [95]; Bcl-2 and resistance to apoptosis [94,96]; and Wnt/β-catenin and acquisition of metastatic potential through epithelial-to-mesenchymal transition [97,98].

Conversely, mutations occurring in tumour-suppressor genes reduce or silence protein activity. Genetic alterations typically include non-sense mutations that introduce premature stop codons, missense mutations that change the amino acid structure of important functional domains, deletions or inversions at the intragenic or chromosomal level and epigenetic silencing through DNA methylation marks [93]. Tumour suppressor genes are typically recessive in nature and require both alleles to be altered in order to permit tumour initiation or progression. Classical examples of tumour suppressors and the canonical pathways they control include; P53 and cell cycle checkpoint for DNA damage [99]; Retinoblastoma protein (Rb) and inhibition of the E2F family of pro-mitotic transcription factors [100]; and Von Hipel Lindau (VHL) and degradation of HIF proteins in the presence of oxygen [101].

Interestingly, while examining retinoblastoma and inheritance patterns, Alfred Knudson observed that tumours only occurred in people with two distinct mutational events and this led to his seminal paper on the “two-hit hypothesis” [102]. He postulated that in inherited forms of cancer, the first mutational event happens in one or both of the parents and is passed on to offspring in germ cells and the second mutation is acquired in somatic cells. In sporadic cases of cancer, both “hits” are mutations that arise in somatic cells and since these are random mutations, retinoblastoma occurs at a much lower frequency [102]. This hypothesis of cancer initiation and progression has since been expanded and experimentally supported [103,104] but the general understanding is that in most cases it is the culmination of multiple mutational events in both tumour suppressors and oncogenes over an organisms lifetime that eventually leads to rapidly proliferating, metastatic and lethal disease.

The dawn of the 21st century used technological advancements, such as high throughput sequencing to delineate the mechanisms of cancer etiology. It is within this timeframe that the genetic landscapes of cancer have slowly become available and have highlighted crucial biological pathways that contribute to the disease. Hallmarks of

cancer include; sustaining proliferative signaling, evading growth suppressors, activating invasion and metastasis, enabling replicative immortality, resisting cell death and inducing angiogenesis [105]. These rapidly growing, immortal cells can also evade host defense systems and often arise from an accumulation of genetic mutations that select for hallmark characteristics [105]. In addition, the identification of genetically heterogeneous cell populations within tumours and the theories that cancer may arise from cancer stem cells or that differentiated cells can transform back to stem-like or mesenchymal-like states have radically changed ideologies and approaches to research and clinical treatment [106-109]. Despite a wealth of new information regarding cancer initiation and progression, several questions and mechanistic knowledge gaps remain.

1.4. Tumour Microenvironment

The tumour microenvironment is defined as the environment in which tumour cells exist, including the availability of nutrients, pH levels, exposure to paracrine, autocrine or hormone signalling molecules, interactions with the extracellular matrix and oxygen tension. The microenvironment contributes to tumour heterogeneity and strongly influences cancer cell evolution through natural selection [110]. Additionally, a chronic inflammatory response induced by invading immune cells and low oxygen availability within the tumour promote tumour growth and metastatic progression. Necrotic tissues, tumour associated macrophages and cells under hypoxic stress release growth factors, interleukins, chemokines, cytokines and reactive oxygen species that increase cancer cell motility and activate angiogenesis [111]. Hence, inflammatory angiogenesis and *de novo* vascularization due to hypoxia support metastasis by providing avenues to the circulatory system whereby invading cancer cells can reach distant organs.

1.4.1. Normoxia and Hypoxia

The atmosphere contains ~21% oxygen, however, alveolar air in the lungs contains ~14% oxygen [112]. Oxygen from the alveoli diffuses into the blood and saturates haemoglobin at ~13% where it then travels throughout the body to be distributed. Not surprisingly, the oxygen tensions of tissues within the body vary greatly depending on the degree of vasculature, the barriers of oxygen dissociation and the

cellular demands for oxygen. For example, the O_2 concentration experienced by cells in the upper respiratory tract is near atmospheric oxygen whereas an O_2 concentration of ~1% can be measured in perisinusoidal bone marrow [113]. Thus, normal oxygen tension (normoxia) is measured in a tissue specific fashion. Normal oxygen tensions in tissues pertinent to this thesis include pO_2 of 52 mmHg in healthy breast tissues [114] and pO_2 of 30.5 mmHg in prostate tissue [115] (corresponding to ~6.5% and ~4% O_2 respectively). Interestingly, the conventional definition of normoxia is in regards to tissue culture and is ~20% O_2, which has recently been criticised due to the fact that "physoxia" (normal physiological oxygen tension) averages ~5% throughout the body [112,115]. Nevertheless, this thesis primarily deals with experiments surrounding cultured cells so the standard definition of normoxia at 20% O_2 applies to following sections.

As with normoxia, hypoxia is a relative term that is defined as a deficiency in the amount of O_2 available to tissues. Additionally, hypoxia can be intermittent or continuous and can be divided into acute, chronic or cycling phases. Acute hypoxia occurs during short periods of low oxygen (20 minutes to several hours) and cells respond through posttranslational modifications of existing proteins [116,117]. Conversely, chronic hypoxia occurs during prolonged exposure to low oxygen (days) and results in altered gene transcription and protein synthesis [116,117]. Cycling hypoxia may occur in instances with fluctuating levels of red blood cells such as temporally regulated blood vessel diameters (vasomotion) or due to dramatic and rapid shifts in microvasculature geometry which is often observed during tumour growth [118]. Hypoxia occurs for a variety of reasons and plays a critical role in pathophysiological conditions such as ischemia, altitude sickness, inflammation and cancer [112,116,119]. Again, the body experiences compartmental physoxia so O_2 partial pressures can fluctuate for physiological definitions of hypoxia depending on the tissue. However, several studies have determined that the majority of tumours experience oxygen levels between 0-2% [114,120,121]. Furthermore, the master regulators of the hypoxic response are hypoxia inducible factor (HIF) proteins who sense low oxygen levels and induce transcriptional programs to combat the effects of hypoxia [116]. Maximal stabilization and transcriptional activation of HIF1α is observed at 0.5% O_2 with half maximal achieved at 1.5-2% O_2 [122]. Thus, hypoxia in the context of tumour biology is an O_2 content <2%.

1.5. Hypoxia Inducible Factors (HIFs)

There are three bHLH-PAS hypoxia-inducible factor (HIF)-α proteins, specifically HIF1α (also named MOP1), HIF2α (also named EPAS1 or MOP2), and HIF3α that dimerize with ARNT when transcriptionally active [30,123-125]. HIF1α is expressed in all tissues whereas HIF2α and HIF3α are restricted to specific tissue types and may have more specialized roles in hypoxic signaling [126]. During normoxia, HIF1α and HIF2α proteins do not accumulate and are inactivated by the presence of prolyl hydroxylases (PHDs) [127-129] and factor inhibiting HIF (FIH) [130,131]. PHDs and FIH use oxygen as a substrate and hydroxylate HIFs at oxygen-dependent degradation domains (ODDs) and C-terminal transactivation domains (C-TADs), respectively (Figure 1.4A). The Von Hippel-Lindau tumor suppressor E3-ligase complex recognizes hydroxylated proline residues within the oxygen-dependent degradation domain [132]. This in turn targets HIF1α for ubiquitination and proteasomal degradation [133-135]. FIHs are asparaginyl hydroxylases that prevent the recruitment of p300/CBP by the C-terminal transactivation domain of HIF, thereby rendering HIF-α transcriptionally inactive under normoxic conditions [130,136]. Although HIF1α and HIF2α share many homologous domains and activities [137], the HIF3α paralog lacks the C-terminal transactivation domain [124] and has several splice variants that have no known role in transcriptional activation. Indeed, the human HIF-3α4 splice variant lacks the oxygen-dependent degradation and C-terminal transactivation domains and is thought to be a dominant-negative regulator of HIF1α activity [138]. In this respect, HIF activity in normal, oxygenated tissues is tightly regulated at the post-translational level (Figure 1.4B).

A characteristic of many solid tumors is that they contain areas that are chronically hypoxic and express elevated levels of HIFs [139,140]. During hypoxia, loss of PHD and FIH activity permit HIF-α proteins to accumulate, translocate to the nucleus, and bind ARNT [30]. Intriguingly, ARNT2 can dimerize with either HIF1α or HIF2α and the HIF1/2α/ARNT2 complexes appear to be the dominant hypoxia sensors in the central nervous system [141-143]. Molecular and computational analyses show that HIF2α and ARNT heterodimerize and associate through analogous PAS-B domain central β-sheets in an anti-parallel manner [144]. In the case of HIF2α, the PAS-B domain is essential for dimerization with ARNT and hypoxic responses are significantly

attenuated without it [144,145]. The HIF complex then binds to hypoxia response elements and recruits coactivators to activate the expression of genes, such as vascular endothelial growth factor (VEGF) and erythropoietin (EPO) [146-148]. Thus the micro-environment of solid tumors is conducive to the activation of HIF-regulated transcriptional programs and these support tumor growth, angiogenesis and metastasis.

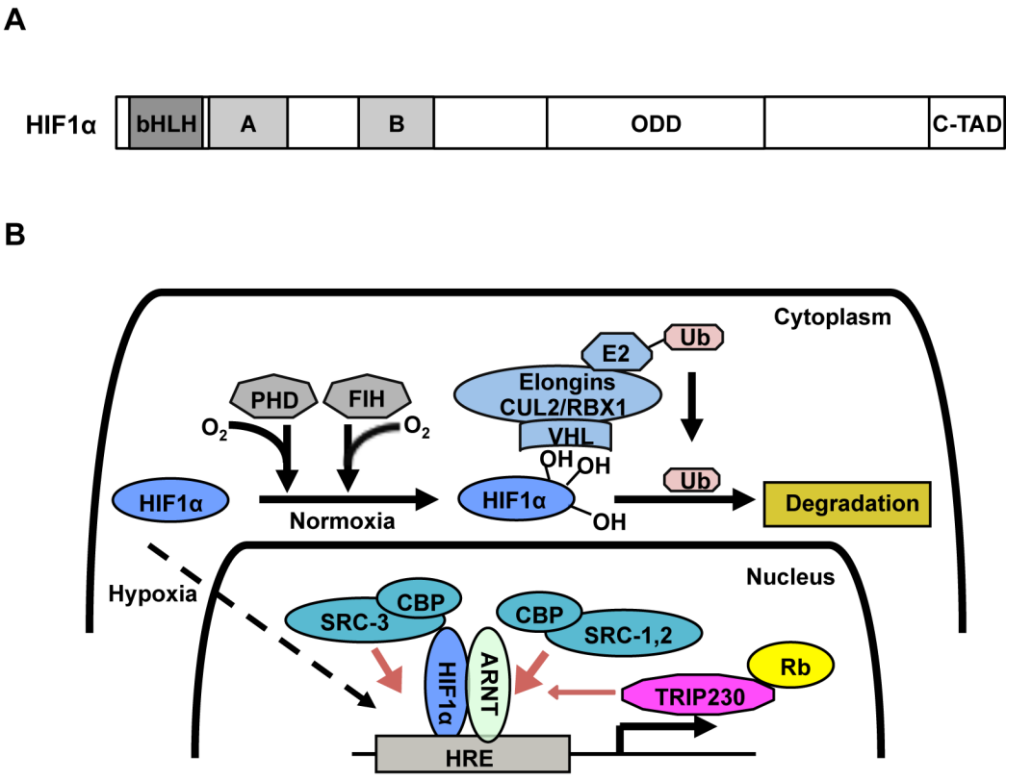

Figure 1.4. Regulation of HIF1α in mammalian systems.
(**A**) Schematic representation of the HIF1α protein and associated domains; bHLH, PAS A and B, oxygen dependent degradation (ODD) domain and C-terminal activation domain (C-TAD). (**B**) During normoxia, HIF1α is kept inactivated in the cytoplasm by factor inhibiting HIF (FIH) and programmed for degradation by prolyl hydroxylases (PHD). Ubiquitination by the Von Hippel-Lindau E3 ligase complex (VHL) leads to degradation of HIF1α proteins. During hypoxia, the HIF1α/ARNT complex binds to hypoxia response elements (HREs) and recruits coactivators such as CBP, SRC, and TRIP230 with its associated coregulator Rb to initiate transcription of hypoxia inducible genes.

1.6. Thyroid hormone receptor/retinoblastoma-interacting protein 230 (TRIP230)

The thyroid hormone receptor/retinoblastoma-interacting protein 230 (TRIP230) is a constitutively expressed protein that was originally identified as an activator of

thyroid hormone receptor (TR)-mediated signaling [149]. Investigators in Wen Hwa-Lee's laboratory determined that TRIP230 bolsters TR-mediated transcriptional responses and is negatively regulated by the Rb protein [149]. Rb-mediated attenuation of TR transcription is significant when Rb is over-expressed and is not due to competition for TRIP230 binding between Rb and TR, although each has a distinct TRIP230 binding region [149]. However, this effect could be due to TRIP230 being functionally inactivated by associating with Rb, which ensures specific and appropriate expression of TR-regulated genes [42,149]. Structurally, TRIP230 is part of the coiled-coil coactivator family and contains an LXXLL motif in its C-terminal domain [150]. This relates well to TRIP230 coactivator function as LXXLL motifs mediate both receptor specific and ligand specific assembly of transcriptional coactivator complexes [151].

The promiscuous nature of TRIP230 has been demonstrated as it is also involved in functions of the cis-Golgi network [152,153] and is an essential coactivator for dioxin and hypoxic signaling [150]. TRIP230 (also known as the Golgi microtubule-associated protein-210; GMAP-210) is important for normal Golgi apparatus morphology and connects the minus ends of microtubules to the cis-Golgi network [152,154]. TRIP230 interacts with microtubules through its basic C-terminus whereas interactions with Golgi membranes occur through its acidic N-terminus [154]. In addition, over-expression of TRIP230 disrupts microtubule networks and results in an enlargement of the Golgi apparatus [154]. Finally, and most importantly, we have demonstrated that TRIP230 is an absolute requirement for AHR and HIF-regulated gene transcription and that it does not interact with either AHR or HIF1α [150]. Thus, TRIP230 represents an attractive therapeutic target because of the roles that AHR and HIFs play in multiple disease states. Although TRIP230 is required for TR-mediated signal transduction and for proper Golgi apparatus morphology, the potential off-target effects of anti-TRIP230 therapeutic strategies may be ameliorated with further characterization of the molecular interactions governing TRIP230 coactivator functions that may highlight specific and targetable differences for biological functions.

1.6.1. TRIP230 and interactions with ARNT

Recruitment of TRIP230 during hypoxia is mediated through the ARNT PAS-B domain interacting with the coiled-coil C-terminal domains of TRIP230 [150,155]. The coiled-coil coactivators bind the same but opposite interface as HIF2α thus mutations affecting the ARNT PAS-B α-helix disrupt coactivator recruitment but still allow HIF2α dimerization [155]. Furthermore, TRIP230 interacts with ARNT through a LXXLL-like nuclear receptor box and mutation of this motif abolishes the TRIP230-ARNT PAS-B interaction [155]. Hence, ARNT represents multiple platforms for the scaffolding of coregulator complexes.

1.7. The Pocket Proteins

The pocket protein family is composed of the retinoblastoma protein (Rb/p105) and the related retinoblastoma-like 1 protein (Rbl1/p107) and retinoblastoma-like 2 protein (Rbl2/p130). The Rb protein was the first pocket protein family member identified and it occurred through studies of inherited retinoblastoma, a malignant retinal cell cancer. Isolation and molecular characterization of the Rb protein laid the groundwork for research identifying tumour suppressor proteins and oncoproteins and was vital to the current understanding of carcinogenesis. Subsequent cloning and functional assays determined that Rb negatively regulates the cell cycle and that it controls the G1-restriction point and blocks S-phase entry by inhibiting E2F transcription factors [100,156]. In parallel, p107 and p130 are also negative regulators of the cell cycle and act through inhibition of E2F transcription factors [157,158]. Although p107 and p130 have several overlapping functions with Rb, p130 activity seems to be restricted to G0 [159] and p107 activity seems to accentuate or support Rb-function, especially during the G1-S phase of proliferating cells [160].

1.7.1. Molecular components of Rb, p107 and p130

The Rb protein has ~30% homology to p107 and p130 whereas p107 and p130 share ~50% homology [161]. Importantly, all family members have a conserved “pocket” domain that mediates interactions with cellular factors such as E2Fs as well LXCXE-

containing proteins such as cyclins and viral oncoproteins [162,163]. The pocket domain consists of A and B subdomains that associate through non-covalent interactions to form a single structural interface [164,165]. Members of the E2F transcription factor family and LXCXE-containing proteins can bind the Rb proteins at the same time as they have distinct pocket domain interaction sites [163]. Additionally, Rb proteins contain an amino-terminal domain (RBN) required for recruitment of chromatin modifying proteins [166,167], an unstructured carboxy-terminal domain (RBC) required for high affinity E2F binding [168] and phosphorylatable linker regions that dictate Rb function [169] (Figure 1.5).

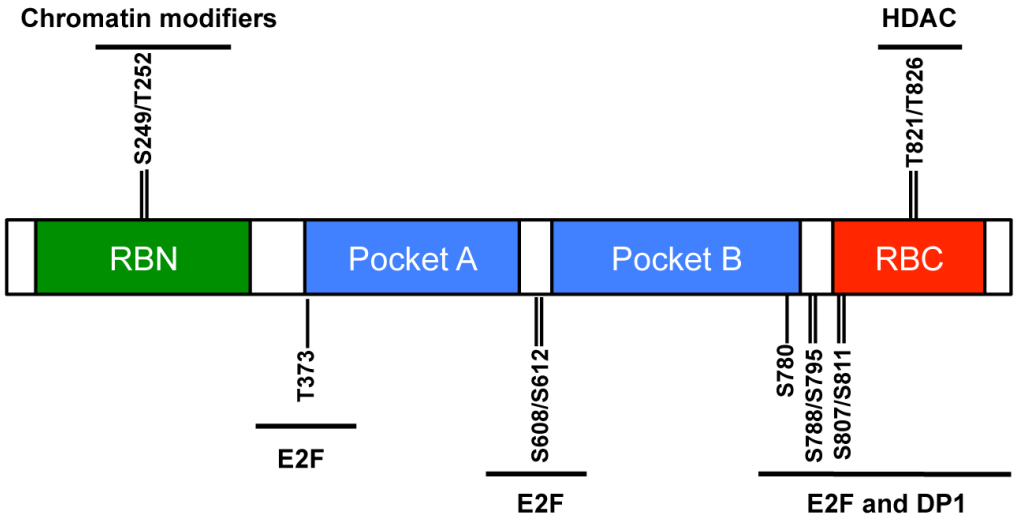

Figure 1.5. Rb structure and the locations of important residues targeted for phosphorylation.

A) A schematic representation of Rb structural domains, amino terminal domain (RBN), pocket domains A and B, carboxy terminal domain (RBC). Rb phosphorylation sites regulating E2F/DP1 and HDAC associations and important locations for coregulator interactions are also highlighted.

1.7.2. Rb and cell cycle control.

The pocket protein family members are posttanslationally modified through phosphorylation and the canonical ideology is that gradual phosphorylation leads to functional inactivation [161,169]. This theory stems from the cell cycle-dependent regulation of the pocket protein family members through cyclin/cyclin dependent kinase (CDK) complexes. CDK and cyclin protein family members are the most important factors regulating the cell cycle. Cyclins A, B, D and E and their respective homologs are LXCXE-containing proteins that have fluctuating expression patterns depending on the

phase of the cell cycle [170]. The cyclins dimerize with CDK1-6 proteins and then cyclin-CDK complexes phosphorylate proteins that ultimately turn on transcriptional programs that promote cell growth and proliferation. Knockout mice studies have highlighted the differences between some of the cyclin-CDK complexes and their functions in cell cycle control and tissue development. For example, Cdk2, Cdk3, Cdk4 and Cdk6 knockout mice are viable whereas Cdk1 knockout is lethal [171-176]. Furthermore, cyclin B1 knockout mice are embryonic lethal, cyclin B2 knockout mice are normal and knockout of any of the D-cyclins (1,2 or 3) causes death mid gestation due to severe hematopoietic and cardiac defects [177,178]. With the exception to CDK1 and cyclin B1 functions, this suggests that some of the CDKs and cyclins have redundant functions that can compensate for deficiencies in the signal transduction cascades of closely related family members. In addition, both CDKs and cyclins exhibit tissue-specific expression and are required for normal development.

The oscillating cyclin protein expression patterns and different CDK dimerization partners have been extensively studied to develop a general theory of cell cycle control in mammalian systems. Cyclin D proteins dimerize with CDK4 or CDK6 in G1 and control the early stages of the cell cycle. Cyclin E-CDK2 complexes mediate S-phase initiation whereas cyclin A-CDK1 and cyclin A-CDK2 complexes mediate S-phase completion. Finally, cyclin B-CDK1 complexes control G2, mitosis and cell cycle exit [170]. Mitogenic stimuli induce transcription of cyclins and initiate the appropriate phases of the cell cycle. For example, growth factor induced activation of the mitogen-activated protein kinases (MAPKs) stimulates AP-1 transcription factor expression and AP-1 stimulates the transcription and expression of cyclin D proteins that control the G1 phase [179]. Fluctuations in cyclin protein expression are regulated by ubiquitin-mediated proteasomal degradation and this allows for the appropriate expression of cyclin proteins throught the cell cycle [180,181]. Since Rb regulates the G1-restriction point, the critical complexes involved in Rb phosphorylation are D-cyclins and CDK4/6 and E-cyclins and CDK2 [182,183]. Additionally, cyclin A-CDK2 complexes are important for phosphorylating p107 and p130 [161]. Taken together, cyclin and CDK proteins are tightly regulated oscillating factors that control a stepwise progression through the cell cycle.

Canonical Rb-function suggests that hypophosphorylated Rb directly interacts with and sterically hinders the transactivation domain of E2F transcription factors to inhibit transcription of genes required for transition from G1 to S phase [184-186]. The Rb-E2F complex binds to the promoters of mitogenic genes and sequential phosphorylation of Rb on approximately 13-15 conserved consensus sites by cyclin-CDK complexes dissociates Rb from E2F [182,183,187,188] (Figure 1.6). A complete picture of the biochemical outputs and structural effects due to Rb phosphorylation remains to be determined, however, serine and threonine sites important for modulating Rb activity include; S249/T252 phosphorylation disrupts Rb interactions with chromatin modifiers [166]; T373 phosphorylation and S608/S612 phosphorylation inhibits the binding of E2F transactivation domains to the Rb pocket domain [189]; S780 and S788/S795 phosphorylation inhibits Rb binding to E2F-DP1 heterodimers [168,190]; T807/T811 phosphorylation is required to facilitate the phosphorylation of other residues important for dissociating the E2F complex [169]; and T821/T826 phosphorylation inhibits HDAC and viral oncoprotein binding to the pocket domain [191]. More work is necessary to determine the degree that each phosphorylated species is expressed and how mono-, di-, tri-, etc., phosphorylation marks change Rb-function.

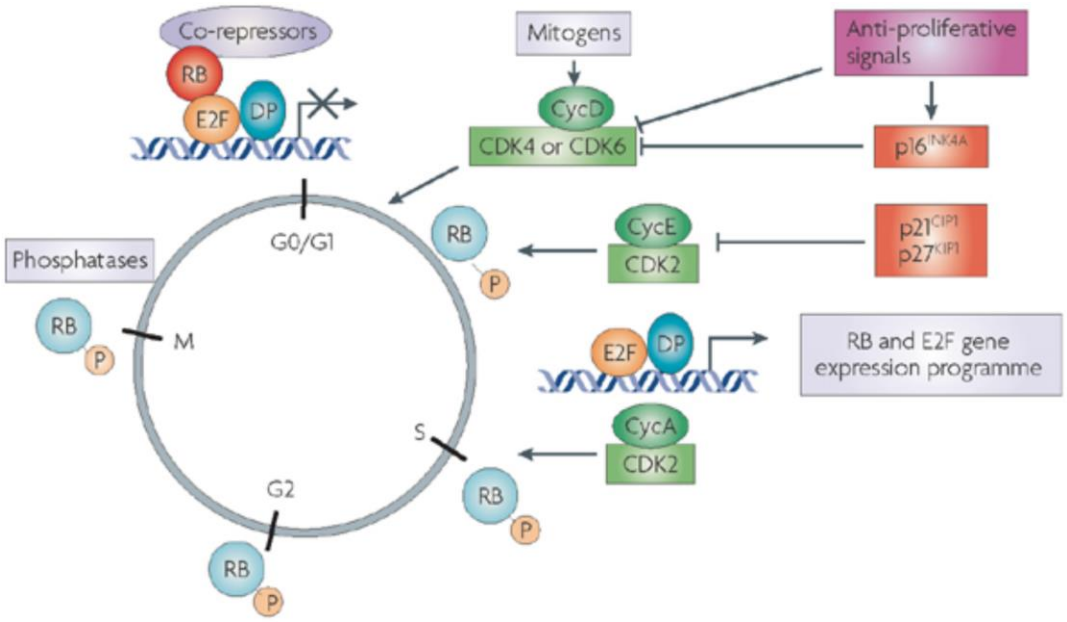

Figure 1.6. Schematic of RB in cell cycle control.
Mitogenic signals stimulate the expression of D-type cyclins (Cyc) and a concomitant increase in cyclin-dependent kinase 4 (CDK4) and CDK6 activity. These factors initiate RB phosphorylation, which is augmented by the activity of CDK2 complexes with cyclins A and E. The phosphorylation of RB disrupts its association with E2F. This inactivation of RB allows for the expression of a transcriptional programme that enables progression through S-phase and mitosis. At the transition from mitosis to G1, RB is dephosphorylated through the action of phosphatases. Importantly, a large number of anti-mitogenic signals function to prevent RB phosphorylation either by limiting the activity of CDK4, CDK6 and CDK2 complexes or by inducing the activity of CDK inhibitors. Reprinted by permission from Macmillan Publishers Ltd: Nature Reviews Cancer, Knudsen, ES. and Knudsen, KE., copyright (2008). [192]

1.7.3. Rb function in apoptosis and the DNA damage response.

The role of Rb in the cell cycle is the most well understood Rb-regulatory pathway, however several research groups have uncovered activities for Rb outside of cell cycle regulation, namely DNA damage repair and apoptosis. With regards to apoptosis, the literature supports both pro- and anti-apoptotic functions for Rb. It has been observed that E2F1 directly regulates the pro-apoptotic gene *p73* and induces its expression in response to DNA damage [193]. Additionally, aberrant E2F1 signalling in Rb-deficient cells induces p53-mediated apoptosis through the stabilization of p14ARF and that re-expression of Rb reduces E2F1-mediated apoptosis [194,195]. Furthermore, Hsieh and colleagues determined that the pro-apoptotic activity of E2F1 was blocked in cells expressing DNA-binding-deficient E2F1 and that Rb-binding-deficient E2F1 induced apoptosis as effectively as wild type E2F1 [196]. Moreover, overexpression of

Rb inhibited apoptosis in cells expressing wild type E2F1 but had no effect on cells expressing Rb-binding-deficient E2F1 [196]. Taken together, this suggests that anti-apoptotic functions of Rb are E2F1-dependent and that molecular safeguards are present to remove cells from the population that have lost normal Rb function.

Conversely, Rb has been shown to exacerbate apoptosis in an E2F1-dependent fashion. Rb and E2F1 are recruited to the *Caspase-7 (CASP7)* gene in response to doxorubicin [197], a DNA intercalating chemotherapeutic. Rb-depletion using shRNA technology showed that Rb-deficient cells had reduced CASP7 mRNA accumulation and less doxorubicin-induced apoptosis compared to Rb-positive control cells [197], suggesting that Rb is a positive regulator of DNA-damage induced apoptosis. Additionally, nonnuclear Rb positively regulates tumour necrosis factor-α (TNF-α)-mediated mitochondrial apoptosis [198]. Apoptosis may occur through an extrinsic pathway, an intrinsic pathway or a combination of the two pathways together. The extrinsic pathway is receptor-mediated and includes activation of death receptors at the plasma membrane and subsequent signal transduction cascades to increase production of pro-apoptotic factors, like caspases [199]. The intrinsic pathway is mitochondria-mediated and relies on BAX and BAK, members of the Bcl-2 protein family, to facilitate mitochondrial outer membrane permeabilization and release of pro-apoptotic factors, such as cytochrome c, that ultimately lead to caspase production and apoptosis [199]. With regards to Rb and mitochondria-mediated apoptosis, cytoplasmic Rb is associated with mitochondria and directly binds and activates BAX to induce mitochondrial outer membrane permeabilization [198]. Interestingly, nonnuclear Rb also includes hyperphosphorylated Rb associated with the mitochondrion [198], suggesting a tumour suppressor function for phosphorylated Rb in a pathway independent from E2F transcription factors. The role of Rb in apoptosis is not the only example of a tumour suppressor role for Rb independent from E2F and the cell cycle. For example, Rb is also known to be involved DNA damage repair and directly participates in non-homologous end-joining (NHEJ) of DNA double strand breaks [200]. Rb associated NHEJ involves the N-terminal domain of Rb interacting with XRCC5 and XRCC6 and this tumour suppressor function for Rb occurs independent of the cell cycle and E2F-transcription factors [200].

In summary, the role of Rb in apoptosis includes both E2F-dependent and E2F-independendt mechanisms. Furthermore, context and cell-specific roles for Rb exists in apoptosis and both the pro- and anti-apoptotic Rb activities provide evolutionary advantages in situations where Rb function is lost. For anti-apoptotic functions, loss of Rb allows cells with a dysregulated cell cycle to be removed from the population providing a molecular safeguard to prevent cancer from occurring. On the other hand, loss of Rb in situations where it displays pro-apoptotic tendencies would be selected for in cancer cells as this would allow for continued genome instability (e.g. aberrations in NHEJ) and lack of cell cycle regulation. Further investigation looking at Rb perturbations and the effects on apoptosis are required, however, these studies highlight the importance of Rb-regulation in pathways distinct from the cell cycle and elaborate on roles for Rb independent of E2F-transcription factors.

1.7.4. Rb and cancer

The Rb protein is the prototypical tumour suppressor protein and loss of Rb function is consistently observed in cancer cells leading to aberrant cell proliferation, tumourigenesis and tumour progression. Deletion, mutation or allelic loss of Rb confers increased susceptibility to cancers of the breast [201], prostate [202], brain and lung. Classical Rb function suggests that the lack of Rb in cancer cells results in loss of the G1-restriction point and permits constitutive E2F-mitogenic signalling, thus explaining the observed increase in cancer susceptibility and tumour progression [203]. However, several studies have shown that Rb has tumour suppressor functions independent from E2F transcription factors and the cell cycle. For example, Sun and colleagues determined that mice expressing an E2F binding-deficient Rb protein ($Rb^{654/654}$) fail to prevent prostate cancer initiation but retain Rb tumour suppressor activity as Rb^{654} prevents progression to invasive and lethal prostate cancer [204]. Thus, Rb/E2F interactions are crucial for preventing tumourigenesis but Rb can use context-dependent mechanisms to restrain tumor progression outside of E2F mechanisms. Finally, loss of Rb in many solid tumours is concomitant or directly precedes the activation of HIF1-regulated genes and correlates with increased VEGF expression, microvascular hyperplasia and metastasis [205,206]. This suggests that Rb and HIF1 signaling pathways may be linked. As most solid tumours contain regions of hypoxia and only

correlative data between HIF1 activity and loss of Rb has been gathered, there is a need to rigorously examine the role of Rb-loss in concert with hypoxia.

1.8. Prostate Cancer

According to the Canadian Cancer Society, prostate cancer is the most common cancer among Canadian males and the 3rd most lethal with an estimated 24,000 new cases and 4,100 deaths in 2015 [207]. The normal prostate is a walnut sized gland surrounding the urethra and is located just below the urinary bladder. Its main functions are to secrete an alkaline fluid to protect and sustain sperm and to facilitate ejaculation through smooth muscle contractions. In general, primary prostate cancers are heterogenous and several histological and molecular subtypes exist. Histologically, adenocarcinomas are the most common prostate cancer variant and account for 90-95% of all cases [208]. On a molecular level, a recent study by the Cancer Genome Atlas Network identified seven distinct prostate cancer subtypes that fall into either gene fusions (*ERG, ETV1/4* and *FL1*) or mutations (*IDH1, SPOP and FOXA1*) [209]. However, more research is required to delineate the exact molecular mechanisms driving cancer cell transformation as ~26% of prostate cancer primary tumours do not fall into these molecular categories [209].

1.8.1. The androgen receptor and roles in prostate cancer.

Prostate cells require androgens, like testosterone and its metabolite dihydrotestosterone (DHT), for growth, maturation and development. Thus, a key transcription factor involved in the normal functions of the prostate gland is the androgen receptor (AR). The AR protein is a member of the nuclear receptor superfamily. Ligand binding activates AR and induces the transcription of genes involved in male secondary sex characteristics, cell growth and proliferation [210]. Additionally, AR signalling is required for the maintenance of the structural and functional integrity of the prostate gland. In prostate cancer, aberrant AR function is commonplace and first line treatments include androgen deprivation therapies (ADTs) that act to interfere with AR signaling and repress AR-target gene expression [211]. However, ADTs are not curative and most

early stage prostate cancers that initially respond to ADT eventually recur as castration-resistant prostate cancer (CRPC), an incurable and ultimately fatal illness.

1.8.2. Neuroendocrine differentiation in prostate cancer

Neuroendocrine (NE) cells are cells that respond to neurotransmitters and other stimuli and release hormones into the blood or in autocrine or paracrine fashions. The normal prostate contains NE cells in all areas of the gland but the highest density of cells tends to localize in the major ducts. In addition, two types of NE cells exist in the prostate; the open-type and closed-type NE cells. Open-type cells have apical processes that extend to the lumen [212]. Closed-type cells do not reach the lumen and are encapsulated by epithelial cells [212]. Both cell types have dendritic extensions that invade adjacent cells and release a multitude of hormones such as serotonin, bombesin and somatostatin [212-214]. Closed-type cells can only receive stimuli from underlying stromal cells (autocrine/paracrine signals), neurotransmitters or hormones from nearby blood vessels whereas open-type cells can also respond to luminal signals such as chemicals and pH [214]. Interestingly, prostatic NE cells are AR negative and appear to be non-proliferative [215,216]. Indeed, androgens are the most important growth-stimulating factor in the prostate and the mechanisms controlling NE cell maintenance remain unclear [217]. Although many similarities between open and closed cell types exist, they are generally regarded as functionally distinct entities. However, research defining individual roles is lacking and further research regarding cell-specific functions and mechanisms of regulatory control may reveal insights into new therapeutic options for neuroendocrine prostate cancers.

In prostate cancer, neuroendocrine differentiation (NED) is a term used to describe conventional adenocarcinomas that display scattered or small nests of NE cells upon histopathologic examination [218]. However, neuroendocrine prostate tumours are heterogeneous in the population and can be classified as exhibiting focal NED (where a small subset of tumour cells display NE features) or pure NED (where every tumour cell displays NE features) [214,218]. Pure NE tumours are represented in cases of small cell carcinoma and carcinoid tumours of the prostate whereas focal NED is represented in cases of adenocarcinoma with neuroendocrine features [218]. Regardless of tumour

composition, neuroendocrine prostate cancer (NEPC) is typically hormone-refractory, has a poor clinical outcome and may represent ~25% of late stage prostate cancer [219,220]. There are two prevailing hypotheses of how NEPC arises: (i) NEPC cells and normal NE cells of the prostate are derived from the same progenitor cell or (ii) NEPC cells are derived from adenocarcinoma cells through the process of neuroendocrine transdifferentiation [221]. The latter model is supported by an abundance of research and hypothesizes that NEPC develops from adenocarcinomas as a mechanism of resistance to androgen-deprivation therapy (ADT).

The prostate cancer NE transdifferentiation model is well characterized and supporting evidence includes clinical specimens [222], genetic and cytological studies comparing NEPC cells and prostate carcinoma cells [223,224] and in vitro and in vivo observations documenting the transdifferentiation process [225-228]. Firstly, archived tumour specimens and retrospective studies illustrate that patients receiving ADT will eventually develop castration resistant prostate cancer (CRPC) [229,230] and develop significantly higher rates of NED the longer that they are on therapy [222,230]. CRPC is a common progression after surgical resection or ADT. The CRPC stage is characteristically hormone refractory (androgen-insensitive) due to constitutively active AR activity or selection of cells that bypass requirements for AR-mediated growth and proliferation [231]. CRPC and NEPC share many similarities but are also distinct diseases and questions remain over the biologic mechanisms driving progression from CRPC to NEPC. Importantly, not all CRPC progresses to NEPC and NEPC may arise before CRPC but it is generally implied that at least a subset of patients on ADT will go from a hormone responsive state at initial presentation to a CRPC/mixed tumour to NEPC in the final stages [214,221,230,232].

Further support for the transdifferentiation model is displayed by the observation that normal prostatic NE cells and NE tumour cells have different protein expression profiles. For example, NE tumour cells and non-NE tumour cells express the β-oxidation enzyme α-methylacyl-CoA-racemase (AMACR) whereas normal NE cells do not, suggesting a close relationship between NE tumour cells and prostate adenocarcinoma cells [223]. Genetic clustering of NE tumour cells, non-NE tumour cells and normal NE cells from clinical specimens determined that NE tumour cells and non-NE tumour cells

are more closely related than NE tumour cells and normal NE cells [224]. Indeed, TMPRSS2-ERG gene fusions frequently occur in prostate cancer [233] and individuals with concurrent adenocarcinoma and small cell carcinoma display identical perturbations of the TRMPRSS2-ERG protein suggesting clonal evolution [234]. In addition, human LNCaP prostate cancer cells are androgen-dependent and epithelial in nature [235], however, transdifferentiation to a NE phenotype occurs after chronic culturing in hormone-deprived media [225,227,236]. Androgen deprived LNCaP cells express characteristic NE markers like ENO2 and show significant decreases in AR and PSA expression [225,227,236]. Finally, patient- derived prostate adenocarcinoma xenograft models showed complete transformation of adenocarcinoma to small cell NEPC after medical-castration [228]. Genomic profiling of the tumour at various time-points during transdifferentiation suggests clonal evolution of adenocarcinoma cells rather than selection of pre-existing NEPC cells [228]. In summary, several avenues of research provide strong evidence for epithelial plasticity in NEPC. However, both the molecular pathways involved and the biomolecules responsible for inducing NED in prostate cancer remain and active area of investigation.

1.8.3. NED and Rb

Rb-loss occurs in 25-50% of cases of prostate cancers [237,238]. Specifically, loss of Rb protein expression occurs in ~90% of small cell prostate cancer cases whereas Rb is normally present in high-grade acinar tumours [239]. Furthermore, mouse models with functional ablation of either p53 or Rb display prostatic intraepithelial neoplasia but functional ablation of both p53 and Rb leads to invasive NEPC [240-242]. Indeed, shRNA-mediated knockdown of Rb in LNCaP and LAPC-4 prostate cancer cells is sufficient to induce a CRPC phenotype [202]. Deregulation of the Rb/E2F1 pathway leads to upregulation of AR mRNA and protein levels and bypass of hormonal therapy [202]. Taken together, this suggests that Rb-loss in prostate cancer is a critical step preceding NED and tumour progression, however, the molecular mechanisms and gene pathways responsible for cancer cell transformation after Rb-ablation remain poorly understood.

1.9. Breast Cancer

According to the Canadian Cancer Society, breast cancer is the most common cancer among Canadian females and the 2nd most lethal with an estimated 25,000 new cases and 5,000 deaths in 2015 [207]. Although males may develop breast cancer, it is rare and occurs in less than 1 case per 100,000 people with an estimated 60 men succumbing to the disease in 2015 [11]. The primary function of the normal female breast is to produce and store milk. The breasts are composed of glandular, milk-producing tissue called lobules, milk-transporting ducts and fatty tissue. Like most cancers, breast cancer is a heterogenous group of diseases that are categorized according to location of the tumour, level of invasiveness and gene expression profiles. Histologically, the most prevalent carcinomas of the breast fall into two distinct categories: ductal or lobular. These classifications are further subcategorized as either in situ or invasive. Breast carcinomas are also categorized according to gene expression profiles and these include the luminal A, luminal B, HER2-enriched or basal-like subtypes [243]. Luminal subtypes are estrogen receptor (ER)-positve and/or progesterone receptor (PR)-positive, HER2- enriched subtypes have extra copies of herceptin receptor 2 (HER2) and the basal subtype is also known as triple-negative breast cancer and does not express any PR, ER or HER2 proteins [243].

1.9.1. Breast cancer and Rb

In breast cancers, familial and sporadic forms of triple-negative breast cancer often display a functional loss of Rb expression [244-246]. Loss of Rb is frequent in aggressive basal-like breast tumours and may contribute to unique therapeutic responses [201]. In addition, DNA microarray data from primary breast tumours paired with patient history determined that an Rb-loss signature in ER-positive primary tumours is associated with worse response to chemotherapy and shorter relapse-free survival compared to ER-positive, Rb-expressing and ER-negative subpopulations [247]. Interestingly, mutations in *RB1* have been identified as a bona fide driver of neoplastic initiation and progression in ER-negative breast cancer [248]. Mutations in *RB1*, as well as *CDKN2A, MAP3K1, PTEN, MAP2K4, ARID1B, FBXW7, MLLT4* and *TP53* account for a significant proportion of recessive driver mutations in breast cancer [248]. Although

several studies have highlighted the importance of Rb-loss in breast cancer initiation and progression, few studies have examined the molecular underpinnings of tumourigenesis and progression. Thus, like prostate cancer, further examination of Rb-loss and hypoxia is warranted in breast cancer models.

1.10. Rationales, Hypotheses and Objectives of this thesis

It has been well established that ARNT is a multifaceted transcriptional coregulator involved in multiple cell signalling pathways. However, the two aspects this thesis will focus on are: 1) The roles of ARNT and AHR in disruption of estrogen receptor mediated signalling; and 2) The role of the ARNT-TRIP230-Rb transcription factor complex in HIF1-regulated transcription.

1.10.1. The roles of ARNT and AHR in disruption of estrogen receptor mediated signalling

Rationale

Polycyclic aromatic hydrocarbons and halogenated aromatic hydrocarbons are ubiquitous in the environment and are well known for their mutagenic and carcinogenic activities. Activators of AHR have been linked to developmental abnormalities, reduced fertility, altered birth sex ratios, and increased incidence of several cancers including breast and prostate [42]. The roles of AHR and ARNT with regards to endocrine disruption are actively being characterized. However, several mechanisms of AHRC-mediated disruption of ER-transcription have been proposed, including competition for ARNT and other transcriptional coactivators [91]. We have previously shown that ER tethers to AHR and ARNT to disrupt TCDD-inducible transcription [73], therefore a reciprocal model at ER-regulated genes is likely. In addition, few novel targets for the amelioration of the toxic affects of AHR activators have yet to emerge. The role of selective modulators for AHR may hold some promise, however elucidation of AHR-ARNT-ER cross-talk will provide us with additional information concerning endocrine disruption, in particular, the molecular determinants regulating these events and identification of potential targets for therapeutic intervention.

Hypothesis

We believe that AHR and ARNT tether to ER at ER-regulated genes to abrogate E2-inducible transcription and that competition for ARNT is not the primary mechanism of AHR-mediated disruption of estrogen signaling.

Objectives

1. Characterize AHRC-mediated disruption of ER-regulated transcription in an ER-positive cell model other than breast cancer cells.

2. Determine the transcriptional and functional consequences of AHR and ARNT knockdown in estrogen signalling.

1.10.2. The role of the ARNT-TRIP230-Rb transcription factor interactions in HIF1-regulated transcription

Rationale

Current chemotherapy tactics have focused on preventing angiogenesis to slow tumour growth and combat metastasis in the hopes of extending patient survival rates. However, these approaches are limited because metastasis is not entirely dependent on angiogenesis. For example, the VEGF antibody bevacizumab (Avastin) has been severely scrutinized due to the lack of evidence supporting an extension or improvement in the quality of life in patients with metastatic breast cancer [249]. Thus, there is a need for a more complete understanding of the molecular mechanisms governing a cancer cell's potential for intravasation and metastasis. A novel approach may involve HIFs, which control the hypoxic response and regulate both cell invasion and angiogenic programs [116,250,251] through the recruitment of TRIP230 and its coregulator Rb. The second part of this thesis focuses on the potential for Rb to regulate cell invasion by virtue of its direct effects on the hypoxia inducible factor 1 complex (HIF1). The benefits of this research are that we intend to use this knowledge to develop better cancer therapeutic agents.

Hypothesis

We believe that the loss of Rb in breast and prostate cancer unmasks the full coactivation potential of TRIP230 and this leads to a dysregulation of HIF1 transcriptional activity that results in angiogenesis, cancer cell invasion and metastatic transformation.

Objectives

1. Delineate the molecular interactions between ARNT, HIF1, TRIP230 and Rb in hypoxia signaling.

2. Identify the transcriptional consequences of Rb knockdown at HIF1-regulated genes.

3. Elucidate the functions and gene signalling pathways that Rb regulates in conjunction with hypoxia in breast and prostate cancer models.

Chapters 2, 3 and 4 contain published work that directly addresses these objectives and are presented in a form as close as possible to the original publication. Chapter 2 uses siRNAs to ablate AHR and ARNT protein levels, real-time PCR, immunoblots and chromatin immunoprecipitation assays in MCF7 and ECC-1 cells to examine AHR and ARNT function at ER-regulated genes. Chapter 3 describes the consequences of Rb-loss at HIF1-regulated genes in cancer cells by knocking down Rb protein with siRNAs and outlines a model for the transcriptional regulation of HIF1 by TRIP230 and Rb. Chapter 4 details the global gene networks affected by Rb-loss and hypoxia in prostate cancer through the use of microarray technology and stably transformed shRNA prostate cancer cell lines that either expressed a shRNA to Rb or a shRNA to a negative control sequence. Finally, chapter 5 contains material in preparation for publication that parallels chapter 4 material but in breast cancer models. Additionally, we use chemical inhibitors of targets identified in our array to ameliorate the loss of Rb in breast cancer cells.

Chapter 2. Distinct roles for aryl hydrocarbon receptor nuclear translocator and Ah receptor in estrogen-mediated signaling in human cancer cell lines.

Published in PLoS ONE January 3, 2012, DOI: 10.1371/journal.pone.0029545

Authors: Mark P. Labrecque, Mandeep K. Takhar, Brett D. Hollingshead, Gratien G. Prefontaine, Gary H. Perdew, Timothy V. Beischlag

Author Contributions: I performed all tissue culture and carried out chromatin immunoprecipitation assays represented in Figures 2.1A and B. I conducted all siRNA treatments specific to ARNT and the scrambled negative control sequence and performed all qPCR, immunoblots and densitometry assays in both MCF7 and ECC-1 cells represented in Figures 2.2, 2.3 and 2.4. I performed all proliferation assays and immunoblots represented in Figure 2.5 and created the cartoon for Figure 2.6. Timothy Beischlag performed the siRNA experiments to AHR and GFP represented in Figures 2.1C-D. Brett Hollingshead performed the immunoblot represented in Figure 2.1E. Timothy Beischlag, Gratien Prefontaine and Gary Perdew helped conceive and design the experiments. I wrote the initial draft of the manuscript and Timothy Beischlag and I wrote the final published version of the manuscript.

2.1. Abstract

The activated AHR/ARNT complex (AHRC) regulates the expression of target genes upon exposure to environmental contaminants such as 2,3,7,8-tetrachlorodibenzo-*p*-dioxin (TCDD). Importantly, evidence has shown that TCDD represses estrogen receptor (ER) target gene activation through the AHRC. Our data indicates that AHR and ARNT act independently from each other at non-dioxin response element sites. Therefore, we sought to determine the specific functions of AHR and

ARNT in estrogen-dependent signaling in human MCF7 breast cancer and human ECC-1 endometrial carcinoma cells. Knockdown of AHR with siRNA abrogates dioxin-inducible repression of estrogen-dependent gene transcription. Intriguingly, knockdown of ARNT does not effect TCDD-mediated repression of estrogen-regulated transcription, suggesting that AHR represses ER function independently of ARNT. This theory is supported by the ability of the selective AHR modulator 3',4'-dimethoxy-α-naphthoflavone (DiMNF) to repress estrogen-inducible transcription. Furthermore, basal and estrogen-activated transcription of the genes encoding *cathepsin-D* and *pS2* are down-regulated in MCF7 cells but up-regulated in ECC-1 cells in response to loss of ARNT. These responses are mirrored at the protein level with cathepsin-D. Furthermore, knock-down of ARNT led to opposite but corresponding changes in estrogen-stimulated proliferation in both MCF7 and ECC-1 cells. We have obtained experimental evidence demonstrating a dioxin-dependent repressor function for AHR and a dioxin-independent coactivator/corepressor function for ARNT in estrogen signaling. These results provide us with further insight into the mechanisms of transcription factor crosstalk and putative therapeutic targets in estrogen-positive cancers.

2.2. Introduction

Elucidating the mechanisms underlying transcription is crucial to our understanding of how cells and organisms respond to physiological signals and environmental stimuli. The aryl hydrocarbon receptor (AHR) and the aryl hydrocarbon receptor nuclear translocator (ARNT) are members of the basic helix-loop-helix/PER-ARNT-SIM (bHLH-PAS) family of proteins and form a heterodimeric transcription factor upon binding a variety of environmental contaminants, including 2,3,7,8-tetrachlorodibenzo-*p*-dioxin (TCDD) [41]. The activated AHR/ARNT complex (AHRC) plays key roles in carcinogenesis and regulates the expression of *Cytochrome P4501A1* (*CYP1A1*) and other xenobiotic target genes to combat the effects of environmental contaminants [41]. In addition, AHR has been shown to be important for normal development and physiological homeostasis [252-254] and is essential for certain functions of the immune response, such as regulation of interleukin-17 producing T-

helper cells [255] and induction of the cytokine interleukin-6 in MCF7 breast cancer cells [256].

Unliganded AHR exists in the cytoplasm as part of a multimeric complex containing two molecules of HSP90, the HSP90 co-chaperone p23, and hepatitis B virus X-associated protein 2 (XAP2) [44-47]. Upon ligand binding, AHR translocates to the nucleus where it associates with ARNT to form a functional transcription factor complex, the AHRC. As an activated complex, the AHRC is capable of recruiting regulatory proteins, such as steroid receptor coactivator-1 (SRC-1), CREB binding protein (CBP/p300), NCoA2/GRIP1 [49,73], receptor-interacting-protein 140 (RIP140) [257], CoCoA [258], GAC63 [259], NcoA4 [260] and TRIP230 [150], which play significant roles in determining the activity of TCDD-induced gene transcription. These coactivators and corepressors incorporate themselves into multimeric complexes that modify chromatin structure, stabilize core transcriptional machinery, and mediate RNA chain elongation [42]. In addition to these classic transcriptional coactivators and corepressors, AHR is recruited by other transcription factors during transcription, including estrogen receptor-α (ERα) [72,73,261] and NF-κB [262] to modify their intrinsic activities.

ERα/β are ligand activated transcription factors that belong to the superfamily of nuclear hormone receptors (NR) [263] and bind 17β-estradiol (E2) to regulate genes involved in reproduction and cellular growth and proliferation [264]. Upon ligand binding, ER forms a functional homodimer and binds its cognate response elements. Interestingly, there is a ligand-dependent reciprocal disruption between ER and AHR signaling. For instance, it has been shown that activated ERα inhibits AHRC activity at *CYP1A1* through direct protein-protein interactions, termed *transrepression* [73]. Conversely, TCDD's anti-estrogenic properties are well documented as it represses the E2-inducible genes *pS2* and *cathepsin-D (CAT-D)* [74,265,266]. However, the mechanisms of repression occurring at E2-responsive genes are unclear. Proposed theories for this repression include: (i) competition for a common pool of coactivators [91]; (ii) a direct down-regulation of *CAT-D* transcription through upstream inhibitory xenobiotic response elements [267]; (iii) activation of a TCDD-inducible inhibitory factor [267]; (iv) an AHR-dependent E3-ligase that degrades proteins crucial for ER-signaling [82], or; (v) a direct transrepression interaction between AHR and ER [73,261].

In this study, we examined the role of AHR and ARNT on ERα-dependent target gene transcription in the human MCF7 breast cancer and the human ECC-1 endometrial-cervical cancer cell lines. Our data suggest that AHR and ARNT act independently from each other at off-target sites and we revealed that ARNT is not essential for TCDD-dependent repression of ER-signaling. In addition, we have demonstrated that ARNT acts as a cell specific coactivator in MCF7 cells, and as a corepressor in ECC-1 cells. Finally, we show that ARNT knockdown not only affects accumulation of mRNA and protein of ERα-target genes, but also has phenotypic consequences by influencing ERα-mediated cell proliferation.

2.3. Results

2.3.1. AHR-dependent repression of estrogen signaling in ECC-1 cells

The presence of AHR, ARNT and ERα at the dioxin-inducible *CYP1A1* enhancer and the E2-inducible *pS2* promoter has already been documented in MCF7 cells and other breast cancer cell lines [72,73,84,261]. Although preliminary studies have identified ECC-1 human endometrial cells as an ideal system to study dioxin disruption of estrogen signaling [268,269] very little is known concerning the roles of AHR, ARNT and ER and their respective interactions in this cell line. We employed the ChIP assay to ascertain the status of these proteins at the *pS2* promoter and *CYP1A1* enhancer in both the presence and absence of E2 and TCDD. ECC-1 cells were treated with DMSO, 10 nM E2, 2 nM TCDD or a combination of E2 and TCDD for 45 min. After chemically cross-linking protein to DNA with formaldehyde, cells were harvested and sonicated. Sheared DNA-protein complexes were precipitated with antibodies specific to AHR, ARNT or ERα and then isolated complexes were reverse-crosslinked and subjected to PCR amplification. Consistent with other investigators' observations in breast cancer cells, we observed the recruitment of AHR and ARNT on the human *CYP1A1* enhancer in a TCDD-dependent fashion and ERα was greatly enriched only after treatment with a combination of 2 nM TCDD and 10 nM E2 (Figure 2.1A). Furthermore, the recruitment of ERα to the *pS2* promoter occurs in an E2-dependent fashion while AHR and ARNT are

present after either E2 or TCDD treatments but are enriched during ligand co-treatment (Figure 2.1B).

We have previously shown that ERα associates with the AHRC to mediate estradiol-dependent transrepression of dioxin-inducible gene transcription [73]. Therefore, we set out to determine the functional significance of AHR in estrogen-inducible gene transcription. We transfected ECC-1 cells with small inhibitory RNA directed towards either AHR (siAHR) or a GFP negative control (siGFP). After transfection, cells were serum starved for 24 h, ligand treated for an additional 24 h and then harvested for total mRNA which was quantified through quantitative PCR. As expected, ablation of AHR and co-treatment with 2 nM TCDD and 10 nM E2 results in the loss of TCDD-induced repression of *pS2* transcription (Figure 2.1C). However, loss of AHR had no measurable effect on basal, or estrogen activated *pS2* mRNA accumulation. As a control for siRNA specificity, Western blots of AHR protein show a greatly reduced expression of AHR protein after transfection and unchanged protein levels of ERα and XAP2 which served as a loading control (Figure 1E). These demonstrate the specificity of the siRNA's to AHR, and that loss of AHR does not affect accumulation or turnover of basal ERα protein levels. Furthermore, the induction of *CYP1A1* transcription with TCDD after AHR knockdown is attenuated when compared to the siGFP negative control (Figure 2.1D). Thus, AHR is a requirement for TCDD-induced repression of E2-responsive gene transcription and the increased transcriptional response with combinatorial treatment is due solely to the loss of AHR and other putative transcriptional modifiers associated with its presence. Finally, we obtained essentially identical results in both MCF7 and ECC-1 cell lines under serum-starved or charcoal-stripped serum conditions suggesting that differences in the cell lines' ability to go through cell cycle does not impact this phenomenon. Together, these results support the concept that the ECC-1 cell line is an excellent alternative cell model to study dioxin-induced disruption of estrogen receptor signaling.

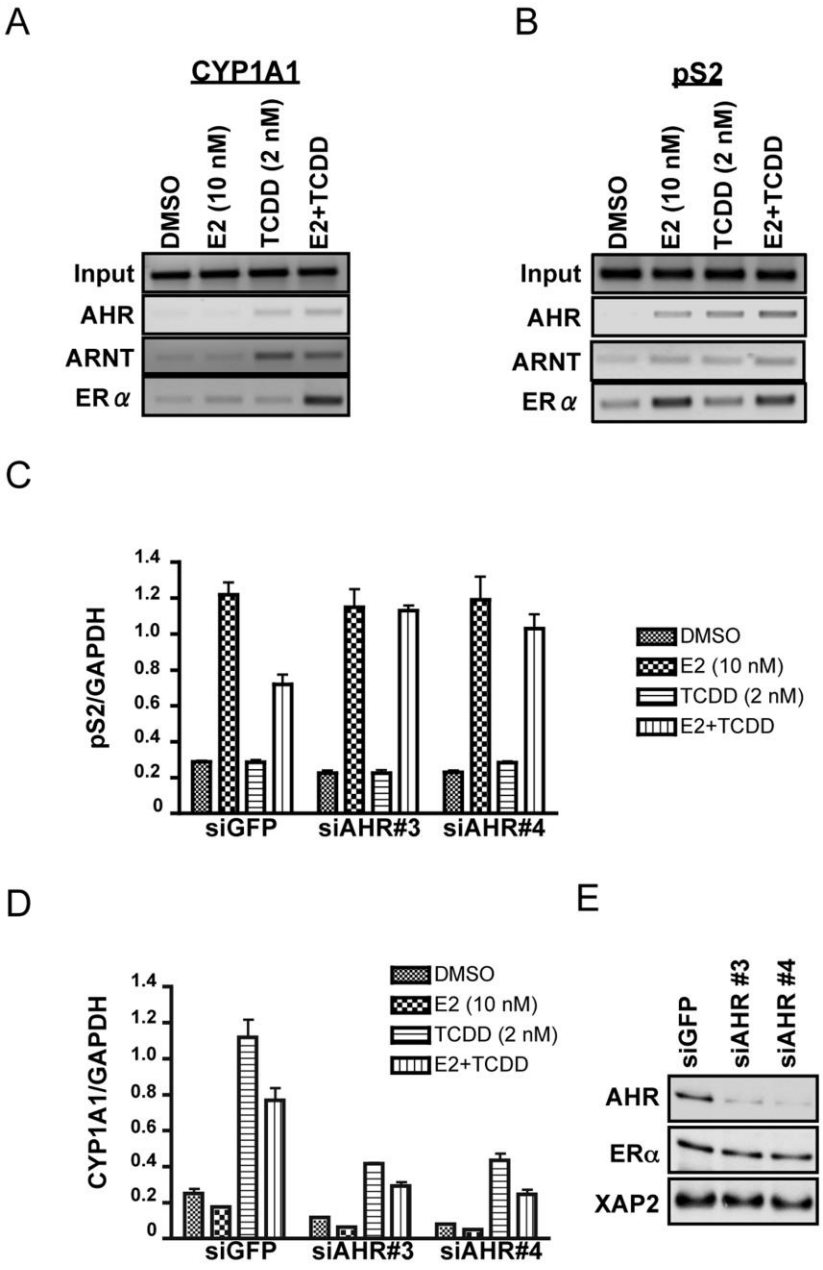

Figure 2.1. AHR is required for TCDD-mediated repression of E2-induced gene transcription.

Chromatin immunoprecipitation assays of the *CYP1A1* enhancer **(A)** and *pS2* promoter **(B)** regions in ECC-1 cells using antibodies targeting AHR, ARNT or ERα. Cells were treated for 45 min with either DMSO, E2 (10 nM), TCDD (2 nM) or a combination of E2 and TCDD. **(C and D)** The functional role of AHR in TCDD-mediated transcription. ECC-1 cells were transfected with siRNAs to either GFP (siGFP) as a negative control or AHR (siAHR#3 or siAHR#4) 24 h prior to ligand treatment, then cells were treated with DMSO, E2 (10 nM), TCDD (2 nM) or a combination of E2 and TCDD. The mRNA levels for *pS2* **(C)** and *CYP1A1* **(D)** were determined through real-time RT-PCR and normalized to constitutively active GAPDH expression. (**E)** ECC-1 cells were transfected with siRNA's to AHR and harvested for whole cell lysates for Western Blot analysis of AHR, ERα and XAP2 protein levels.

2.3.2. ARNT has cell specific coactivator/corepressor functions

The identification of ARNT as a coactivator in estrogen signaling [84,91], juxtaposed with the known transrepressor effects of TCDD, led us to investigate the role played by ARNT in TCDD-mediated transrepression of ER function in various human cancer cell lines, namely MCF7 and ECC-1 cells. Through siRNA directed towards ARNT and a scrambled negative control (siSCX), and subsequent qPCR analysis of endogenous *pS2* and *CAT-D* gene transcription, we made several interesting observations. First, ARNT displays corepressor properties in ECC-1 cells. Accumulation of *pS2* (Figure 2.2A) and *CAT-D* (Figure 2.2B) mRNA levels are exacerbated during E2 treatments after loss of ARNT suggesting a cell specific function for ARNT independent of AHR. Furthermore, we observed this phenomena with three separate siRNAs directed towards ARNT (siRNA's 1 and 3 are shown in Figure 2.1A). We used at least two siRNA's for all other experimental parameters with essentially identical results, but for brevity, hereafter we only present data depicting the use of one siRNA. Secondly, consistent with the findings of several other investigators, ARNT displayed coactivator properties in MCF7 cells [84,91]. Indeed, knockdown of ARNT protein dampens E2-induced transcription of *pS2* (Figure 2.2C) and *CAT-D* (Figure 2.2D). Finally, in a dose response experiment, we observed a concomitant decrease of CAT-D protein levels with increasing concentrations of TCDD in both ECC-1 and MCF7 cells (Figure 2.2E). These data indicate that ARNT function as it relates to ER signaling is likely dictated by other factors specific to the cellular environment.

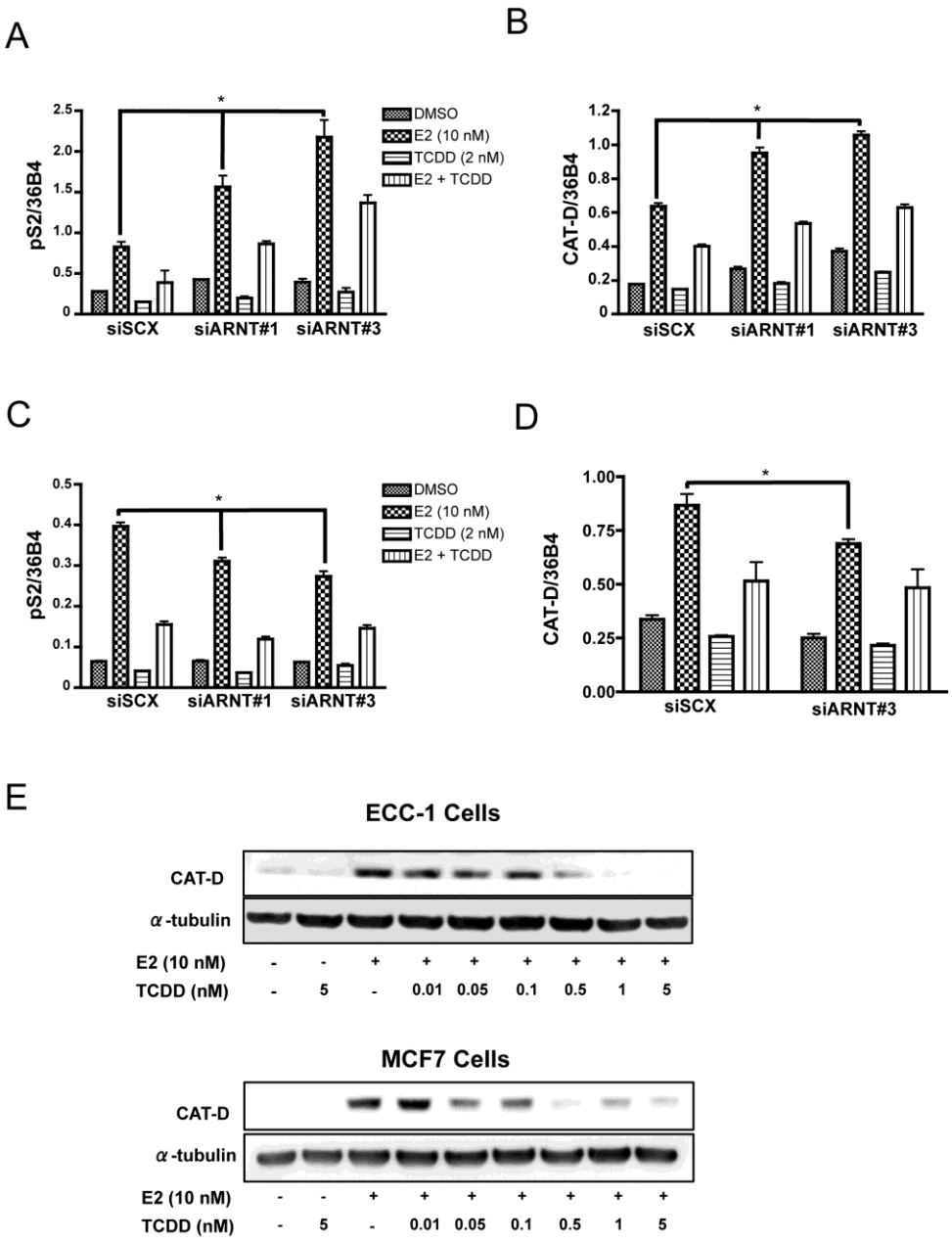

Figure 2.2. Loss of ARNT shows a cell specific coactivator or corepressor transcriptional function.

ECC-1 cells **(A and B)** and MCF7 cells **(C and D)** were transfected with either scrambled siRNA (siSCX) or siRNA directed to ARNT (siARNT#1 or siARNT#3). Twenty-four hours after transfection, cells were treated with vehicle (DMSO), E2 (10 nM), TCDD (2 nM) or a combination of E2 and TCDD. Gene expression was determined by real-time RT-PCR after isolation and reverse transcription of total RNA. *CAT-D* and *pS2* expression was normalized to constitutively active 36B4 gene expression. **(E)** Western blot analysis of CAT-D protein levels in MCF7 and ECC-1 cells. Cells were treated with DMSO or E2 (10 nM) and varying concentrations of TCDD (10 pM, 50 pM, 100pM, 500pM, 1 nM or 5 nM). After 24 hours of treatment, whole cell lysates were harvested, and Western Blot assays were performed using antibodies directed against CAT-D and α-tubulin. Error bars represent ± S.D. * $p < 0.05$.

To determine if the modulation of transcriptional activity translated into similar protein expression profiles, we used Western blot analysis to visualize the level of CAT-D protein after ARNT knockdown. Cells were transfected and ligand treated under identical conditions as the qPCR parameters. When compared to the scrambled negative control, CAT-D protein expression after E2 treatment is blunted in ECC-1 cells with ARNT knockdown (Figure 2.3A). Conversely, MCF7 cells transfected with ARNT siRNA resulted in an exacerbated expression of CAT-D protein during E2 treatment. Furthermore, ERα levels remained consistent, regardless of ARNT status (Figure 2.3C and 2.3D). Most importantly, dioxin-induced repression of ER signaling was maintained at the protein level after ARNT knockdown (Figure 2.3A and C). The representative blots were normalized to α-tubulin and fluorescence was measured using GeneTools 4.01.2 software (Syngene). These normalized values showed a two-fold induction of CAT-D in ECC-1 cells with ARNT knockdown after E2 treatment (Figure 2.3B, Lanes 2 and 6), whereas in MCF7 cells, knock-down of ARNT resulted in a 40% decrease in E2-dependent CAT-D expression (Figure 2.3D, Lanes 2 and 6). These results provide concrete evidence that the level of protein expression mirrors the transcriptional response in both cell lines and that physiological consequences must ensue with loss of ARNT.

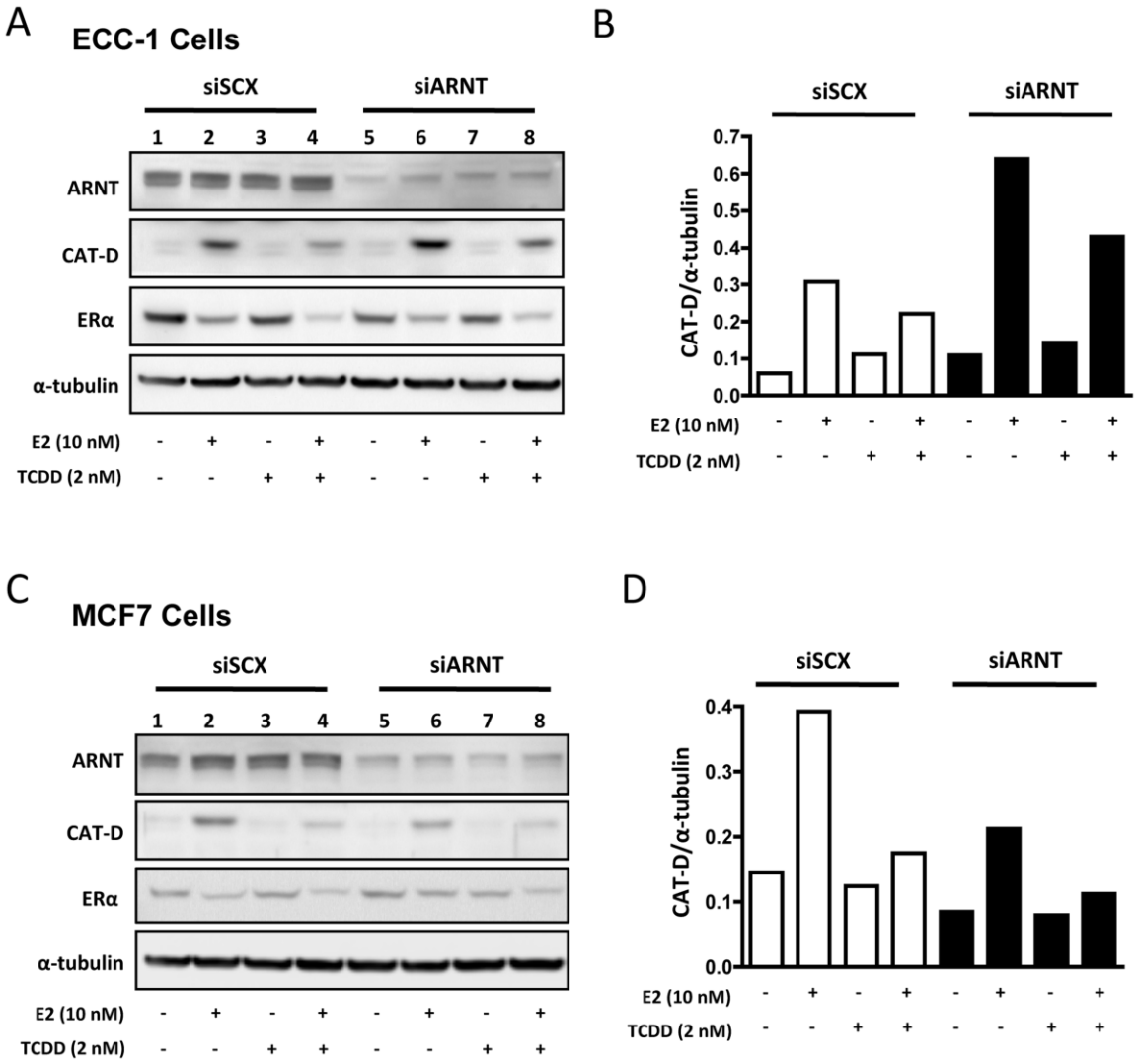

Figure 2.3. Effect of ARNT knockdown on ARNT, CAT-D and ERα protein levels. ECC-1 **(A and B)** and MCF7 **(C and D)** cells were transfected with either siSCX or siARNT and ligand treated as described in Figure 2.2. **(A and C)** Representative Western blots of ARNT, CAT-D, ERα and α-tubulin protein levels. Bar graphs of CAT-D protein levels in ECC-1 **(B)** and MCF7 **(D)** cells after normalizing fluorescence values to α-tubulin. Open bars represent ligand treatments after siRNA to scrambled negative control (siSCX) and closed (black) bars represent ligand treatments after siRNA to ARNT (siARNT). Experiments were performed three times with essentially identical outcomes.

These surprising results were coupled with the observation that TCDD-induced repression of ER-signaling is maintained in both cell lines after ARNT knockdown (Figure 2.2 and 2.3) thus providing evidence that ARNT is not required for TCDD/AHR-dependent repression of ERα signaling. This hypothesis is supported by the ability of a selective aryl hydrocarbon receptor modulator (SAHRM) to repress estrogen signaling.

We examined the ability of the known SAHRM, DiMNF [270,271] to repress E2-mediated transcription by RT-PCR in MCF7 and ECC-1 cells (Figure 2.4). One μM DiMNF was as effective at repressing CAT-D mRNA accumulation as TCDD. DiMNF is a potent antagonist of AHR and effectively displaces TCDD from the receptor at 1 μM [271]. In addition, DiMNF fails to induce AHR-ARNT-dioxin response element formation in an electrophoretic mobility shift assay, suggesting that AHR-ARNT dimerization may not occur [271], thus, it seems likely that AHR's transrepressor function is entirely ARNT-independent.

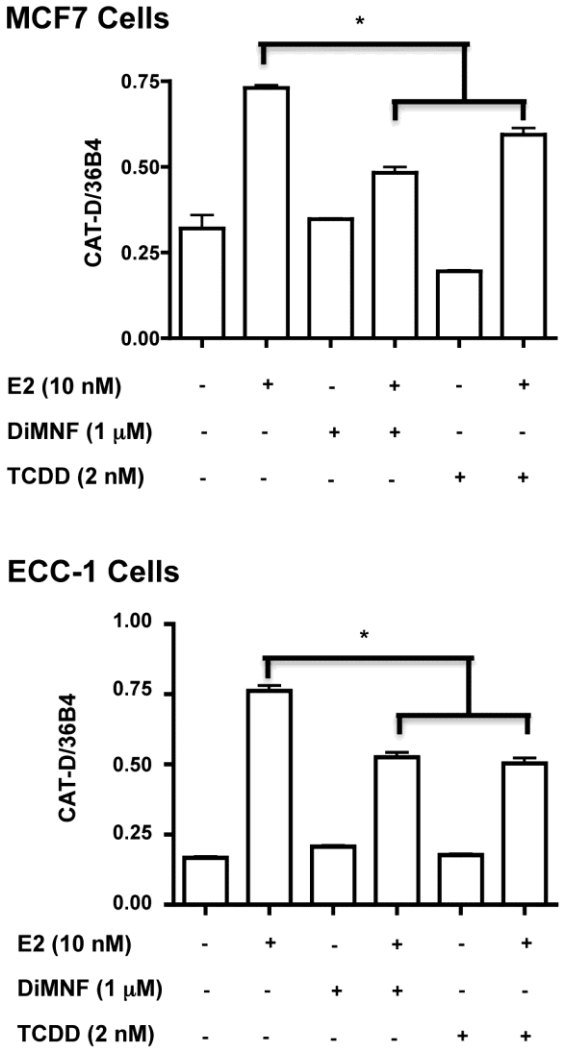

Figure 2.4. Effect of selective aryl hydrocarbon receptor modulators on estrogen-inducible transcription.

The effect of 1 μM DiMNF on E2-inducible CAT-D expression in MCF7 and ECC-1 cells. Cells were treated with the indicated ligands for 24 h prior to RNA isolation. Gene expression was determined as described above. Error bars represent ± S.D. * $p < 0.05$.

2.3.3. ARNT knockdown causes increased proliferation in ECC-1 cells and decreased proliferation in MCF7 cells.

Sensitivity to estrogen has been linked to proliferation and cell transformation in ER-positive carcinoma cells [272]. To establish if ARNT can influence E2-dependent cellular proliferation, we performed proliferation assays on ECC-1 and MCF7 cells after ARNT siRNA treatment. Consistent with our quantitative PCR and Western blot data, ECC1 and MCF7 cells displayed altered rates of proliferation after ARNT knockdown compared to cells transfected with the scrambled negative control siRNA (Figure 2.5A and B). Knockdown of ARNT was monitored for 72 h and the significant knock-down observed was unchanged essentially at each time point (Figure 2.5C). Neither cell line displayed altered growth patterns until the 48 hour time point. At 48 hours, ECC-1 cells in both the siSCX and siARNT conditions showed a modest response to E2 treatments. At the 96 hour time point, there was a highly significant increase in E2-inducible proliferation of ECC-1 cells treated with siARNT, compared to scrambled control treated cells. Intriguingly, ARNT knockdown increased basal growth rates and caused an exacerbated response to E2 with the cell number nearly doubling in the siARNT E2 treatments compared to the siSCX E2 treatments. Conversely, MCF7 cells showed a decreased proliferation rate after ARNT knockdown (Figure 2.5B). The growth rates were not significantly different until the 48 h time point, when the E2-inducible proliferative response in the scrambled negative control was apparent. The siARNT transfected cells had a blunted growth response during both control and E2 conditions. At 96 hours, the cells began losing sensitivity to E2 and entered into a senescent state. Whether or not this was due to the growth conditions is unclear. However, these data further support the hypothesis that ARNT has corepressor properties in ECC-1 cells and coactivator properties in MCF7 cells. Moreover, the sensitivity to E2 and the reciprocal growth responses exhibited by the two cell lines are bona fide phenotypic consequences of ARNT ablation.

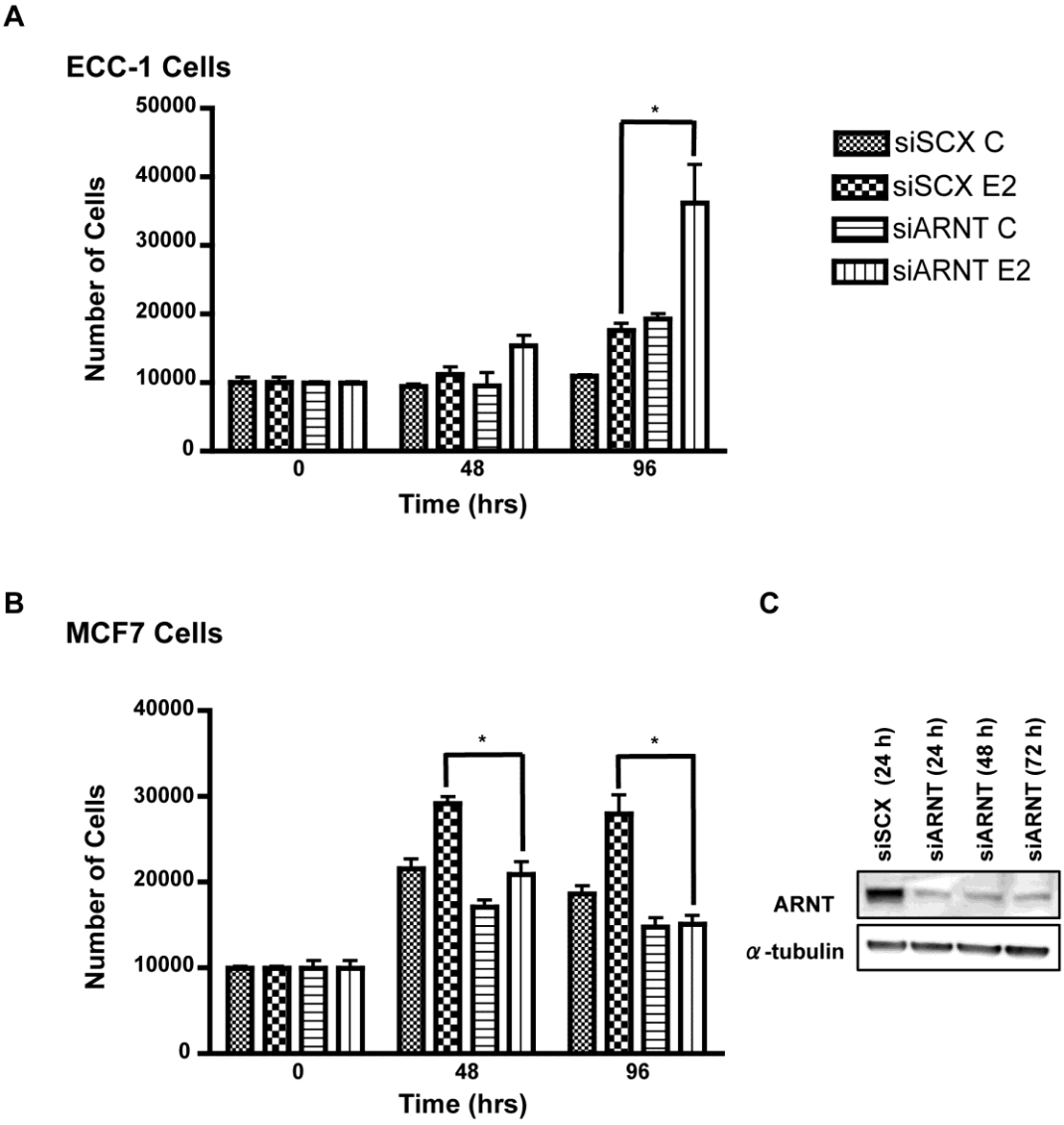

Figure 2.5. Loss of ARNT promotes cell proliferation in ECC-1 cells and attenuates growth in MCF7 cells.

ECC-1 **(A)** and MCF7 **(B)** cells were transfected with either siSCX or siARNT for 6 hours and then trypsinized and reseeded at 10,000 cells/well in 12-well dishes. Twenty-four hours after seeding, cells were treated with either DMSO or E2 (10 nM) and cell counts were conducted at 0, 48 and 96 hours after treatments with a Fuchs-Rosenthal Counting Chamber. At the 48 h time point, cells were treated a second time with 10 nM E2. Experiments were done in triplicate and each trial was counted three times. **(C)** Western blot analysis of ARNT after siRNA knock-down reveals that significant knock-down was achieved and persists over a 72 h period. Error bars represent ± S.D. * $p < 0.05$.

2.4. Discussion

Many environmental contaminants that serve as activators of the aryl hydrocarbon receptor are known as putative endocrine disrupting compounds. Exposure to many of these compounds occur on a daily basis and represents significant risks to human health. In particular, the repressive effects elicited by ligands of the AHR on ER signaling have been well documented [73,261,273-275]. Other reports have described the coactivator potential of ARNT for ER-mediated transcription [91]. Despite the growing body of evidence to support roles for AHR and ARNT in ER function, little is known about the normal physiological role of these proteins as they relate to estrogen signaling or the molecular determinants of toxicant-induced transrepression of ER function by AHR. Finally, this investigation revealed that ARNT is not essential for AHR-mediated off-target transrepression. In order to delineate the molecular mechanisms underlying AHR-mediated transrepression we sought to uncouple AHR and ARNT function in ER-positive human cancer cell lines. In doing so, we discovered that ARNT attenuates activated ER-target gene transcription in ECC-1 cells, in direct contrast to its coactivator function described in MCF7 cells [91].

ARNT was originally identified as a bona fide transcription factor [16] and dimerization partner of AHR [276]. Beyond its canonical transcription factor function, ARNT can interact with several other transcription factors, including ERα [73] and its coactivator function for ER signaling has been well described [84,91]. Therefore, we expected that knockdown of ARNT in ECC-1 endometrial-cervical cancer cells would result in a diminution of ER target gene expression. The resulting increase in mRNA accumulation, protein expression and E2-inducible proliferation strongly suggests that ARNT acts as a transcriptional corepressor in this cell line. The molecular mechanism(s) underlying the differences observed in MCF7 and ECC-1 cells likely is related to differences in the nature and composition of the ancillary transcriptional machinery recruited by ARNT in each cell line. ARNT presents several different protein-protein interaction domains for the recruitment of coactivator proteins, including a carboxy-terminal transactivation domain [42], its PAS-B region [277] and its basic-helix-loop-helix domain [49]. In addition, an association between ARNT and the transcriptional corepressor protein, SMRT has been demonstrated [278]. However, we believe that this

is the first demonstration that ARNT has dual coactivator/corepressor function in a cell-specific fashion (Figure 2.6). In addition, the repercussions of these transcriptional effects can be observed at the translational and phenotypic levels.

Several models have been hypothesized to explain the molecular mechanisms underlying transcription factor mediated cross-talk, particularly the ability of one transcription factor to repress another's function [42]. Reugg and colleagues, among others, have suggested that transcription factor-mediated transrepression might be the result of competition for a limited pool of coactivator proteins [91]. However, the identification of ARNT as a corepressor in ECC-1 cells unmasks a more complex mechanism of transrepression at E2-inducible genes than the coactivator competition model suggests. While these data do not definitively disprove this model, we believe that our data suggest that it is unlikely because coactivator competition cannot account for TCDD-inducible repression in ECC-1 cells as activated AHR should squelch ARNT's corepressor function. In addition, ARNT, a protein that has demonstrated the ability to recruit numerous coactivators [49,150,155,259,277,279] should elicit an effect similar to ligand-activated AHR if coactivator pools were in such limited supply that competition would hinder individual transcription factor function. This clearly is not the case in the ECC-1 cell line.

The experimental evidence presented above indicates that AHR does not require ARNT to mediate its off-target transrepressor effects. Loss of ARNT in both MCF7 and ECC-1 cells failed to abrogate the repressive effects of TCDD on E2-inducible transcription and protein expression (Figures 2.2 and 2.3). DRE-binding independency for the effects of DiMNF-bound AHR has been clearly established as DiMNF does not retard the movement of a labeled dioxin response element probe in gel shift assays [271]. Furthermore, AHR-ARNT dimerization is a requirement for DNA binding, suggesting that this may not occur in the presence of DiMNF. This represents a paradigm shift in our understanding of AHR function and has implications for the use and effectiveness of selective AHR modulators. Indeed, a novel AHR antagonist has proven to be a potent promoter of AHR-dependent stem cell expansion [280]. Thus, antagonists that do not elicit AHR-ARNT dimerization might be more effective repressors of ER function than pure agonists as AHR would not be squelched by ARNT binding. The

SARHM DiMNF is a potent AHR-dependent repressor of cytokine signaling [270,271]. Furthermore, DiMNF was effective in repressing ER-regulated target gene expression (Figure 2.4). Molecular modelling studies suggest that DiMNF forms an extra hydrogen bond with AHR at Thr289 [271], a characteristic not shared with the partial agonist α-naphthoflavone suggesting that the DiMNF-AHR adopts a unique confirmation. Thus, the flavonoids represent a class of compounds that may be attractive targets for further testing and development to determine their effects on ER target gene expression.

Our experimental evidence demonstrates a TCDD-dependent repressor function for AHR and a TCDD/AHR-independent coactivator/corepressor function for ARNT in estrogen signaling. These results provide us with further insight into the mechanisms of transcription factor crosstalk and putative therapeutic targets in estrogen-positive cancers. Taken together, our data suggest a more complex mechanism of ARNT function and AHR-mediated transrepression of ER-signaling than previously suggested. The clinical utility of these findings remains to be tested and will be the subject of future investigations.

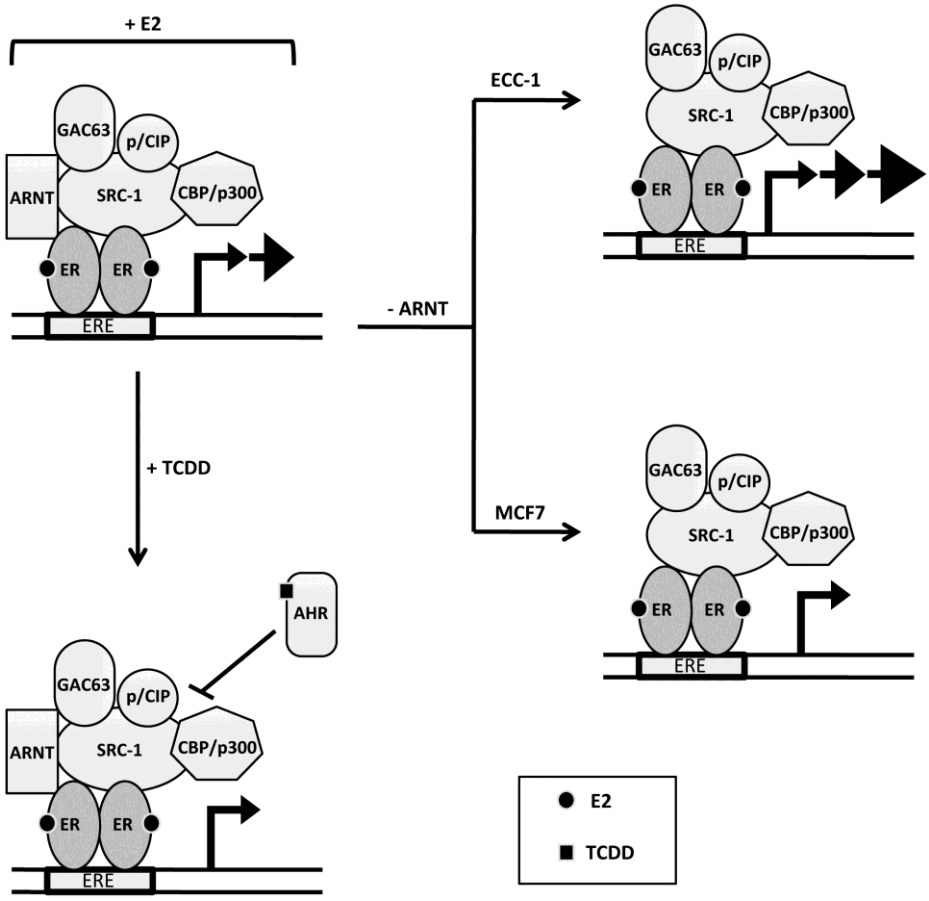

Figure 2.6. A schematic representation of estrogen signaling, describing the transcriptional functions of ER, AHR and ARNT in ECC-1 and MCF7 cells.

The presence of E2 facilitates the assembly of transcriptional modifiers that induce transcription of E2-responsive genes. Ligand activated AHR represses ER-signaling independent of ARNT. The loss of ARNT in ECC-1 cells, where it acts as a corepressor, leads to increased sensitivity to E2 and increased transcriptional activity at ER regulated genes. The loss of ARNT in MCF7 cells, where it acts as a coactivator, leads to decreased sensitivity to E2 and decreases transcriptional activity at ER regulated genes.

2.5. Materials and Methods

2.5.1. Materials and Cell Culture

3',4'-dimethoxy-α-naphthoflavone (DiMNF) was obtained commercially (Indofine Chemical Co., Hillsborough, NJ). ECC-1 and MCF7 cells (ATCC) were maintained in Dulbecco's Modified Eagle's Medium (DMEM; BioWhittaker, Lonza,) with 10% fetal bovine serum (FBS; HyClone, PerBio, Thermo Fisher Scientific Inc.) and supplemented

with 100 units/ml potassium penicillin-100 µg/ml streptomycin sulphate (BioWhittaker, Lonza) at 37ºC, 20% O_2, and 5% CO_2. Twenty-four h before any experimental perturbation, cells were washed 2x with PBS, and maintained in Phenol-Red-free media without FBS [88].

2.5.2. Chromatin immunoprecipitation assays

Chromatin immunoprecipitation (ChIP) assays were performed as described previously [150]. Briefly, cells were plated into 150 cm^2 dishes and serum-starved 24 h before treatment. Treatment of cells was done in serum-free media supplemented with 3 mg/mL bovine serum albumin for 45 min. Chromatin complexes were chemically cross-linked using a 1% formaldehyde/0.7 mol/L HEPES solution (final concentration), and complexes were sonicated to yield DNA fragments of 200 to 900 bp size. Complexes were precleared with protein A agarose resin (CalBiochem) and incubated overnight with specific antibodies [ERα rabbit polyclonal or ARNT goat polyclonal (Santa Cruz) or AHR rabbit polyclonal described previously [281]]. Immunoadsorbed complexes were captured on protein A agarose resin and washed twice with 0.5X RIPA, followed by three washes with 10 mmol/L Tris-HCl (pH 8.0) and 0.5 mol/L EDTA. Samples were eluted off of the resin using 100 mmol/L NaHCO3 and 1% SDS, and cross-links were reversed at 65°C overnight. Immuno-adsorbed DNA was analyzed by PCR. Primers for the *CYP1A1* enhancer and pS2 promoter have been described previously [72,282].

2.5.3. Transient transfections

MCF7 and ECC-1 cells were cultured in the conditions described above until approximately 70% confluent before siRNA transfection. Cells were transfected with either Green Fluorescence Protein (GFP) siRNA (Dharmacon), scrambled (SCX) siRNA (DS Scrambled negative control siRNA, Integrated DNA Technologies Inc.), AHR siRNAs (Dharmacon) or ARNT siRNAs (Integrated DNA Technologies Inc., Cat. No. HSC.RNAI.N187426.11.1, HSC.RNAI.N178426.11.2, HSC.RNAI.N178426.11.3; siARNT 1, siARNT 2, and siARNT 3 respectively). Cells were transfected with 10 – 15 nM siRNA using 0.3% (v/v) Trifectin (Integrated DNA Technologies) according to manufacturer's protocol. The cells were allowed to incubate in transfection mix for 6 h at 37°C, and 5%

CO_2 after which the transfection mix was removed and replaced with serum free medium.

2.5.4. Reverse transcription and Real-Time PCR

Reverse transcription and real-time PCR were performed as described previously [73]. In brief, cells were treated either with DMSO (Me_2SO), TCDD (2 nM), E2 (10 nM), or a combination of TCDD and E2, for 24 h. For studies involving the selective AHR modulator 1 μM 3',4'-dimethoxy-α-naphthoflavone (DiMNF) with either DMSO, E2 (10 nM), diMNF (1 μM) or E2 and diMNF in combination. Cells were harvested in TRI Reagent (Sigma) and total RNA was isolated and subjected to reverse transcription using a High Capacity cDNA Archive kit (Applied Biosystems). Complimentary DNA was amplified by real-time PCR using a Power SYBR Green PCR kit (Applied Biosystems) according to manufacturer's protocols. Oligonucleotide pairs used to amplify human cDNA sequences were described previously [73]. DNA was amplified for 45 cycles in a StepOne Plus Real-Time PCR System (Applied Biosystems). Oligonucleotides for amplification of CYP1A1 enhancer chromatin isolated using the ChIP assay were identical to those reported by Hestermann and Brown [282].

2.5.5. Western blot analysis

In order to determine the effects of TCDD on E2-inducible protein levels, MCF7 and ECC-1 cells were treated either with vehicle (Me_2SO), TCDD (2 nM), E2 (10 nM), or a combination of TCDD and E2 for 24 h. For protein analysis that included siRNA treatment, cells were transfected for 6 h and then starved in serum free media for 24 h prior to ligand treatments. Cells were harvested and the protein concentration estimated by the RC DC protein assay (Bio-Rad). Equal amounts of proteins from the samples were resolved on a SDS-acrylamide gel then transferred to polyvinylidene fluoride (PVDF) membrane. Upon completion of transfer, the membrane was wetted with 100% methanol then probed with anti-ARNT (goat polyclonal IgG; Santa Cruz Biotechnology, Inc.), anti-AHR (rabbit polyclonal, Biomol, GmbH), anti-CAT-D (rabbit polyclonal IgG; Santa Cruz Biotechnology, Inc.), anti-ERα (rabbit polyclonal IgG; Santa Cruz Biotechnology, Inc.), anti-α-tubulin (mouse monoclonal IgG; Santa Cruz Biotechnology,

Inc.). or anti-XAP2 mouse monoclonal antibody. The detection was performed using horseradish peroxidase conjugated anti-mouse or anti-rabbit or anti-goat IgG and ECL detection kit (GE Healthcare).

2.5.6. Proliferation Assay

MCF7 cells and ECC-1 cells at 75-80% confluency were transfected with either ARNT or scrambled negative control siRNA. After 6 h, cells were washed 2 times with PBS, trypsinized and seeded into 12-well plates at 10,000 cells/well in DMEM with 2.5% charcoal-stripped FBS. Twenty-four hours after plating, E2 was added directly to half the wells to a final concentration of 10 nM. Cells were counted at; 0 (control), 12, 24, 48 and 96 h following E2 administration. A second treatment of E2 (10 nM) was added to the cells at 48 hrs. Determinations were performed in triplicate and each sample was counted three times.

2.5.7. Statistical analysis

Statistical analyses were performed using GraphPad Prism 4.0. For multiple comparisons (i.e. siRNA experiments) statistical significance was determined using a 2-way ANOVA with Tukey's Multiple Comparison test. Values are presented as means +/- standard error of the mean (SEM). A P value < 0.05 was considered to be significant.

Chapter 3. A TRIP230-retinoblastoma protein complex regulates hypoxia-inducible factor-1α-mediated transcription.

Published in PLoS ONE June 11, 2014, DOI: 10.1371/journal.pone.0099214

Authors: Mark P. Labrecque, Mandeep K. Takhar, Julienne M. Jagdeo, Kevin J. Tam, Christina Chiu, Te-Yu Wang, Gratien G. Prefontaine, Michael E. Cox, Timothy V. Beischlag

Author Contributions: I performed all siRNA treatments and obtained qPCR results represented in Figure 3.1. I performed all immunoblots represented in Figure 3.2. Timothy Beischlag and I performed the chromatin immunoprecipitation (ChIP) assays represented in Figures 3.2B and F and Timothy Beischlag performed the ChIPs and ChIP-re-ChIPs performed in Figures 3.2D, E and H. I performed the siRNA treatments and immunoblots represented in Figure 3.3B and D. Timothy Beischlag conducted the qPCR experiments shown in Figures 3.3A and C. Mandeep Takhar conducted the siRNA treatments and immunoblot represented in Figure 3.3E. Julienne Jagdeo performed the siRNA treatments and immunoblots represented in the top panels of Figure 3.4A and I performed the rest of the immunoblots shown in Figure 3.4 (bottom panels of A and all of B). I performed all Matrigel invasion assays represented in Figure 3.5. Christina Chiu performed the proliferation assay represented in Figure 3.5C. Kevin Tam performed the cell sorting and analysis of cell cycle represented in Figure 3.5D and E. Timothy Beischlag performed the GST-assays and co-immunoprecipitation assays represented in Figure 3.6. Te-Yu Wang performed the reporter assays shown in Figure 3.6. Timothy Beischlag, Gratien Prefontaine and Michael Cox helped conceive and design the experiments. Timothy Beischlag and I wrote the draft of the manuscript and Timothy Beischlag, Michael Cox and I wrote the final published manuscript.

3.1. Abstract

Localized hypoxia in solid tumours activates transcriptional programs that promote the metastatic transformation of cells. Like hypoxia-inducible hyper-vascularization, loss of the retinoblastoma protein (Rb) is a trait common to advanced stages of tumour progression in many metastatic cancers. However, no link between the role of Rb and hypoxia-driven metastatic processes has been established. We demonstrated that Rb is a key mediator of the hypoxic response mediated by HIF1α/β, the master regulator of the hypoxia response, and its essential coactivator, the thyroid hormone receptor/retinoblastoma-interacting protein (TRIP230). Furthermore, loss of Rb unmasks the full coactivation potential of TRIP230. Using small inhibitory RNA approaches *in vivo*, we established that Rb attenuates the normal physiological response to hypoxia by HIF1α. Notably, loss of Rb results in hypoxia-dependent biochemical changes that promote acquisition of an invasive phenotype in MCF7 breast cancer cells. In addition, Rb is present in HIF1α-ARNT/HIF1β transcriptional complexes associated with TRIP230 as determined by co-immunoprecipitation, GST-pulldown and ChIP assays. These results demonstrate that Rb is a negative modulator of hypoxia-regulated transcription by virtue of its direct effects on the HIF1 complex. This work represents the first link between the functional ablation of Rb in tumour cells and HIF1α-dependent transcriptional activation and invasion.

3.2. Introduction

Hypoxia inducible factor-1α (HIF1α), its orthologue HIF2α, and their dimerization partner the aryl hydrocarbon receptor nuclear translocator, (ARNT or HIF1β) which make up the HIF1 complex [126,283] regulates a cell's response to conditions of low oxygen. In healthy tissue, the HIF1 complex directs the ordered and tightly regulated expression of genes controlling the *de novo* synthesis of new vasculature to support tissue growth or tissue re-perfusion. During hypoxia, HIF1α accumulates, translocates to the nucleus, and binds ARNT. The HIF1 complex recruits coactivators including CBP/p300 [279], and Brm/Brg-1[284] and activates the expression of genes, such as vascular endothelial growth factor (VEGF), erythropoietin (EPO) and the metastatic markers, CXCR4 and

procollagen lysyl hydroxylase 2 (PLOD2) [126,285,286]. Evidence suggests that the HIF1 complex can activate gene expression independently or in concert with other transcription factors [287,288]. Demonstration that HIF1α is capable of interacting with c-Myc, Notch and more recently FOXA2 to direct ordered transcription and enhance tumour formation [289-291] leaves open the possibility that the HIF1 complex is a core transcriptional unit that modulates multiple intracellular signaling networks, many of which may be involved in metastatic transformation. Thus, many of the molecules that control different aspects of HIF1 function have yet to be identified.

The HIF1 complex carries out this function by recruiting transcriptional coactivator proteins including the thyroid hormone receptor/retinoblastoma protein-interacting protein-230 (TRIP230) to the regulatory regions of hypoxia-responsive genes to activate transcription [150]. TRIP230, was initially identified as a thyroid hormone receptor (TR)-interacting protein that enhanced TRs activity [292]. In addition, TRIP230 has been isolated as part of the p160 coactivator complex [293], a bona fide ARNT coactivator complex [49]. Importantly, we have demonstrated that TRIP230 is recruited by ARNT as a transcriptional coactivator and it is essential for the transcriptional activity of the HIF1 complex [150]. Furthermore, it was shown that TRIP230 interacts with Rb and that Rb attenuates TRIP230-enhanced TR-driven transcription [149]. A subsequent study demonstrated that only the hyper-phosphorylated form of Rb interacts with TRIP230 [153] highlighting a function for Rb distinct from its canonical E2F-dependent regulation of cell cycle, specific to its hypo-phosphorylated form.

Loss of *RB1*, the gene that codes for Rb [156], and or loss-of-function of Rb is associated with the development and metastatic progression of many other solid tumours including cancers of the ovary, lung, breast, prostate and brain [202,205,294-296]. The best understood function of Rb is that of cell cycle regulator repressing E2F transcription factor function thereby mediating cell proliferation and differentiation [297]. Hypo-phosphorylated Rb blocks cell cycle progression by binding to E2F transcription factors and effecting E2F-dependent transcriptional outcomes. It does so by recruiting chromatin-remodeling transcriptional repressor proteins such as Sin3a/b, HDACs, SUV39H1 and DNMT1 [298-300]. Hyper-phosphorylated Rb fails to repress E2Fs and allows them to activate or repress various gene expression programs [297].

Recent studies suggest that Rb may have physiologic roles in addition to its canonical E2F function [301]. Previously, we demonstrated a direct interaction between TRIP230 and ARNT [150]. In addition, we demonstrated that TRIP230 was indispensable for transcription mediated by two distinct dimerization partners of ARNT, namely the aryl hydrocarbon receptor and HIF1α [150]. In this report, we provide the first evidence for the existence an Rb-TRIP230-ARNT complex that mediates HIF1 transcription. In addition, we demonstrate that Rb attenuates the activity of ARNT transcriptional complexes by virtue of its association with TRIP230 and independent of E2F. Ultimately, this work reveals the ability of Rb to modulate HIF1-activated gene expression with consequences for cancer cell transformation.

3.3. Results

3.3.1. HIF1-regulated gene expression is enhanced by siRNA knock-down of Rb

TRIP230 is known to bind directly to TR and ARNT [149,150]. Given that hyper-phosphorylated-Rb represses TRIP230 coactivated TR activity [153] and that TRIP230 expression is required for transcriptional activity of the ARNT partners, AHR and HIF1α [150], we hypothesized that Rb might attenuate hypoxia-inducible gene transcription. In order to examine the role of Rb on the accumulation of hypoxia-inducible target gene mRNA species, we depleted Rb in human cancer cell lines by siRNA-mediated gene *knock-down*. MCF7 and LNCaP cells were transfected with either scrambled (SCX) control siRNA or two Rb-specific siRNAs and mRNA accumulation of HIF1 target genes exposed to normoxia and hypoxia were compared (Figure 3.1). Rb RNA and protein levels were equivalently suppressed under both normoxic and hypoxic conditions (Figures 3.1A, E and 3.3A). No change was observed in CXCR4 or VEGF expression in Rb siRNA transfected cells under normoxic conditions, however an increase in PLOD2 mRNA accumulation under normoxic conditions was observed in MCF7 cells (Figure 3.1D) but not in LNCaP cells (Figure 3.1E). In addition, MCF7 cells transfected with the Rb-specific siRNAs exhibited significantly increased mRNA accumulation of the HIF1 target genes CXCR4, VEGF and PLOD2 under hypoxic conditions (Figure 3.1B-D). A similar hypoxia-dependent effect on, CXCR4, VEGF and PLOD2 induction was observed

in response to suppressed Rb expression in LNCaP prostate cancer cells (Figure 3.1E) suggesting that this observation is not cell type specific.

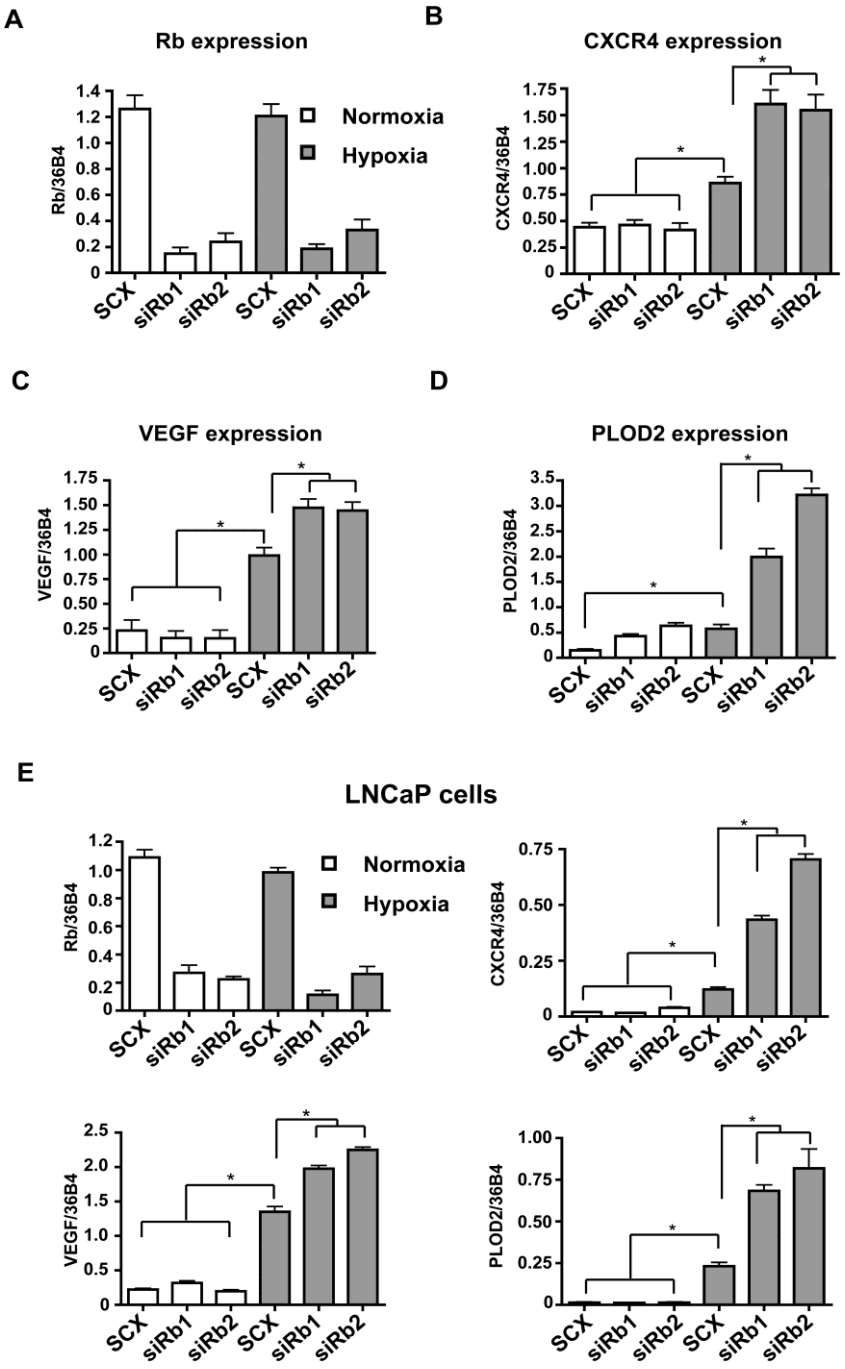

Figure 3.1. Rb represses HIF1-regulated target gene mRNA in MCF7 human breast cancer cells and LNCaP human prostate cancer cells.

MCF7 cells **(A,B, C and D)** and LNCaP cells **(E)** were transfected with either scrambled siRNA (SCX) or Rb siRNAs siRb 1, and siRb 2. Twenty-four hours after transfection cells were either maintained under normoxic conditions or 1% O_2 for a further 24h. Gene expression was determined by quantitative real-time PCR after isolation and reverse transcription of total RNA. VEGF, CXCR4, PLOD2 and Rb expression were normalized to constitutively active 36B4 gene expression. Open bars represent normoxia (20% O_2) and closed (grey) bars represent hypoxia (1% O_2). Error bars represent ± S.D. * $p < 0.05$.

3.3.2. Rb and Rb-associated repressor proteins are recruited to the regulatory regions of hypoxia inducible genes during activated transcription.

We observed that loss of Rb resulted in exaggerated expression of HIF1 target genes in a hypoxia-dependent fashion. Thus, we were interested to determine if the presence of Rb could be recorded over the regulatory regions HIF1-regulated genes harboring well characterized hypoxia response elements during activated transcription; namely the VEGF promoter and EPO enhancer. A schematic of these regions and the placement of oligonucleotides for PCR amplification of chromatin are depicted in Figure 3.2A. Chromatin immunoprecipitation (ChIP) analysis revealed that Rb associates with regulatory regions of the HIF1-regulated genes, VEGF and EPO in a hypoxia-dependent fashion in MCF7 cells (Figure 3.2B). To ensure that our experimental conditions produced the appropriate response to hypoxia, we also precipitated chromatin with antibodies to HIF1α, ARNT, TRIP230 or a control rabbit IgG. Control IgG was incapable of precipitating chromatin containing the VEGF and EPO regulatory regions. As we have demonstrated previously [150], we were more readily able to amplify chromatin precipitated from hypoxia treated lysates than from those derived from lysates maintained under normoxic conditions using the HIF1α, ARNT, TRIP230 and Rb antibodies. We could amplify low levels of the VEGF promoter and EPO enhancer under normoxic conditions (Figure 3.2B) when precipitating chromatin with our TRIP230 antibody, therefore, we cannot discount the possibility that TRIP230 associates with HREs at low levels despite normal oxygen tension. However, our inability to detect HIF1α or HIF2α under these conditions (Figure 3.2C) suggests the possibility that Rb is not recruited to these HRE regions under normoxic conditions.

We expanded our investigations in an attempt to determine if TRIP230 and Rb have the ability to interact with individual DNA elements in concert with HIF1α and ARNT at hypoxic response elements. We performed a sequential two-step ChIP assay, first isolating chromatin with affinity-purified antibodies to ARNT or HIF1α followed by precipitation of these purified chromatin fractions with antibodies to TRIP230 and Rb. In each case VEGF promoter DNA was amplified by PCR in a hypoxia-dependent fashion (Figure 3.2D and E) strongly suggesting that HIF1α, ARNT, TRIP230 and Rb are

present at HREs in a multi-protein complex. In addition, knockdown of Rb as assessed by immuno-blot (Figure 3.2G), did not result in further enrichment of TRIP230 at the VEGF promoter (Figure 3.2F) suggesting that Rb does not interfere with TRIP230 recruitment to HIF1 responsive elements.

Finally, we were interested to see if known Rb-associated repressor complexes [299,300] were present at these elements during hypoxia-driven transcription. ChIP analysis revealed the Sin3a/b, HDAC1 and HDAC3 were enriched at the HIF-responsive regulatory regions of both the VEGF and EPO genes under hypoxic conditions (Figure 3.2H) supporting our hypothesis that Rb is part of transcriptional repressor complex acting on HIF1-regulated transcription. In contrast, HDAC2 behaved in a more canonical fashion and was dismissed from these regions in a hypoxia-dependent fashion (Figure 3.2H). These data suggest that transcriptional repressor proteins are recruited to hypoxia-regulated genes during activated transcription. Furthermore, these observations support the hypothesis that transcription must be attenuated to ensure the appropriate transcriptional response.

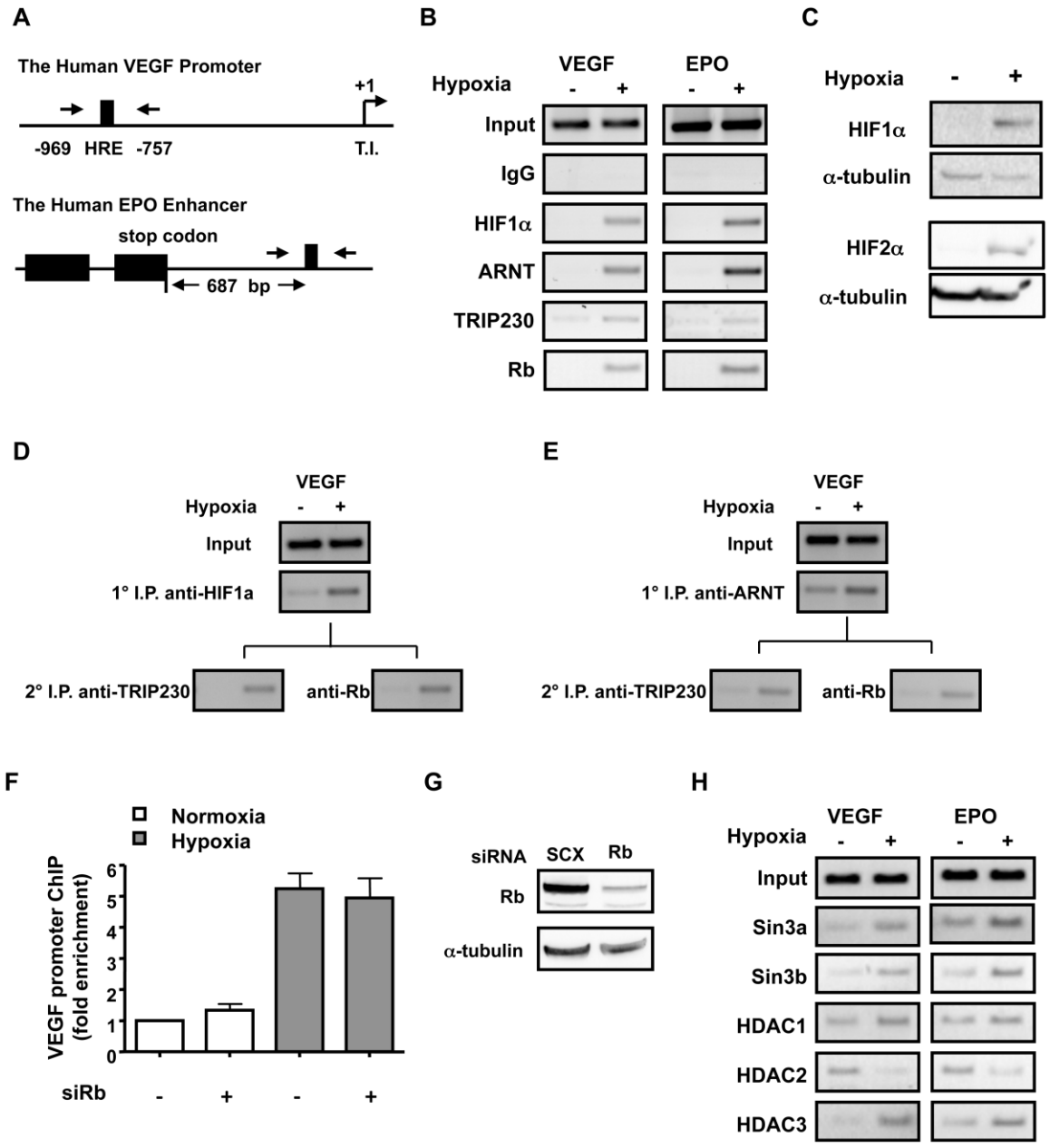

Figure 3.2. **HIF1α, ARNT, TRIP230, Rb and Rb-associated repressor proteins occupy hypoxia responsive regulatory regions of HIF1-regulated genes in a hypoxia-dependent fashion.**

(A) A schematic of the VEGF proximal promoter and EPO enhancer and the relative location of oligonucleotides used for PCR amplification. **(B)** The status of HIF1α, ARNT, TRIP230, and Rb at the VEGF promoter and EPO enhancer in MCF7 cells as assayed by chromatin-immuno-precipitation (ChIP) and polymerase chain reaction (PCR) and compared to amplification reactions derived from lysates precipitated with control IgG. All ChIPs were performed at least three times except where indicated. **(C)** HIF1α and HIF2α protein levels are dramatically enriched during hypoxia in MCF7 cells. MCF7 cells were maintained in culture in either 20% or 1% O_2 for 24 h. Nuclear extracts were analyzed by immuno-blot and membranes were probed with affinity-purified antibodies to HIF1α and α-tubulin. Sequential ChIP of the proximal VEGF promoter and EPO enhancer using either anti-HIF1α **(D)** or anti-ARNT **(E)** affinity purified antibodies followed by immuno-precipitation with anti-TRIP230 and anti-Rb antibodies. **(F)** ChIP of the VEGF promoter after in MCF7 cells after transfection with either scrambled siRNA or siRb1 and immuno-precipitation with anti-TRIP230 antibody. Values are expressed as fold enrichment over control and were determined by quantitative real-time PCR. Each experimental value was corrected for input and experiments were performed twice. **(G)** Immuno-blot analysis of siRNA-transfected MCF7 cell lysates used in ChIP experiments. **(H)** ChIP of Rb-repressor complex proteins in MCF7 cells. Cells were treated as described above and chromatin complexes were isolated with affinity-purified antibodies directed to Sin3a, Sin3b, and HDACs 1-3.

3.3.3. ARNT and TRIP230 are essential for Rb-regulation of HIF1 activity.

Since Rb and TRIP230 are interacting proteins, the quantitative RT-PCR experiments were repeated using a siRNA directed to TRIP230. Hypoxic gene induction of CXCR4 mRNA accumulation was severely impaired upon knock-down of TRIP230 (Figure 3.3A and B). Knock-down of Rb under these conditions, as evidenced by immuno-blot analysis (Figure 3.3B) did not result in any significant increase in CXCR4 mRNA, providing further evidence that this effect is TRIP230-dependent. Images of whole immuno-blots can be found in Supplemental Figure S1. Furthermore, loss of Rb did not lead to an increase in CXCR4 mRNA accumulation in cells ablated for ARNT by siRNA-mediated knock-down further suggesting that the effect mediated by Rb is hypoxia-dependent (Figure 3.3C and D). In addition, siRNA-mediated suppression of DP1 expression in MCF7 cells responded to hypoxia as readily as control cells (Figure 3.3C and E) indicating that the modulatory function of Rb on HIF-regulated genes is independent of E2F and uncoupled from Rb's canonical role as a cell cycle mediator.

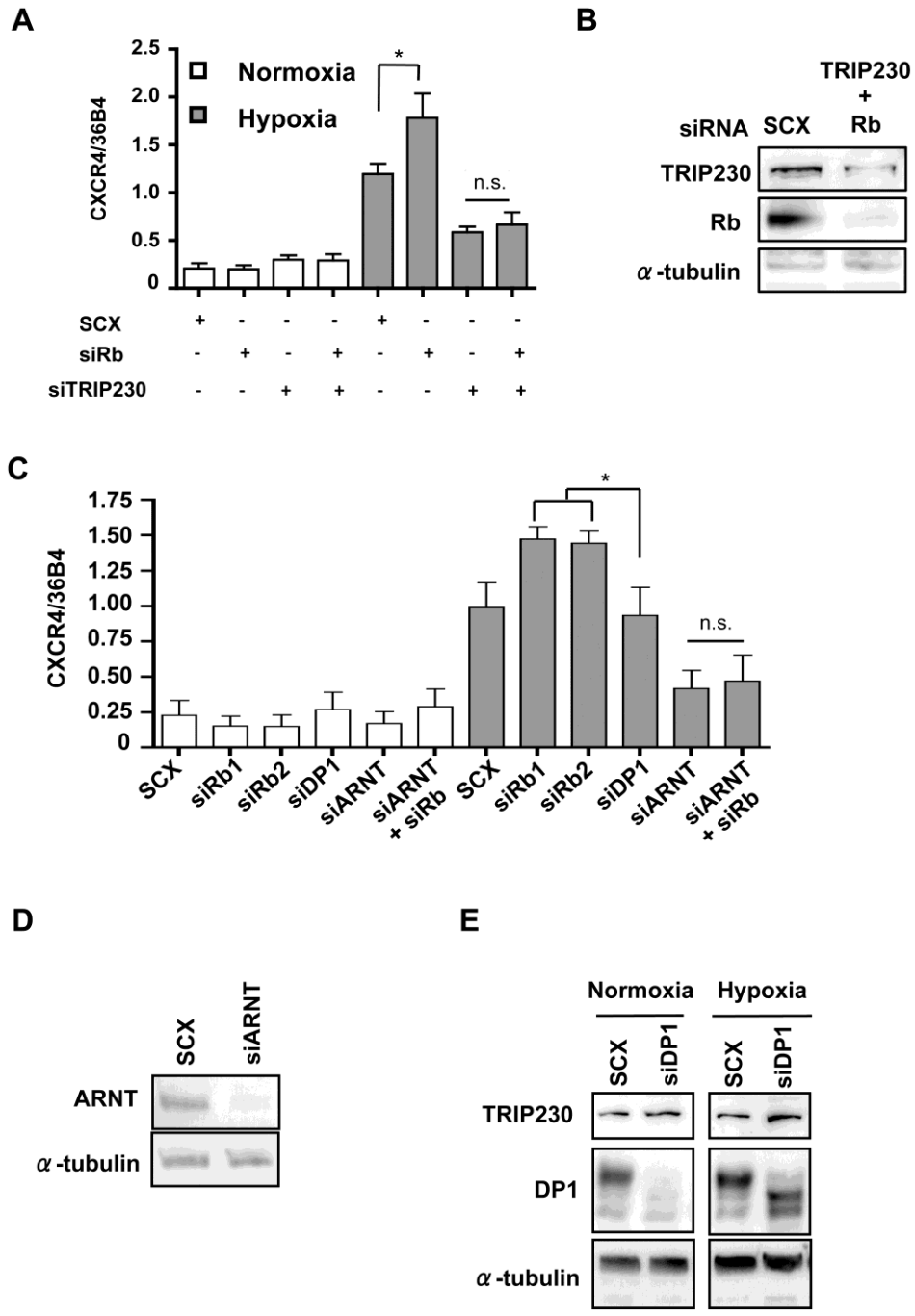

Figure 3.3. ARNT and TRIP230 are essential for Rb-regulation of HIF1.

(**A**) MCF7 cells were transfected with either scrambled siRNA (SCX) or Rb siRNAs siRb 1, and siRb 2, or a combination of TRIP230 siRNA and siRb1. Twenty-four hours after transfection cells were either maintained under normoxic conditions or 1% O_2 for a further 24h. Gene expression was determined by quantitative real-time PCR after isolation and reverse transcription of total RNA. CXCR4 expression was normalized to constitutively active 36B4 gene expression. **(B)** Immunoblot analysis of TRIP230 and Rb after siRNA transfection with either scrambled siRNA, or a combination of siTRIP230 and siRb. Alpha-tubulin (α-tubulin) was used as a loading control. (**C**) MCF7 cells were transfected with either scrambled siRNA (SCX) or Rb siRNAs siRb 1, and siRb 2, or ARNT, or DP1 siRNA or a combination of ARNT/Rb1 siRNA and treated as described above. (**D**) Immuno-blot of ARNT and α-tubulin after transfection with either scrambled control of siRNA directed to ARNT. (**E)** Immuno-blot of DP1, TRIP230 and α-tubulin. MCF7 cells were transfected with either scrambled control (SCX) or siRNA directed to DP1. Data in figure 3A and 3C were analyzed using a two-way-ANOVA. *$p < 0.01$.

3.3.4. Loss of Rb leads to an increase in HIF1 target gene protein expression.

We were interested to determine if the effect of Rb-loss on mRNA accumulation was reflected at the protein level of HIF1 target genes and, in particular if pro-metastatic factors were affected. Thus, we also examined the role of Rb in the expression of downstream metastatic markers that are sensitive to hypoxia. Loss of Rb resulted in a concomitant increase in CXCR4 protein levels after 48 h of hypoxia and PLOD2 after 96 h of hypoxia (Figure 3.4A). Furthermore, a 24 h exposure to hypoxia with Rb knock-down also resulted in an increase in the expression of the mesenchymal marker, vimentin (Supplemental Figure S2A). In addition, loss of Rb did not increase endogenous levels of HIF1α (Figure 3.4A), suggesting that the observed hypoxic effect was not due to an increase in HIF1α expression or stability. Finally, previous reports demonstrated that TRIP230 associates with hyper-phosphorylated Rb [149,153]. Immuno-blotting lysates from MCF7 and LNCaP cells with antibodies directed to Rb, Rb-phospho-serine780 and Rb-phospho-serine807/811 demonstrate that there is a significant amount of phosphorylated Rb in MCF7 and LNCaP cells (Figure 3.4B).

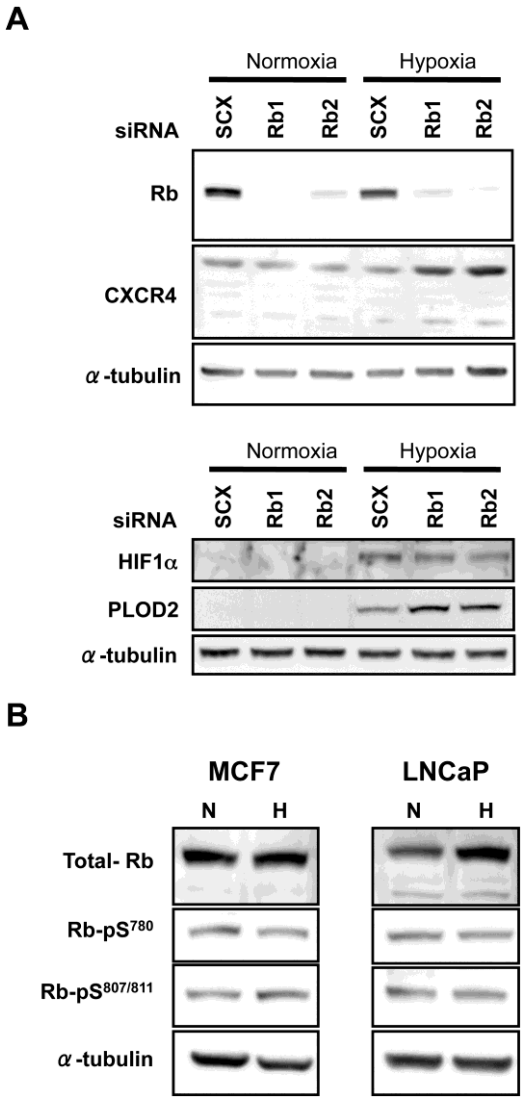

Figure 3.4. Rb represses HIF1-regulated target gene protein accumulation in MCF7 human breast cancer cells and is phosphorylated at serines 780 and 807/811.

MCF7 cells (**A**) were transfected with either scrambled siRNA (SCX) or Rb siRNAs siRb 1, and siRb 2. Rb, CXCR4, HIF1α, PLOD2 and α-tubulin protein levels were assessed by immuno-blot after exposure to atmospheric O_2 or 1% O_2 for 48 h (Rb and CXCR4) or 96 h (HIF1α, and PLOD2). (**B**) Immuno-blots of whole cell lysates from MCF7 and LNCaP cells either left at normoxia (N) or treated with 1% O_2 for 6 h (H). Blots were probed with primary antibodies to total Rb, Rb-phospho-serine^{780} (Rb-pS^{780}), Rb-phospho-serine$^{807/811}$ (Rb-pS$^{807/811}$), or α-tubulin as a loading control.

3.3.5. Loss of Rb Promotes an Invasive Phenotype in MCF7 Breast Cancer Cells.

The ability of Rb knock-down to enhance HIF1 complex transcriptional activity and protein expression led us to assess whether Rb suppression might also enhance hypoxia-induced cell invasion in traditionally non–invasive MCF7 breast cancer cells [302]. For cells with a complete complement of Rb (i.e. cells transfected with SCX control siRNA), hypoxia had no effect on invasion of MCF7 cells into the matrigel (Figure 3.5A and B). However, siRNA knock-down of Rb led to increased invasion of MCF7 cells under hypoxic conditions but had no effect on invasion under normoxic conditions (Figure 3.5A and B). These data support the role of Rb as a tumour suppressor of hypoxia-regulated metastatic programs.

We were concerned that the increased invasiveness might be due to a dramatic increase in cell proliferation due to loss of Rb control of the cell cycle. To avoid periods of prolonged, severe hypoxia, we demonstrated that the HIF1α stabilizing agent $CoCl_2$ would mimic the effects of hypoxia in the matrigel assay (Supplemental Figure S2C). These data further support our hypothesis that the observed effects are mediated via the HIF1 complex. With $CoCl_2$ established as an effective mimic of hypoxia after knock-down of Rb in the matrigel assay, we were able to determine if the observed increase in cell invasion was due to an increase in cell proliferation (Figure 3.5C). MCF7 cell growth dynamics were monitored at regular intervals by counting viable cells over a 72 h period. In cells transfected with either SCX control siRNA or Rb siRNA and with separate samples of each maintained either in the presence or absence of $CoCl_2$, we observed that loss of Rb decreased proliferation in both un-treated and $CoCl_2$-treated cells (Figure 3.5C) with no significant difference between the other treatments. Likewise, matrigel invasion of SCX control cells was indistinguishable under either condition. Cell sorting after propidium iodide staining revealed a larger proportion of the Rb knock-down cells in the sub-G1 phase of the cell cycle (Figure 3.5D and E). Taken together, these data strongly suggest that loss of Rb promotes cell invasion in a hypoxia-dependent fashion and that these effects are not due to increased cell number or proliferation.

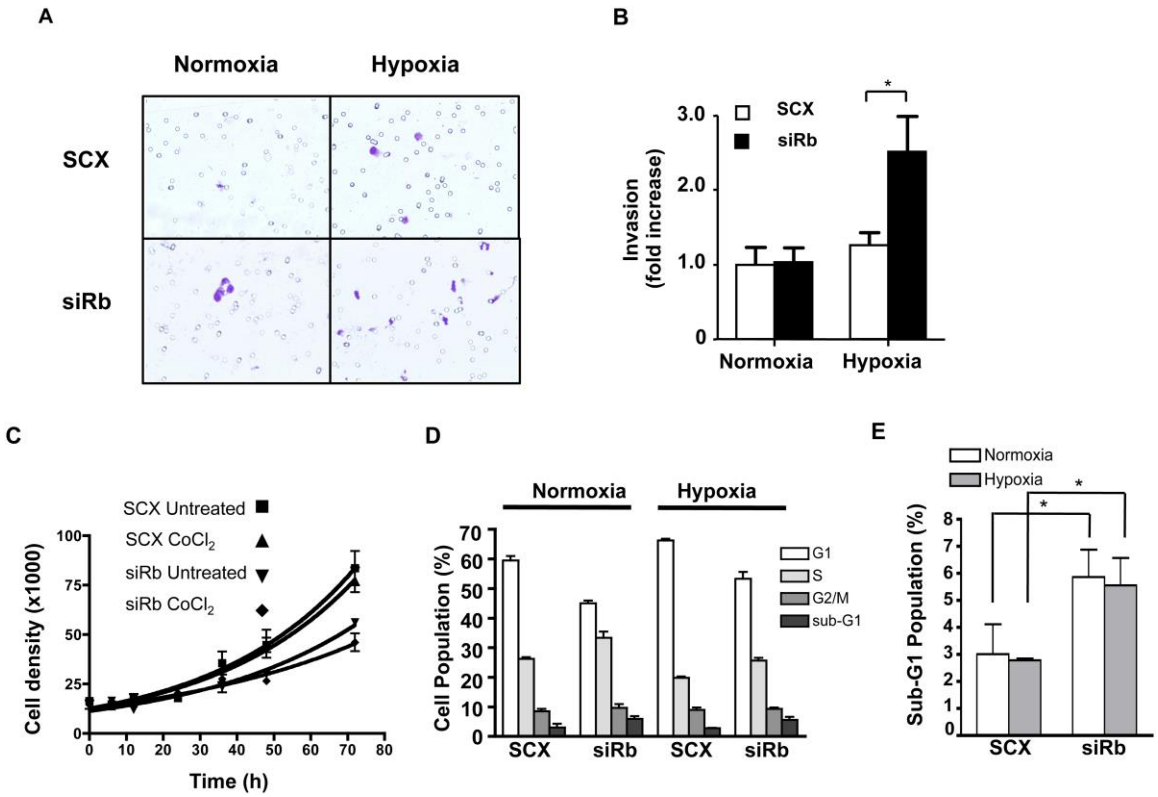

Figure 3.5. Loss of Rb promotes hypoxia-dependent invasiveness in MCF7 cells in a Matrigel Invasion Assay.

MCF7 cells were transfected with scrambled siRNA (SCX) or Rb siRNA as described above. Twenty-four hours after siRNA transfection, the cells were subjected to the Matrigel™ invasion assay. Plates were incubated in normoxic (20% O_2) or hypoxic conditions (1% O_2) at 37°C for 24 h and invading cells were fixed and visualized with toluidine blue. **(A)** Photomicrographs of matrigel-embedded MCF7 cells. **(B)** Numerical representation of relative invasion of matrigel-embedded MCF7 cells after treatment with SCX or siRb and exposure to normoxic or hypoxic conditions (n=6), **(C)** Knock-down of Rb in MCF7 cells does not alter cell proliferation in response to $CoCl_2$. Cells were transfected with siRNA's as described above. Twenty-four h after transfection, cells were treated with vehicle or 100 µM $CoCl_2$ to activate HIF1α and cells were counted at 0, 6, 12, 24, 36 48, and 72 h later. Error bars represent ± S.E.M. * $p < 0.01$. **(D)** Cell cycle and **(E)** Sub-G1 status was determined by propidium iodide (PI) staining and flow cytometry. MCF7 cells with a scrambled negative control or with Rb ablated, were treated with hypoxia or left at normoxic conditions for 36-hours. The percentage of cells in each stage of the cell cycle was determined using FlowJo analysis software based on the PI staining profile of FSC/SSC-gated population. Assay was performed three times and each sample was read in triplicate. Error bars represent ± S.E.M.

3.3.6. Rb associates with the PAS-B/TRIP230-interaction domain of the ARNT protein.

The possibility that ARNT, TRIP230 and Rb could be part of a multimeric complex was explored by immuno-precipitation of TRIP230 associated complexes from

the nuclear extracts of MCF7 cells incubated for 6 h under hypoxic conditions (Figure 3.6A). Immuno-blot analysis revealed ARNT and Rb to be present in the anti-TRIP230 immuno-precipitate while none of the three factors were detected in precipitates of lysates performed with non-immune IgG. These results provide strong evidence that native TRIP230 protein is capable of protein-protein interactions with ARNT and Rb.

Given that previous *in vitro* interaction studies determined that Rb does not directly interact with ARNT [303], we therefore were interested to determine if the TRIP230 interaction domain within ARNT could be used to isolate Rb from MCF7 cell nuclear extracts. Partch and colleagues have identified that the TRIP230 interaction domain within ARNT is located in its PAS-B region [155]. We fused amino acids 344-479 harboring the expanded PAS-B domain of mouse ARNT to GST. Using this minimal interaction domain was done in part to reduce the potential for ARNT to interact with other nuclear proteins. Pull-down of TRIP230 and Rb from nuclear extracts of hypoxia-conditioned MCF7 cells was dramatically enriched using the GST-ARNT-PAS-B domain compared to GST alone (Figure 3.6B). Thus, it is possible that an ARNT complex including TRIP230 and Rb is formed through the ARNT PAS-B domain. This domain mediates the interaction between ARNT and multiple coactivators that are essential for ARNT-mediated transcription: namely, TRIP230 [150], the p160/NCoA/SRC-family of transcriptional coactivators [49], and CoCoA [304].

Finally, we wished to determine specifically, if hyper-phosphorylated Rb was involved in HIF1-regulated gene transcription. We probed immuno-blots with an anti-phospho-serine^{780} Rb-specific antibody after pull-down using GST-PAS-B. In this fashion, we observed hyper-phosphorylated Rb in blots generated from normoxic and hypoxic MCF7 cell nuclear extracts (Figure 3.6C). In addition, interrogation of the transcriptional regulatory regions of the HRE-containing VEGF promoter and EPO enhancer revealed the presence of Rb-pSer^{780} in a hypoxia-dependent fashion (Figure 3.6D).

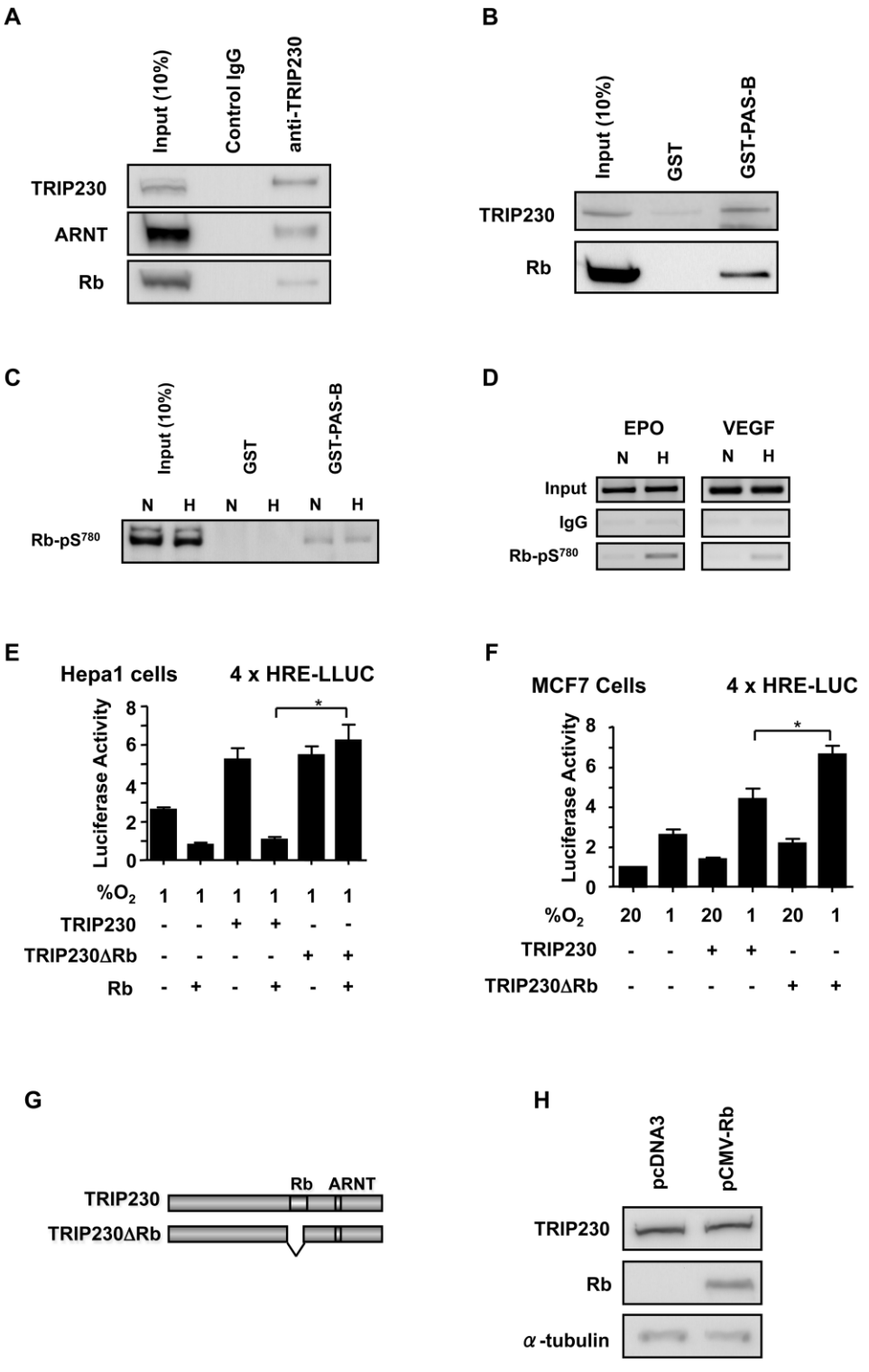

Figure 3.6. Rb mediates its transcriptional effects on hypoxia-inducible gene regulation through an ARNT-TRIP230-Rb complex.

(A) Immuno-blot of complexes precipitated using either a mouse monoclonal antibody directed to TRIP230 or mouse control IgG from the nuclear extracts of MCF7 cells. Blots were probed for the presence of TRIP30, ARNT and Rb. The left hand lane of each blot contains nuclear extract representing 10% of input. (B) GST-ARNT-PAS-B is capable of pulling down TRIP230 and Rb. Immuno-blot analysis of GST-ARNT-PAS-B pull-down and GST pull-down of TRIP230 and Rb from MCF7 nuclear extracts. GST moieties were fixed to glutathione-agarose beads and incubated for 90 min at 4 degrees C with 500 μg of MCF7 cell nuclear extract. Input lanes were loaded with 250 μg of nuclear extract. Complete blots for panels A and B can be found in Supplemental Figure S1. GST-ARNT-PAS-B is capable of pulling down phosphorylated Rb. (C) Immuno-blot analysis of GST-ARNT-PAS-B pull-down and GST pull-down of Rb-phospho-serine780 (Rb-pS780) from MCF7 nuclear extracts harvested from cells left at normoxia (N) or treated with 1% O2 for 6h (H). (D) Chromatin immunoprecipitation assay of EPO enhancer and VEGF promoter regions in MCF7 cells using control or Rb-phospho-serine780 antibodies. Cells were treated as described above. Rb attenuates TRIP230-mediated coactivation of ARNT-dependent transcriptional activity. The Rb- and ARNT-interaction domains are indicated. Hepa-1c1c7 cells (E) and MCF7 cells (F) were transfected with a hypoxia responsive 4xHRE-driven luciferase construct as a reporter, expression plasmids for TRIP230, TRIP230ΔRB and Rb as indicated and subjected to 1% O2 or atmospheric (20%) O2 for 24 h. Whole cell lysates were assayed for luciferase activity. (G) A schematic of the TRIP230ΔRB mutant. (H) TRIP230 protein levels are unaffected by transfection of Rb expression plasmid into Hepa1c1c7 cells. Whole cell lysates were analyzed by immuno-blot and membranes were probed with affinity-purified antibodies to TRIP230, Rb and α-tubulin. * $p<0.05$.

3.3.7. TRIP230 mediates the repressive effects of Rb on HIF-regulated transcription.

We have established that Rb co-purifies with TRIP230 and that Rb attenuates the accumulation of hypoxia-inducible target gene mRNA and protein levels. In order to determine if the ability of Rb to modulate HIF1-regulated transcriptional activity was mediated via TRIP230, we examined effects of Rb on the expression of a hypoxia-responsive reporter construct using deletion mutants of TRIP230 in Rb-negative and –positive cell lines. Rb-negative Hepa1c1c7 cells were transfected with an expression plasmid encoding TRIP230, or a transcriptionally competent deletion-mutant of TRIP230 (TRIP230ΔRb; schematic in Figure 3.6G) lacking the Rb-interaction domain [153], an Rb cDNA expression plasmid, and a synthetic luciferase reporter construct containing a multimerized hypoxia-responsive element (HRE) promoter (Figure 3.6E). Rb abrogated hypoxic induction of reporter activity in cells transfected with wild-type TRIP230, but was ineffective in cells transfected with the mutant TRIP230. Transfection of Rb into the Hepa1c1c7 cell line had no effect on levels of endogenous TRIP230 protein (Figure 3.6H). Indeed, titration of increasing amounts of Rb-expression plasmid repressed hypoxia-inducible reporter activity in a dose-dependent manner (Supplemental Figure S2B). Transfection of the mutant TRIP230 into Rb-positive MCF7 human breast cancer

cells further enhanced expression of the reporter gene (Figure 3.6F), thus acting as a dominant negative likely by competing for HREs with the endogenous wild-type TRIP230. These data collectively suggest that Rb's attenuating effects on HIF1 transcriptional activity appear to be mediated by TRIP230.

3.4. Discussion

We have determined that Rb attenuates the physiological response to hypoxia by HIF1α and that it is an integral and indispensable part of the HIF1 transcriptional complex by virtue of a direct interaction with TRIP230. This effect is independent of other protein-protein interactions as the repressive effect of Rb was lost in cells over-expressing a transcriptionally competent mutant of TRIP230 lacking the Rb-interaction domain (Figure 3.6E and F) and in cells depleted of TRIP230 (Figure 3.3A). In addition, siRNA-mediated knock-down of Rb led to a concomitant increase of known HIF1 target genes in a hypoxia-dependent fashion in human breast MCF7 and in human prostate LNCaP cancer cell lines (Figure 3.1). Furthermore, we were able to record Rb over well-characterized HREs in the EPO and VEGF regulatory regions (Figure 2) suggesting that Rb may regulate expression of these genes at the transcriptional level.

The TRIP230 coactivator was cloned and characterized based on its ability to interact with the thyroid hormone receptor (TR) and enhance its transactivation function [149,292], and by virtue of its ability to interact with Rb [149]. In this latter report, evidence was presented that supported a role for Rb as a transcriptional attenuator of thyroid hormone receptor function, likely mediated through the TRIP230 transcriptional coactivator. TRIP230 was later found to act as an essential coactivator for ARNT-dependent transcriptional activities, including hypoxia-inducible gene expression [150]. Importantly, we found that TRIP230 did not interact with HIF1α in a yeast two-hybrid assay (T. Beischlag, unpublished data). Our immuno-precipitation studies employing antibodies directed to TRIP230 demonstrate that endogenous ARNT and Rb interact with TRIP230 in MCF7 cells (Figure 3.6A) further supporting our hypothesis that Rb is part of a HIF1 transcriptional complex.

To further delineate the nature of this putative complex and to determine if ARNT, TRIP230 and Rb exist in a single complex, we eliminated other known protein-protein interaction interfaces within ARNT and used a GST pull-down strategy to affinity capture TRIP230 and Rb. The comprehensive analysis by GST pull-down performed by Elferink and colleagues failed to demonstrate a direct interaction with ARNT and Rb *in vitro* [303]. In addition, based on our previous studies characterizing the interaction between ARNT and TRIP230 [150], Partch and colleagues identified amino acids within the ARNT PAS-B domain that mediate the ARNT-TRIP230 interaction [155]. We designed a GST-ARNT-PAS-B fusion thus eliminating other protein interaction domains within ARNT. The ability of the ARNT-PAS-B region to pull-down Rb supports the existence of a multimeric complex containing ARNT, TRIP230 and Rb (Figure 3.6B). Indeed, the PAS-B domain has emerged as a bona fide platform for the recruitment of multiple forms of transcriptional co-regulatory complexes [49,150,155,259].

The HIF1 complex regulates the cell's adaptive response to low oxygen mediating angiogenesis and alternative energy utilization via glucose metabolism. Hypoxia is also a hall-mark of solid tumours and has been implicated in tumour cell transformation. We found an exacerbated hypoxia-dependent accumulation of PLOD2 and CXCR4 mRNA in MCF7 and LNCaP cells depleted of Rb (Figure 3.1) and a concomitant increase in protein in MCF7 cells (Figure 3.4A).

This work represents the first link between the functional ablation of Rb in tumor cells and HIF1α-dependent invasion. These data support a hitherto unrecognized mode of action for Rb that is uncoupled from its canonical cell cycle/tumour suppressor function. Loss-of-function of Rb or genetic ablation of *RB1* has been implicated in advanced stages of brain cancers [305,306], prostate cancer [307,308], breast cancer, and lung cancer [294]. Furthermore, the loss of Rb and the activation of HIF1-regulated genes such as increased VEGF expression, microvascular hyperplasia and metastasis are traits that are common to progression in many solid tumours [205], however no direct link between the Rb and HIF pathways has been established. As a result, we were interested in further investigating the physiological connection between Rb function and hypoxia inducible gene expression, especially HIF1-regulated transcriptional programs involved in cancer cell transformation.

The observation that CXCR4 and PLOD2 protein (Figure 3.4A) and vimentin mRNA (Supplemental Figure S2A) levels were elevated upon depletion of Rb from MCF7 cells led us to investigate the effects of Rb-loss on the invasive phenotype of MCF7 cells. CXCR4 expression is likely to be a key effector of the invasive phenotype observed in Figure 5 [309,310]. CXCR4 promotes many key steps in epithelial to mesenchymal transition (EMT) and metastasis including detachment from neighboring cells, extra-vasation, metastatic colonization, angiogenesis and proliferation [311]. Furthermore, Gilkes and colleagues recently demonstrated that the metastatic marker PLOD2 is a hypoxia-inducible gene and is required for breast cancer metastasis to lymph and lung [312]. PLOD2 is an enzyme required for collagen production and plays a role in extracellular matrix re-modelling [313]. Under normoxic conditions MCF7 cells maintain an epithelial and non-invasive phenotype regardless of Rb status. Upon knock-down of Rb, hypoxia and $CoCl_2$ treatment triggered invasion in nearly 3% of the cells seeded in the matrigel assay (Figure 3.5A, B and Supplemental Figure S2C). This represents a change in the invasive potential of the MCF7 cells and it seems likely that loss of Rb contributes to HIF1-inducible tumour cell transformation. Our data suggests that Rb attenuates HIF1 function to ensure the appropriate levels of HIF1-target gene expression. Thus, we propose that loss of Rb or breakdown of this pathway primes cancer cells for metastatic transformation by allowing for the over-expression of pro-metastatic factors such as PLOD2 and CXCR4.

In addition, we were interested to see if known Rb-associated repressor complexes [299,300] could be recorded over well-characterized HREs during hypoxia-driven transcription. ChIP analysis revealed the presence of Sin3a/b, HDAC1 and HDAC3 on the HIF-responsive regulatory regions of both the VEGF and EPO genes (Figure 3.2H). In light of the abundance of data suggesting that HDACs are required for HIF1-mediated transcription [314-316], we do not dismiss the theory that HDACs are essential for the initiation and maintenance of HIF1-regulated transcription. However, we are also cognizant that they may have pleiotropic effects and be recruited in a different fashion to attenuate the hypoxic response. Whether targeting these factors has any functional or therapeutic utility remains to be seen and will be the focus of future research efforts.

The hypothesis that ARNT, TRIP230 and Rb act in concert to regulate hypoxia-inducible gene transcription is supported by several lines of investigation. First, our data derived from the sequential chromatin immuno-purifications using ARNT, HIF1α, TRIP230 and Rb affinity purified antibodies (Figure 3.2D and E) suggest that all 4 proteins are present at HIF1-regulatory elements at the same time. Second, a transcriptionally competent mutant of TRIP230 (TRIP230ΔRb) overcomes the repressive effect of Rb over-expression on hypoxia-inducible transcription in Rb-negative Hepa1 cells (Figure 3.6E). Third, TRIP230ΔRb was more efficacious in coactivating hypoxia-inducible transcription in Rb-positive MCF7 cells (Figure 3.6F). Finally, loss of Rb did not exacerbate the hypoxic response in cells depleted of TRIP230 (Figure 3.3A). Taken together, there is strong evidence that Rb is a negative regulator of the TRIP230-HIF1 complex and that loss of Rb unmasks the full coactivation potential of TRIP230 (Figure 7).

While we have not ruled out the involvement of hypo-phosphorylated Rb in HIF1 function, the presence of hyper-phosphorylated Rb at HIF regulatory elements and after GST pull-down by the ARNT-PAS-B domain (Figure 3.6C and D) supports the observations of other investigators [149,153]. Since there was no appreciable difference in the ability of the GST-ARNT-PAS-B moiety to pull-down Rb from either normoxic or hypoxic extracts, it seems as if neither HIF1α nor HIF2α is essential for this interaction. Additionally, it seems clear that the modulatory effect of Rb on HIF function is uncoupled from E2F as evidenced by the unaltered transcriptional response observed after knock-down of DP1 (Figure 3.3C**).** Furthermore, the abundance of phospho-Rb (serine^{780} and serine$^{807/811}$) (Figure 3.4B) indicates that Rb is in a permissive state for uncoupling from E2F [317]. Thus, our data suggest that Rb plays an essential role in regulating the amplitude of the hypoxic response for genes regulating both angiogenesis and metastasis and that loss of Rb leads to exacerbated expression of HIF1α target genes that regulate tumour progression.

Targeting angiogenesis has been an attractive strategy for combating cancer [318] however, there are caveats to anti-angiogenic therapies. Avastin, a monoclonal antibody to VEGF failed to extend survival rates in patients suffering from breast cancer [319], and is of limited benefit in other types of cancer [320]. Furthermore, there is

experimental evidence that anti-angiogenic drugs exacerbate tumour progression [321]. Therefore, a novel approach to combating tumour progression may involve specifically targeting the HIF1α/β-TRIP230-Rb complex that regulates both angiogenic and cell invasion programs [322]. We have demonstrated that Rb represses or attenuates the coactivation function of TRIP230 and thereby regulates the transcriptional response to hypoxia. In addition, this work demonstrates that Rb plays a hitherto unidentified role in tumour suppression by virtue of effects on HIF1α/β that are distinct from its classic tumour suppressor role mediated through repression of E2F transcription factors. These data provide the first direct link between the loss of Rb and HIF1-regulated pro-metastatic and pro-angiogenic processes. Therefore, targeting this pathway could yield novel therapies to better combat solid tumour progression and metastasis.

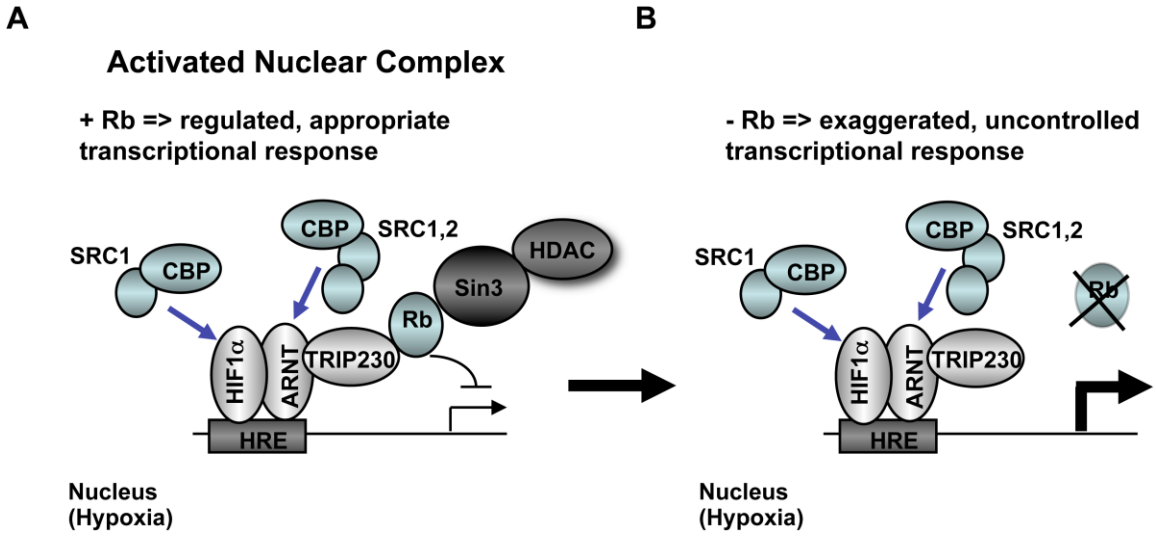

Figure 3.7. Illustration describing the transcriptional regulation of HIF-target genes in cells either expressing or lacking Rb.

(A) In cells that are Rb-positive, the full transcriptional activation capacity of the HIF1-TRIP230 complex is repressed or muted resulting in regulated expression of HIF1 target genes. **(B)** In cells lacking Rb, gene expression mediated by HIF1 becomes uncontrolled.

3.5. Materials and Methods

3.5.1. Cell culture, transient transfections, luciferase assays and RNA interference.

Hepa1c1c7 and HEK293T cells (ATCC) were maintained in Dulbecco's Modified Eagle's Medium (DMEM; BioWhittaker, Lonza) with 10% fetal bovine serum (FBS; HyClone, Perbio, Thermo Fisher Scientific Inc.). MCF7 cells were maintained under similar conditions but were supplemented with 100 units/ml potassium penicillin-100 μg/ml streptomycin sulphate (BioWhittaker, Lonza), and 4.5 g/L glucose and 4.5 g/L L-glutamine at 37°C, 20% O_2, and 5% CO_2. LNCaP cells were maintained in RPMI 1640 medium with L-Glutamine (BioWhittaker, Lonza) supplemented with 10% FBS and 100 units/ml potassium penicillin-100 μg/ml streptomycin sulphate. Transient transfections and luciferase assays were performed as described previously [150]. Rb, and TRIP230 wild-type and TRIP230 mutant expression plasmids were generously provided by Dr. Y. Chen (Univ. of Texas, San Antonio) and were described previously [149].

MCF7 or LNCaP cells were transfected with either scrambled (SCX) siRNA (DS Scrambled negative control siRNA, Integrated DNA Technologies Inc.), Rb siRNAs (Integrated DNA Technologies Inc., Cat. No. HSC.RNAI.N000321.9.1, HSC.RNAI.N000217.9.2; siRb 1, and siRb 2, respectively), ARNT siRNA (Integrated DNA Technologies Inc., Cat. No. HSC.RNAI.N178426.11.3), TRIP230 siRNA (Integrated DNA Technologies Inc., Cat. No. HSC.RNAI.N004239.12.1) or DP1 siRNA (Integrated DNA Technologies Inc., Cat. No. HSC.RNAI.N007111.11.1). MCF7 cells were transfected with 10 – 15 nM siRNA using 0.3% (v/v) Lipofectamine RNAiMAX (Invitrogen Inc) according to manufacturer's protocol. The cells were allowed to incubate in transfection mix for 6 h at 37°C, 20% O_2, and 5% CO_2 after which the transfection mix was removed and replaced with complete media.

3.5.2. Antibodies

The mouse anti-TRIP230 IgG was kindly provided by Dr. Y. Chen (University of Texas, San Antonio). Anti-Rb (rabbit polyclonal, Santa Cruz Biotechnology Inc., SC-7905), anti-phospho-Rb (Ser^{780}) (Cell Signaling, 9307), anti-phospho-Rb ($Ser^{807/811}$) (Cell

Signaling, 9308), anti-PLOD2 (mouse polyclonal, Abnova, H00005352-B01P), anti-HIF1α (rabbit polyclonal, Santa Cruz Biotechnology Inc., SC-10790), anti-DP1 (rabbit polyclonal, Santa Cruz Biotechnology Inc., SC-610), anti-ARNT (goat polyclonal, Santa Cruz Biotechnology Inc., SC-8076), anti-CXCR4 (rabbit polyclonal, Abcam Inc., ab2074), anti-α-tubulin (mouse monoclonal, Santa Cruz Biotechnology Inc., SC-8035), anti- HIF2α (mouse monoclonal, Santa Cruz Biotechnology Inc., SC-46691), goat anti-rabbit IgG-HRP (Santa Cruz Biotechnology Inc., SC-2004), goat anti-mouse IgG-HRP (Santa Cruz Biotechnology Inc., SC-2005), donkey anti-goat IgG-HRP (Santa Cruz Biotechnology Inc., SC-2020)

3.5.3. Quantitative Real-Time PCR

For quantitative real-time PCR (RT-PCR) experiments, MCF7 or LNCaP cells were incubated under hypoxic conditions (1% O_2) for 24 h in a humidified CO_2 incubator. The mRNA levels of VEGF, EPO, CXCR4, vimentin, PLOD2, RB1, and 36B4 were determined using quantitative real-time PCR. The primer pairs for VEGF EPO and 36B4 were described previously [284]. The other primer pairs used were; CXCR4: 5'-CAGTGGCCGACCTCCTCTT-3' and 5'-GGACTGCCTTGCATAGGAAGTT-3'; RB1: 5'-CATCGAATCATGGAATCCCT-3' and 5'- GGAAGATTAAGAGGACAAGC -3'; PLOD2 5'-GCGTTCTCTTCGTCCTCATC-3' and 5'-GTGTGAGTCTCCCAGGATGC-3', and; Vimentin: 5'-TTCCAAACTTTTCCTCCCTGAACC-3' and 5'-TCAAGGTCATCGTGATGCTGAG-3'; Total RNA was isolated using TRI reagent (Sigma, Cat. No. T9424-200ML) according to the manufacturer's protocol. Reverse transcription was performed using High Capacity cDNA Reverse Transcription Kit (Applied Biosystems, Part No.4368814) according to the manufacturer's protocol. A total of 2 – 4 µg of RNA was used in a 20 µL reaction amplified by cycling between 25^{o}C for 5 min, 37^{o}C for 120 min, and 85^{o}C for 5 min (Veriti 96 Well Thermal Cycler, Applied Biosystems). From each experiment, a sample that was both transfected with Rb-specific siRNA and pre-conditioned with hypoxia was used to generate a relative standard curve in which the sample was diluted 1:10 in five serial dilutions resulting in dilutions of 1:10, 1:100, 1:1,000, 1:10,000, and 1:100,000 whereas the samples were diluted 1:30; the analysis was done using StepOnePlus System (Applied Biosystems).

3.5.4. Chromatin immunoprecipitation assays

Chromatin immuno-precipitations (ChIPs), and sequential ChIP assays were performed as described previously [73,150]. Oligonucleotide sequences for PCR amplification of human VEGF and EPO regulatory regions were as described previously [150]. All antibodies were supplied by Santa Cruz Biotechnology Inc. or as described above.

3.5.5. Immuno-blotting

Protein analysis was performed by immuno-blotting as described previously [86]. Briefly, MCF7 cells were incubated under hypoxic conditions (1% O_2) for either 48 h or 96 h. Cells were harvested and the protein concentration estimated by the Bradford assay. Equal amounts of proteins from the samples were resolved on a SDS-acrylamide gel then transferred to polyvinylidene fluoride (PVDF) membrane. Membranes were incubated with diluted primary antibodies in 5% w/v skim milk powder, 1X TBS, 0.1% Tween-20 at 4°C with gentle shaking, overnight. The detection was done using horseradish peroxidase conjugated anti-mouse or anti-rabbit IgG (Santa Cruz Biotechnology Inc.) and ECL Prime detection kit (GE Healthcare).

3.5.6. Matrigel invasion and cell proliferation assays

MCF7 cells were transfected with scrambled siRNA or Rb siRNA as described above. Twenty-four hours after siRNA transfection, the cells were washed, trypsinized, and re-suspended in culture medium, and subjected to invasion assay using BD BioCoat Matrigel Invasion Chamber (BD Sciences, Cat. No. 354480) according to the manufacturer's protocol. Briefly, the suspended chambers were rehydrated in warm bicarbonate-based medium for 2 h. MCF7 cells were reverse transfected according to manufacturer's protocols and seeded into invasion chambers in DMEM without FBS at a density of 10,000 cells/chamber. Chambers were placed in 24-well plates with chemo-attractant (complete medium containing 10% FBS) in the well. The plates were incubated in normoxic (20% O2) or hypoxic conditions (1% O2) at 37oC for 24 h or treated with vehicle or 100 µM CoCl2 for 24h. Before mounting the invasion membrane

to microscope slides, the non-invading cells were removed by cotton swab and invading cells in the membrane were fixed with 100% methanol and stained with 1% toluidine blue. All the cells in the invasion membrane were counted using light microscopy at 10-40 × magnification. Assays were performed in triplicate and each membrane was counted three times.

MCF7 cells grown to 75-80% confluence were transfected with either Rb or scrambled negative control siRNA (SCX). Media was changed after eight hours. Twenty-four h post-transfection, cells were washed 2 times with PBS, trypsinized and seeded into 6-well plates at 10,000 cells/well. Twenty-four h after plating, CoCl2 was added directly to half the wells to a final concentration of 100 μM. Cells were counted at; 0 (control), 6, 12, 24, 36, 48 and 72 h following CoCl2 administration. Determinations were performed in triplicate and each sample was counted three times.

3.5.7. Flow cytometry and sub-G1 status

Cell cycle status was determined by propidium iodide (PI) staining and flow cytometry. MCF7 cells treated with a scrambled negative control or with Rb knocked-down, were treated with hypoxia or left at normoxic conditions for 36-hours and then harvested using trypsin. Biological triplicates of 5x105 cells were fixed in 70% ethanol on ice for 15 minutes and then cells were centrifuged for 3 minutes at 1500 rpm to remove the ethanol and incubated in 0.5 ml of propidium iodide staining solution (50 μg/mL PI, 0.05% Triton X-100, 0.1 mg/mL RNase A, in PBS) for 40 min at 37ºC. Following staining, cells were washed with PBS then run on a BD FACSCanto II flow cytometer (488 nm excitation, 617 emission, 375 volts, PI) where 20,000 events were collected. The percentage of cells in each stage of the cell cycle was determined using FlowJo analysis software based on the PI staining profile of FSC/SSC-gated population.

3.5.8. Co-immuno-precipitation and glutathione-s-transferase pull-down assays

Immuno-precipitation of complexes from MCF7 cell nuclear extracts was performed essentially as described previously [49], with minor modifications. MCF7 cells

were maintained in 1% O_2 for 6 h in a humidified CO2 incubator and nuclear extracts were prepared following our established protocol [323]. Approximately, 1 mg of nuclear extract was incubated with 5 μg of either affinity purified anti-TRIP230 or control mouse IgG at 4° C for 90 min on a spinning wheel. Approximately, 50 μl of pre-cleared Protein-G sepharose beads were added to each mixture and incubated for a further 90 min. Samples were washed vigorously and fractionated by SDS-PAGE. Precipitates were transferred to nylon membrane for immuno-blotting and blots were probed with antibodies to TRIP230, ARNT and Rb.

Glutathione-*s*-transferase (GST) pull-down assays were performed as described previously with minor modifications [49]. In order to construct the GST-ARNT-PAS-B fusion moiety, a mouse ARNT cDNA encoding amino acids 344-479 was PCR-amplified and cloned into pGEX-5X-1 using Bam H1 and XhoI. Approximately 30 μl of GST or GST-ARNT-PAS-B beads were incubated with 250 μg of nuclear extract at 4° C for 90 min on a spinning wheel, washed and eluted as described previously [49]. Eluted samples were fractionated by SDS-PAGE, transferred to PVDF membrane and analyzed by immuno-blot for the presence of TRIP230, Rb or phospho-Rb (Ser^{780}).

3.5.9. Statistical analysis

Statistical analyses were performed using GraphPad Prism 4.0. For multiple comparisons (i.e. siRNA experiments) statistical significance was determined using a 2-way ANOVA with Tukey's Multiple Comparison test. Values are presented as means ± standard deviation (S.D.). A P value < 0.05 was considered to be significant.

3.6. Supporting Information

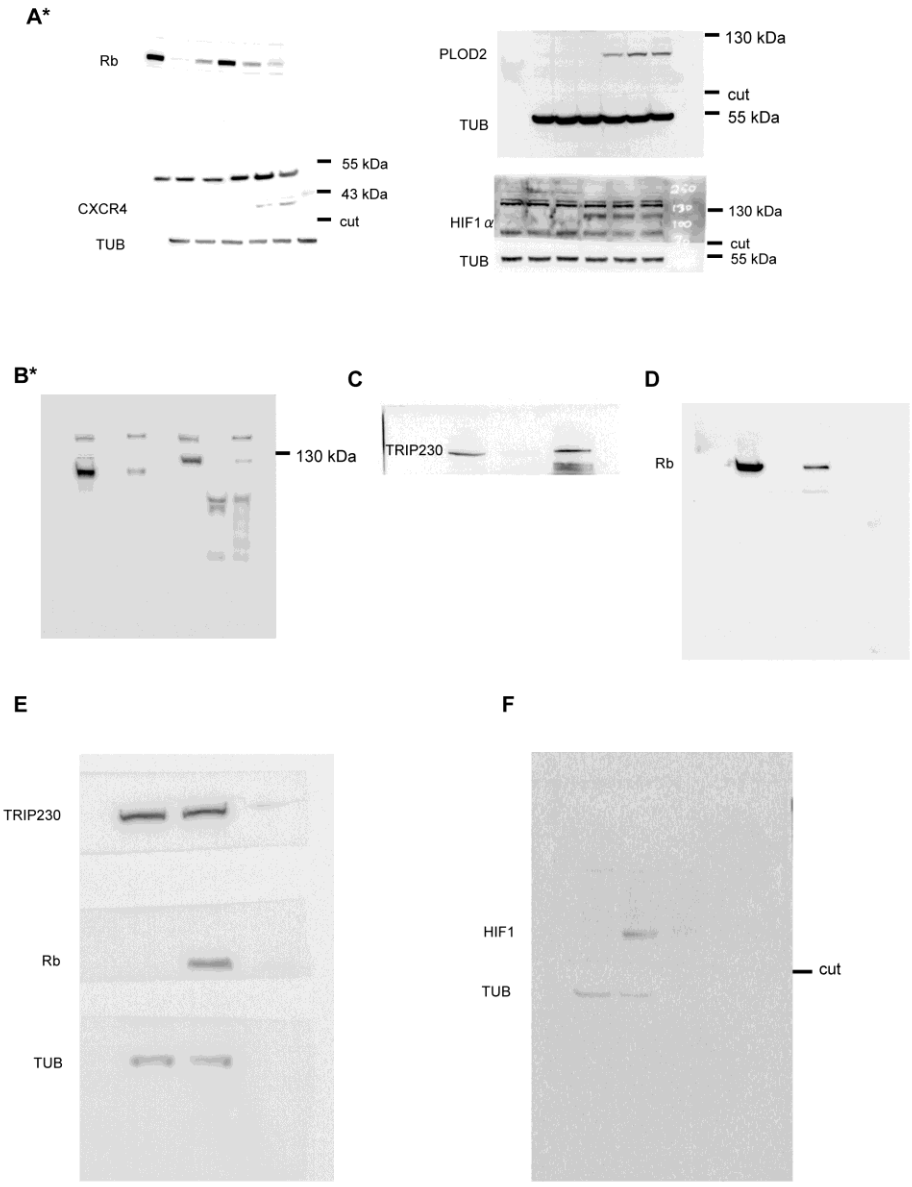

Figure 3.8. Supplemental Figure 1
Complete digital images of **(A)** immuno-blots depicted in manuscript Figures 4A, **(B)** 6A, **(C and D)** 6B **(E)** 6H and **(F)** 2C. When necessary, blots were cut into strips at encompassing the appropriate molecular weights to that different proteins of interest of different molecular weights could be analyzed from the same sample and expt. For GST pull-down experiments, the entire blot cut into two sections is shown. However, we used the pull-down of TRIP230 from another identical experiment (Supplemental Figure 1B) as a representative blot because the signal was stronger. In some cases, brightness and contrast of the images have been altered (*) in order for the boundary of the cut blots or for the molecular weight markers to be clearly visible.

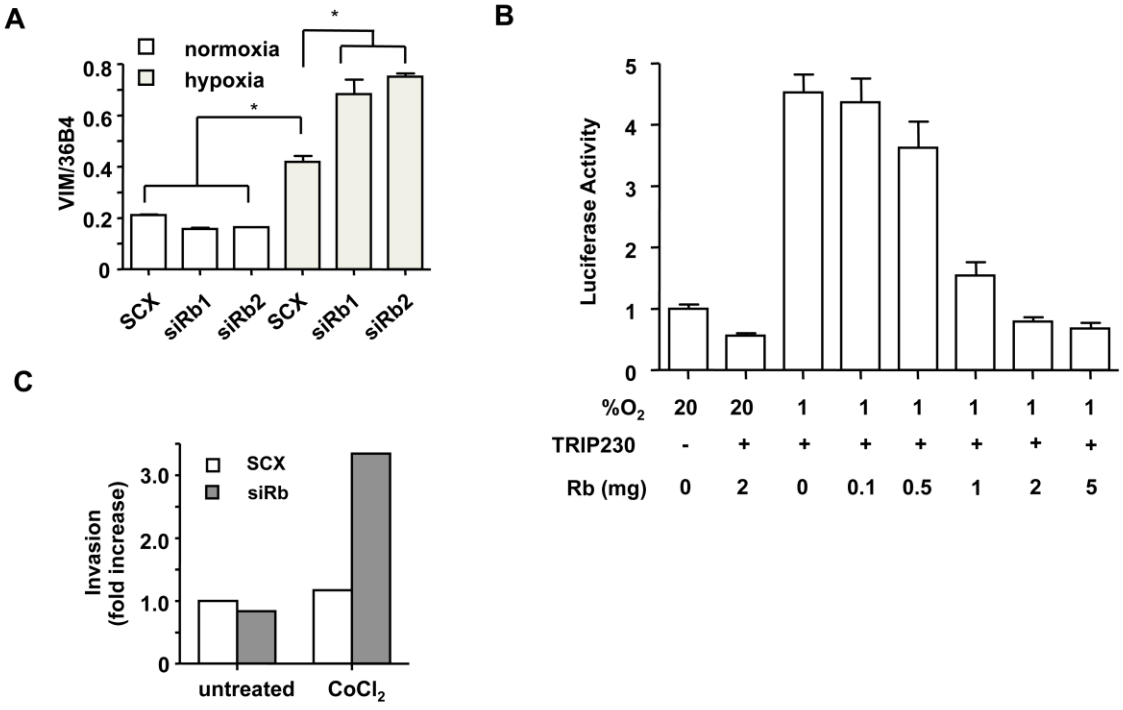

Figure 3.9. Supplementary Figure 2
(A) Relative mRNA levels of vimentin under similar conditions described in Figure 1. Open bars represent normoxia (20% O_2) and closed (grey) bars represent hypoxia (1% O_2). * $p < 0.05$. **(B)** Titration of Rb expression vector into Hepa1C1C7 cells. Increasing amounts of Rb expression vector was co-transfected with pCMV-TRIP230 and an HRE-driven luciferase vector (see Materials and Methods and Figure 6 legend). (**C**) Numerical representation of relative invasion of matrigel-embedded MCF7 cells after treatment with SCX or siRb and treatment with the HIF1 activator, $CoCl_2$ (100 μM).

3.7. Acknowledgements

The authors would like to thank Dr. Yumay Chen (Dept. of Medicine, University of Texas Health Science Center) for TRIP230 antibody and the Rb expression vector.

Chapter 4. The retinoblastoma protein regulates HIF1-mediated genetic programs, tumor cell invasiveness and neuroendocrine differentiation in prostate cancer cells.

Published in Oncotarget 2016 Mar 23. doi: 10.18632/oncotarget.8301. [Epub ahead of print]

Authors: Mark P. Labrecque, Mandeep K. Takhar, Rebecca Nason, Stephanie Santacruz, Kevin J. Tam, Shabnam Massah, Ann Haegert, Robert H. Bell, Manuel Altamirano-Dimas, Collin C. Collins, Frank J. Lee, Gratien G. Prefontaine, Michael E. Cox and Timothy V. Beischlag.

Author Contributions: I performed all tissue culture and generated the shRNA cell lines in both LNCaP and 22Rv1 cells. I conducted the qPCR and immunoblots represented in Figure 4.1. I performed the Matrigel invasion assay and proliferation assay show in Figures 4.2A and 4.2B. Kevin Tam performed the flow cytometry and cell cycle analysis represented in Figure 4.2C. Ann Haegert conducted the microarray. Timothy Beischlag and I worked in collaboration with Robert Bell, Manuel Altamirano-Dimas and Collin Collins to analyze the microarray data and perform gene ontology analysis. Shabnam Massah mapped our identified array genes to their chromosomal locations and Robert Bell conducted the gene clustering statistical analysis. I performed the *in sillico* consensus ARNT:HIF1α binding sequence analysis and created the Venn Diagrams and the cartoon represented in Figure 4.3 and the heatmap shown in figure 4.4A. I validated the microarray results through qPCR in shRNA LNCaP and shRNA 22Rv1 cells shown in Figure 4.5. Rebecca Nason, Stephanie Santacruz and I worked in collaboration to produce the immunoblots represented in Figure 4.6. Frank Lee conducted the calcium mobilization assay. Mandeep Takhar performed the immunocytochemistry and subsequent data analysis. Timothy Beischlag, Gratien Prefontaine and Michael Cox

conceived and designed the experiments. I wrote the initial draft of the manuscript and Timothy Beischlag and I wrote the final published version of the manuscript.

4.1. Abstract

Loss of tumor suppressor proteins, such as the retinoblastoma protein (Rb), results in tumor progression and metastasis. Metastasis is facilitated by low oxygen availability within the tumor that is detected by hypoxia inducible factors (HIFs). The HIF1 complex, HIF1α and dimerization partner the aryl hydrocarbon receptor nuclear translocator (ARNT), is the master regulator of the hypoxic response. Previously, we demonstrated that Rb represses the transcriptional response to hypoxia by virtue of its association with HIF1. In this report, we further characterized the role of Rb in hypoxia-regulated genetic programs by stably ablating Rb expression with retrovirally-introduced short hairpin RNA in LNCaP and 22Rv1 human prostate cancer cells. DNA microarray analysis revealed that loss of Rb in conjunction with hypoxia leads to aberrant expression of hypoxia-regulated genetic programs that increase cell invasion and promote neuroendocrine differentiation. For the first time, we have established a direct link between hypoxic tumor environments, Rb inactivation and progression to late stage metastatic neuroendocrine prostate cancer. Understanding the molecular pathways responsible for progression of benign prostate tumors to metastasized and lethal forms will aid in the development of more effective prostate cancer therapies.

4.2. Introduction

A characteristic of many solid tumors is that they contain regions of low oxygen availability (hypoxia) and express elevated levels of hypoxia inducible factors (HIFs) [139]. The HIF1 complex, HIF1α and dimerization partner the aryl hydrocarbon receptor nuclear translocator (ARNT/HIF1β), is the master regulator of the hypoxic response. During hypoxia, HIFs accumulate, translocate to the nucleus, and bind ARNT [38]. The HIF1 complex then binds to hypoxia response elements and recruits coactivators such as the thyroid hormone receptor/retinoblastoma-interacting protein 230 (TRIP230) [150], CBP/p300 [279] and Brm/Brg-1[284] to modulate the expression of genes. Typical HIF1-

regulated genes include angiogenic and metabolic targets, such as vascular endothelial growth factor (VEGF) [148] and GLUT1 [324] but also include metastatic markers, like CXCR4 [325] and procollagen-lysine 2-oxoglutarate 5-dioxygenase 2 (PLOD2) [326]. Thus, the microenvironment of solid tumors is conducive to the activation of hypoxia-regulated genetic programs and these support tumor growth.

Rb is a tumor suppressor protein with a well characterized and canonical function as a cell cycle regulator by repression of E2F-mediated transcriptional activity [161]. Hypo-phosphorylated Rb binds E2F and prevents transcription of E2F-dependent mitotic and cell cycle programs. Thus, loss of Rb expression or function is a crucial step preceding tumor development [161,297]. However, we recently demonstrated that TRIP230 and Rb form a complex with HIF1 and that hyper-phosphorylated Rb represses the function of TRIP230 and the transcriptional response to hypoxia [327]. Additionally, loss of Rb combined with hypoxia led to exacerbated HIF1-mediated transcriptional responses and concomitant increases in target protein expression and invasion in MCF7 breast cancer cells [327]. Interestingly, loss of Rb function is also associated with progression of several other cancers, including brain [306], lung [296] and prostate [202,237,328].

In prostate cancer, Rb-loss occurs in 25-50% of cases [237,238]. Despite the high frequency of Rb inactivation, few studies have addressed the impact of this on the cellular response to hypoxia. In this study, we examined the consequences of Rb-loss and hypoxia in two different prostate cancer cell lines, 22Rv1 and LNCaP. Using short-hairpin RNA in LNCaP cells to knockdown Rb expression in concert with DNA micro-array technology, we found that Rb-loss deregulates the expression of hypoxia-mediated transcriptional programs that govern angiogenesis, metastasis and neuroendocrine differentiation (NED). Ultimately, this leads to acquisition of a more invasive phenotype and expression of bona fide NED protein markers in human prostate cancer cells.

4.3. Results

4.3.1. Loss of Rb leads to deregulation of hypoxia-regulated genes and hypoxia-dependent acquisition of an invasive phenotype.

Previously, we demonstrated that ARNT, TRIP230 and Rb form a complex and that Rb represses the function of TRIP230 and the transcriptional response to hypoxia [327]. To more clearly define the role of Rb in hypoxia-mediated signaling, we used a retroviral vector expressing a short-hairpin (sh) RNA directed to Rb to permanently knockdown Rb expression in LNCaP prostate cancer cells. Stably infected LNCaP cells had either wild type Rb expression from a scrambled negative control vector (shSCX) or a stably ablated Rb protein (shRb). Total Rb mRNA and protein levels were significantly attenuated in the LNCaP-shRb cells during both normoxia and hypoxia (Figure 4.1A and B). In addition, VEGF and CXCR4 mRNA accumulation in LNCaP-shSCX cells displayed typical hypoxia induction profiles, however, significantly exacerbated transcriptional responses occurred in LNCaP-shRb cells subjected to 24 hours of hypoxia when compared to scrambled controls (Figure 4.1C and D). Taken together, this data supports our notion that loss of Rb leads to dysregulation of hypoxia-inducible transcriptional processes in prostate cancer and reinforces the shRNA LNCaP lines as appropriate models to study this paradigm.

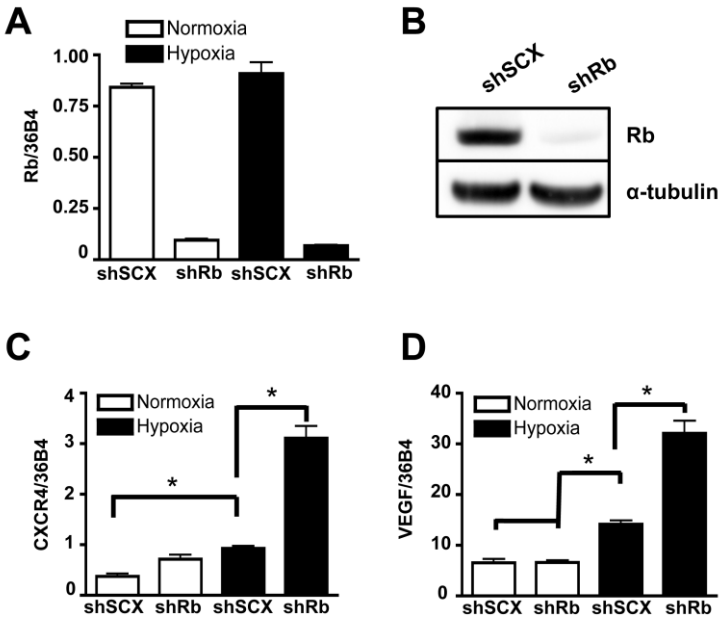

Figure 4.1. Ablation of Rb leads to transcriptional dysregulation of HIF1-target genes involved in metastasis and angiogenesis

(A) LNCaP cells stably infected with either a shRNA to Rb (shRb) or a scrambled negative control shRNA (shSCX) were maintained in normoxic conditions or at 1% O_2 for 24h then gene expression was determined by quantitative real-time PCR after isolation and reverse transcription of total RNA. Rb expression was normalized to the constitutively active 36B4 gene expression. **(B)** Immunoblot analysis of whole cell extracts from shSCX and shRb LNCaP cells using anti-Rb or anti-α-tubulin primary antibodies. α-tubulin is the loading control. (**C)** CXCR4 and **(D)** VEGF mRNA accumulation was determined by RT-PCR after shSCX and shRb LNCaP cells were treated as described in (A). Open bars represent normoxia (20% O_2) and closed black bars represent hypoxia (1% O_2). Error bars represent ± S.D. * $p < 0.05$.

Exacerbated expression of the metastatic marker CXCR4 with Rb-loss and hypoxia led us to hypothesize that LNCaP cells lacking Rb may acquire a more invasive phenotype compared to control cells. In order to determine this, we used Matrigel invasion chambers in concert with 36 hours of hypoxia or normoxia and shRb or shSCX LNCaP cells to test cell-line specific invasive potentials. A significant increase in invasion occurred only in cells depleted of Rb that had been exposed to hypoxia (Figure 4.2A). Next, we monitored cell growth over a 72-hour period to ascertain if increased growth characteristics contributed to the observed increase in invasion. Indeed, loss of Rb alone did not affect proliferation rates when compared to scrambled controls (Figure 4.2B). However, proliferation was significantly inhibited in both shSCX and shRb cells after 72-hours of hypoxia ($p<0.05$) supporting the findings of others [329,330]. Furthermore, subjecting shRNA LNCaP cells to hypoxia and then FACS sorting after propidium iodide

staining revealed no significant differences between treatments and any of the stages of the cell cycle [G1, G2, S or sub-G1] (Figure 4.2C). Hence, these data strongly suggest that loss of Rb in LNCaP cells promotes cell invasion in a hypoxia-dependent fashion and that this effect is not due to increased cell growth or proliferation.

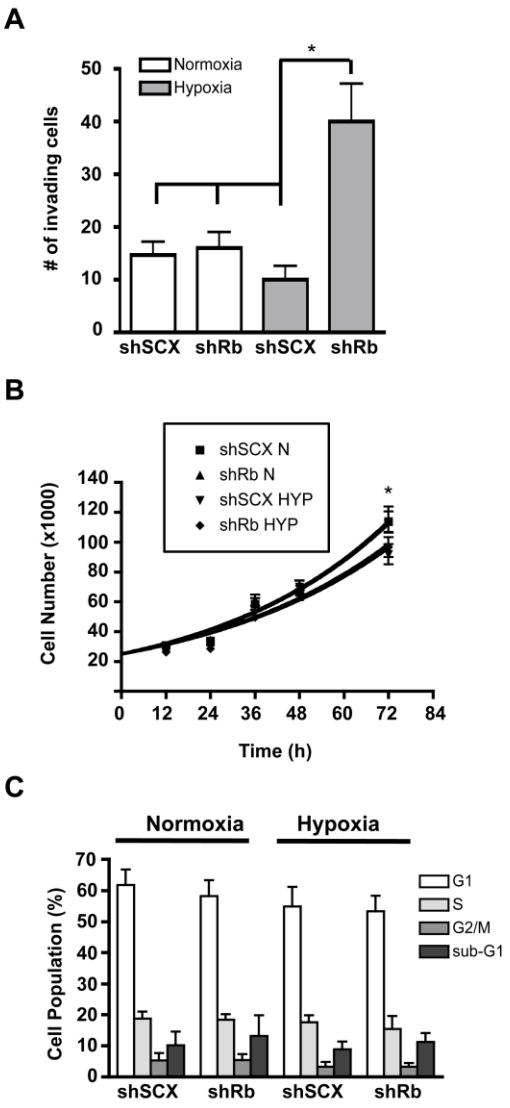

Figure 4.2. Hypoxia-inducible increase in invasion but not cell cycle or proliferation in LNCaP prostate cancer cells lacking Rb

(A) shRNA LNCaP cells ($1x10^4$) were seeded in Matrigel invasion chambers and then maintained in normoxic conditions or at 1% O_2 for 36h. Chambers were then prepared according to manufacturers protocols and cells were counted under a microscope. Assays were performed in triplicate. **(B)** Knock-down of Rb in LNCaP cells does not alter cell proliferation in response to hypoxia. Cells were either left at normoxia or treated with 1% O_2 and cells were counted at 0, 12, 24, 36 48, and 72 h later. Error bars represent ± S.E.M. * $p < 0.05$. **(C)** Knock-down of Rb in LNCaP cells does not alter cell cycle in response to hypoxia. Cell cycle status was determined by propidium iodide (PI) staining and flow cytometry. LNCaP cells with a scrambled negative control or with Rb ablated, were treated with hypoxia or left at normoxic conditions for 36-hours. The percentage of cells in each stage of the cell cycle was determined using FlowJo analysis software based on the PI staining profile of FSC/SSC-gated population. Assay was performed three times and each sample was read in triplicate. Error bars represent ± S.E.M.

4.3.2. Rb regulates specific hypoxia-regulated genetic programs.

With the shRNA cell lines validated, we next used Agilent Genome-Wide human expression arrays and shRNA LNCaP cells either left at normoxia or treated with 1% O2 to delineate the role of Rb in hypoxia-regulated transcriptional programs. We narrowed our scope to focus only on genes whose expression was further exaggerated by loss of Rb in a hypoxia-dependent fashion as these are the genes that are most likely regulated by the HIF1-Rb complex. Thus, we selected genes from the shRb-hypoxia-treated data set that were up- or down-regulated significantly ($p<0.05$) at least 2.0 fold when compared to the other treatments.

For all up-regulated genes (Hyp-Rb vs. all other conditions; > 2-fold increase), micro-array analysis revealed that there are 383 genes that are significantly up-regulated by loss of Rb and hypoxia (Supplementary Data File 1, Table 1). In addition, of the 383 up-regulated genes, 69 are hypoxia inducible (Hyp-SCX vs Norm-SCX; > 2-fold increase), 27 are sensitive to loss of Rb (Norm-Rb vs Norm-SCX; > 2-fold increase) and 10 genes are both hypoxia inducible and sensitive to Rb-loss. Thus, 297 up-regulated genes are not sensitive to either loss of Rb or hypoxia alone but have exacerbated transcriptional responses with Rb-loss and hypoxia in combination (Figure 4.3A). We realize that due to our arbitrary 2-fold increase cut-off, many of these 297 genes are likely regulated by hypoxia or are sensitive to Rb-loss but these changes are ignored in this analysis. Nevertheless, the analysis narrowed our focus so that only the most sensitive targets were highlighted for subsequent investigation, as these targets are likely the true effectors of cancer cell transformation via the Rb-HIF1 transcriptional complex. The complete dataset from the arrays can be viewed at (http://www.ncbi.nlm.nih.gov/geo/query/acc.cgi?acc=GSE78245).

Evidence in the literature suggests that Rb may mediate transcriptional repression by recruiting chromatin modifiers to manipulate chromatin structure [327,331-334]. Furthermore, knockdown or loss of epigenetic regulators can affect distinct chromosomes or modulate specific gene clusters [335-337]. Thus, we were interested to determine if Rb attenuates hypoxia-regulated transcription in the same fashion. A pie chart of all the up- and down-regulated genes and their associated chromosome is presented in Figure 4.3B. A Fisher's exact test demonstrated that the total number of

genes on each chromosome from our list is not significantly different from the normal distribution of genes in the genome on each chromosome. However, we used the BioMart program and Ensemble Genes 70 and Homo sapiens genes (GRCh37.p10) databases to arrange significantly up- and down-regulated genes on chromosomes according to their annotated start and stop base pairs. When genes were mapped in this fashion, for example on chromosomes 1 and 21, a clustering pattern was observed (Figure 4.3C) for a large number of genes. Graphical representation of all genes and associated chromosomal start and stop locations are presented in the Supplementary Data File 2. To test if these distributions are different the distance between genes was calculated for genes on chromosome 1 and 21. This was done once for the genes of interest and then for 65 randomly chosen genes from chromosome 1 and 21. For these genes the median distance was calculated. The random choosing was repeated 100 times to generate a distribution of random medians. For both chromosome 1 and 21, the difference between the distribution of genes on our list and the randomly chosen genes was significantly different (p-value = 2.156e-05 and p-value < 2.2e-16, respectively). This pattern was observed on many other chromosomes (Supplementary Data File 2) suggesting that many of the Rb-sensitive hypoxia-regulated genes are in close proximity to one another (over several million basepairs). Taken together, our data suggest that the Rb regulates well-ordered hypoxia-inducible genetic programs. In addition, loss of Rb function permits exaggerated expression of gene within specific genomic regions and this may facilitate prostate cancer progression.

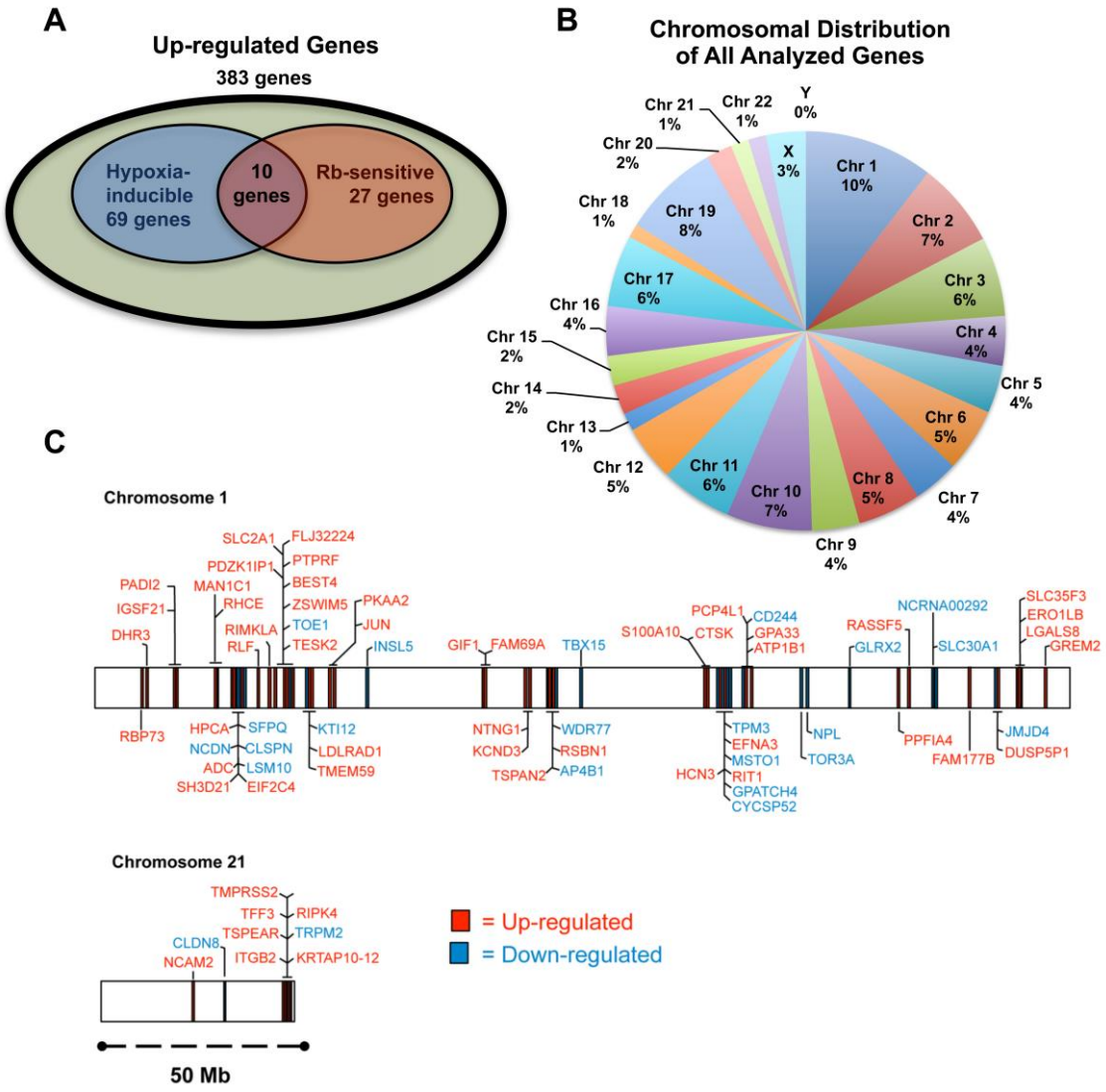

Figure 4.3. The role of Rb in HIF1-mediated transcription.
LNCaP cells infected with either a short-hairpin control RNA (shSCX) or a short-hairpin to Rb (shRb) were maintained under hypoxic (1% O_2) or normoxic (20% O_2) conditions for 24 h. Extracted RNA was subjected to microarray analysis. Experiments were performed in triplicate and only genes that were up- or down-regulated at least 2-fold under hypoxic conditions with a p-value <0.05 were considered significant. **(A)** Venn diagram of up-regulated genes, showing the overlap between hypoxia inducible genes, genes sensitive to loss of Rb and up-regulated genes sensitive to Rb-loss and hypoxia in combination. Olive shaded area represents genes that are from the shRb-hypoxia-treated data set that were up-regulated significantly (p<0.05) at least 2.0 fold when compared to the other treatments. Blue shaded area represents genes that are hypoxia-inducible. Red shaded area represents genes that are up-regulated by Rb-loss. **(B)** A pie chart was used to illustrate the percentage of genes on each chromosome that were up- or down-regulated in Rb knockdown LNCaP cells. (**C)** Genes regulated by the Rb-HIF1 complex cluster at certain loci on select chromosomes. Chromosome maps of all the up- and down-regulated genes according to their annotated start and stop sites, chromosomes 1 and 21 are represented to scale.

4.3.3. Loss of Rb dysregulates hypoxia-mediated metastatic and neuroendocrine transcriptional programs in human prostate cancer cells.

We identified a cohort of genes whose hypoxia-inducible transcriptional activity is either bolstered or activated by loss of Rb (383 genes). Conversely, we have also identified a cohort of down-regulated genes whose transcription is further repressed by Rb-loss and hypoxia (155 genes, Supplementary Data File 1, Table 2). Surprisingly, of the top 25 genes identified whose transcription is enhanced after Rb-loss under hypoxic conditions, 7 are neuronal markers or are associated with neuroendocrine differentiation (NED), including HTR5A [338], RORA [339], KISS1R [340], ALDOC [341], and ENO2 (a clinical hallmark of NED) [342]. Furthermore, 7 genes in the top 25 are associated with metastasis and/or angiogenesis, such as CXCR4, ANGPTL4 [343], PLOD2 [250], NDRG1[344] and STC1[345]. Finally, 15 of the top 25 up-regulated genes are directly regulated by either HIF1α or HIF2α or are known to be hypoxia-inducible (Table 4.1) [326,346-357]. For the 10 remaining up-regulated genes, we performed an in silico consensus ARNT:HIF1α binding site analysis using reported DNA sequences and the JASPAR database [358,359]. The analysis determined that all 10 genes contained multiple consensus sequences for HIF1 binding sites that may bind the ARNT:HIF1α transcriptional complex (Supplementary Data File 1). This data supports our previous findings that Rb regulates the HIF1 transcriptional complex [327] and that Rb-loss under hypoxic stress leads to aberrant expression of HIF1 target genes involved in metastases and NED.

Table 4.1. The top 25 up-regulated genes that are induced greater than 2-fold by a combination of loss of Rb and hypoxia when compared to negative controls. The (*) denotes genes containing putative HREs identified in the *in silico* consensus ARNT:HIF1α binding sequence analysis (Supplementary Data File 1).

Gene Name	Probe Name	Fold Induction (vs shSCX-N)			Hypoxia Inducible/HIF1-regulated
		shRb-N	shSCX-HYP	shRb-HYP	
HTR5A	A_23_P42565	2.07	27.41	256.40	[353]
PLOD2	A_33_P3318581	2.53	24.26	219.02	[326,351,353]
SLC16A3	A_23_P158725	1.73	24.85	200.17	[354]
ATP4A	A_23_P430728	2.46	12.53	157.93	*
PLA2G4D	A_33_P3361611	1.15	10.05	97.72	*
NIM1	A_23_P254863	1.32	5.73	91.57	*
CYP26A1	A_23_P138655	1.15	2.87	68.51	*
CXCR4	A_23_P102000	1.30	2.65	62.56	[352]
KISS1R	A_33_P3231357	0.61	8.51	61.94	*
ANGPTL4	A_33_P3295358	1.92	3.63	53.17	[348,353]
GPR26	A_23_P305581	0.98	9.84	53.00	*
MYBPC2	A_33_P3257182	1.18	3.74	50.39	*
FOS	A_23_P106194	1.47	1.41	49.01	[353]
PPFIA4	A_23_P420692	1.61	8.32	39.76	[356]
CA9	A_23_P157793	1.18	2.09	28.63	[351,353,357]
NFATC4	A_33_P3250083	1.52	4.70	21.97	[351]
PFKFB4	A_24_P362904	1.53	2.94	21.82	[350,351,353]
PCP4L1	A_32_P214665	1.97	2.51	21.02	*
RORA	A_23_P26124	1.40	2.57	20.81	[349]
AMPD3	A_24_P304154	0.91	0.89	19.43	*
ALDOC	A_23_P78108	1.46	4.85	19.33	[351,353]
ENO2	A_24_P236091	1.80	2.61	19.09	[351]
SCNN1G	A_23_P206626	1.10	1.30	19.01	*
STC1	A_23_P314755	1.10	4.42	19.00	[347]
NDRG1	A_23_P20494	1.19	6.80	18.60	[346,355]

Hierarchical clustering was performed using Ingenuity Pathway Assist (IPA) on the top 50 genes whose expression was most up-regulated with Rb-loss and hypoxia (Figure 4.4A). Interestingly, the top two diseases associated with the 50 genes are

cancer (32 molecules) and neurological disease (17 molecules). Moreover, the top two cellular and molecular functions associated with these genes are cell death and survival (10 molecules) and cellular movement (17 molecules). Importantly, gene ontology analysis revealed that the top two associated transcription factors were HIF1α (p-value of overlap = 2.49E-15) and EPAS/HIF2α (p-value of overlap = 2.30E-14), thus strengthening our hypothesis that this phenomenon is mediated via a HIF-regulated mechanism and not an idiosyncratic effect of the short hairpin RNA. The summary of the IPA analysis can be found in Supplementary Data File 3. Taken together, this analysis indicates that the top 50 up-regulated genes support prostate cancer initiation or progression through up-regulation of pro-metastatic and neuroendocrine programs.

Although the IPA analysis of the top 50 up-regulated genes provided valuable insight on hypoxia-inducible oncogenic targets, the true consequences of Rb-loss on hypoxia-regulated transcriptional programs were highlighted when the top 50 down-regulated targets were also included in the analysis. IPA analysis determined that the top physiological system development and function associated with these 100 genes are 1) nervous system development and function (21 molecules), 2) tissue morphology (24 molecules), 3) organismal development (32 molecules), 4) digestive system development (12 molecules) and 5) organ morphology (23 molecules). The top molecular functions are cell morphology (27 molecules) and cellular movement (24 molecules). For all physiological systems and molecular pathways involved, the –logP values are all greater than 4 and this suggests a highly significant relationship between the identified genes and associated pathways (Figure 4.4B). Finally, the top two associated network functions are (1) Cellular Movement, Hematological System Development and Function, Immune Cell Trafficking (Supplementary Data File 1, Figure 1) and (2) Neurological Disease, Psychology Disorders, Cardiovascular Disease (Figure 4.4C). The complete IPA analysis summary can be found in the Supplementary Data File 3 and all identified networks can be found in the Supplementary Data File 1 (Figures 1-6). Analysis of the neurological disease network identified several key up-regulated targets such as HTR5A, KISS1R and GPR146. Moreover, the network analysis identified nodes in signaling cascades like PI3K, MAPK and NFκB as the ultimate downstream targets for disease progression. There were no significantly down-regulated genes identified in the neurological disease network however, the power of the

analysis relies only on the known associations in the literature. We have confirmed the array data for the putative neuroendocrine markers ENO2, KISS1R, HTR5A and PLOD2 through qRT-PCR (Figure 4.5A). Likewise, the array confirmed PLOD2 and CXCR4 as bona fide targets of the Rb-HIF1 complex that we reported previously [327]. Importantly, knockdown of DP1 protein with siRNA did not significantly alter the hypoxia inducible accumulation of ENO2, KISS1R, HTR5A or PLOD2 in our shRb knockdown cells (Supplementary Data File 1, Figure 7). This strongly suggests that these genes are not E2F regulated.

LNCaP cells are classically defined as AR positive, hormone-responsive and metastatic prostate cancer cells [360]. Furthermore, LNCaP cells can transition to a neuroendocrine state through androgen deprived culturing methods [227]. Thus, we were interested in determining if the observed transcriptional responses could be recapitulated in another prostate cancer cell line that is already androgen-insensitive. We therefore retrovirally introduced the shSCX and shRb constructs into 22Rv1 prostate cancer cells and subjected transformed cells to normoxic or hypoxic conditions. The shSCX 22Rv1 cells expressed Rb protein while the shRb cells had significant Rb knockdown. Notably, ENO2, KISS1R and PLOD2 transcriptional levels in the shRNA 22Rv1 cells mirrored the LNCaP shRNA transcription profiles and were exacerbated under hypoxic conditions with loss of Rb (Figure 4.5B). Interestingly, HTR5A did not respond in the same fashion but this may be due to a cell-type specific response. Nevertheless, this data suggests that Rb modulates hypoxia-regulated gene programs in prostate cancer independent of clinical stage or cell-type.

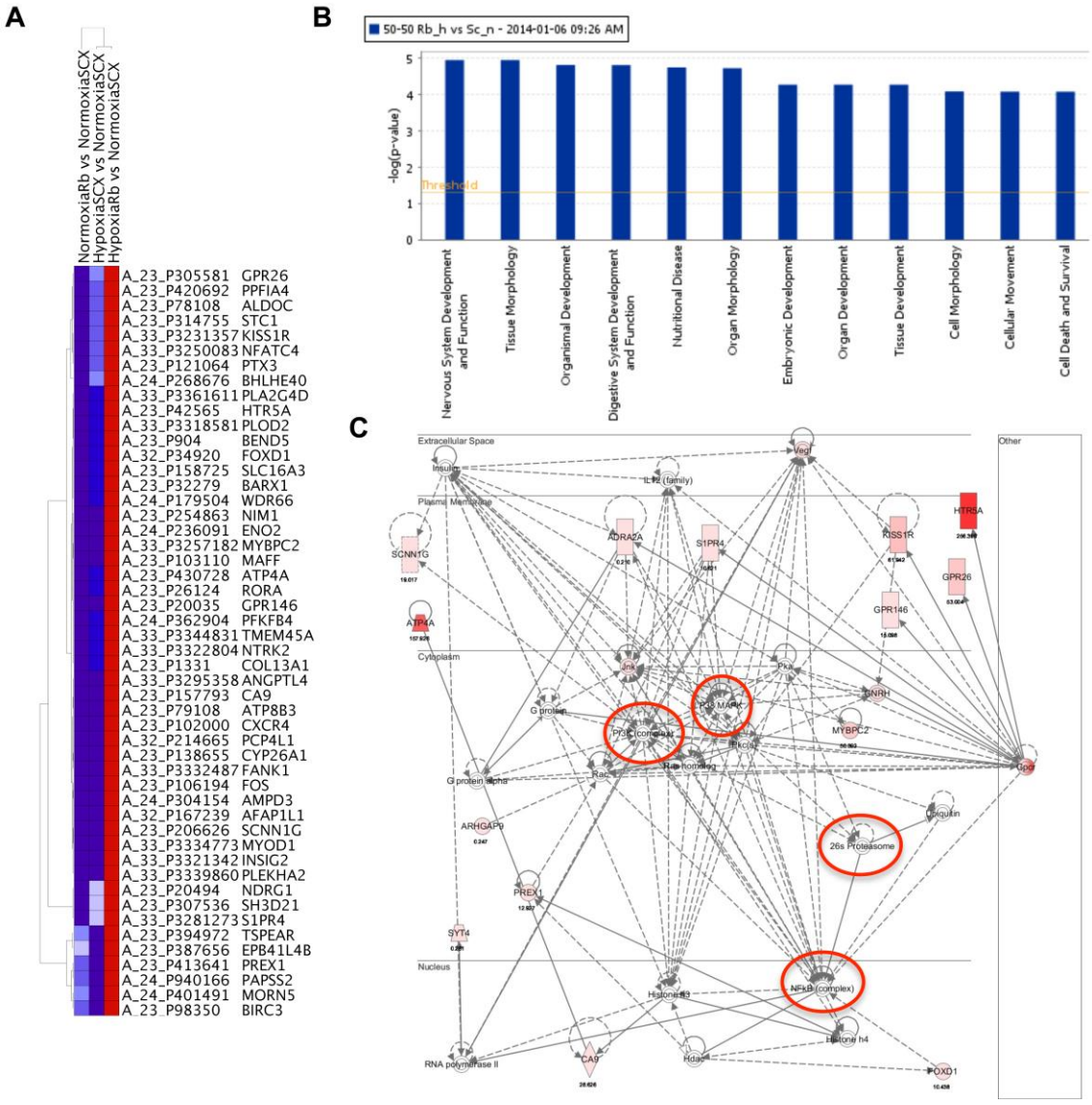

Figure 4.4. Rb-loss leads to transcriptional dysregulation of HIF1-target genes involved in metastasis, angiogenesis and neuroendocrine differentiation.

(A) Heat map of the 50 genes displaying the largest increase in fold gene expression in response to hypoxia after knock-down of Rb. **(B)** The top systems and diseases identified by Ingenuity Pathway Assist (IPA) analysis. The top 12 systems and diseases associated with the 50 most up-regulated and 50 most down-regulated hypoxia sensitive genes after knock-down of Rb. The –log of the p-value is represented on the ordinate. **(C)** Nervous system development and function network identified by IPA analysis. Nodes identified are indicated with red circles. Up-regulated genes identified in our micro-array screen are filled with varying shades of pink and red with the most highly expressing genes shaded red and the lower expressing genes shaded pink.

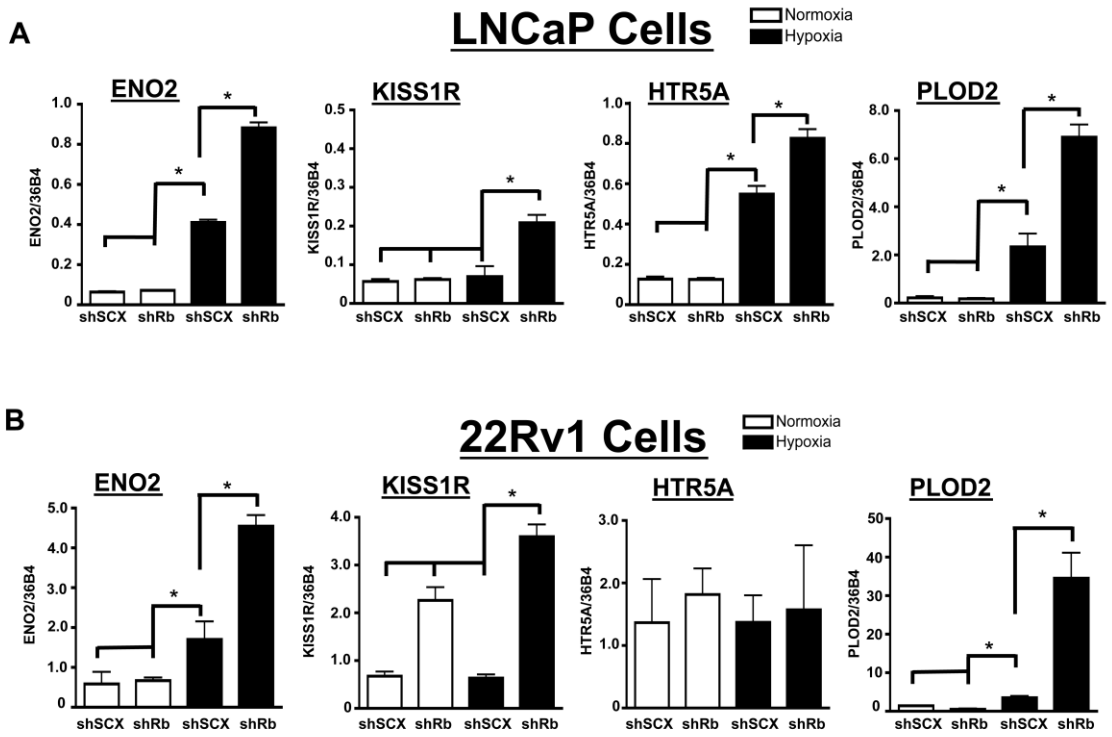

Figure 4.5. Confirmation of Rb-sensitive and HIF1-regulated neuroendocrine targets identified through microarray analysis.

(A) LNCaP or **(B)** 22Rv1 cells infected with either a short-hairpin control RNA (shSCX) or a short-hairpin to Rb (shRb) were maintained under hypoxic (1% O_2) or normoxic (20% O_2) conditions for 24 h. Extracted RNA was subjected to qRT-PCR. Transcriptional responses of ENO2, KISS1R, HTR5A and PLOD2 are displayed and expression was normalized to the constitutively active 36B4 gene expression. Open bars represent normoxia (20% O_2) and closed black bars represent hypoxia (1% O_2). Error bars represent ± S.D. * $p < 0.05$.

4.3.4. Rb-loss results in a hypoxia-dependent increase in expression of proteins involved in metastasis and neuroendocrine differentiation in human prostate cancer cells.

To further validate the array, we used the shRNA expressing LNCaP and 22Rv1 cells and immunoblotting to measure the level of protein expression for identified genes. The shRNA cell lines were exposed to normal O_2 levels or 1% O_2 for various times up to 7 days. Protein levels for the most highly expressing genes (HTR5A, KISS1R, PLOD2, ENO2, NDRG1 and RORα) imitated the transcriptional responses observed in the array (Figure 4.6A and B). In addition, shRb cells exposed to chronic hypoxia (2-7 days) exhibited a more exacerbated protein expression for the targets of interest than cells that

were treated with acute hypoxia (24 hrs). This observation supports our hypothesis that the key effectors of cellular transformation and metastasis require both transcriptional and translational processes for exacerbated accumulation with Rb-loss and hypoxia. Additionally, these data support a role for the Rb-HIF1 complex in the maintenance of normal cell physiology and the loss of Rb leads to activation of hypoxia-regulated networks involved in cellular movement and transformation that drive prostate cancer cells to acquire metastatic and neuroendocrine phenotypes.

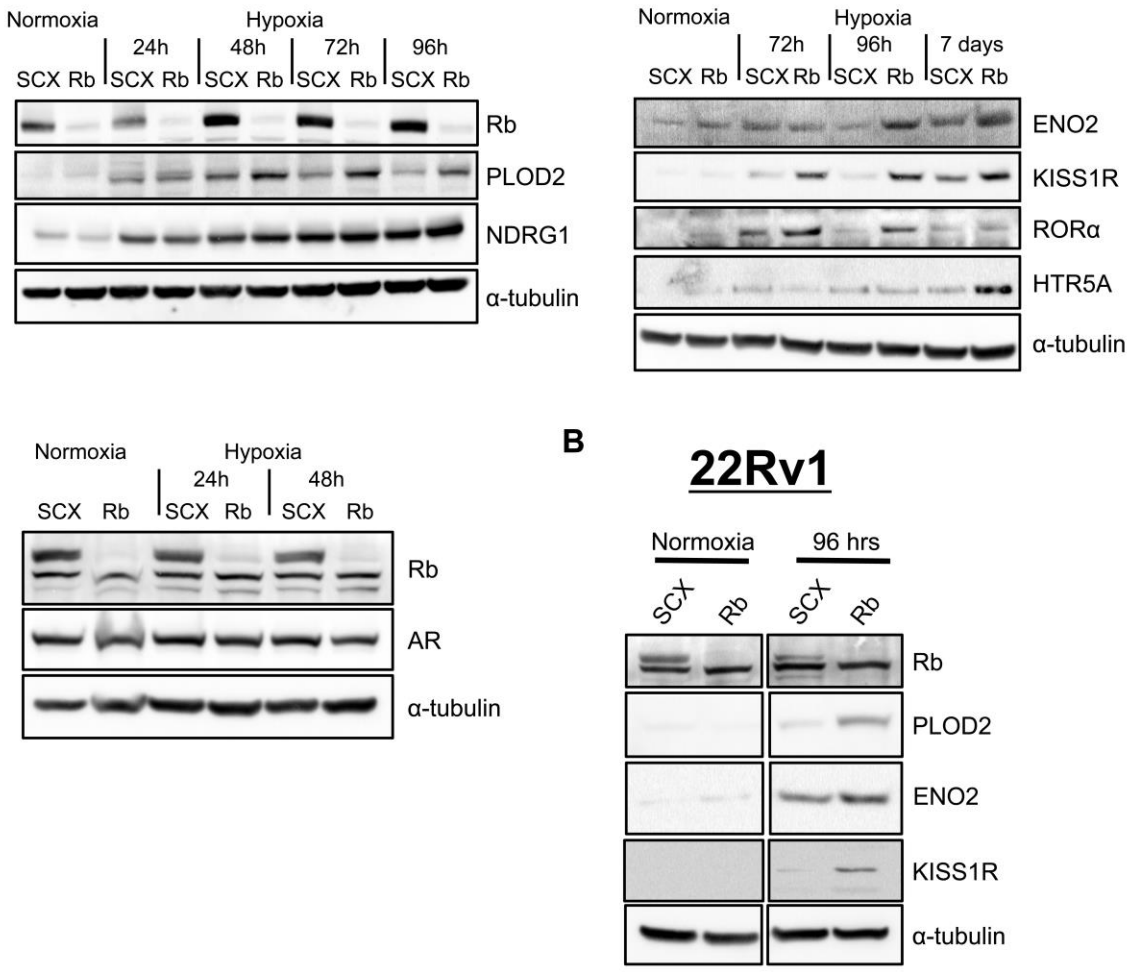

Figure 4.6. Loss of Rb results in increased expression of proteins involved in metastasis and neuroendocrine differentiation in prostate cancer cells in a hypoxia-dependent fashion.

(A) LNCaP and **(B)** 22Rv1 shRNA cells were exposed to normal O_2 levels or 1% O_2 for various times up to 7 days as indicated. Whole cell lysates were fractionated by SDS-PAGE and examined by immunoblotting using affinity purified antibodies to α–tubulin, Rb, ENO2, KISS1R, RORα, PLOD2, NDRG1 and HTR5A.

4.3.5. KISS1R is linked to intracellular calcium mobilization in 22Rv1 cells.

The significant increases in both mRNA and protein expression after Rb-loss and hypoxia for several of our identified array genes suggests that functional consequences specific to these genes may be present. Kisspeptin/KISS1R interactions and activation

of the Gqα–p63RhoGEF signaling cascade has been identified as a driver of metastasis in breast cancer cells [361]. Additionally, activation of Gqα is canonically coupled to an increase in cellular calcium mobilization. Thus, to establish if KISS1R expression can influence sensitivity to kisspeptin in prostate cancer, we performed fluorescence based calcium mobilization assays in control (shSCX) and shRb LNCaP and 22Rv1 cells after normoxia or hypoxia treatments. Despite strong immunocytochemical staining of KISS1R in the cytoplasm and cell membrane in hypoxia treated shRb LNCaP cells (Supplementary Data File 1, Figure 8), 1 uM Kisspeptin-10 failed to produce a detectable calcium mobilization response in LNCaP cells (Figure 4.7A). However, in shRb 22Rv1 cells subjected to 96 hours of hypoxia, application of 1 uM Kisspeptin-10 peptide led to a significant increase in intracellular calcium levels compared to shSCX hypoxia cells and to shRb and shSCX normoxia cells (Figure 4.7B). Many possible explanations exist for why kisspeptin-10 failed to trigger intracellular calcium release in hypoxic shRb-LNCaP cells. Most GPCRs require proper folding and targeting to the membrane in order to function [362]. Indeed, many GPCRs exist in the membrane and are non-functional due to improper folding [363]. Another possible explanation is that LNCaP cells do not express the Gq subunit required for KISS1R coupling or that KISS1R is coupled to another signal transducer. Taken together, these data suggest that PCa cells that lose Rb in a hypoxic environment undergo dramatic molecular, biochemical, physiological and phenotypic changes. These adaptations enable them to better tolerate an oxygen-deprived environment and aid in the transformation to a more aggressive cancer phenotype.

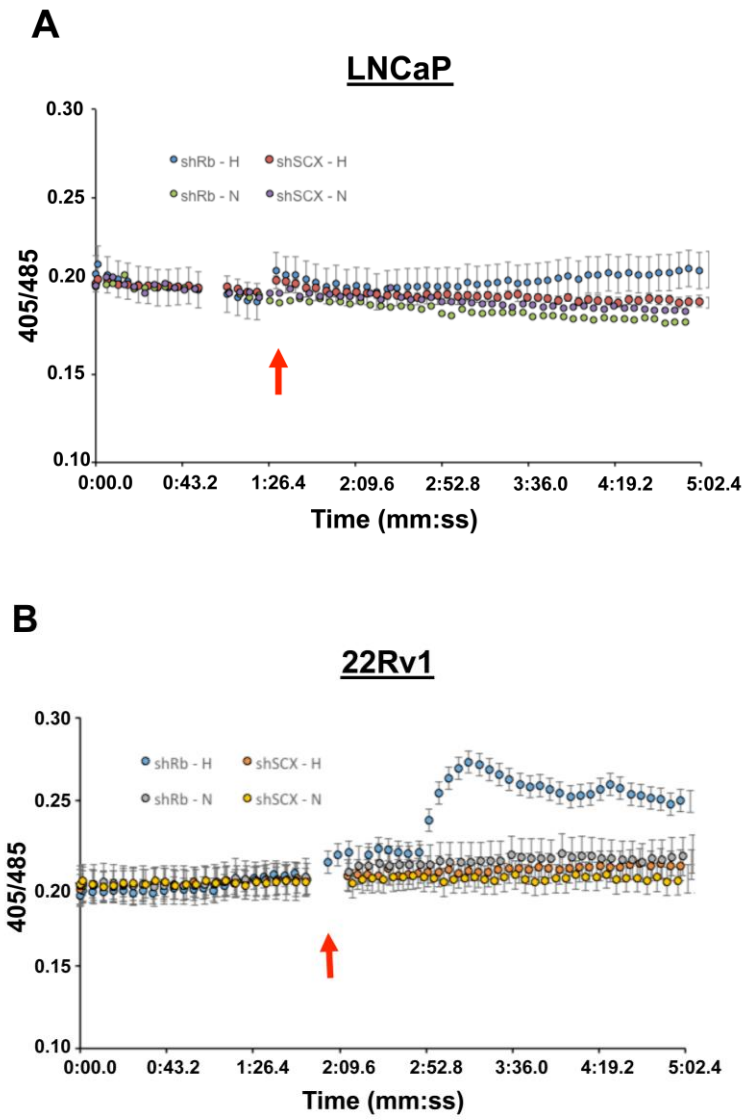

Figure 4.7. Kisspeptin-10 activates calcium signaling in 22Rv1 cells.
Application of 1 uM Kisspeptin-10 peptide in **(A)** LNCaP or (**B**) 22rV1 cells lacking Rb (shRb) and subjected to 96 hours of hypoxia led to a significant increase in intracellular calcium levels compared to control scrambled (shSCX) hypoxia cells and to normoxia cells (both shRb and shSCX) in 22Rv1 cells only. After hypoxia or normoxia treatment, cells were loaded with 2 uM indo-1AM dye (30 min at 37°C) and then imaged on an inverted fluorescent microscope. Application of 1 uM Kisspeptin-10 (indicated by red arrows) led to a significant increase intracellular calcium levels in 22Rv1 cells as indexed by ratiometric fluorescence measurements taken at 405 and 485 nm. Black arrow represents application of 2 uM ionomycin. One-way ANOVA followed by post-hoc Tukey test. * $p<0.05$, ** $p< 0.01$ vs 1:20 time point, n = 5.

4.4. Discussion

In healthy tissue, HIF proteins are tightly regulated and hypoxia via the HIF1 complex activates genetic programs regulating key physiological functions in a coordinated fashion [126]. However, chronic hypoxia in solid tumor microenvironments leads to activation of HIF1 transcriptional programs, microvascular hyperplasia and metastasis and this promotes tumor progression [364]. In addition, loss of Rb function or genetic ablation of RB1 has been implicated in advanced stages of brain cancers [305,306], lung cancer [294] and in 25-50% of late stage prostate cancer cases [237,238]. As a result, we were interested in further investigating the physiological connection between Rb function and hypoxia-inducible gene expression, especially hypoxia-regulated transcriptional programs involved in cancer cell transformation. Previously, we demonstrated that Rb attenuates the HIF1-mediated physiological response to hypoxia and that it is an integral and indispensable part of the HIF1 transcriptional complex by virtue of a direct interaction with TRIP230 [150,327]. The TRIP230 protein is a member of the coiled-coil coactivator family of proteins and was first isolated as a thyroid hormone-dependent coactivator of TR-mediated signaling [149]. In addition, Rb associates with TRIP230 through distinct interaction motifs and this association dampens TRIP230 coactivator potential [149,327]. Subsequent studies have established a function for Rb independent from its role in E2F-mediated regulation of cell cycle by determining that only the hyper-phosphorylated form of Rb interacts with TRIP230 [153,327]. Further characterization of TRIP230 revealed that it is also a part of the p160 coactivator complex [293] a bona fide transcriptional coactivator complex associated with ARNT during activated transcription [49]. Finally, TRIP230 interacts with ARNT as a coactivator in hypoxia signaling and HIF1-mediated transcriptional activity is abolished in cells depleted of TRIP230 [150,155]. Thus, TRIP230 is a multifaceted coactivator protein that is required for the physiological response to hypoxia.

In this study, we examined the consequences of Rb-loss and hypoxia in LNCaP and 22Rv1 prostate cancer cells. Permanent Rb knockdown led to a concomitant dysregulation of hypoxia-inducible transcriptional activity and increased invasiveness in a hypoxia-dependent fashion (Figures 4.2 and 4.5). In addition, we used DNA microarray technology to identify novel gene targets regulated by the Rb-HIF1 complex and to

determine how Rb-loss and hypoxia affect the genetic landscape in prostate cancer evolution. The micro-array analysis identified 383 up-regulated genes and 155 down-regulated genes sensitive to Rb-loss and hypoxia (Figure 4.3A). Interestingly, these genes highlight a function for Rb in the attenuation of hypoxia-regulated transcriptional programs that govern both metastasis and neuroendocrine differentiation (NED). Thus, loss of Rb expression or function in combination with hypoxia leads to up-regulation of bona fide and newly discovered neuroendocrine and metastatic markers at the protein level and highlights a hitherto unrecognized mode of cellular transformation in prostate cancer models. Clinically, loss of Rb implies either ablation of gene/protein or loss-of function. Loss-of-function of pRb while retaining protein immuno-reactivity is well documented in prostate cancer and other solid tumor types [192,365,366]. We mimicked loss of Rb using retroviral expression of short-hairpin RNAs to knock-down Rb in the LNCaP and 22Rv1 cells lines. Thus, attempts to correlate pRb levels with neuroendocrine markers of any other gene candidates culled from our experiments likely would be uninformative.

We recognize that a limitation to our analysis is that some bona fide hypoxia-sensitive and Rb-sensitive targets are shifted to the hypoxia-insensitive or Rb-insensitive classes due to the arbitrary 2-fold induction requirement. However, this analysis narrowed the focus to targets that are most sensitive to Rb-loss and hypoxia and elucidated four intriguing possibilities in our paradigm. Firstly, that many genes are directly hypoxia-inducible and contain hypoxia response elements (HREs) in their regulatory regions and that loss of Rb unmasks the full coactivation potential of TRIP230 during HIF1-mediated transcription. This permits exacerbated expression of pro-metastatic and neuroendocrine markers in solid tumor microenvironments that are not normally expressed or are expressed at low levels in oxygenated tissues or in cells expressing functional Rb. Secondly, there is the possibility that the TRIP230-Rb interaction exists with other transcription factors on the affected genes and these parallel pathways are also affected by Rb-loss. This likelihood should be the focus of future investigations. Thirdly, some of these genes may also be downstream effectors of primary HIF1/Rb target genes. However, we exposed cells to hypoxia for only 24 hours in an attempt to minimize noise from expression of downstream targets. Finally, Rb in the context of the HIF1α-ARNT-TRIP230 complex, may be involved in long-range

genomic interactions and genes in close proximity to HIF1α-ARNT-TRIP230-regulated genes are significantly impacted by loss of Rb. Interestingly, the latter point is further supported by statistical analysis and chromosome maps for up- and down-regulated genes displaying base pair start and stop sites (Figure 4.3C). The analysis revealed that many of the Rb-sensitive hypoxia-regulated target genes are relatively close to each other on many chromosomes. This suggests that Rb may be important for maintaining proper chromatin structure. The ability for Rb to recruit chromatin modifying proteins to DNA-regulatory elements has been well established with confirmed interactions between SUV39H1 [332], HDACs [327,333], DNMT1 [334] and SIN3a/b [327]. Moreover, 3-dimensional chromatin interactions such as chromatin looping, constitute a primary mechanism for regulating transcription in mammalian genomes and has been demonstrated for ERα-regulated transcriptional programs [336] and CTCF-mediated chromatin organization and transcriptional regulation [337]. It was previously determined that ~15% of HREs in the genome are in long-range relationship to genes (>50 kb) and this suggests that a significant number of HIF1-regulated genes could be affected by long-range transcriptional activities [367]. Undoubtedly, more research is required to determine the exact mechanisms Rb employs to attenuate HIF1 transcription, however we speculate that the HIF1-TRIP230-Rb complex regulates some genetic programs through long-range chromatin interactions, such as chromatin looping, and Rb-loss leads to deregulation of these chromatin interactions.

One of the startling revelations of this research was the observation that certain clinical and prognostic markers of advanced stages of prostate cancer were manifested in hypoxic LNCaP and 22Rv1 cells after loss of Rb. The evolution of prostate cancer from initial diagnosis and treatment ultimately determines clinical outcome. Neuroendocrine prostate cancer (NEPC) is an androgen receptor-negative prostate cancer subtype that can occur sporadically but most commonly evolves from primary prostate adenocarcinoma [220]. In addition, NEPC has a poor clinical outcome and may represent ~25% of late stage prostate cancer [219,220]. Recent molecular characterization of NEPC showed up-regulation of AURKA and MYCN expression and co-operative function to induce neuroendocrine differentiation in prostate cancer cells [368]. However, molecular determinants of NED remain understudied and poorly characterized. We have demonstrated that Rb-loss in conjunction with hypoxia leads to

acquisition of a more invasive phenotype in LNCaP cells (Figure 4.2A) and expression of neuroendocrine markers in prostate cancer cells (Figure 4.6A and B). Microarray analysis using IPA identified a network of genes that may contribute to NED, namely HTR5A, KISS1R and ENO2. ENO2 (neuron-specific enolase, NSE) is a marker that is characteristically expressed in neuroendocrine prostate cancers and is used in clinical settings to determine prostate cancer progression [342]. Thus, the exacerbated expression of ENO2 in shRb cells exposed to hypoxia provides further support that Rb-loss in late stage prostate cancers permits transformation to a neuroendocrine state (Figure 6A and B).

A hallmark of NEPC is sensitivity to serotonin and other neuro-signaling molecules that support cell growth and proliferation [369]. The striking up-regulation of HTR5A mRNA and protein levels only in prostate cancer cells exposed to hypoxia and lacking Rb expression (Figure 4.4 and 4.5) leads to the possibility that NE cells may develop sensitivity to serotonin in this fashion. This is the first time HTR5A has been implicated in prostate cancer progression and development of HTR5A antagonists may prove to be a viable treatment option for men who develop neuroendocrine prostate cancer. Moreover, we identified exacerbated expression of KISS1R protein in both LNCaP-shRb and 22Rv1-shRb cells when exposed to hypoxia (Figure 4.5). The KISS1 molecule was originally identified as a metastasis inhibitor and potent activator of KISS1R (GPR54) [370]. However, the KISS1/KISS1R signaling cascade is also critical for controlling the gonadotropic axis by stimulating GnRH release from neurons in the hypothalamus [371]. Chronic exposure to KISS1 analogs desensitizes KISS1R and attenuates GnRH release leading to decreased plasma testosterone levels [372,373]. Hence, the therapeutic potential of KISS1R agonists in treating men with prostate cancer has recently been investigated. Phase 1 trials for TAK-448 revealed that it is an inhibitor of the hypothalamic-pituitary-gonadal axis and that sustained exposure potently decreased testosterone levels and prostate-specific antigen through KISS1R desensitization [374]. However, therapeutic programs using KISS1 agonists to modulate KISS1R-expressing neurons likely activate KISS1/KISS1R signaling in individual cancer cells. KISS1R expression has been identified as a driver of metastasis in breast cancer cells [361]. Activation of Gqα–p63RhoGEF signaling cascade through autocrine KISS1/KISS1R signaling [361] and transactivation of EGFR through direct association

with KISS1R [375] are thought to be the key pathways involved in KISS1R-mediated metastasis. Interestingly, our microarray analysis determined that shRb LNCaP cells exposed to hypoxia led to a 7.56-fold increase in EGFR expression (Supplementary Data File 1, Table 1). Additionally, our data suggests that KISS1R may be linked to Gq to initiate intracellular calcium mobilization in at least some compromised prostate cancer cells (Figure 7B). This may have implications for the therapeutic use of kisspeptin agonists and antagonists in the treatment of metastatic castration resistance prostate cancer (mCRPC), however the clinical significance and relationship between EGFR up-regulation and pro-metastatic KISS1R-signaling remains to be determined. Our observed increases in KISS1R expression in both LNCaP and 22Rv1 cells after Rb-loss and hypoxia were surprising as a previous report suggested that KISS1 inhibits metastasis and that both KISS1 and KISS1R protein levels appear to decrease with prostate cancer progression [376]. However, Wang and colleagues suggest that the anti-metastatic activity of KISS1 is likely elicited through pathways independent of KISS1R [376]. Furthermore, our data suggests that KISS1R expression only occurs in hypoxic tumor environments after Rb-loss and these parameters were not determined for the tissue specimens in the previous report.

The identification of PI3K, MAPK and NFκB through IPA analysis as central nodes of the Rb-dependent hypoxia signal in the neurological disease network leads to the intriguing possibilities of new drug targets for late stage prostate cancer (Figure 4.4C). The NFκB system mediates the inflammatory response and is associated with the invasive cancer cell phenotype [377]. Nuclear localization and activation of NFκB targets is also associated with metastasis and prostate cancer progression [378,379]. Seventeen of the highest expressing genes in this network were identified in our screen as being hypoxia-inducible and sensitive to loss of Rb. Nine of these seventeen genes transduce signals to modulate NFκB activity. This suggests a role for Rb-loss and hypoxia in NFκB signaling and that activation of the NFκB pathway in prostate cancer may signal a progression to metastatic, castrate-resistant or neuroendocrine disease. Likewise, the PI3K pathway is crucial for LNCaP survival in androgen deprived environments and PI3K inhibition stabilizes p27kip1 expression [380]. Lastly, eight of the 17 genes in this network that were identified in our screen directly activate the ERK1/2 pathway, which was identified as a major node of this network and is a mediator of

neoplastic cell invasion and transformation [381]. The over expression of several Rb-sensitive hypoxia-inducible factors promote invasion including CXCR4 [382], ANGPTL4 [343], PLOD2 [250], NDRG1[344] and STC1[345]. The identified nodes pose an avenue of further research to determine if prostate cancer cell transformation can be blocked through inhibitors of the MAPK signaling cascade or if targeting the individual up-regulated factors with chemotherapeutic agents can effectively combat neuroendocrine cancers.

Castration Resistant Prostate Cancer (CRPC) is a common progression after surgical resection or hormone deprivation therapy for initial prostate tumors. The CRPC stage is characteristically hormone refractory (androgen-insensitive) due to constitutively active AR activity or selection of cells that bypass requirements for AR-mediated growth and proliferation [231]. Furthermore, transition to metastatic CRPC is associated with a poor prognosis and treatment options become limited and rarely curative [231]. We determined that permanently ablated Rb expression in the 22Rv1 cell line leads to hypoxia-mediated increases in pro-metastatic genes (Figure 6B). This suggests that loss of Rb in CRPC contributes to the progression and lethality of the disease and that cellular transformation through the Rb-TRIP230-HIF1 complex is not just a function of hormone-sensitive or early stage prostate cancers. A previous study determined that Rb-loss in LNCaP cells is sufficient for progression to CRPC and that this was due to E2F-mediated up-regulation of androgen receptor (AR) signaling [202]. However, the oxygen status of these tumor xenografts is unknown. Nevertheless our array data revealed that AR transcriptional levels were not affected by hypoxia or Rb-loss nor were protein levels after 24 and 48 hours (Figure 4.6A). In addition, observations by several other groups support our working paradigm in prostate cancer. Firstly, HIF1 expression may be required for CRPC progression [383]. Second, previous in vivo experiments support a tumor suppressor role for E2F-binding deficient Rb in prostate cancer [204]. Sun and colleagues determined that the E2F/Rb interaction is critical for preventing tumor initiation but that Rb can use context-dependent mechanisms to restrain tumor progression outside of E2F mechanisms as Rb654 retains the ability to significantly delay progression to invasive and lethal prostate cancer [204]. This strongly supports our findings that progression to lethal and metastatic prostate cancer occurs independently of E2F-mechanisms [327]. Finally, the tumor suppressor activities of Rb in neoplastic

tissues may indeed be attributed primarily to the attenuation of TRIP230 coactivator potential on HIF1-mediated transcriptional responses. Thus, we cannot discount the evidence that supports a role for Rb as a regulator of HIF1-mediated signaling via TRIP230 in prostate cancer progression.

In summary, during the course of activated transcription Rb attenuates the coactivation function of TRIP230 resulting in the appropriate magnitude of mRNA production mediated by the HIF1 complex. Loss of Rb results in the unmasking of the full coactivation potential of TRIP230 leading to exaggerated HIF1 transcriptional output and concomitant up-regulation in target protein expression. The result of this failure is the over-expression of specific hypoxia-regulated transcriptional programs mediating cell transformation and metastasis.

4.5. Materials and Methods

4.5.1. Cell Culture

LNCaP (ATCC) and 22Rv1 cells were maintained in RPMI-1640 Media (BioWhittaker, Lonza) with 10% fetal bovine serum (FBS; HyClone, Perbio, Thermo Fisher Scientific Inc.) supplemented with 100 units/mL potassium penicillin-100 μg/mL streptomycin sulphate (BioWhittaker, Lonza), and 4.5 g/L glucose and 4.5 g/L L-glutamine at 37oC, 20% O2, and 5% CO2. HEK293T cells (ATCC) were maintained in similar conditions as describe above but in Dulbecco's Modified Eagle's Medium (DMEM; BioWhittaker, Lonza) with 10% fetal bovine serum (FBS; HyClone, Perbio, Thermo Fisher Scientific Inc.).

4.5.2. Quantitative Real-Time PCR

Real-time PCR (RT-PCR) experiments were performed as described previously. Breifly, LNCaP cells were incubated under hypoxic conditions (1% O2) for 24 h in a humidified CO2 incubator. The mRNA levels of VEGF, CXCR4, RB1, PLOD2, ENO2, HTR5A, KISS1R, NDRG1and 36B4 were determined using quantitative real-time PCR. The primer pairs for VEGF, CXCR4, RB1, PLOD2 and 36B4 were described previously

[284,327]. The other primer pairs used were; ENO2: 5'-AGCCATCGACACGGCTGGCTAC -3' and 5'- TGGACCAGGCAGCCCAATCATC -3', KISS1R: 5'- CGTTCGGTGCAGTTTCGTTGTGAA -3' and 5'-CTGGAATGATCCAGAAAGTCCTGTG -3'; NDRG1: 5'-CGCCAGGACATTGTGAATGAC -3' and 5'- TTTGAGTTGCACTCCACCACG -3'; and; HTR5A: 5'- GGCGGACCGTGAACACCAT-3' and 5'-ACTCTCCGCTGTCATCTCTCTGG -3'; Total RNA was isolated using TRI reagent (Sigma, Cat. No. T9424-200ML) according to the manufacturer's protocol. Reverse transcription was performed using High Capacity cDNA Reverse Transcription Kit (Applied Biosystems, Part No.4368814) according to the manufacturer's protocol. A total of 2 – 4 µg of RNA was used in a 20 µL reaction amplified by cycling between 25oC for 5 min, 37oC for 120 min, and 85oC for 5 min (Veriti 96 Well Thermal Cycler, Applied Biosystems). From each experiment, a sample that was both infected with viral Rb-specific shRNA and pre-conditioned with hypoxia was used to generate a relative standard curve in which the sample was diluted 1:10 in five serial dilutions resulting in dilutions of 1:10, 1:100, 1:1,000, 1:10,000, and 1:100,000 whereas the samples were diluted 1:30; the analysis was done using StepOnePlus System (Applied Biosystems).

4.5.3. Immunoblotting

Protein analysis was performed by immunoblotting as described previously [86]. Briefly, LNCaP or 22Rv1 cells were incubated under hypoxic conditions (1% O_2) for 24 h or up to 7 days as indicated. Cells were harvested and the protein concentration estimated by the Bradford assay. Equal amounts of proteins from the samples were resolved on a SDS-acrylamide gel then transferred to polyvinylidene fluoride (PVDF) membrane. Membranes were probed with primary antibodies and the detection was done using horseradish peroxidase conjugated anti-mouse or anti-rabbit IgG (GE Healthcare,) and ECL Prime detection kit (GE Healthcare).

4.5.4. Antibodies

Anti-Rb (rabbit polyclonal, Santa Cruz Biotechnology Inc., SC-7905), anti-PLOD2 (mouse polyclonal, Abnova, H00005352-B01P), anti-KISS1R (rabbit polyclonal, Sigma,

SAB2700212), anti-HTR5A (rabbit polyclonal, Sigma, SAB2101110), anti-NDRG1 (rabbit polyclonal, Santa Cruz Biotechnology Inc., SC-30040), anti-AR (rabbit polyclonal (PG-21), EMD Millipore, 06-680), anti-RORα (goat polyclonal, Santa Cruz Biotechnology Inc., SC-6062), anti-ENO2 (rabbit polyclonal, Cell Signaling, 9536), anti-α-tubulin (mouse monoclonal, Santa Cruz Biotechnology Inc., SC-8035), goat anti-rabbit IgG-HRP (Santa Cruz Biotechnology Inc., SC-2004), goat anti-mouse IgG-HRP (Santa Cruz Biotechnology Inc., SC-2005), donkey anti-goat IgG-HRP (Santa Cruz Biotechnology Inc., SC-2020).

4.5.5. Short-hairpin RNA interference in prostate cancer cells

LNCaP or 22Rv1 cells were stably infected with short-hairpin RNAs (shRNA) according to the method described by Wang et al [384]. The pQCXIPgfp vector was obtained from Dr. Oliver Hankinson (UC, Los Angeles). Oligonucleotides encoding short-hairpin RNAs directed to RB1 were annealed and cloned into the pQCXIPgfp vector 3-prime of the mouse U6 promoter. The RB1 forward and reverse primers were; RB1-CDS/13-14-F – TTTGGGATCTCAGCGATAGAAACTTCAAGAGAGTTTGTATCGCTGTGATCCTTTTT, and; RB1-CDS/13-14-R - AATTAAAAAGGATCACAGCGATACAAACTCTCTTGAAGTTTCTATCGCTGAGATCC

Human embryonic kidney 293T cells were transfected with the shRNA vectors and the pCL10A1 packaging vector using Lipofectamine 2000 (Invitrogen) and maintained in DMEM supplemented with 10% FBS and 1% penicillin/streptomycin. Twenty-four h after transfection, media was replaced and viral supernatants were collected 24 h later. LNCaP and 22RV1cells were seeded into 6-well plates (2x105 cells/well) and spin infections were performed using 2 mL of viral supernatant and centrifugation at 2500 rpm for 90 min at 30° C. Twenty-four hours post-infections media was supplemented with 3 μg/mL puromycin. Infection was monitored by immunoflourescence of GFP and knockdown was determined by immunoblotting.

4.5.6. Matrigel invasion and cell proliferation assays

shRNA LNCaP cells were washed, trypsinized, and re-suspended in culture medium, and subjected to invasion assay using BD BioCoat Matrigel Invasion Chamber (BD Sciences, Cat. No. 354480) according to the manufacturer's protocol. Briefly, the suspended chambers were rehydrated in warm bicarbonate-based medium for 2 h. shRNA LNCaP cells were seeded into invasion chambers in DMEM without FBS at a density of 10,000 cells/chamber. Chambers were placed in 24-well plates with chemo-attractant (complete medium containing 10% FBS) in the well. The plates were incubated in normoxic (20% O2) or hypoxic conditions (1% O2) at 37oC for 36 h. Before mounting the invasion membrane to microscope slides, the non-invading cells were removed by cotton swab and invading cells in the membrane were fixed with 100% methanol and stained with 1% toluidine blue. All the cells in the invasion membrane were counted using light microscopy at 10 – 40 × magnification.

shRNA LNCaP cells either expressing Rb (shSCX) or lacking Rb (shRb) were washed 2 times with PBS, trypsinized and seeded into 6-well plates at 10,000 cells/well. Twenty-four h after plating, cells were either maintained at normal oxygen tensions or treated with 1% O2. Cells were counted at; 0 (control), 12, 24, 36, 48 and 72 h following O2 treatments. Determinations were performed in triplicate and each sample was counted three times.

4.5.7. Flow Cytometry

Cell cycle status was determined by propidium iodide (PI) staining and flow cytometry. shRNA LNCaP cells were either treated with hypoxia or left at normoxic conditions for 36-hours and then harvested using trypsin. Biological triplicates of 5x105 cells were fixed in 70% ethanol on ice for 15 minutes and then cells were centrifuged for 3 minutes at 1500 rpm to remove the ethanol and incubated in 0.5 mL of propidium iodide staining solution (50 µg/mL PI, 0.05% Triton X-100, 0.1 mg/mL RNase A, in PBS) for 40 min at 37ºC. Following staining, cells were washed with PBS then run on a BD FACSCanto II flow cytometer (488 nm excitation, 617 emission, 375 volts, PI) where 20,000 events were collected. The percentage of cells in each stage of the cell cycle

was determined using FlowJo analysis software based on the PI staining profile of FSC/SSC-gated population.

4.5.8. Gene expression-array analysis

Gene expression microarray analysis was performed at the Laboratory for Advanced Genome Analysis (Vancouver Prostate Centre, Vancouver, Canada). Messenger RNA from LNCaP cells stably expressing either short-hairpin scrambled RNA (shSCX) or shRb was isolated using TRI reagent (Sigma) according to the manufacturer's protocol. Total RNA was quantified using a NanoDrop ND-1000 UV-VIS spectrophotometer to measure A260/280 and A260/230 ratios. We performed quality control checks of total RNA using an Agilent 2100 Bioanalyzer. One hundred ng of total RNA was converted to cRNA using T7 RNA polymerase in the presence of cyanine 3 (Cy3)-labeled CTP using an Agilent One-Color Microarray-Based Gene Expression Analysis Low Input Quick Amp Labeling v6.0 kit. Experiments were performed in triplicate and cRNAs were hybridized to Agilent GE Human Whole Genome 4x44Kv2 microarrays (Design ID 026652).

Arrays were scanned with an Agilent DNA Microarray Scanner at a 3 μm resolution and data was processed using Agilent Feature Extraction 10.10 software. Green processed signal was quantile normalized with Agilent GeneSpring 11.5.1. To find significantly regulated genes, fold changes between the RB1 shRNA and the scrambled shRNA control groups and p-values gained from t-test between the same groups were calculated with a Benjamini-Hochberg multiple testing correction. The t-tests were performed on log transformed normalized data and the variances were not assumed to be equal between sample groups. The data discussed in this publication have been deposited in NCBI's Gene Expression Omnibus [385] and are accessible through GEO Series accession number GSE78245 (http://www.ncbi.nlm.nih.gov/geo/query/acc.cgi?acc=GSE78245)

Up- and down-regulated genes with P values < 0.05 and fold difference ≥2.0 compared to the control or to the hypoxia scrambled control group were selected for further analysis. Heat maps were created using the Hierarchical clustering program from

the GenePattern website (http://genepattern.broadinstitute.org). To map the genes to chromosomal locations, we used the BioMart program located at http://uswest.ensembl.org. The Ensemble Genes 70 and Homo sapiens genes (GRCh37.p10) were chosen as databases for analysis. Selected genes from the microarray analysis were mapped on chromosomes by filtering using the Agilent Human Gene Expression 4x44K v2 Microarrays (Design ID 026652) probe's IDs.

4.5.9. Calcium mobilization assay

shRNA LNCaP and shRNA 22Rv1 cells were either left at normoxia or treated with 1% O_2 for 96 hours. After hypoxia or normoxia treatment, cells were loaded with 2 μM indo-1AM dye (30 min at 37°C) and then imaged on an inverted fluorescent microscope. Cells were then treated with Kisspeptin-10 peptide and intracellular calcium levels were indexed by ratiometric fluorescence measurements taken at 405 and 485 nm.

4.5.10. In silico data and statistical analysis

DNA sequences for ATP4A, PLA2G4D, NIM1K, CYP26A1, KISS1R, GPR26, MYBPC2, PCP4L1, AMPD3 and SCNN1G were located and defined using the UCSC Genome Browser on Human Dec. 2013 (GRCh38/hg38) Assembly. Annotated DNA sequences as well as 2 Kb upstream of indicated start sites and 2 Kb downstream of indicated stop sites were analyzed for HIF1α:ARNT binding sites using the JASPAR database (http://jaspar.genereg.net) [358,359]. A 95% relative profile score threshold was used to screen for consensus sequence HIF1 binding sites. If DNA sequences were longer than 20,000 bp then sequential DNA segments were analyzed.

Statistical analyses were performed using GraphPad Prism 4.0. Values for transcriptional responses are presented as means ± standard deviation (S.D.). A P value < 0.05 was considered to be significant. Values for growth curves are presented as means ± standard error of the mean (S.E.M.). A P value < 0.05 was considered to be significant. For our gene clustering analysis, we used a Wilcoxon rank test in addition to a Student's t-test to determine if the distance between target genes was different from

the distance between all genes on chromosomes 1 and 21. This was done once for the genes of interest and then for 65 randomly chosen genes from chromosome 1 and 21. For these genes the median distance was calculated. The random choosing was repeated 100 times to generate a distribution of random medians.

4.6. Acknowledgements

We would like to thank Mr. Shawn Anderson (Vancouver Prostate Centre) for his help preparing the micro-array data file.

4.7. Disclosure of potential conflicts of interest

The authors have no conflicts of interest to report.

4.8. Grant support

This work was supported by a Discovery Grant from the Natural Sciences and Engineering Research Council of Canada to T.V.B. and by CIHR/Terry Fox Program Project to M.E.C.

4.9. Supplementary Data

Table 4.2. Supplementary Table 1: All up-regulated genes that are induced greater than 2-fold by a combination of loss of Rb and hypoxia when compared to all other treatments

Gene Name	Probe Name	Fold Increase (vs shSCX-N)		
		shRb-N	shSCX-HYP	shRb-HYP ± S.D.
LOC100128264	A_33_P3375279	2.59	61.55	581.19 ± 63.98
HTR5A	A_23_P42565	2.07	27.41	256.40 ± 202.60
PLOD2	A_33_P3318581	2.53	24.26	219.02 ± 25.25
SLC16A3	A_23_P158725	1.73	24.85	200.17 ± 48.02
ATP4A	A_23_P430728	2.46	12.53	157.93 ± 32.25
PLA2G4D	A_33_P3361611	1.15	10.05	97.72 ± 10.46
NIM1	A_23_P254863	1.32	5.73	91.57 ± 80.55
CYP26A1	A_23_P138655	1.15	2.87	68.51 ± 11.92
CXCR4	A_23_P102000	1.30	2.65	62.56 ± 16.56
KISS1R	A_33_P3231357	0.61	8.51	61.94 ± 13.15
ANGPTL4	A_33_P3295358	1.92	3.63	53.17 ± 13.27
GPR26	A_23_P305581	0.98	9.84	53.00 ± 14.08
MYBPC2	A_33_P3257182	1.18	3.74	50.39 ± 4.90
FOS	A_23_P106194	1.47	1.41	49.01 ± 18.72
PPFIA4	A_23_P420692	1.61	8.32	39.76 ± 5.66
CA9	A_23_P157793	1.18	2.09	28.63 ± 6.14
NFATC4	A_33_P3250083	1.52	4.70	21.97 ± 5.61
PFKFB4	A_24_P362904	1.53	2.94	21.82 ± 4.29
PCP4L1	A_32_P214665	1.97	2.51	21.02 ± 0.82
RORA	A_23_P26124	1.40	2.57	20.81 ± 5.43
AMPD3	A_24_P304154	0.91	0.89	19.43 ± 4.15
ALDOC	A_23_P78108	1.46	4.85	19.33 ± 3.21
ENO2	A_24_P236091	1.80	2.61	19.09 ± 2.99
SCNN1G	A_23_P206626	1.10	1.30	19.02 ± 6.66
STC1	A_23_P314755	1.10	4.42	19.00 ± 7.29
NDRG1	A_23_P20494	1.19	6.80	18.6 ± 1.61
TSPEAR	A_23_P394972	5.97	1.71	17.31 ± 7.26
TMEM45A	A_33_P3344831	1.46	2.61	17.07 ± 1.63
MAFF	A_23_P103110	1.23	2.02	16.52 ± 2.85

Gene Name	Probe Name	Fold Increase (vs shSCX-N)		
		shRb-N	shSCX-HYP	shRb-HYP ± S.D.
ATP8B3	A_23_P79108	1.92	2.36	15.52 ± 2.42
GPR146	A_23_P20035	1.35	2.14	15.1 ± 4.01
LOC728276	A_33_P3394362	1.93	1.29	14.94 ± 6.63
BARX1	A_23_P32279	1.50	3.12	14.9 ± 1.80
BEND5	A_23_P904	1.27	2.58	14.25 ± 1.96
NTRK2	A_33_P3322804	1.45	2.36	13.14 ± 3.40
LOC100132354	A_33_P3216282	1.20	1.55	12.94 ± 1.80
PREX1	A_23_P413641	3.01	1.54	12.93 ± 1.44
PAPSS2	A_24_P940166	3.87	2.51	12.81 ± 9.06
C4orf47	A_33_P3247175	1.01	3.09	12.58 ± 3.01
C2orf72	A_33_P3227676	1.18	2.82	12.29 ± 2.69
COL13A1	A_23_P1331	1.37	2.27	12.17 ± 2.00
AFAP1L1	A_32_P167239	1.65	1.58	11.72 ± 1.89
SH3D21	A_23_P307536	0.68	2.72	11.46 ± 1.20
BHLHE40	A_24_P268676	0.94	1.99	11.38 ± 2.29
C20orf46	A_23_P120504	1.66	1.81	11.16 ± 2.12
PLEKHA2	A_33_P3339860	2.02	1.82	10.98 ± 1.40
S1PR4	A_33_P3281273	1.09	4.34	10.62 ± 2.42
FOXD1	A_32_P34920	1.09	2.05	10.44 ± 0.70
LOC442132	A_33_P3406843	0.80	2.50	10.01 ± 5.01
LOC285965	A_33_P3432135	0.83	1.66	10.00 ± 4.16
LOC100291851	A_33_P3328410	1.03	1.80	9.98 ± 1.52
MYOD1	A_33_P3334773	1.03	1.13	9.69 ± 0.80
MORN5	A_24_P401491	3.43	1.81	9.61 ± 6.03
EPB41L4B	A_23_P387656	2.14	0.93	9.59 ± 1.28
PTX3	A_23_P121064	1.34	2.54	9.56 ± 2.18
WDR66	A_24_P179504	1.06	2.09	9.51 ± 2.11
INSIG2	A_33_P3321342	1.22	1.26	9.46 ± 1.53
BIRC3	A_23_P98350	2.90	1.43	9.43 ± 1.47
FLJ44715	A_33_P3671729	1.28	3.57	9.30 ± 0.90
RHOXF1	A_23_P85082	1.69	0.77	8.98 ± 3.28
ANKRD37	A_24_P237586	0.84	2.75	8.80 ± 1.97
BNIP3	A_33_P3419785	1.11	3.20	8.50 ± 1.48
LDLRAD1	A_24_P491397	2.62	1.01	8.45 ± 2.91

Gene Name	Probe Name	Fold Increase (vs shSCX-N)		
		shRb-N	shSCX-HYP	shRb-HYP ± S.D.
STON1	A_23_P302005	2.13	1.09	8.26 ± 1.07
CYB5R2	A_23_P2181	1.13	1.72	8.14 ± 0.89
C8orf22	A_32_P80741	0.71	0.84	8.02 ± 11.98
NEDD9	A_23_P344555	2.04	1.85	7.84 ± 3.40
P4HA1	A_33_P3214481	1.10	3.35	7.81 ± 0.87
PHGR1	A_33_P3323501	3.23	1.84	7.78 ± 0.66
LGALS8	A_33_P3349883	3.61	1.80	7.70 ± 1.76
KRTAP10-12	A_33_P3357651	1.53	1.21	7.60 ± 2.00
EGFR	A_23_P215790	0.80	1.96	7.57 ± 0.53
ITPKA	A_23_P65918	2.21	1.28	7.53 ± 0.30
CYS1	A_33_P3398156	1.01	1.11	7.44 ± 1.63
PFKP	A_33_P3413962	0.88	2.57	7.41 ± 0.83
PFKFB3	A_24_P261259	0.89	1.80	7.28 ± 0.82
HES7	A_33_P3368695	1.47	1.43	7.27 ± 1.28
LOC644192	A_24_P795371	0.96	1.43	7.20 ± 1.14
LOC154761	A_24_P918907	1.06	2.39	7.18 ± 2.09
C10orf11	A_23_P113034	1.66	1.37	7.09 ± 1.25
SYT17	A_23_P163697	1.34	2.14	7.06 ± 0.55
NPR3	A_23_P58676	0.99	2.18	6.99 ± 2.53
CXCL12	A_24_P412156	3.22	2.68	6.92 ± 3.48
TUBB2B	A_24_P314477	2.04	2.05	6.88 ± 1.19
GREM2	A_24_P40626	0.74	0.92	6.86 ± 1.47
BNIP3L	A_23_P134925	1.00	2.42	6.82 ± 0.82
LOX	A_23_P122216	1.11	1.92	6.79 ± 2.27
FLJ26484	A_33_P3741022	0.92	1.32	6.71 ± 5.13
NRXN2	A_24_P261470	1.87	1.65	6.65 ± 1.16
DLEC1	A_23_P18282	1.34	1.15	6.61 ± 1.76
VEGFB	A_23_P1594	1.59	2.33	6.54 ± 0.37
LOC100128988	A_32_P202125	1.23	1.06	6.53 ± 1.75
DHRS3	A_23_P33759	1.75	1.66	6.47 ± 0.57
TMEM45B	A_23_P1682	1.67	1.61	6.35 ± 0.66
TCP11L2	A_23_P419107	1.01	1.42	6.34 ± 1.20
CYBRD1	A_24_P345451	2.41	1.74	6.33 ± 0.44
LOC388242	A_32_P135336	1.67	1.29	6.33 ± 0.92

Gene Name	Probe Name	Fold Increase (vs shSCX-N)		
		shRb-N	shSCX-HYP	shRb-HYP ± S.D.
FLJ37644	A_24_P497464	1.83	1.18	6.29 ± 2.58
PTH1R	A_23_P167030	2.26	2.53	6.23 ± 2.31
FAM110C	A_32_P47643	1.92	1.39	6.20 ± 1.06
KDM3A	A_23_P395075	1.17	2.41	6.18 ± 1.78
PAQR5	A_33_P3368750	1.31	1.60	6.15 ± 1.19
SGCE	A_33_P3229617	2.95	1.78	6.05 ± 1.95
RASGEF1A	A_33_P3287760	1.87	1.58	6.03 ± 3.84
ARAP3	A_23_P167389	2.11	2.14	5.89 ± 0.85
CYP1B1	A_23_P209625	1.02	2.45	5.87 ± 1.54
LOC399715	A_33_P3291619	0.55	2.14	5.86 ± 1.33
GAD1	A_23_P374689	0.56	1.73	5.84 ± 3.48
ASGR1	A_23_P118722	1.92	1.75	5.83 ± 0.76
VNN2	A_23_P122724	1.55	1.41	5.77 ± 0.73
C15orf62	A_32_P183970	1.67	1.30	5.69 ± 1.64
PPP1R3B	A_24_P201064	1.04	1.53	5.65 ± 0.69
ODAM	A_23_P58228	1.59	2.16	5.62 ± 0.64
WISP2	A_23_P102611	1.23	1.89	5.60 ± 2.38
EPO	A_23_P145669	0.95	2.16	5.57 ± 2.53
SEC14L5	A_24_P254850	1.00	1.03	5.57 ± 1.48
DUSP5P	A_24_P367602	1.09	2.23	5.56 ± 0.84
STAB1	A_23_P32500	1.36	2.65	5.56 ± 1.37
ASCL2	A_32_P171061	1.14	2.55	5.55 ± 0.69
SH2D3C	A_33_P3293918	2.61	2.02	5.36 ± 2.26
PADI2	A_24_P187970	1.99	1.42	5.35 ± 0.44
CCDC147	A_33_P3257297	1.59	1.37	5.35 ± 1.40
ATP8A2	A_23_P258612	1.35	1.52	5.34 ± 2.58
GATA5	A_23_P371835	1.16	1.86	5.31 ± 1.58
ANKZF1	A_23_P119907	1.16	2.03	5.23 ± 0.93
SRRM3	A_23_P331700	2.12	1.73	5.22 ± 1.37
ZNF395	A_23_P146077	1.27	1.64	5.20 ± 0.85
P4HA2	A_23_P30363	1.01	1.77	5.08 ± 0.35
VIM	A_23_P161190	0.59	2.22	5.01 ± 0.30
MAP3K15	A_23_P308483	1.06	1.58	5.01 ± 0.84
TCAM1P	A_24_P68088	1.46	0.79	5.00 ± 3.75

Gene Name	Probe Name	Fold Increase (vs shSCX-N)		
		shRb-N	shSCX-HYP	shRb-HYP ± S.D.
C20orf195	A_33_P3405459	1.50	1.49	4.97 ± 0.42
KIAA2022	A_32_P169505	0.80	1.55	4.96 ± 1.17
STON1-GTF2A1L	A_23_P79488	0.71	0.93	4.91 ± 3.19
SH3PXD2A	A_23_P35456	1.59	1.41	4.91 ± 0.23
ADAM12	A_33_P3310929	1.00	1.32	4.87 ± 0.75
DNAI2	A_33_P3419239	1.16	1.00	4.87 ± 2.20
PGK1	A_23_P125829	0.98	2.00	4.85 ± 0.30
AKAP12	A_23_P111311	0.62	1.72	4.82 ± 1.44
FAM115C	A_24_P237912	0.98	1.73	4.81 ± 1.03
SH3GL3	A_23_P48988	1.63	1.29	4.80 ± 0.46
TG	A_23_P32454	0.95	1.61	4.79 ± 0.67
ARC	A_23_P365738	0.80	1.98	4.77 ± 1.56
SCN4B	A_23_P303833	0.89	1.65	4.75 ± 0.68
DPYSL4	A_23_P331049	0.86	1.72	4.74 ± 0.82
GPR155	A_32_P132317	1.73	1.30	4.70 ± 0.40
FLJ31356	A_33_P3364062	1.02	1.26	4.68 ± 1.47
ZNF292	A_32_P113584	0.94	1.54	4.67 ± 0.50
EPAS1	A_23_P210210	1.49	1.06	4.65 ± 0.69
RAB33A	A_23_P147025	1.05	1.61	4.64 ± 0.77
PHF21B	A_24_P113572	1.52	1.40	4.62 ± 2.65
CDKN1C	A_23_P428129	1.32	1.65	4.61 ± 0.47
C11orf96	A_32_P74409	1.08	1.32	4.60 ± 0.77
OSBPL7	A_33_P3358740	0.82	2.02	4.60 ± 1.43
MMP24	A_33_P3398331	0.91	1.74	4.56 ± 0.59
CACNA1H	A_33_P3218960	0.72	1.20	4.55 ± 0.87
PDK1	A_24_P37441	0.98	1.90	4.52 ± 0.19
IGFBP6	A_23_P139912	1.43	1.07	4.52 ± 0.92
CCDC110	A_23_P383325	1.54	1.68	4.51 ± 0.56
LCN15	A_33_P3263938	1.36	1.26	4.50 ± 0.50
MAP7D2	A_24_P367645	0.64	1.86	4.44 ± 4.22
TFF3	A_23_P393099	2.17	1.42	4.43 ± 0.33
FUT11	A_23_P413788	0.92	2.10	4.43 ± 0.49
TCF7L1	A_23_P142872	1.50	0.76	4.38 ± 3.43
MUC6	A_33_P3314500	1.36	1.10	4.38 ± 1.10

Gene Name	Probe Name	Fold Increase (vs shSCX-N)		
		shRb-N	shSCX-HYP	shRb-HYP ± S.D.
PLK5	A_32_P50223	1.20	0.96	4.32 ± 0.70
GADD45B	A_24_P239606	1.12	1.52	4.30 ± 0.23
SPRY1	A_23_P144476	0.83	1.47	4.28 ± 0.45
EFNA3	A_24_P114032	1.81	1.67	4.27 ± 1.51
DSP	A_33_P3402565	1.21	1.53	4.23 ± 0.62
CIB2	A_33_P3308914	1.76	1.26	4.22 ± 0.07
SEMA4G	A_23_P127068	1.64	1.35	4.19 ± 0.51
LOC727869	A_32_P110016	1.09	1.57	4.17 ± 0.46
FAM167A	A_23_P334955	1.79	1.18	4.15 ± 1.31
RIMKLA	A_23_P349406	0.84	1.52	4.15 ± 0.41
CA8	A_23_P83838	2.03	1.01	4.14 ± 0.81
FAM13A	A_33_P3691916	1.33	1.34	4.13 ± 1.11
SLC1A1	A_23_P216468	1.10	1.75	4.13 ± 0.78
ZC3H6	A_24_P826348	1.21	1.17	4.10 ± 0.49
YPEL2	A_24_P787947	1.39	1.04	4.06 ± 0.55
RNF182	A_23_P399255	1.75	1.32	4.05 ± 0.46
UNC5CL	A_23_P428298	1.28	1.36	4.05 ± 1.03
LRAT	A_32_P113066	1.00	0.99	4.04 ± 0.56
ST3GAL6	A_23_P250800	1.05	0.74	4.01 ± 0.71
NCRNA00324	A_23_P362191	1.25	1.57	4.01 ± 1.09
HES1	A_23_P6596	1.73	1.14	4.01 ± 0.68
TGFB1	A_24_P79054	0.94	0.94	3.98 ± 1.41
S100A10	A_23_P137984	0.75	1.76	3.97 ± 0.43
HPCA	A_33_P3246133	1.53	0.89	3.97 ± 0.77
TMPRSS2	A_23_P29067	1.64	1.21	3.94 ± 0.31
RAB6B	A_24_P475349	1.58	1.32	3.90 ± 0.18
CLIP3	A_23_P50786	1.18	1.42	3.89 ± 1.03
GPA33	A_24_P319374	1.88	1.51	3.88 ± 1.01
SLC2A1	A_23_P571	0.85	1.81	3.88 ± 0.39
DUSP1	A_23_P110712	1.01	0.88	3.85 ± 1.10
ARMCX4	A_33_P3211864	1.21	1.27	3.85 ± 0.79
EFEMP2	A_33_P3367830	1.05	1.39	3.84 ± 0.62
GBE1	A_23_P121082	0.84	1.47	3.83 ± 0.41
ERO1L	A_23_P106145	0.97	1.30	3.83 ± 0.51

Gene Name	Probe Name	Fold Increase (vs shSCX-N)		
		shRb-N	shSCX-HYP	shRb-HYP ± S.D.
LDHC	A_23_P53039	0.95	1.57	3.82 ± 0.78
NCAM1	A_33_P3363799	1.41	1.16	3.81 ± 1.27
ITGB2	A_23_P329573	1.00	1.80	3.80 ± 0.61
C4orf3	A_23_P388433	0.92	1.67	3.79 ± 0.12
NHEDC1	A_23_P415611	1.37	0.84	3.78 ± 0.97
STBD1	A_23_P254079	1.20	1.30	3.77 ± 1.55
MVP	A_33_P3294608	1.29	0.89	3.77 ± 0.52
ZNF404	A_23_P90333	1.34	1.33	3.76 ± 0.35
PRPH	A_23_P13713	0.90	1.65	3.74 ± 0.23
CCND2	A_24_P278747	0.98	1.57	3.72 ± 1.32
VEGFA	A_24_P12401	0.94	1.86	3.72 ± 0.69
C1orf51	A_23_P410717	1.13	1.61	3.70 ± 0.98
PCP2	A_24_P399500	1.14	1.21	3.67 ± 0.18
B3GNT4	A_23_P76071	1.36	1.50	3.65 ± 0.38
ASB2	A_23_P205370	0.92	1.63	3.64 ± 0.10
GLDN	A_24_P49199	1.76	1.54	3.64 ± 1.15
NOTCH3	A_33_P3313055	1.66	1.37	3.64 ± 0.61
LOC100130691	A_24_P400172	1.46	1.01	3.63 ± 2.75
SPTB	A_32_P134968	1.41	1.19	3.61 ± 0.24
FZD7	A_23_P209449	1.47	1.18	3.60 ± 0.59
MXI1	A_33_P3383029	0.90	1.43	3.57 ± 0.67
LOC100240735	A_32_P170481	1.58	1.58	3.55 ± 1.67
RNF165	A_33_P3319680	0.71	1.33	3.55 ± 0.87
ARHGEF37	A_32_P222695	1.19	1.71	3.53 ± 0.23
BEST4	A_33_P3244808	1.28	1.19	3.51 ± 0.55
LRP1	A_23_P124837	1.24	1.32	3.51 ± 0.71
MLLT3	A_23_P216693	1.14	0.91	3.51 ± 0.35
CREG2	A_23_P394986	0.92	1.18	3.49 ± 0.59
RNASE4	A_23_P205531	1.44	1.70	3.49 ± 0.65
C5orf41	A_23_P404606	0.93	1.24	3.49 ± 0.58
PNMA2	A_24_P389415	1.59	1.32	3.48 ± 0.41
ZNF511	A_33_P3384885	1.08	1.38	3.47 ± 0.36
KIAA1984	A_33_P3293511	1.07	1.49	3.45 ± 1.18
ARID3A	A_33_P3272921	0.90	1.35	3.44 ± 0.50

Gene Name	Probe Name	Fold Increase (vs shSCX-N)		
		shRb-N	shSCX-HYP	shRb-HYP ± S.D.
KLHL3	A_23_P133543	1.49	1.70	3.44 ± 0.58
TTC6	A_33_P3226575	1.26	1.23	3.44 ± 0.29
FOSL2	A_23_P348121	1.09	1.10	3.44 ± 0.47
LOC284998	A_24_P498854	0.62	1.58	3.43 ± 0.53
VIPR2	A_32_P153071	1.50	1.64	3.42 ± 0.44
RLF	A_23_P126037	0.98	1.55	3.40 ± 0.29
NLGN1	A_33_P3214690	1.66	0.87	3.40 ± 1.02
VPS37D	A_33_P3293573	1.12	1.30	3.38 ± 0.24
SCNN1B	A_32_P83098	0.98	0.87	3.33 ± 0.66
C4orf6	A_23_P7048	0.67	1.18	3.32 ± 1.34
NOTUM	A_33_P3257125	1.12	1.13	3.31 ± 0.67
VSTM2A	A_33_P3347193	1.03	1.42	3.31 ± 0.38
LAMB2P1	A_33_P3413815	1.29	0.77	3.31 ± 0.38
RNF112	A_23_P107116	0.65	1.44	3.26 ± 0.31
GRID1	A_23_P32805	1.31	1.37	3.25 ± 0.76
LOC100129617	A_33_P3343516	1.15	1.35	3.25 ± 1.01
PNRC1	A_23_P145074	1.21	1.25	3.25 ± 0.17
GLYAT	A_23_P75749	1.06	1.06	3.24 ± 0.69
SLC35F3	A_23_P422212	0.98	1.27	3.24 ± 0.51
GLIS2	A_33_P3333224	1.35	1.01	3.23 ± 0.31
CCNG2	A_24_P12065	1.37	1.53	3.23 ± 0.86
ABTB1	A_33_P3297444	1.28	1.28	3.22 ± 0.16
IL10RA	A_23_P203173	1.06	1.55	3.22 ± 0.71
JAK3	A_24_P59667	1.25	1.16	3.21 ± 0.46
TBC1D8B	A_23_P325887	1.19	1.22	3.19 ± 0.42
TLE6	A_33_P3400147	1.24	1.23	3.18 ± 0.37
RASD1	A_23_P118392	1.03	1.19	3.18 ± 0.98
TNNT1	A_33_P3397865	1.18	1.42	3.17 ± 0.36
PPP2R5B	A_23_P35796	1.26	1.19	3.17 ± 0.41
BCL3	A_23_P4662	0.97	1.02	3.16 ± 0.40
CLK3	A_32_P20691	0.94	1.18	3.15 ± 0.21
ZNF713	A_33_P3409710	1.39	0.86	3.14 ± 1.55
SEC31B	A_23_P35564	1.34	1.35	3.14 ± 0.70
BRSK2	A_33_P3273480	1.26	1.24	3.13 ± 0.30

Gene Name	Probe Name	Fold Increase (vs shSCX-N)		
		shRb-N	shSCX-HYP	shRb-HYP ± S.D.
PRKAA2	A_32_P94160	1.27	1.25	3.12 ± 0.21
GATA2	A_33_P3550894	1.12	1.11	3.12 ± 0.51
MYO15A	A_23_P27229	0.91	1.32	3.11 ± 1.43
DUSP5	A_23_P150018	0.90	1.13	3.10 ± 1.13
CD300A	A_24_P159434	0.89	0.85	3.10 ± 0.77
CLRN3	A_23_P127107	1.09	0.92	3.09 ± 0.58
JUND	A_33_P3324909	1.36	1.03	3.08 ± 1.00
IGFL3	A_33_P3243454	1.09	1.47	3.07 ± 1.84
C7orf68	A_23_P20022	0.77	1.13	3.06 ± 0.11
HMOX1	A_23_P120883	0.82	0.99	3.04 ± 0.19
GUCY1A2	A_23_P350001	0.89	1.37	3.04 ± 1.39
ALOX5	A_23_P104464	1.42	1.26	3.03 ± 0.32
TGFBI	A_23_P156327	1.51	1.27	3.01 ± 0.55
CLEC3B	A_23_P69497	0.99	1.11	2.99 ± 0.14
TSC22D3	A_33_P3237634	0.91	1.28	2.98 ± 0.34
ZBTB20	A_23_P40866	1.02	0.87	2.97 ± 0.42
BLNK	A_33_P3363637	1.41	1.29	2.97 ± 0.19
FRY	A_33_P3223495	0.97	1.46	2.95 ± 0.43
PLTP	A_23_P5983	1.26	1.34	2.95 ± 0.23
COX8C	A_33_P3372069	0.87	0.96	2.93 ± 0.63
YPEL1	A_32_P88120	1.07	1.25	2.92 ± 0.39
CRYM	A_23_P77731	1.37	1.31	2.91 ± 0.26
SMCR6	A_33_P3877728	1.27	1.34	2.91 ± 0.51
RNF122	A_23_P134744	0.86	1.37	2.90 ± 0.24
HERC3	A_24_P51201	0.51	0.86	2.87 ± 0.68
CAMK1D	A_23_P124252	0.88	1.32	2.87 ± 0.46
VASN	A_23_P129695	1.14	1.35	2.84 ± 0.27
YEATS2	A_23_P69437	0.86	1.20	2.84 ± 0.08
MTL5	A_23_P161507	1.14	1.30	2.83 ± 0.43
ZSWIM5	A_23_P383118	0.99	0.93	2.82 ± 0.54
GAL3ST1	A_23_P120863	0.61	0.92	2.81 ± 0.98
CARHSP1	A_33_P3260307	1.30	1.19	2.81 ± 0.15
LOC284930	A_33_P3436935	0.93	1.21	2.79 ± 0.54
MST1	A_24_P148796	1.14	1.26	2.79 ± 0.29

Gene Name	Probe Name	Fold Increase (vs shSCX-N)		
		shRb-N	shSCX-HYP	shRb-HYP ± S.D.
KIAA1467	A_23_P394567	1.13	1.22	2.79 ± 0.42
C17orf39	A_33_P3381771	1.25	1.29	2.79 ± 0.29
LOC283070	A_33_P3464555	0.87	1.32	2.78 ± 0.44
IFITM10	A_33_P3358601	1.08	1.22	2.76 ± 0.74
KLHL24	A_24_P521994	0.82	1.26	2.76 ± 0.37
DDRGK1	A_33_P3299781	0.89	1.15	2.75 ± 1.00
BHLHA15	A_33_P3312730	1.10	1.22	2.73 ± 0.33
PNCK	A_23_P62377	0.82	1.16	2.71 ± 1.50
MICALL2	A_24_P303524	1.25	1.26	2.70 ± 0.10
HIVEP2	A_23_P214766	1.19	0.98	2.70 ± 0.36
LPIN3	A_33_P3393341	1.07	1.30	2.70 ± 0.24
RSBN1	A_33_P3888365	0.97	1.12	2.70 ± 0.34
C7orf63	A_33_P3615922	0.93	0.86	2.68 ± 0.32
WSB1	A_23_P4353	1.03	1.19	2.67 ± 0.48
PYGL	A_23_P48676	0.98	1.17	2.67 ± 0.35
ACLY	A_33_P3415042	1.19	1.21	2.66 ± 0.44
MICAL3	A_24_P366082	1.20	1.15	2.66 ± 0.54
CCDC114	A_33_P3261054	1.22	1.32	2.65 ± 0.42
DCDC2	A_33_P3212109	1.06	0.99	2.65 ± 0.87
EIF2C4	A_23_P23171	1.00	1.25	2.65 ± 0.39
SYNPO	A_33_P3397658	1.14	1.06	2.63 ± 0.64
HLA-A	A_23_P408353	1.23	1.09	2.62 ± 0.18
IRS1	A_24_P802145	1.28	0.99	2.61 ± 0.44
TNIP1	A_23_P30435	1.28	1.16	2.60 ± 0.35
CITED2	A_23_P214969	1.02	1.13	2.59 ± 0.24
IGSF21	A_32_P78101	0.72	1.28	2.58 ± 0.15
PLXND1	A_24_P376391	1.24	1.18	2.57 ± 0.17
LUC7L3	A_33_P3246997	1.16	1.13	2.55 ± 0.51
RIPK4	A_24_P125871	1.16	1.19	2.55 ± 0.23
ANKRD12	A_33_P3294524	1.00	1.18	2.54 ± 0.60
JUN	A_33_P3323298	0.95	1.05	2.54 ± 0.73
PTGER4	A_23_P148047	1.13	1.01	2.54 ± 0.20
DENND3	A_33_P3321130	0.99	1.06	2.52 ± 0.84
CDKN1B	A_24_P81841	1.20	1.06	2.52 ± 0.31

Gene Name	Probe Name	Fold Increase (vs shSCX-N)		
		shRb-N	shSCX-HYP	shRb-HYP ± S.D.
C8orf58	A_23_P310483	1.12	1.06	2.52 ± 0.31
CHST6	A_23_P106922	1.21	0.94	2.52 ± 0.37
NRG3	A_33_P3229417	1.12	0.62	2.51 ± 0.51
SAV1	A_24_P287473	1.05	1.16	2.50 ± 0.22
SNTB1	A_23_P95029	0.92	0.93	2.49 ± 0.57
MRC2	A_33_P3364741	0.97	1.23	2.49 ± 0.57
PPP1R13L	A_23_P119095	1.10	1.20	2.49 ± 0.30
GSN	A_33_P3423365	1.24	1.12	2.48 ± 0.37
YPEL5	A_33_P3281408	1.00	1.16	2.48 ± 0.37
PRTN3	A_23_P142345	1.04	0.87	2.48 ± 0.51
LOC100131346	A_33_P3289338	1.15	1.05	2.48 ± 0.20
RIT1	A_33_P3394075	0.68	0.90	2.46 ± 0.47
ARL4C	A_33_P3323722	0.90	1.06	2.45 ± 0.34
C16orf89	A_33_P3296862	0.96	1.20	2.45 ± 0.42
MKNK2	A_23_P142310	1.16	1.11	2.45 ± 0.22
PIAS2	A_33_P3349269	0.93	1.11	2.44 ± 0.23
STC2	A_23_P416395	0.90	1.19	2.44 ± 0.28
MYO1E	A_33_P3297978	1.09	1.07	2.44 ± 0.35
LOC100134285	A_33_P3240972	0.82	0.92	2.43 ± 0.96
EFCAB3	A_33_P3264042	0.86	1.15	2.43 ± 0.29
LOC283050	A_33_P3394140	0.71	1.07	2.40 ± 0.35
FLJ41455	A_33_P3520835	0.95	1.15	2.40 ± 0.41
CECR5-AS1	A_32_P131143	0.96	1.11	2.39 ± 0.36
FLJ32224	A_33_P3694746	1.04	0.93	2.38 ± 0.20
C17orf76	A_23_P368484	1.03	1.04	2.37 ± 0.34
MAPT	A_24_P224488	0.66	1.10	2.37 ± 0.53
KIAA1958	A_33_P3404744	1.04	0.92	2.35 ± 0.24
EVC2	A_33_P3319880	0.90	0.83	2.32 ± 1.43
RNF24	A_24_P333019	1.11	1.09	2.32 ± 0.58
KIAA1715	A_32_P31771	1.03	1.16	2.32 ± 0.16
BRWD3	A_32_P489130	1.06	1.11	2.32 ± 0.52
DMGDH	A_33_P3387716	0.95	0.81	2.31 ± 0.52
EPB41L4A	A_24_P257579	0.97	0.85	2.27 ± 0.43
WTIP	A_33_P3381948	0.99	1.04	2.26 ± 0.47

Gene Name	Probe Name	Fold Increase (vs shSCX-N)		
		shRb-N	shSCX-HYP	shRb-HYP ± S.D.
TNFRSF10D	A_33_P3326588	1.11	1.04	2.25 ± 0.21
GRIN3B	A_33_P3394213	0.98	0.91	2.24 ± 0.34
TNFRSF25	A_33_P3234530	0.85	0.76	2.22 ± 1.20
CASC2	A_33_P3213362	1.05	0.83	2.20 ± 0.32
GSDMB	A_33_P3221999	1.10	1.07	2.19 ± 0.17
BBC3	A_23_P382775	0.93	1.00	2.14 ± 0.14
AQPEP	A_33_P3251522	0.88	0.83	2.13 ± 1.22
CRHR1	A_33_P3320443	0.94	1.02	2.12 ± 0.18
FAM117B	A_32_P195401	0.92	0.99	2.11 ± 0.25
PAGE2B	A_33_P3420862	0.91	1.02	2.11 ± 0.26
PARD3	A_24_P35478	0.89	0.85	2.09 ± 0.62
CDKL3	A_23_P110643	0.94	0.99	2.09 ± 0.20
APOE	A_33_P3223592	0.98	0.84	2.05 ± 0.23
LOC100127885	A_33_P3278813	0.99	0.73	2.05 ± 1.12

Table 4.3. Supplementary Table 2: All down-regulated genes that are attenuated greater than 2-fold by a combination of loss of Rb and hypoxia when compared to all other treatments.

Gene Name	Probe Name	Fold Decrease (vs shSCX-N)		
		shRb-N	shSCX-HYP	shRb-HYP ± S.D.
SPIC	A_32_P148275	2.00	0.95	8.55 ± 2.91
DSC1	A_23_P38696	2.24	0.89	7.92 ± 1.67
KBTBD8	A_23_P431252	1.75	1.21	7.83 ± 2.00
UGT2B4	A_23_P386912	1.65	1.09	7.66 ± 3.60
PTPRQ	A_33_P3309471	2.39	1.00	7.21 ± 1.32
EOMES	A_24_P97374	1.50	1.03	6.84 ± 1.43
FLJ45684	A_33_P3288219	1.60	1.27	6.48 ± 1.82
CLEC2A	A_33_P3295348	1.05	0.94	6.11 ± 2.65
TARP	A_33_P3225625	2.68	0.87	6.11 ± 2.63
KLHL1	A_23_P2825	1.63	1.38	6.08 ± 0.96
TAF9B	A_24_P391431	1.31	1.27	5.92 ± 0.89
INSL5	A_23_P51479	1.11	1.15	5.77 ± 2.23
LRRTM4	A_24_P174294	2.61	0.99	5.63 ± 0.77
TBX15	A_24_P128442	2.55	1.42	5.46 ± 0.94

Gene Name	Probe Name	Fold Decrease (vs shSCX-N)		
		shRb-N	shSCX-HYP	shRb-HYP ± S.D.
NAP1L3	A_23_P125717	1.17	1.26	5.37 ± 1.07
CNGB3	A_23_P216376	1.57	1.68	4.89 ± 1.81
POLR3G	A_33_P3396527	2.30	1.22	4.82 ± 0.46
KLB	A_23_P350617	1.71	0.86	4.65 ± 0.82
MARS2	A_23_P108492	1.04	1.27	4.32 ± 1.98
ASZ1	A_33_P3217258	1.72	1.14	4.19 ± 0.56
ZNF365	A_24_P226970	1.13	1.20	4.17 ± 0.78
GBX2	A_33_P3423969	1.15	1.31	4.16 ± 0.44
ARHGAP9	A_23_P64661	1.64	1.09	4.04 ± 0.67
DPF3	A_33_P3240946	1.59	1.46	4.02 ± 1.81
PKHD1L1	A_33_P3254136	0.78	0.85	3.89 ± 1.47
MPV17L2	A_23_P165130	1.19	1.31	3.87 ± 0.40
NCRNA00167	A_24_P359030	0.83	1.04	3.84 ± 1.67
FLJ40606	A_33_P3388636	1.27	1.14	3.82 ± 0.68
PSPC1	A_33_P3232173	1.65	1.05	3.73 ± 0.96
POP1	A_23_P341275	1.44	1.47	3.69 ± 0.37
CLEC7A	A_24_P235988	1.66	0.92	3.60 ± 0.85
HSPH1	A_33_P3348752	1.21	0.98	3.53 ± 0.35
CNDP1	A_23_P9869	0.75	0.50	3.51 ± 0.88
SCAF11	A_33_P3283196	1.29	1.07	3.49 ± 0.52
CSMD1	A_33_P3230249	1.45	1.50	3.47 ± 0.98
FGFBP3	A_24_P201381	1.59	1.05	3.47 ± 0.79
AREG	A_33_P3419190	1.00	1.09	3.43 ± 1.04
MSMB	A_24_P146683	1.09	1.18	3.39 ± 0.64
UFSP1	A_33_P3327500	1.31	1.09	3.38 ± 0.43
LRRN4CL	A_33_P3221129	1.00	1.23	3.35 ± 0.78
CHAC2	A_32_P194264	1.00	1.09	3.34 ± 0.67
AGPAT9	A_23_P69810	1.36	1.21	3.33 ± 1.00
SLC2A13	A_33_P3354514	1.52	0.93	3.32 ± 0.96
POLR1B	A_24_P942112	1.39	1.27	3.27 ± 0.39
PIGW	A_23_P379794	1.14	1.06	3.24 ± 0.57
SNAPC5	A_33_P3335746	0.95	1.12	3.19 ± 0.45
SFPQ	A_33_P3318292	1.00	1.08	3.17 ± 0.19
FZD8	A_23_P396858	1.40	1.03	3.16 ± 0.61

Gene Name	Probe Name	Fold Decrease (vs shSCX-N)		
		shRb-N	shSCX-HYP	shRb-HYP ± S.D.
NUP98	A_23_P308032	1.18	1.10	3.15 ± 0.20
MAPK10	A_23_P45025	1.05	1.24	3.14 ± 1.08
YIF1B	A_23_P142239	0.93	1.41	3.13 ± 0.67
ZNF597	A_24_P378402	1.07	1.46	3.12 ± 0.97
PNLIPRP3	A_33_P3368193	0.98	0.87	3.04 ± 1.14
SLC30A1	A_23_P23815	1.29	1.43	3.03 ± 0.36
AP1S3	A_33_P3288995	0.98	1.28	3.03 ± 0.41
GPATCH4	A_33_P3211263	1.08	1.11	3.00 ± 0.19
SGOL1	A_23_P29723	0.98	1.03	2.94 ± 0.59
ING3	A_33_P3356711	1.20	1.45	2.94 ± 0.32
SLC43A2	A_24_P296508	1.41	1.15	2.93 ± 0.26
RRS1	A_23_P146187	1.24	1.31	2.88 ± 0.14
WT1	A_23_P116280	0.98	1.27	2.87 ± 0.48
FITM2	A_24_P203407	1.19	1.10	2.87 ± 0.13
OXNAD1	A_24_P927189	1.38	1.27	2.86 ± 0.57
CROT	A_33_P3355208	1.32	1.26	2.82 ± 0.30
TMEM177	A_23_P5339	0.89	1.12	2.80 ± 0.53
ELAC1	A_23_P15944	1.15	1.04	2.79 ± 0.30
HGD	A_23_P250164	1.36	0.91	2.79 ± 0.29
CD244	A_33_P3234292	1.05	1.14	2.78 ± 0.43
MSGN1	A_33_P3291379	1.07	0.86	2.78 ± 1.58
GLRX2	A_23_P160503	1.37	1.05	2.78 ± 0.29
CYCSP52	A_33_P3261132	1.23	1.27	2.76 ± 0.74
CHORDC1	A_33_P3502037	1.18	0.99	2.75 ± 0.35
STIM2	A_24_P180242	1.13	1.10	2.74 ± 0.95
GNRH2	A_24_P323072	1.09	1.08	2.74 ± 0.30
SLC5A6	A_24_P247732	1.13	1.24	2.74 ± 0.53
TM4SF18	A_24_P120251	1.30	1.06	2.72 ± 0.89
MAGOHB	A_24_P330112	0.92	1.12	2.71 ± 0.30
PGAM5	A_23_P319719	1.25	1.13	2.70 ± 0.30
KTI12	A_23_P103276	1.25	1.23	2.69 ± 0.15
FLJ13744	A_33_P3806965	1.09	1.08	2.68 ± 0.33
NOP2	A_23_P204364	1.04	1.19	2.68 ± 0.55
SURF6	A_24_P21447	1.19	1.25	2.66 ± 0.14

Gene Name	Probe Name	Fold Decrease (vs shSCX-N)		
		shRb-N	shSCX-HYP	shRb-HYP ± S.D.
PNN	A_33_P3218694	1.29	1.00	2.64 ± 0.25
PYCRL	A_23_P383278	1.08	1.05	2.63 ± 0.36
PCYT2	A_33_P3394809	1.11	1.13	2.63 ± 0.30
ADAT1	A_23_P141100	0.91	1.03	2.62 ± 0.40
PNO1	A_24_P336853	1.12	1.10	2.62 ± 0.44
TRPM2	A_24_P27977	1.02	1.05	2.61 ± 0.26
SRSF7	A_24_P222911	1.20	0.91	2.61 ± 0.27
ARL4A	A_32_P806841	1.09	1.27	2.59 ± 0.17
RPS6KL1	A_33_P3334419	1.13	1.07	2.58 ± 0.27
NCDN	A_23_P97736	0.97	1.11	2.57 ± 0.32
UQCR10	A_24_P66001	1.25	1.15	2.57 ± 0.09
TIMM13	A_33_P3413845	1.24	1.18	2.56 ± 0.43
NDUFAF4	A_24_P171983	1.10	1.17	2.56 ± 0.21
SRPRB	A_23_P80773	1.15	1.10	2.56 ± 0.32
L1CAM	A_33_P3374443	1.15	0.82	2.56 ± 0.76
ADRB1	A_33_P3310189	1.15	1.21	2.54 ± 0.32
PDSS1	A_23_P161152	1.22	1.12	2.53 ± 0.34
AP4B1	A_23_P160729	1.03	1.07	2.52 ± 0.22
FUS	A_23_P106887	0.78	0.95	2.51 ± 0.43
FAM203A	A_23_P61268	1.06	1.16	2.51 ± 0.18
CLDN8	A_23_P427014	0.73	1.11	2.49 ± 0.67
JMJD4	A_33_P3306113	1.24	1.15	2.49 ± 0.28
NDUFC2	A_24_P364236	1.11	0.99	2.49 ± 0.11
HAS3	A_23_P393034	0.91	1.21	2.47 ± 0.25
MSTO1	A_23_P630	1.23	1.13	2.47 ± 0.35
TOE1	A_24_P19828	0.99	1.10	2.46 ± 0.26
TOR3A	A_24_P130962	1.01	1.02	2.45 ± 0.30
NOP56	A_23_P79927	0.96	1.01	2.44 ± 0.51
RRP9	A_23_P6802	1.13	1.18	2.43 ± 0.15
CDC25A	A_24_P397107	1.00	1.08	2.43 ± 0.44
TRAM1L1	A_23_P18518	1.02	1.06	2.42 ± 0.17
CLN6	A_23_P117797	1.01	1.05	2.41 ± 0.25
PLG	A_23_P30693	0.73	0.80	2.40 ± 0.43
MKI67IP	A_23_P50897	1.19	1.05	2.38 ± 0.25

Gene Name	Probe Name	Fold Decrease (vs shSCX-N)		
		shRb-N	shSCX-HYP	shRb-HYP ± S.D.
ZBTB9	A_23_P8119	1.10	1.14	2.37 ± 0.45
SLC27A4	A_24_P257971	0.91	0.99	2.37 ± 0.67
MUM1	A_23_P208961	0.92	1.04	2.37 ± 0.23
NOL6	A_24_P21410	0.99	1.15	2.37 ± 0.37
NRADDP	A_33_P3386150	0.90	1.08	2.36 ± 0.46
SRSF3	A_33_P3232828	1.04	1.08	2.35 ± 0.07
RPP30	A_33_P3233666	1.12	1.01	2.35 ± 0.36
ABCA1	A_24_P235429	0.68	1.14	2.34 ± 0.25
SLC25A20	A_23_P72025	0.98	1.11	2.34 ± 0.23
CCNE2	A_33_P3217819	0.95	1.06	2.33 ± 0.42
DOLK	A_23_P10870	0.91	1.11	2.32 ± 0.18
FAM86FP	A_33_P3339336	1.15	1.15	2.32 ± 0.34
LSM10	A_24_P216681	1.07	1.15	2.31 ± 0.24
F2	A_23_P94879	0.95	0.88	2.30 ± 0.18
ALG1	A_24_P586523	1.12	1.02	2.30 ± 0.26
SRSF2	A_33_P3412945	0.90	1.00	2.28 ± 0.33
CHAC1	A_33_P3376965	0.99	0.86	2.27 ± 0.40
LRRC31	A_24_P240259	0.71	0.89	2.26 ± 0.34
ANKRD42	A_33_P3224135	0.89	1.01	2.25 ± 0.43
TBC1D30	A_32_P206050	0.92	0.99	2.25 ± 0.71
KBTBD10	A_23_P17190	1.12	0.91	2.25 ± 0.59
CLSPN	A_23_P126212	1.09	0.94	2.24 ± 0.64
CHMP6	A_23_P10156	1.06	0.98	2.23 ± 0.39
TPM3	A_32_P119197	1.04	0.92	2.21 ± 0.49
WDR77	A_23_P115149	1.03	1.05	2.19 ± 0.12
DCTPP1	A_23_P33613	0.92	1.04	2.18 ± 0.33
NCRNA00292	A_33_P3299811	0.92	1.07	2.17 ± 0.39
ALKBH8	A_33_P3318357	0.99	1.03	2.17 ± 0.21
IKZF3	A_23_P376060	0.63	0.79	2.16 ± 0.66
POLA2	A_23_P161615	0.94	0.94	2.14 ± 0.36
NPL	A_33_P3316456	0.83	0.98	2.14 ± 0.34
NPY1R	A_23_P69699	1.06	0.90	2.13 ± 0.27
RFC3	A_23_P14193	0.97	1.06	2.13 ± 0.46
WDR5B	A_33_P3259548	0.88	1.04	2.08 ± 0.28

Gene Name	Probe Name	Fold Decrease (vs shSCX-N)		
		shRb-N	shSCX-HYP	shRb-HYP ± S.D.
ZNF552	A_23_P38830	0.99	1.03	2.08 ± 0.13
DSCC1	A_23_P252740	0.95	0.90	2.02 ± 0.21
FEN1	A_24_P84898	1.00	0.95	2.02 ± 0.28
FAM86B1	A_33_P3628675	0.98	0.99	2.01 ± 0.31
FLJ30679	A_23_P346327	0.82	0.96	2.00 ± 0.66

In silico consensus ARNT:HIF1α binding sequence analysis using the JASPAR database:

ATP4A

GRCh38:chr19:35549443-35564658:

7 putative sites were predicted with these settings (95%) in sequence named **chromosome:GRCh38:19:35549443:35564658:-1**

Model ID	Model name	Score	Relative score	Start	End	Strand	predicted site sequence
MA0259.1	ARNT::HIF1A	10.987	0.993674439370933	544	551	-1	GCACGTGC
MA0259.1	ARNT::HIF1A	10.987	0.993674439370933	544	551	1	GCACGTGC
MA0259.1	ARNT::HIF1A	10.321	0.973806031368894	8723	8730	-1	CTACGTGC
MA0259.1	ARNT::HIF1A	10.184	0.969718986479586	10051	10058	1	ACACGTGC
MA0259.1	ARNT::HIF1A	10.987	0.993674439370933	12380	12387	-1	GCACGTGC
MA0259.1	ARNT::HIF1A	10.987	0.993674439370933	12380	12387	1	GCACGTGC
MA0259.1	ARNT::HIF1A	9.817	0.958770479367351	13501	13508	-1	GGACGTGA

Comment: This type of analysis has a high sensitivity but abysmal selectivity. In other words: while true functional will be detected in most cases, most predictions will correspond to sites bound in vitro but with no function in vivo. A number of additional contraints of the analysis can improve the prediction; phylogenetic footprinting is the most common. We recommend using the ConSite service, which uses the JASPAR datasets.

The review Nat Rev Genet. 2004 Apr;5(4):276-87 gives a comprehensive overview of transcription binding site prediction

-1

PLA2G4D

GRCh38:chr15:42063009-42082008:-1

3 putative sites were predicted with these settings (95%) in sequence named **PLA2G4D_GRCh38:42063009:42082008:-1**

Model ID	Model name	Score	Relative score	Start	End	Strand	predicted site sequence
MA0259.1	ARNT::HIF1A	9.694	0.955101088700307	11044	11051	1	GTACGTGA
MA0259.1	ARNT::HIF1A	9.739	0.956443548700445	16508	16515	-1	GCACGTGG
MA0259.1	ARNT::HIF1A	10.232	0.971150943813066	16508	16515	1	CCACGTGC

Comment: This type of analysis has a high sensitivity but abysmal selectivity. In other words: while true functional will be detected in most cases, most predictions will correspond to sites bound in vitro but with no function in vivo. A number of additional contraints of the analysis can improve the prediction; phylogenetic footprinting is the most common. We recommend using the ConSite service, which uses the JASPAR datasets.

The review Nat Rev Genet. 2004 Apr;5(4):276-87 gives a comprehensive overview of transcription binding site prediction

GRCh38:chr15:42082009-42098554:-1

7 putative sites were predicted with these settings (95%) in sequence named **PLA2G4D_GRCh38:15:42082009-42098554:-1**

Model ID	Model name	Score	Relative score	Start	End	Strand	predicted site sequence
MA0259.1	ARNT::HIF1A	9.817	0.958770479367351	3899	3906	1	GGACGTGA
MA0259.1	ARNT::HIF1A	10.232	0.971150943813066	6727	6734	-1	CCACGTGC
MA0259.1	ARNT::HIF1A	9.739	0.956443548700445	6727	6734	1	GCACGTGG
MA0259.1	ARNT::HIF1A	10.184	0.969718986479586	8863	8870	1	ACACGTGC
MA0259.1	ARNT::HIF1A	9.657	0.95399728825575	11047	11054	-1	GAACGTGC
MA0259.1	ARNT::HIF1A	10.184	0.969718986479586	13637	13644	-1	ACACGTGC
MA0259.1	ARNT::HIF1A	9.951	0.962768026923317	14182	14189	1	GGACGTGG

Comment: This type of analysis has a high sensitivity but abysmal selectivity. In other words: while true functional will be detected in most cases, most predictions will correspond to sites bound in vitro but with no function in vivo. A number of additional contraints of the analysis can improve the prediction; phylogenetic footprinting is the most common. We recommend using the ConSite service, which uses the JASPAR datasets.

The review Nat Rev Genet. 2004 Apr;5(4):276-87 gives a comprehensive overview of transcription binding site prediction

NIM1K

hg38:chr5:43190068-43209000:+1

3 putative sites were predicted with these settings (95%) in sequence named **NIM1K_hg38:chr5:43190068-43209000:+1**

Model ID	Model name	Score	Relative score	Start	End	Strand	predicted site sequence
MA0259.1	ARNT::HIF1A	10.987	0.993674439370933	8988	8995	-1	GCACGTGC
MA0259.1	ARNT::HIF1A	10.987	0.993674439370933	8988	8995	1	GCACGTGC
MA0259.1	ARNT::HIF1A	11.075	0.996299694482314	14160	14167	-1	GTACGTGC

Comment: This type of analysis has a high sensitivity but abysmal selectivity. In other words: while true functional will be detected in most cases, most predictions will correspond to sites bound in vitro but with no function in vivo. A number of additional contraints of the analysis can improve the prediction; phylogenetic footprinting is the most common. We recommend using the ConSite service, which uses the JASPAR datasets.

The review Nat Rev Genet. 2004 Apr;5(4):276-87 gives a comprehensive overview of transcription binding site prediction

hg38:chr5:43,209,01-43,228,000:+1

0 putative sites were predicted with these settings (95%) in sequence named **NIM1K_hg38:chr5:43209001:43228000:+1**

Model ID	Model name	Score	Relative score	Start	End	Strand	predicted site sequence

Comment: This type of analysis has a high sensitivity but abysmal selectivity. In other words: while true functional will be detected in most cases, most predictions will correspond to sites bound in vitro but with no function in vivo. A number of additional contraints of the analysis can improve the prediction; phylogenetic footprinting is the most common. We recommend using the ConSite service, which uses the JASPAR datasets.

The review Nat Rev Genet. 2004 Apr;5(4):276-87 gives a comprehensive overview of transcription binding site prediction

hg38:chr5:43228001-43247000:+1

3 putative sites were predicted with these settings (95%) in sequence named **NIM1K_hg38:chr5:43228001-43247000:+1**

Model ID	Model name	Score	Relative score	Start	End	Strand	predicted site sequence
MA0259.1	ARNT::HIF1A	10.321	0.973806031368894	2882	2889	1	CTACGTGC
MA0259.1	ARNT::HIF1A	9.828	0.959098636256273	3940	3947	-1	GTACGTGG
MA0259.1	ARNT::HIF1A	9.951	0.962768026923317	17317	17324	1	GGACGTGG

Comment: This type of analysis has a high sensitivity but abysmal selectivity. In other words: while true functional will be detected in most cases, most predictions will correspond to sites bound in vitro but with no function in vivo. A number of additional contraints of the analysis can improve the prediction; phylogenetic footprinting is the most common. We recommend using the ConSite service, which uses the JASPAR datasets.

The review Nat Rev Genet. 2004 Apr;5(4):276-87 gives a comprehensive overview of transcription binding site prediction

hg38:chr5:43247001-43266000:+1

0 putative sites were predicted with these settings (95%) in sequence named **NIM1K_hg38:chr5:43247001-43266000:+1**

Model ID	Model name	Score	Relative score	Start	End	Strand	predicted site sequence

Comment: This type of analysis has a high sensitivity but abysmal selectivity. In other words: while true functional will be detected in most cases, most predictions will correspond to sites bound in vitro but with no function in vivo. A number of additional contraints of the analysis can improve the prediction; phylogenetic footprinting is the most common. We recommend using the ConSite service, which uses the JASPAR datasets.

The review Nat Rev Genet. 2004 Apr;5(4):276-87 gives a comprehensive overview of transcription binding site prediction

hg38:chr5:43266001-43282850:+1

2 putative sites were predicted with these settings (95%) in sequence named **NIM1K_hg38:chr5:43266001-43282850:+1**

Model ID	Model name	Score	Relative score	Start	End	Strand	predicted site sequence
MA0259.1	ARNT::HIF1A	9.590	0.951998514477767	10481	10488	-1	GGACGTGT
MA0259.1	ARNT::HIF1A	10.184	0.969718986479586	14294	14301	-1	ACACGTGC

Comment: This type of analysis has a high sensitivity but abysmal selectivity. In other words: while true functional will be detected in most cases, most predictions will correspond to sites bound in vitro but with no function in vivo. A number of additional contraints of the analysis can improve the prediction; phylogenetic footprinting is the most common. We recommend using the ConSite service, which uses the JASPAR datasets.

The review Nat Rev Genet. 2004 Apr;5(4):276-87 gives a comprehensive overview of transcription binding site prediction

CYP26A1

hg38:chr10:93071890-93079890:+1

3 putative sites were predicted with these settings (95%) in sequence named **CYP26A1:hg38:chr10:93071890-93079890:+1**

Model ID	Model name	Score	Relative score	Start	End	Strand	predicted site sequence
MA0259.1	ARNT::HIF1A	9.817	0.958770479367351	73	80	-1	GGACGTGA
MA0259.1	ARNT::HIF1A	10.321	0.973806031368894	2928	2935	1	CTACGTGC
MA0259.1	ARNT::HIF1A	10.444	0.977475422035937	3153	3160	1	CGACGTGC

Comment: This type of analysis has a high sensitivity but abysmal selectivity. In other words: while true functional will be detected in most cases, most predictions will correspond to sites bound in vitro but with no function in vivo. A number of additional contraints of the analysis can improve the prediction; phylogenetic footprinting is the most common. We recommend using the ConSite service, which uses the JASPAR datasets.

The review Nat Rev Genet. 2004 Apr;5(4):276-87 gives a comprehensive overview of transcription binding site prediction

KISS1R

hg38:chr19:915342-923015:+1

11 putative sites were predicted with these settings (95%) in sequence named **KISS1R_hg38:chr19:915342-923015:+1**

Model ID	Model name	Score	Relative score	Start	End	Strand	predicted site sequence
MA0259.1	ARNT::HIF1A	9.817	0.958770479367351	3219	3226	1	GGACGTGA
MA0259.1	ARNT::HIF1A	9.828	0.959098636256273	3456	3463	1	GTACGTGG
MA0259.1	ARNT::HIF1A	10.232	0.971150943813066	3508	3515	-1	CCACGTGC
MA0259.1	ARNT::HIF1A	9.739	0.956443548700445	3508	3515	1	GCACGTGG
MA0259.1	ARNT::HIF1A	10.232	0.971150943813066	3607	3614	-1	CCACGTGC
MA0259.1	ARNT::HIF1A	9.739	0.956443548700445	3607	3614	1	GCACGTGG
MA0259.1	ARNT::HIF1A	9.694	0.955101088700307	4202	4209	1	GTACGTGA
MA0259.1	ARNT::HIF1A	9.542	0.950566557144287	4240	4247	-1	GGGCGTGC
MA0259.1	ARNT::HIF1A	9.590	0.951998514477767	4321	4328	-1	GGACGTGT
MA0259.1	ARNT::HIF1A	10.232	0.971150943813066	4476	4483	-1	CCACGTGC
MA0259.1	ARNT::HIF1A	9.739	0.956443548700445	4476	4483	1	GCACGTGG

Comment: This type of analysis has a high sensitivity but abysmal selectivity. In other words: while true functional will be detected in most cases, most predictions will correspond to sites bound in vitro but with no function in vivo. A number of additional contraints of the analysis can improve the prediction; phylogenetic footprinting is the most common. We recommend using the ConSite service, which uses the JASPAR datasets.

The review Nat Rev Genet. 2004 Apr;5(4):276-87 gives a comprehensive overview of transcription binding site prediction

GPR26

hg38:chr10:123664355-123683000:+1

5 putative sites were predicted with these settings (95%) in sequence named **GPR26_hg38:chr10:123664355-123683000:+1**

Model ID	Model name	Score	Relative score	Start	End	Strand	predicted site sequence
MA0259.1	ARNT::HIF1A	9.951	0.962768026923317	411	418	-1	GGACGTGG
MA0259.1	ARNT::HIF1A	9.605	0.952446001144479	2196	2203	-1	GCACGTGA
MA0259.1	ARNT::HIF1A	11.075	0.996299694482314	2622	2629	-1	GTACGTGC
MA0259.1	ARNT::HIF1A	10.184	0.969718986479586	3960	3967	-1	ACACGTGC
MA0259.1	ARNT::HIF1A	10.184	0.969718986479586	6350	6357	-1	ACACGTGC

Comment: This type of analysis has a high sensitivity but abysmal selectivity. In other words: while true functional will be detected in most cases, most predictions will correspond to sites bound in vitro but with no function in vivo. A number of additional contraints of the analysis can improve the prediction; phylogenetic footprinting is the most common. We recommend using the ConSite service, which uses the JASPAR datasets.

The review Nat Rev Genet. 2004 Apr;5(4):276-87 gives a comprehensive overview of transcription binding site prediction

hg38:chr10:123683001-123696607:+1

2 putative sites were predicted with these settings (95%) in sequence named **GPR26_hg38:chr10:123683001-123696607:+1**

Model ID	Model name	Score	Relative score	Start	End	Strand	predicted site sequence
MA0259.1	ARNT::HIF1A	10.184	0.969718986479586	1330	1337	1	ACACGTGC
MA0259.1	ARNT::HIF1A	9.951	0.962768026923317	2025	2032	-1	GGACGTGG

Comment: This type of analysis has a high sensitivity but abysmal selectivity. In other words: while true functional will be detected in most cases, most predictions will correspond to sites bound in vitro but with no function in vivo. A number of additional contraints of the analysis can improve the prediction; phylogenetic footprinting is the most common. We recommend using the ConSite service, which uses the JASPAR datasets.

The review Nat Rev Genet. 2004 Apr;5(4):276-87 gives a comprehensive overview of transcription binding site prediction

MYBPC2

hg38:chr19:50430903-50450000:+1

3 putative sites were predicted with these settings (95%) in sequence named **MYBPC2_hg38:chr19:50430903-50450000:+1**

Model ID	Model name	Score	Relative score	Start	End	Strand	predicted site sequence
MA0259.1	ARNT::HIF1A	9.951	0.962768026923317	5621	5628	1	GGACGTGG
MA0259.1	ARNT::HIF1A	10.232	0.971150943813066	18793	18800	-1	CCACGTGC
MA0259.1	ARNT::HIF1A	9.739	0.956443548700445	18793	18800	1	GCACGTGG

Comment: This type of analysis has a high sensitivity but abysmal selectivity. In other words: while true functional will be detected in most cases, most predictions will correspond to sites bound in vitro but with no function in vivo. A number of additional contraints of the analysis can improve the prediction; phylogenetic footprinting is the most common. We recommend using the ConSite service, which uses the JASPAR datasets.

The review Nat Rev Genet. 2004 Apr;5(4):276-87 gives a comprehensive overview of transcription binding site prediction

hg38:chr19:50450001-50468321:+1

6 putative sites were predicted with these settings (95%) in sequence named **MYBPC2_hg38:chr19:50450001-50468321:+1**

Model ID	Model name	Score	Relative score	Start	End	Strand	predicted site sequence
MA0259.1	ARNT::HIF1A	9.951	0.962768026923317	4148	4155	1	GGACGTGG
MA0259.1	ARNT::HIF1A	10.987	0.993674439370933	9173	9180	-1	GCACGTGC
MA0259.1	ARNT::HIF1A	10.987	0.993674439370933	9173	9180	1	GCACGTGC
MA0259.1	ARNT::HIF1A	9.605	0.952446001144479	10330	10337	1	GCACGTGA
MA0259.1	ARNT::HIF1A	10.987	0.993674439370933	10843	10850	-1	GCACGTGC
MA0259.1	ARNT::HIF1A	10.987	0.993674439370933	10843	10850	1	GCACGTGC

Comment: This type of analysis has a high sensitivity but abysmal selectivity. In other words: while true functional will be detected in most cases, most predictions will correspond to sites bound in vitro but with no function in vivo. A number of additional contraints of the analysis can improve the prediction; phylogenetic footprinting is the most common. We recommend using the ConSite service, which uses the JASPAR datasets.

The review Nat Rev Genet. 2004 Apr;5(4):276-87 gives a comprehensive overview of transcription binding site prediction

PCP4L1

hg38:chr1:161256727-161273000:+1

3 putative sites were predicted with these settings (95%) in sequence named **PCP4L1_hg38:chr1:161256727-161273000:+1**

Model ID	Model name	Score	Relative score	Start	End	Strand	predicted site sequence
MA0259.1	ARNT::HIF1A	9.590	0.951998514477767	2771	2778	1	GGACGTGT
MA0259.1	ARNT::HIF1A	10.987	0.993674439370933	14921	14928	-1	GCACGTGC
MA0259.1	ARNT::HIF1A	10.987	0.993674439370933	14921	14928	1	GCACGTGC

Comment: This type of analysis has a high sensitivity but abysmal selectivity. In other words: while true functional will be detected in most cases, most predictions will correspond to sites bound in vitro but with no function in vivo. A number of additional contraints of the analysis can improve the prediction; phylogenetic footprinting is the most common. We recommend using the ConSite service, which uses the JASPAR datasets.

The review Nat Rev Genet. 2004 Apr;5(4):276-87 gives a comprehensive overview of transcription binding site prediction

hg38:chr1:161273001-161287450:+1

0 putative sites were predicted with these settings (95%) in sequence named **PCP4L1_hg38:chr1:161273001-161287450:+1**

Model ID	Model name	Score	Relative score	Start	End	Strand	predicted site sequence

Comment: This type of analysis has a high sensitivity but abysmal selectivity. In other words: while true functional will be detected in most cases, most predictions will correspond to sites bound in vitro but with no function in vivo. A number of additional contraints of the analysis can improve the prediction; phylogenetic footprinting is the most common. We recommend using the ConSite service, which uses the JASPAR datasets.

The review Nat Rev Genet. 2004 Apr;5(4):276-87 gives a comprehensive overview of transcription binding site prediction

AMPD3

hg38:chr11:10453320-10472000:1+

1 putative sites were predicted with these settings (95%) in sequence named **AMPD3_hg38:chr11:10453320-10472000:1+**

Model ID	Model name	Score	Relative score	Start	End	Strand	predicted site sequence
MA0259.1	ARNT::HIF1A	9.657	0.95399728825575	2583	2590	-1	GAACGTGC

Comment: This type of analysis has a high sensitivity but abysmal selectivity. In other words: while true functional will be detected in most cases, most predictions will correspond to sites bound in vitro but with no function in vivo. A number of additional contraints of the analysis can improve the prediction; phylogenetic footprinting is the most common. We recommend using the ConSite service, which uses the JASPAR datasets.

The review Nat Rev Genet. 2004 Apr;5(4):276-87 gives a comprehensive overview of transcription binding site prediction

hg38:chr11:10472001-10490500:+1

3 putative sites were predicted with these settings (95%) in sequence named **AMPD3_hg38:chr11:10472001-10490500:+1**

Model ID	Model name	Score	Relative score	Start	End	Strand	predicted site sequence
MA0259.1	ARNT::HIF1A	10.987	0.993674439370933	13390	13397	-1	GCACGTGC
MA0259.1	ARNT::HIF1A	10.987	0.993674439370933	13390	13397	1	GCACGTGC
MA0259.1	ARNT::HIF1A	9.605	0.952446001144479	16429	16436	1	GCACGTGA

Comment: This type of analysis has a high sensitivity but abysmal selectivity. In other words: while true functional will be detected in most cases, most predictions will correspond to sites bound in vitro but with no function in vivo. A number of additional contraints of the analysis can improve the prediction; phylogenetic footprinting is the most common. We recommend using the ConSite service, which uses the JASPAR datasets.

The review Nat Rev Genet. 2004 Apr;5(4):276-87 gives a comprehensive overview of transcription binding site prediction

hg38:chr11:10490501-10509579:+1

3 putative sites were predicted with these settings (95%) in sequence named **AMPD3_hg38:chr11:10490501-10509579:+1**

Model ID	Model name	Score	Relative score	Start	End	Strand	predicted site sequence
MA0259.1	ARNT::HIF1A	9.657	0.95399728825575	4343	4350	1	GAACGTGC
MA0259.1	ARNT::HIF1A	10.184	0.969718986479586	10160	10167	1	ACACGTGC
MA0259.1	ARNT::HIF1A	9.657	0.95399728825575	10984	10991	-1	GAACGTGC

Comment: This type of analysis has a high sensitivity but abysmal selectivity. In other words: while true functional will be detected in most cases, most predictions will correspond to sites bound in vitro but with no function in vivo. A number of additional contraints of the analysis can improve the prediction; phylogenetic footprinting is the most common. We recommend using the ConSite service, which uses the JASPAR datasets.

The review Nat Rev Genet. 2004 Apr;5(4):276-87 gives a comprehensive overview of transcription binding site prediction

SCNN1G

hg38:chr16:23180715-23199500:+1

1 putative sites were predicted with these settings (95%) in sequence named **SCNN1G_hg38:chr16:23180715-23199500:+1**

Model ID	Model name	Score	Relative score	Start	End	Strand	predicted site sequence
MA0259.1	ARNT::HIF1A	9.542	0.950566557144287	5513	5520	-1	GGGCGTGC

Comment: This type of analysis has a high sensitivity but abysmal selectivity. In other words: while true functional will be detected in most cases, most predictions will correspond to sites bound in vitro but with no function in vivo. A number of additional contraints of the analysis can improve the prediction; phylogenetic footprinting is the most common. We recommend using the ConSite service, which uses the JASPAR datasets.

The review Nat Rev Genet. 2004 Apr;5(4):276-87 gives a comprehensive overview of transcription binding site prediction

hg38:chr16:23199501-23218803:1+

5 putative sites were predicted with these settings (95%) in sequence named **SCNN1G_hg38:chr16:23199501-23218803:1+**

Model ID	Model name	Score	Relative score	Start	End	Strand	predicted site sequence
MA0259.1	ARNT::HIF1A	9.951	0.962768026923317	3823	3830	1	GGACGTGG
MA0259.1	ARNT::HIF1A	10.232	0.971150943813066	8501	8508	-1	CCACGTGC
MA0259.1	ARNT::HIF1A	9.739	0.956443548700445	8501	8508	1	GCACGTGG
MA0259.1	ARNT::HIF1A	9.951	0.962768026923317	9428	9435	-1	GGACGTGG
MA0259.1	ARNT::HIF1A	9.542	0.950566557144287	18379	18386	1	GGGCGTGC

Comment: This type of analysis has a high sensitivity but abysmal selectivity. In other words: while true functional will be detected in most cases, most predictions will correspond to sites bound in vitro but with no function in vivo. A number of additional contraints of the analysis can improve the prediction; phylogenetic footprinting is the most common. We recommend using the ConSite service, which uses the JASPAR datasets.

The review Nat Rev Genet. 2004 Apr;5(4):276-87 gives a comprehensive overview of transcription binding site prediction

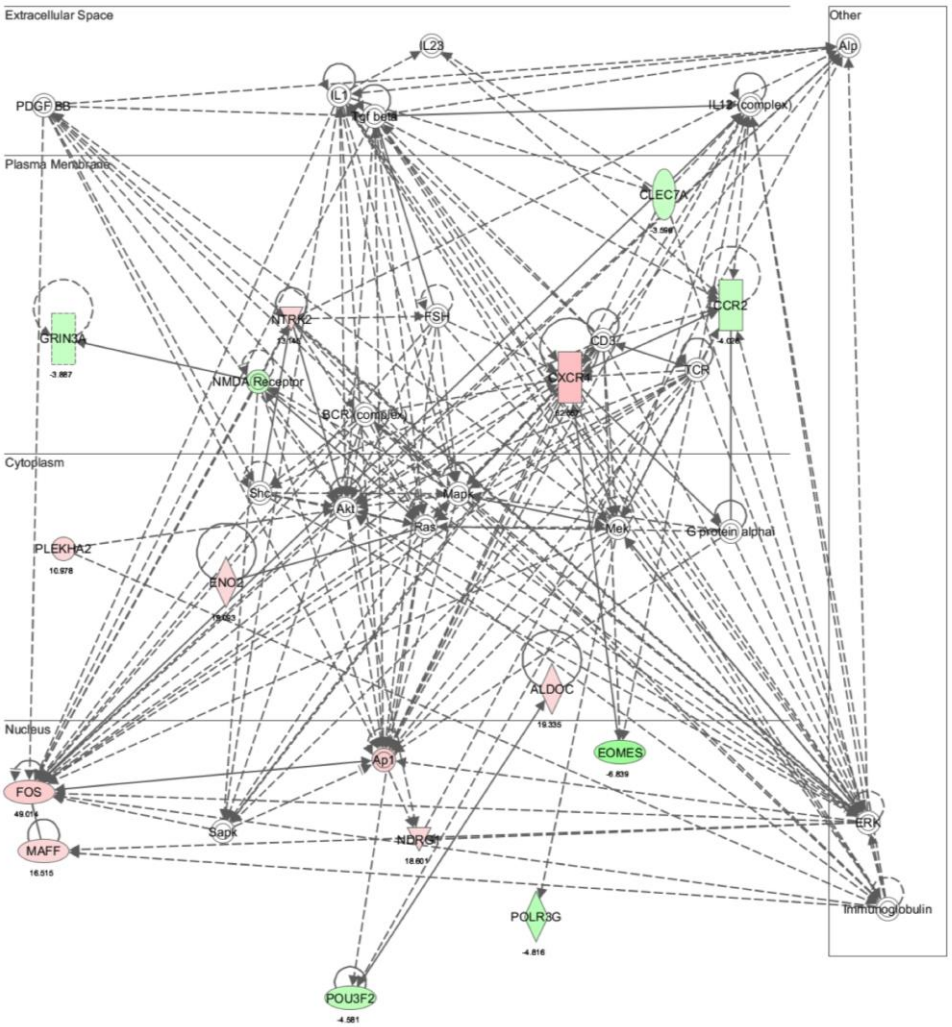

Figure 4.8. Supplementary Figure 1.
Cellular Movement, Hematological System Development and Function, Immune Cell Trafficking Network. A network identified after Ingenuity Pathway Assist analysis of the top 50 up-regulated genes and top 50 down-regulated genes that are most sensitive to Rb-loss and hypoxia from the shRNA LNCaP microarray.

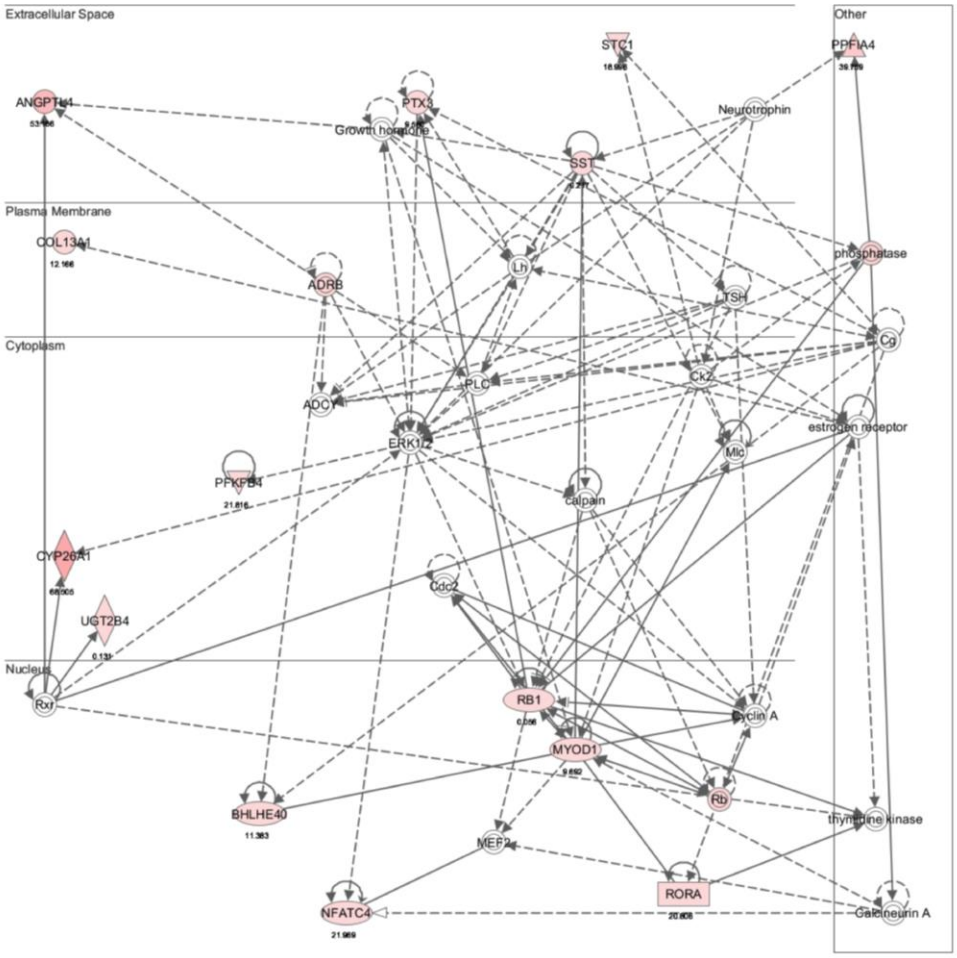

Figure 4.9. Supplementary Figure 2.
Cardiovascular System Organismal Development, Skeletal and Muscular System Network. A network identified after Ingenuity Pathway Assist analysis of the top 50 up-regulated genes and top 50 down-regulated genes that are most sensitive to Rb-loss and hypoxia from the shRNA LNCaP microarray.

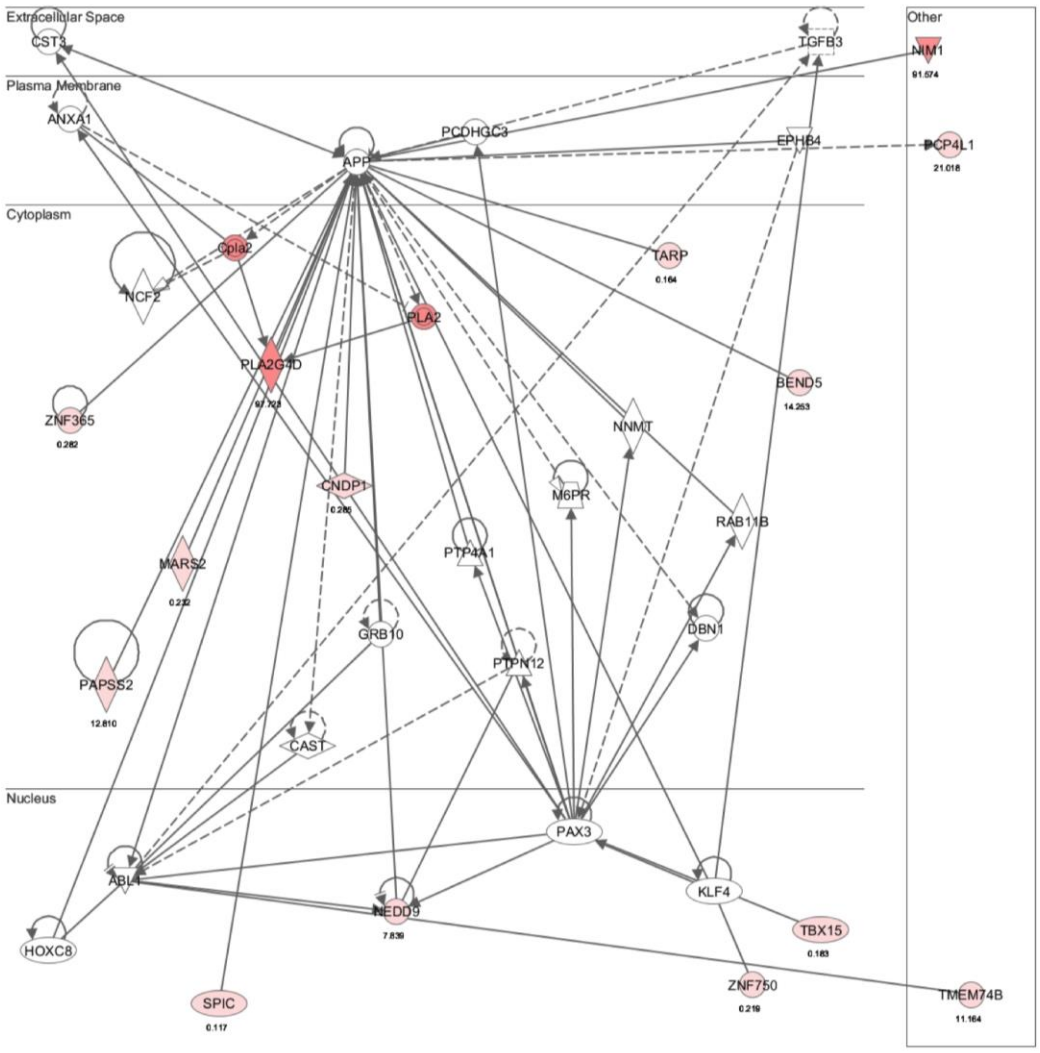

Figure 4.10. Supplementary Figure 3.
Cardiovascular Disease Developmental Disorder, Hereditary Disorder Network. A network identified after Ingenuity Pathway Assist analysis of the top 50 up-regulated genes and top 50 down-regulated genes that are most sensitive to Rb-loss and hypoxia from the shRNA LNCaP microarray.

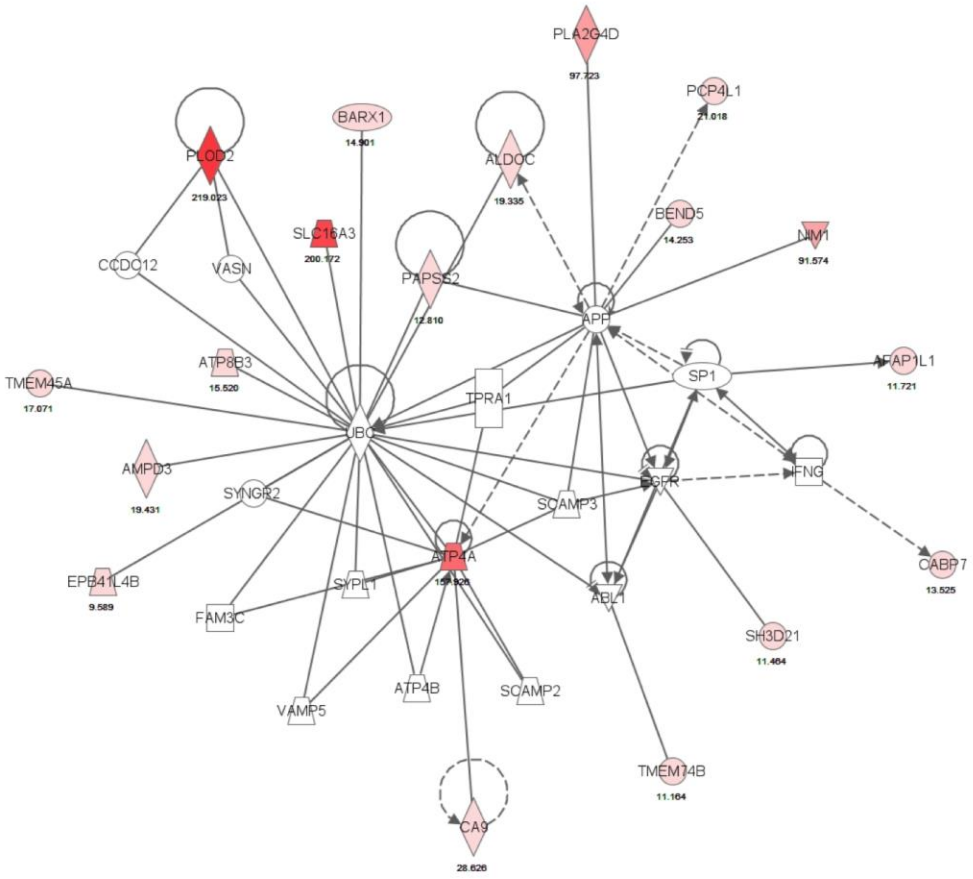

Figure 4.11. Supplementary Figure 4.
Cardiac Arteriopathy, Cardiovascular Disease, Hematological Disease Network. A network identified after Ingenuity Pathway Assist analysis of the top 50 up-regulated genes and top 50 down-regulated genes that are most sensitive to Rb-loss and hypoxia from the shRNA LNCaP microarray.

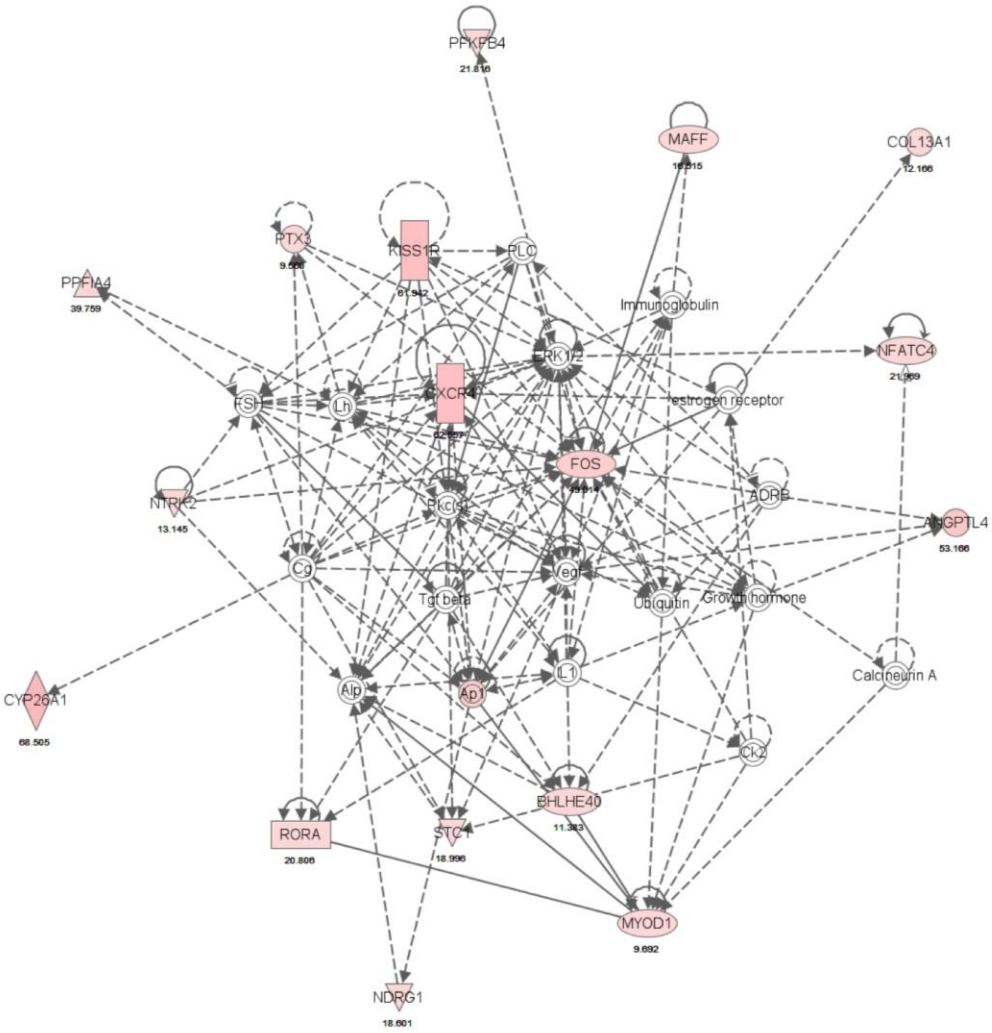

Figure 4.12. Supplementary Figure 5.
Organ Morphology, Organismal Development, Reproductive System Development and Function Network. A network identified after Ingenuity Pathway Assist analysis of the top 50 up-regulated genes and top 50 down-regulated genes that are most sensitive to Rb-loss and hypoxia from the shRNA LNCaP microarray.

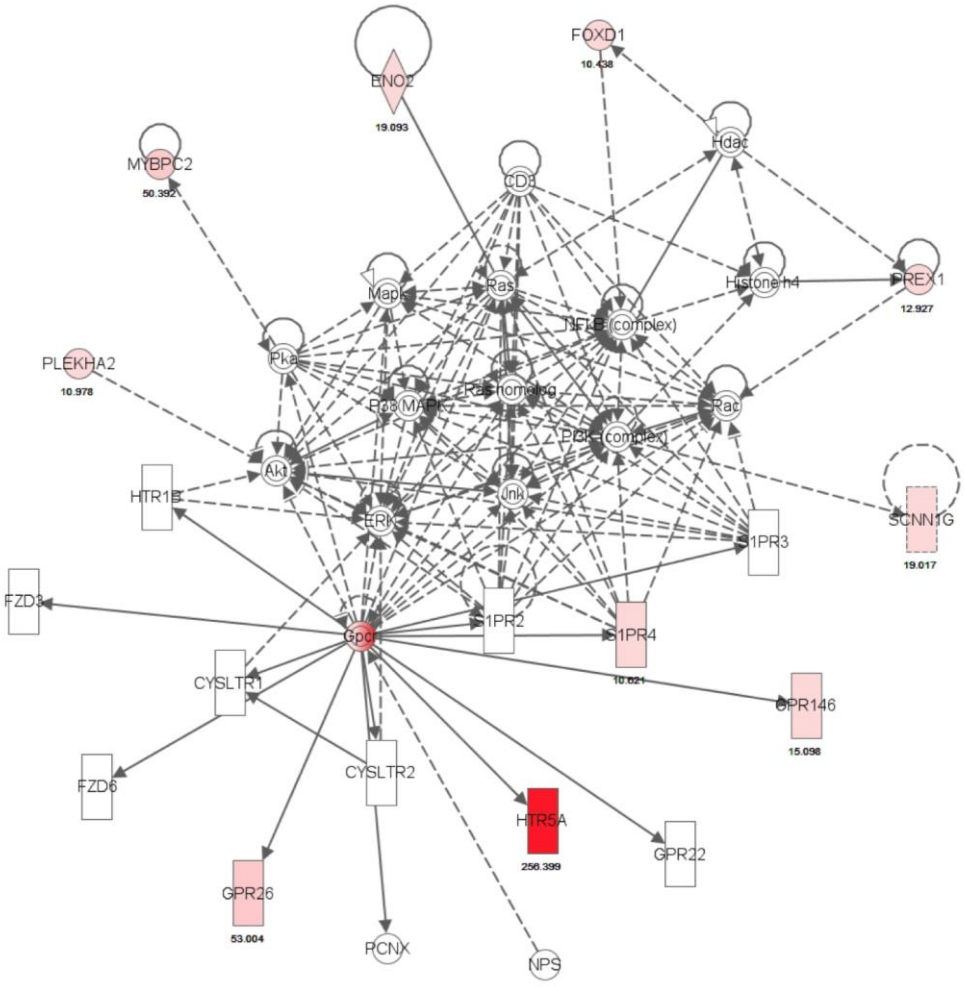

Figure 4.13. Supplementary Figure 6.
Cellular Development, Cellular Growth and Proliferation, Hematological System Development and Function Network. A network identified after Ingenuity Pathway Assist analysis of the top 50 up-regulated genes and top 50 down-regulated genes that are most sensitive to Rb-loss and hypoxia from the shRNA LNCaP microarray.

MATERIALS AND METHODS:

Transient Transfections: LNCaP and shRb LNCaP cells were transfected with 10–15 nM of either scrambled (siSCX) siRNA or DP1 siRNAs (siDP1-i and siDP1-ii) using 0.3% (v/v) Lipofectamine RNAiMAX (Invitrogen Inc) according to manufacturer's protocol. The cells were allowed to incubate in transfection mix for 6 h at 37°C, 20% O2, and 5% CO2 after which the transfection mix was removed and replaced with complete media.

Slide Preparation and Hypoxia Treatment: 18 mm round slides were soaked in 1 N Nitric Acid overnight, then washed two- three times with mili-Q water and stored in 70% Ethanol. Before use, the slides were washed twice with sterile PBS and coated with polyethylenamine for 30 min at 37 °C. LNCaP shSCX and shRb cells were seeded at 62,500 cells/slide on 18 mm round glass slides in a 12-well plate. One of the plates was placed into a hypoxia chamber set at 37 °C, 1% O2, and 5% CO2, while the other plate was left at 37 °C, 20% O2, and 5% CO2 for 96 h.

Immunostaining: Following 96 h of hypoxia or normoxia the slides were washed two times with ice cold PBS, and fixed with ice cold Methanol at -20 °C for 10 min. The slides were then washed two times with ice cold PBS and blocked in 5% Normal Donkey Serum (Jackson ImmunoResearch Laboratories) and 0.3 M Glycine in PBS for 30 min at room temperature. Next, the slides were incubated with either PBS or KISS1R primary antibody (1/100 dilution; abcam; ab140839) overnight at 4 °C. Following incubation, the slides were washed two times with ice cold PBS for 5 min at room temperature. The slides were then incubated with Alexa Flour® 680 donkey anti-rabbit IgG (1/1000, Life technologies; A10043) in PBS for 1 h at room temperature, then washed two times with ice cold PBS for 5 min. Slides were stained with Hoescht (1/10,000) in PBS for 1 min, followed by two washes of ice cold PBS. Lastly, the slides were mounted using FlourSave (Calbiochem), and imaged at 60x using water and the Metamorph software. *Number of Foci/cell was counted using the Metamorph software. (using a threshold of 450 and dot range of 10-120)*

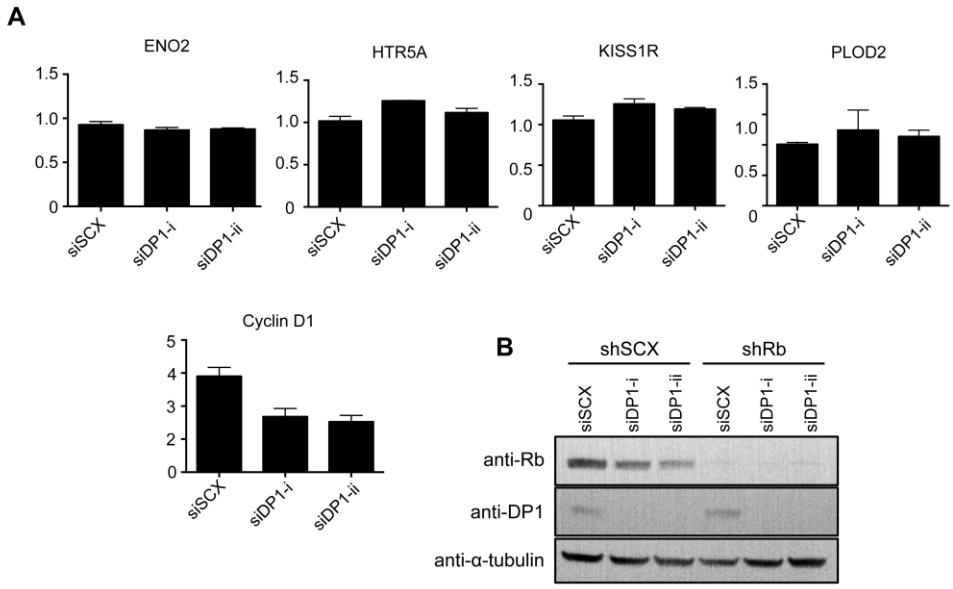

Figure 4.14. Supplementary Figure 7.
siRNA-mediated suppression of DP1 expression in shRb LNCaP cells does not affect HIF1-regulated transcription of identified array genes. (A) shRb LNCaP cells were transfected with either scrambled siRNA (siSCX) or DP1 siRNAs (siDP1-i and siDP1-ii). Twenty-four hours after transfection cells were treated with 1% O2 for a further 24 h. Gene expression was determined by quantitative real-time PCR after isolation and reverse transcription of total RNA. Target gene expression was normalized to constitutively active 36B4 gene expression. Cyclin D1 expression was used as a positive control as it is directly regulated by E2F-DP1 transcription factors. Error bars represent ± S.D. (B) Immunoblot of Rb, DP1 and α-tubulin. shRNA LNCaP cells were transfected with either scrambled control (siSCX) or two siRNA directed to DP1. Forty-eight hours after transfection, whole cell lysates were collected, analyzed and fractionated by SDS-PAGE. Alpha-tubulin (α-tubulin) was used as a loading control.

A

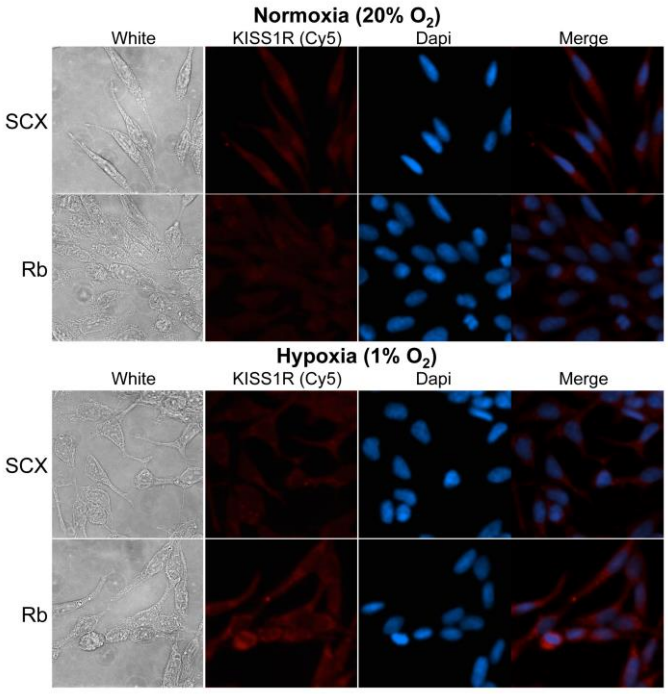

B

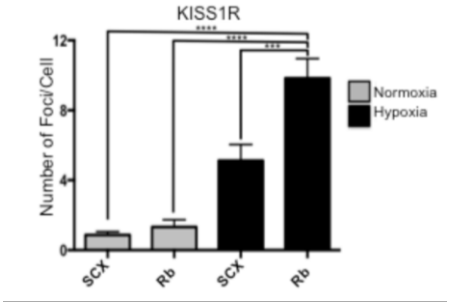

Figure 4.15. Supplementary Figure 8.
Cytoplasmic and membrane KISS1R protein expression is increased in Rb-ablated LNCaP cells exposed to hypoxia. **(A)** Immunocytochemistry of shRNA LNCaP cells treated with either normoxia or hypoxia for 96 hours. Cells were stained with KISS1R primary antibody and Hoescht and then imaged on a fluorescent microscope at 60x using water and the Metamorph software. **(B)** Number of Foci per cell was counted using the Metamorph software and a threshold of 450 and dot range of 10-120. Error bars represent ± S.D. ***p<0.05.

Chapter 5. A retinoblastoma protein-hypoxia-inducible factor-1/2α complex regulates hypoxia inducible transcriptional programs, actin reorganization and cancer cell invasiveness in breast cancer cells

This chapter is in preparation for publication.

Authors: Mark P. Labrecque, Mandeep K. Takhar, Samaneh Khakshour, Anne Haegert, Robert H. Bell, Manuel Altamirano-Dimas, Colin C. Collins, Gratien G. Prefontaine, Michael E. Cox, and Timothy V. Beischlag

Author Contributions: I performed all tissue culture and generated the shRNA cell lines for both MCF7 and MDA-MB-231 cells. I conducted the immunoblot represented in Figure 5.1A. Ann Haegert performed the microarray. Timothy Beischlag and I worked in collaboration with Robert Bell, Manuel Altamirano-Dimas and Collin Collins to analyze the microarray data and perform gene ontology analysis. I validated the microarray results through qPCR in shRNA MCF7 and shRNA MDA-MB-231 cells shown in Figure 5.3. Mandeep Takhar produced the immunoblots represented in Figure 5.4. Samaneh Khakshour constructed the optical tweezer and manipulated cells to measure the normalized amplitude of resultant bead movement (NARBM) shown in Figure 5.5A. I performed the migration assays represented in Figure 5.5B. Timothy Beischlag, Gratien Prefontaine and Michael Cox conceived and designed the experiments. I wrote the initial draft of the manuscript and Timothy Beischlag, Michael Cox and I wrote the final published version of the manuscript.

5.1. Abstract

Localized hypoxia in solid tumors activates transcriptional programs that promote the metastatic transformation of cells. Like hypoxia-inducible hyper-vascularization, loss

of the retinoblastoma protein (Rb) is a trait common to advanced stages of tumor progression in many metastatic cancers. We recently demonstrated that Rb is a key mediator of the hypoxic response controlled by HIF1α/β, the master regulator of the hypoxia response, and its essential coactivator, the thyroid hormone receptor/retinoblastoma-interacting protein (TRIP230). Here, using short-hairpin RNA approaches and microarray analysis, we identified hypoxia-inducible gene programs that are further exacerbated with loss of Rb expression in MCF7 breast cancer cells. Additionally, suppressed Rb expression in conjunction with hypoxia lincreases mRNA and protein levels of identified array genes in shRNA MCF7 and MDA-MB-231 human breast cancer cells. Finally, hypoxia and Rb-depletion significantly exacerbates actin reorganization and cell migration in MCF7 breast cancer cells and chemical inhibitors of ERK1/2 and AKT1/2 block these effects. These results demonstrate that Rb mediates specific hypoxia-regulated transcriptional programs that promote both cell motility and metastasis by virtue of its direct effects on the HIF1 complex.

5.2. Introduction

Targeting angiogenic factors has been an attractive strategy for the development of anti-tumor therapies. However, such approaches are limited because metastasis is not entirely dependent on angiogenesis and tumors progress to metastatic states despite existing anti-angiogenic therapies [386]. Importantly, the *de novo* vascularization of tumors, and cell transition from epithelial to invasive phenotypes that lead to metastasis are determined by the tumor's micro-environment [387]. In particular, all solid tumors of significant size have regions of hypoxia that initiate angiogenesis and trigger cells to become more invasive thereby promoting metastasis [387]. Thus, innovations in cancer therapeutics require better understanding of the molecular determinants of cell invasion that also contribute to metastasis.

Primary factors regulating angiogenesis and cell invasion include the hypoxia inducible factor-1α (HIF1α), its homologue HIF2α, and their dimerization partner the aryl hydrocarbon receptor nuclear translocator, ARNT or HIF1β which make up the HIF1 complex [126,283]. In healthy tissue, the HIF complex directs the ordered and tightly

regulated expression of genes controlling the *de novo* synthesis of new vasculature to support tissue growth or tissue re-perfusion. Cancerous tissue is characterized by hypervasculature displaying aberrant structure and morphology, suggesting a breakdown in the structured process of angiogenesis [205]. Furthermore, HIF1α stabilization is associated with increased micro-vessel density and VEGF expression in various carcinomas and is correlated with increased risk of mortality in several cancers [126]. During hypoxia, HIF1α accumulates, translocates to the nucleus, and binds ARNT. The HIF1 complex recruits coactivators including CBP/p300 [279] and Brm/Brg-1 [284] to activate the expression of genes, such as vascular endothelial growth factor (VEGF) and erythropoietin (EPO) [126]. Additionally, The HIF1 complex recruits the transcriptional coactivator thyroid hormone receptor/retinoblastoma protein-interacting protein-230 (TRIP230) to the regulatory regions of hypoxia-responsive genes to activate transcription [150]. TRIP230, was initially identified as a thyroid hormone receptor (TR)-interacting protein that enhanced TRs activity [292]. In addition, TRIP230 has been isolated as part of the p160 coactivator complex [293], a bona fide ARNT coactivator complex [49]. Importantly, we have demonstrated that TRIP230 is recruited by ARNT as a transcriptional coactivator and it is essential for the transcriptional activity of the HIF1 complex [150]. Furthermore, it was shown that TRIP230 interacts with Rb and that Rb attenuates TRIP230-enhanced TR-driven transcription [149]. Subsequent studies demonstrated that only the hyper-phosphorylated form of Rb interacts with TRIP230 [153] and that loss of Rb function unmasks the full coactivator potential of TRIP230 and exacerbates HIF1 transcription factor functions [327], thus highlighting a role for Rb distinct from its canonical E2F-dependent regulation of cell cycle, specific to its hypo-phosphorylated form.

Loss of *RB1*, the gene that codes for Rb [156], and or loss-of-function of Rb is associated with the development and metastatic progression of many solid tumors including cancers of the ovary, lung, breast and brain [205,294-296]. The best understood function of Rb is that of cell cycle regulator repressing E2F transcription factor function thereby mediating cell proliferation and differentiation [297]. Hypo-phosphorylated Rb blocks cell cycle progression by binding to E2F transcription factors and modulating E2F-dependent transcriptional outcomes. It does so by recruiting chromatin-remodeling transcriptional repressor proteins such as Sin3a/b, HDACs,

SUV39H1 and DNMT1 [298-300]. Hyperphosphorylated Rb fails to repress E2Fs and allows them to activate or repress various gene expression programs [297].

Recent studies suggest that hyperphosphorylated Rb may have physiologic roles in addition to its canonical E2F function [301]. Previously, we demonstrated a direct interaction between TRIP230 and ARNT [150]. In addition, we demonstrated that TRIP230 was indispensable for transcription mediated by two distinct dimerization partners of ARNT, namely the aryl hydrocarbon receptor and HIF1α [150]. Finally, we showed that loss of Rb expression dysregulates HIF1-mediated transcription [327] and that hypoxia in conjunction with Rb-loss promotes a more invasive and neuroendocrine phenotype in prostate cancer cells [388]. In this report, we further characterize the role that Rb plays in HIF-mediated signalling in breast cancer and identify gene networks responsible for metastatic cell transformation. In addition, we demonstrate that Rb-loss in combination with hypoxia significantly increases actin reorganization and cell migration in breast cancer cells and that treatment with chemical inhibitors of MEK1/2 and AKT1/2 block these effects. Ultimately, this work reveals the ability of Rb to modulate HIF1-activated transcription, gene expression and cancer cell invasion and metastasis in breast cancer.

5.3. Results

5.3.1. Rb regulates specific HIF1-regulated transcriptional programs in human breast cancer cells

In order to more clearly understand the role of Rb in HIF1-mediated gene regulation, we interrogated the transcriptomes of Rb-positive and Rb-negative MCF7 breast cancer cells under normoxic and hypoxic conditions. Probes were made from RNA derived from retrovirally infected MCF7 cells expressing either a scrambled control (shSCX) shRNA or a shRNA directed to Rb (shRb) and maintained under either normoxic or hypoxic conditions for 24 h. The shSCX control cells had high levels of Rb while the shRb cells were deficient in Rb protein (Figure 5.1A). Previous studies indicated that Rb acts to attenuate hypoxia-mediated gene expression [327,388], therefore we focused on genes whose hypoxia-regulated expression was further

exaggerated by loss of Rb. Genes from the shRb-hypoxia-treated data set that were up- or down-regulated significantly ($p<0.05$) at least 1.5 fold compared to all other conditions were selected. Hypoxia regulated genes whose expression patterns were accentuated significantly ($p<0.05$) upon loss of Rb and Rb-regulated genes whose expression patterns were accentuated upon exposure to hypoxia were selected for further analysis (see Figure 5.1B).

Microarray analysis revealed that of the 914 annotated genes that were significantly up-regulated by hypoxia, 100 were sensitive to loss of Rb (further up-regulated) and of the 656 hypoxia down-regulated genes, 36 were sensitive to loss of Rb regardless of oxygen status. Strikingly, of the top 25 upregulated genes from the shRb-HYP dataset, 12 genes have known cell motility functions (migration, invasion or metastasis) including; NDRG1 [389], SPAG4 [390], S1PR4 [391] and STC1 [392] (Table 5-1). Moreover, 6 of the 25 genes have known roles in epithelial-to-mesenchymal transition (EMT) including PLAC8 [393], LRP4 [394], and LOXL2 [395]. This data implicates Rb-loss and hypoxia as drivers of metastatic transformation in breast cancer cells.

Table 5.1. List of the top 25 genes significantly up-regulated in MCF7 cells in response to a combination of hypoxia and Rb-depletion. *Epithelial-to-mesenchymal transition (EMT)

Gene Name	Probe Number	Pathway	Fold Induction (vs shSCX-N)		
			shRb-Norm	shSCX-HYP	shRb-HYP
SEMA5B	NM_001031702		2.6819	12.192	45.9407
ASB2	NM_016150	Migration	1.665	23.8445	34.7281
NDRG1	NM_006096	Invasion/EMT	1.8595	20.7463	34.488
SPAG4	NM_003116	Migration	2.2649	9.4096	15.369
PLAC8	NM_016619	EMT	4.1006	3.9889	14.6663
FGD5	NM_152536		1.2365	3.4061	14.6056
S1PR4	NM_003775	Metastasis	2.4918	5.804	14.001
STC1	NM_003155	Migration/Invasion	1.7672	8.5651	13.8954
VTCN1	NM_024626	Metastasis	4.061	4.8074	13.1332
FAM13A	NM_014883		1.5326	6.8521	12.6826
LRP4	NM_002334	EMT	0.8321	7.7775	12.1727
LDLRAD1	NM_001010978		1.7046	3.7053	11.5997
PADI1	NM_013358		4.3484	1.5704	11.2928
EPHA3	NM_005233	Metastasis/Angiogenesis	3.5866	1.9329	10.6874
GAL3ST1	NM_004861		1.0588	3.3125	10.4002
TLE6	NM_001143986		3.6094	5.383	9.7791
LOXL2	NM_002318	EMT/Metastasis	2.2852	4.5204	9.5369
UCA1	NR_015379		5.1983	1.8198	9.3181
WNT11	NM_004626	Migration/Invasion	4.2943	1.7271	8.6906
HOXA13	NM_000522	EMT/Metastasis	2.329	4.0701	8.0788
SCNN1G	NM_001039		1.4687	3.1485	7.9785
PTGS1	NM_000962	Metastasis	4.613	1.6494	7.9169
HEY1	NM_001040708	EMT/Metastasis	1.1653	4.0239	7.5989
EGLN3	NM_022073		1.144	5.3624	7.2161
EFCAB3	NM_001144933		1.8567	4.0265	7.0963
CPXM2	NM_198148		2.0749	1.3417	6.978

Of the 100 hypoxia-inducible genes sensitive to loss of Rb, 49 of these were up-regulated after loss of Rb under normoxic conditions and demonstrated either an additive or synergistic increase in mRNA accumulation under both conditions and the

other 51 were sensitive to loss of Rb only in a hypoxia-dependent fashion (i.e similar to the expression profile observed for CXCR4 and VEGF presented in Figure 5.1C). Twenty-nine genes whose expression was significantly enhanced by loss of Rb under normoxic conditions were not hypoxia inducible in short-hairpin-scrambled cells (shSCX) genes but had significantly higher mRNA levels in the shRb expressing cells under hypoxia. Venn diagrams for these relationships are presented in Figure 5.1B. Furthermore, there were an additional 60 genes that were not significantly up-regulated by loss of Rb or hypoxia alone, but demonstrated a significant increase in mRNA accumulation when interrogated under both experimental conditions (Figure 5.1B).

Similarly, of the 83 genes down regulated by a combination of loss of Rb and hypoxia, 36 of these were repressed by hypoxia alone (Supplementary Information, Table 5-3). Many of these genes expression were repressed by loss of Rb under normoxic conditions and demonstrated a multiplicative or synergistic effect when exposed to a combination of low oxygen and Rb loss and 25 were sensitive to loss of Rb only in a hypoxia-dependent fashion. Twenty-two genes whose expression was significantly repressed by loss of Rb under normoxic conditions were not hypoxia-repressible in short-hairpin-scrambled cells (shSCX) genes but had significantly lower mRNA levels in the shRb expressing cells under hypoxia. Finally, there were 25 genes that were not significantly repressed in either shRb expressing cells under normoxic conditions, or in shSCX cells during hypoxia that showed significantly lower mRNA levels in shRb cells under hypoxic conditions (Supplemental Information, Table 5-2).

Hierarchical clustering was performed using Ingenuity Pathway Assist. Ninety-six up-regulated genes clustered into the 5 top networks identified. Interestingly, 82 of the up-regulated genes were involved in 4 associated network functions that regulate organ and tissue development and cellular movement. In addition, heat maps for these 96 genes demonstrating these relationships are presented in Figure 5.1D. Gene ontology (GO) analysis reveals that hypoxia-regulated genes that are sensitive to loss of Rb solely in a hypoxia-dependent fashion are not randomly dispersed but cluster together (Figure 5.1D, purple shaded gene names). Similarly, hypoxia-regulated genes that were sensitive to loss of Rb under normoxic conditions but demonstrated a synergistic hyper-activation under both conditions (yellow shaded gene names, Figure

5.1D) also segregated with genes that were sensitive to loss of Rb in a hypoxia dependent fashion. Genes that were affected by both loss of Rb and hypoxia, but only in an additive fashion are not shaded and were distributed in a more random fashion in the map. Importantly, GO analysis revealed that the top two associated transcription factors were HIF1α (p-value of overlap = 2.62E-08) and EPAS/HIF2α (p-value of overlap = 5.81E-05), thus validating our results and our hypothesis that loss of Rb perturbs HIF-controlled gene programs.

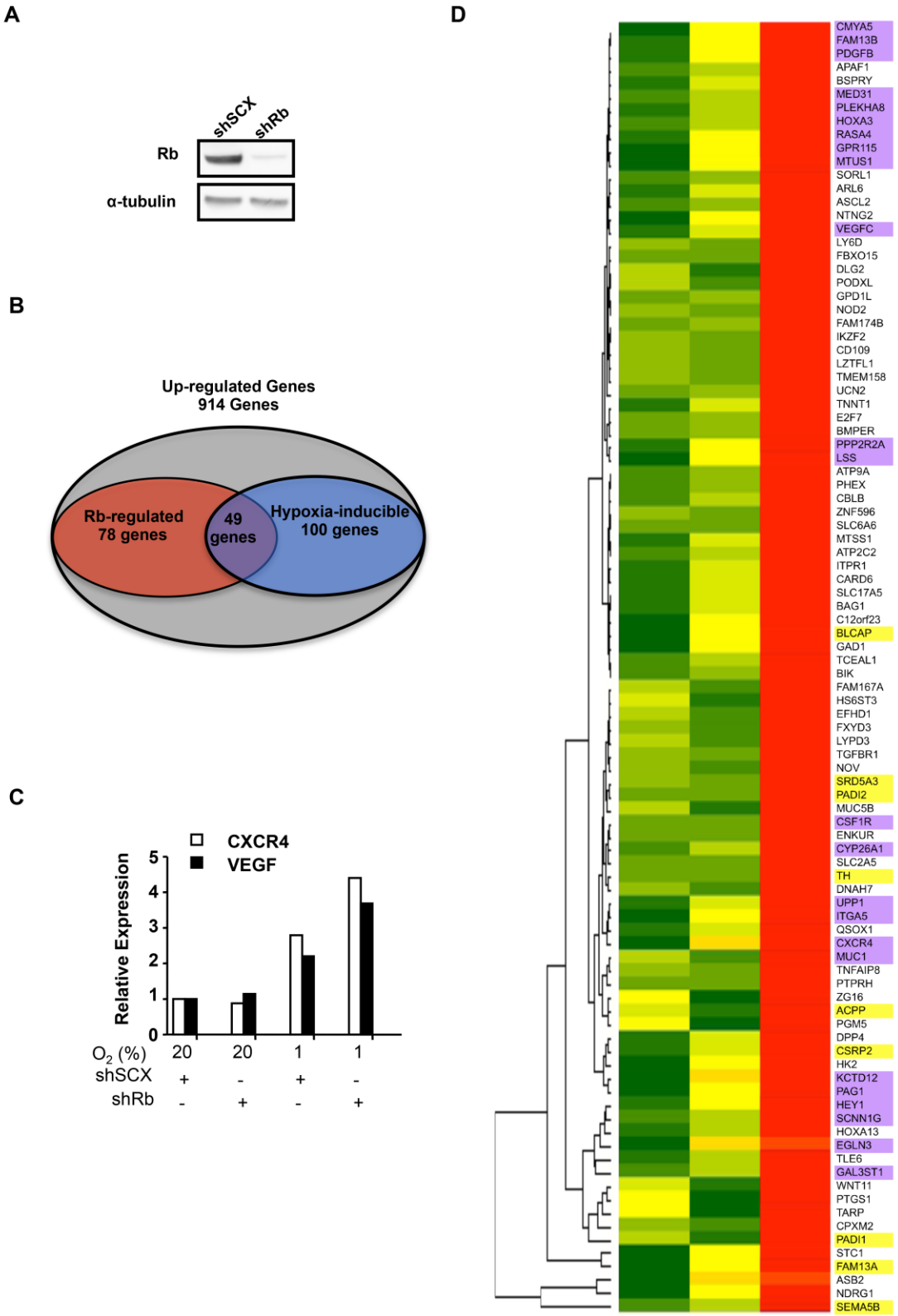
A
shSCX
shRb
Rb
α-tubulin
B
Up-regulated Genes
914 Genes
Rb-regulated
78 genes
49
genes
Hypoxia-inducible
100 genes
C
CXCR4
VEGF
Relative Expression
5
4
3
2
1
0
O2 (%) 20 20 1 1
shSCX + - + -
shRb - + - +
D
CMYA5
FAM13B
PDGFB
APAF1
BSPRY
MED31
PLEKHA8
HOXA3
RASA4
GPR115
MTUS1
SORL1
ARL6
ASCL2
NTNG2
VEGFC
LY6D
FBXO15
DLG2
PODXL
GPD1L
NOD2
FAM174B
IKZF2
CD109
LZTFL1
TMEM158
UCN2
TNNT1
E2F7
BMPER
PPP2R2A
LSS
ATP9A
PHEX
CBLB
ZNF596
SLC6A6
MTSS1
ATP2C2
ITPR1
CARD6
SLC17A5
BAG1
C12orf23
BLCAP
GAD1
TCEAL1
BIK
FAM167A
HS6ST3
EFHD1
FXYD3
LYPD3
TGFBR1
NOV
SRD5A3
PADI2
MUC5B
CSF1R
ENKUR
CYP26A1
SLC2A5
TH
DNAH7
UPP1
ITGA5
QSOX1
CXCR4
MUC1
TNFAIP8
PTPRH
ZG16
ACPP
PGM5
DPP4
CSRP2
HK2
KCTD12
PAG1
HEY1
SCNN1G
HOXA13
EGLN3
TLE6
GAL3ST1
WNT11
PTGS1
TARP
CPXM2
PADI1
STC1
FAM13A
ASB2
NDRG1
SEMA5B

Figure 5.1. Specific hypoxia-regulated gene programs are sensitive to loss of Rb.

MCF7 cells infected with either a short-hairpin control RNA (shSCX) or a short-hairpin to Rb (shRb) were maintained under hypoxic (1% O_2) or normoxic conditions for 24 h. Extracted RNA was used to probe Agilent 60K Genome Wide Expression arrays. Experiments were performed in triplicate and only genes that were up- or down-regulated at least 1.5-fold under hypoxic conditions with a p-value <0.05 were considered significant. **(A)** Knock-down of Rb was confirmed by immunoblotting with affinity-purified antibodies to Rb and α-tubulin as a loading control. **(B)** Venn diagrams of all up regulated genes sensitive to hypoxia (blue) and /or loss of Rb (red). **(C)** Results obtained from microarray analysis for alterations in mRNA accumulation for VEGFC and CXCR4 and expressed as fold increase in expression. **(D)** Heat maps of the 96 genes sensitive to loss of Rb under hypoxic conditions that clustered into 5 associated network functions identified by Ingenuity Pathway Assist gene ontology analysis. Hypoxia-regulated genes sensitive to loss of Rb solely in a hypoxia-dependent fashion are highlighted in purple and those that are sensitive to both Rb loss under normoxic conditions and hypoxia independently but demonstrated a synergistic effect when examined in combination are highlighted in yellow.

5.3.2. Rb-knockdown and hypoxia activates gene networks involved in migration, invasion and cellular transformation.

The top two associated network functions identified by IPA were (1) organ development, skeletal and muscular system development and function, cellular movement with a network score of 47 (Figure 5.2A), and (2) drug metabolism, small molecule biochemistry, cellular movement with a network score of 41 (Figure 5.2B). The complete IPA analysis summary can be found in the Supplementary Information. Both associated networks contained only genes that were hypoxia-inducible and further sensitive to loss of Rb further supporting our hypothesis that Rb regulates specific HIF-regulated transcriptional programs. In addition, the top molecular and cellular functions identified in the IPA analysis were cellular movement (37 molecules), cell morphology (19 molecules), cellular development (33 molecules), cell-to-cell signalling and interaction (18 molecules) and cellular function and maintenance (20 molecules). Interestingly, the network analysis identified NFκB, AKT and ERK1/2 as downstream regulators of cancer cell transformation. No negatively regulated genes were identified in any of the top associated network functions. We confirmed the array data for the metastatic markers NDRG1, STC1, S1PR4 and GAL3ST1 through quantitative real-time PCR (Figure 5.3A). The transcriptional responses to hypoxia for these genes mimicked the array data and Rb-loss significantly bolstered the HIF1-mediated transcriptional response to hypoxia.

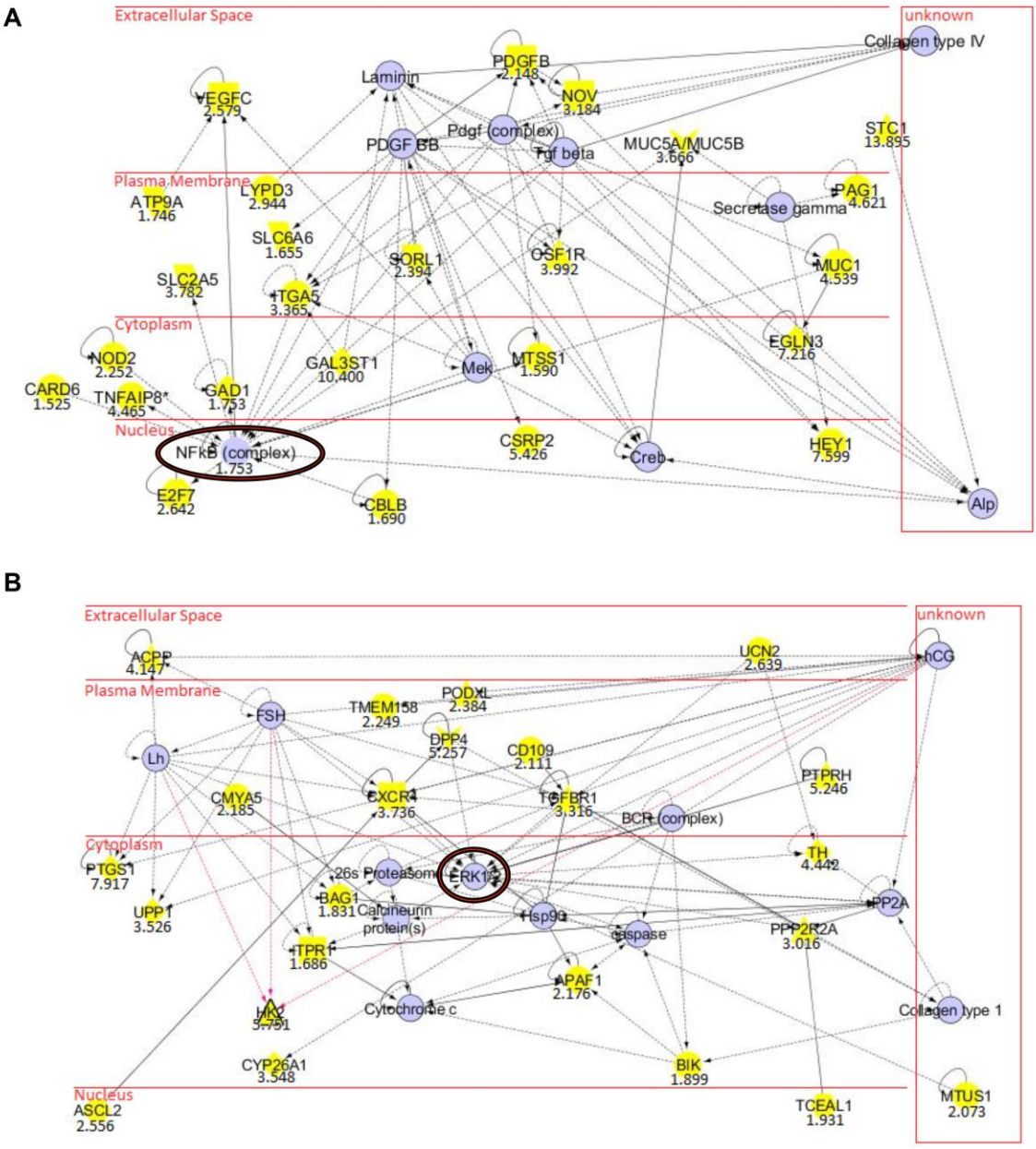

Figure 5.2. Rb-loss dysregulates hypoxia-inducible gene networks involved in cell migration, invasion and metastasis

Gene ontology analysis using Ingenuity Pathway Assist (IPA) software identified gene networks with modified expression under hypoxia and loss of Rb in shRNA MCF7 cells. Schematic illustrations of the **(A)** organ development and cellular movement network and **(B)** drug metabolism and cellular movement network. Hypoxia inducible genes up-regulated by Rb-loss are presented in yellow. The genes presented in blue are absent from our list but are suggested as part of the network by IPA.

Cultured MCF7 cells are hormone sensitive and minimally invasive and represent an early stage breast cancer phenotype [302,396]. Thus, we wanted to examine a more advanced breast cancer cell type to determine if we could reproduce the observed transcriptional profiles with loss of Rb and hypoxia. We retrovirally introduced the shSCX and shRb constructs into triple negative MDA-MB-231 breast cancer cells and ablated Rb protein levels (Figure 5.3B). Indeed, loss of Rb in conjunction with hypoxia imitated the MCF7 cell data and significantly exacerbated STC1, NDRG1 and PLOD2 mRNA expression when compared to all other conditions (Figure 5.3C). Taken together, this data suggests that Rb modulates hypoxia-regulated gene programs in breast cancer irrespective of clinical stage or cell-type. Additionally, these data unambiguously demonstrate the requirement for Rb in the regulated and stringently controlled expression of HIF1-regulated genes.

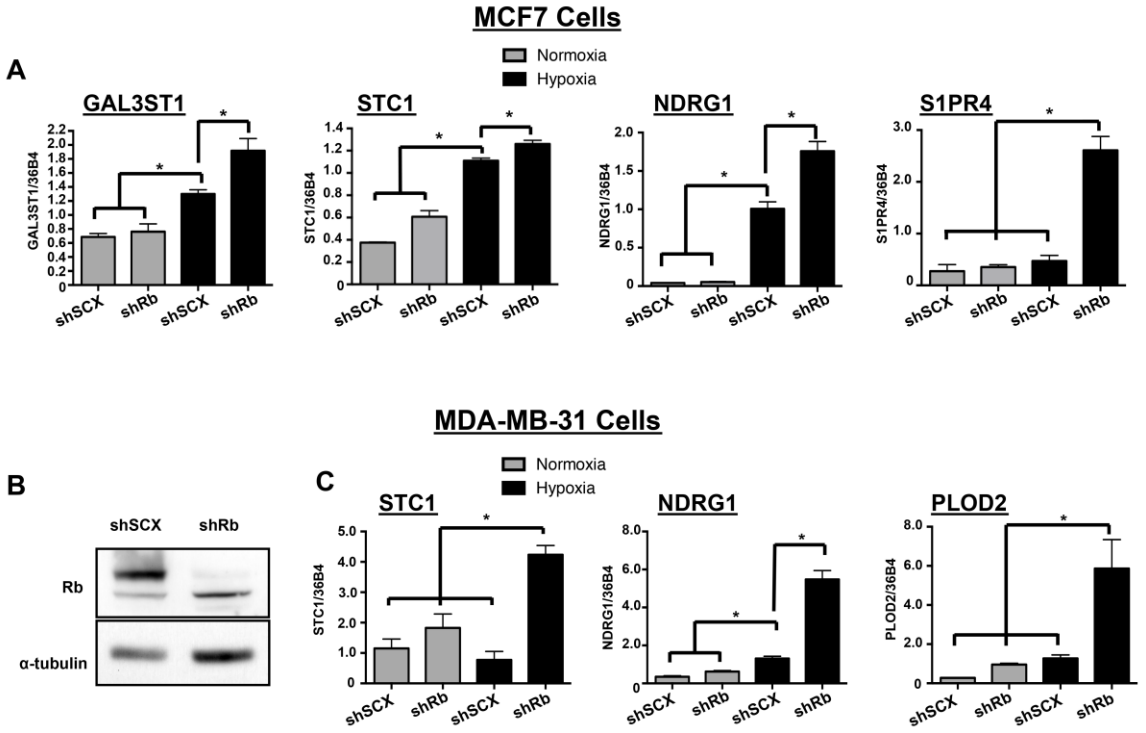

Figure 5.3. Confirmation of Rb-regulated and hypoxia-inducible genes identified by microarray analysis.

(A) MCF7 and **(C)** MDA-MB-231 shSCX and shRb cells were placed in hypoxia (1% O_2) or normoxia for 24 h. S1PR4, GAL3ST1, NDRG1, STC1 and PLOD2 transcript levels were quantified by qRT-PCR following isolation and reverse transcription of total RNA. All mRNA levels were normalized against 36B4. Grey bars represent normoxia and black bars represent hypoxia (1% O_2). Values are presented as means + S.D. (N=3). * $p<0.05$. **(B)** Immunoblot of shSCX and shRb MDA-MB-231 cells using primary antibodies to Rb and α-tubulin.

5.3.3. Rb-loss results in a hypoxia-dependent increase in expression of proteins involved in metastasis in human breast cancer cells.

To further validate the microarray, we used shSCX and shRb MCF7 cells and immunoblotting to measure the level of protein expression for identified genes. The shRNA cell lines were exposed to normal O2 levels or 1% O2 for various time points up to 7 days. Protein accumulation for NDRG1 and S1PR4 reflected the transcriptional responses observed in the microarray with Rb-depleted cells exposed to hypoxia expressing significantly more protein compared to other conditions (Figure 5.4). Furthermore, longer exposures to hypoxia (4–7 days) led to accumulation of more protein for the targets of interest compared to cells that were treated with 2-3 days of hypoxia. This observation supports our hypothesis and suggests that the key effectors of cellular transformation and metastasis require both transcriptional and translational processes for exacerbated accumulation with Rb-loss and hypoxia. Additionally, these data support a role for the Rb-HIF1 complex in the maintenance of normal cell physiology.

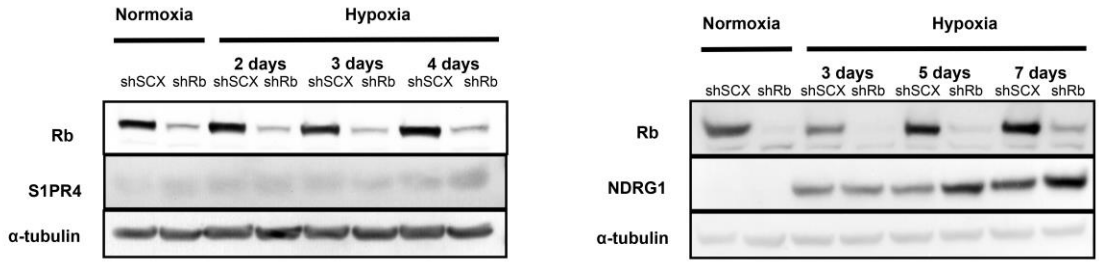

Figure 5.4. Loss of Rb and hypoxia increases expression of S1PR4 and NDRG1 protein levels in shRNA MCF7 cells.

shSCX and shRb MCF7 cells were exposed to normoxia or hypoxia (1% O_2) for 2-7 days as indicated. Cells were harvested and then whole-cell lysates were quantified, run on SDS-PAGE and then transferred to PVDF membrane. Representative immunoblots were probed with primary antibodies to Rb, NDRG1, S1PR4 and α-tubulin. α-tubulin was used as the loading control.

5.3.4. Hypoxia-inducible actin reorganization and cell migration is dependent on AKT and ERK in Rb-depleted breast cancer cells.

The gene ontology analysis suggests that Rb-deficient MCF7 cells exposed to hypoxia are more invasive and migratory compared to the other conditions. Additionally,

the analysis identified AKT and ERK1/2 signalling pathways as critical downstream regulators of hypoxia-inducible invasion and migration in Rb-depleted MCF7 cells. To test these observations, we examined the normalized amplitude of resultant bead movement (NARBM) in response to an oscillating optical tweezer applied force in control and Rb-deficient MCF7 cells under hypoxic and normoxic conditions [397]. NARBM measures tripeptide Arg-Gly-Asp (RGD)-coated microbead displacement in cells after manipulation with the optical tweezer and corresponds to cellular actin reorganization [397]. We found that only the MCF7 cells lacking Rb and exposed to hypoxia were able to significantly impede bead movement, suggesting a stiffer cytoskeletal structure (Figure 5.5A). Additionally, phalloidin staining determined that Rb-depleted cells conditioned with hypoxia had significantly more actin polymerization compared to all other treatments (T.Beischlag, unpublished data). Treating cells with either 10 μM of the MEK1/2 inhibitor U0126 or 2 μM of the AKT1/2 inhibitor A6730 blocked hypoxia inducible actin reorganization in Rb-depleted cells (Figure 5.5A). Furthermore, to determine if actin reorganization corresponds to increased cell migration, we treated shRNA MCF7 cells with hypoxia or normoxia and used a cell migration assay to measure the total number of migrating cells. Indeed, shRb MCF7 cells exposed to hypoxia migrated at a significantly higher rate compared to scrambled negative controls and to normoxic shRb cells (Figure 5.5B). Additionally, treatment with 10 μM U0126 or 2 μM A6730 significantly impeded hypoxia-inducible migration in shRb MCF7 cells compared to the untreated control. This suggests that Rb-depleted MCF7 cells under hypoxic stress adopt a more migratory phenotype through mobilization of actin filaments. In addition, blocking the AKT and ERK signaling pathways inhibits hypoxia-inducible metastatic transformation in breast cancer cells that have lost functional Rb.

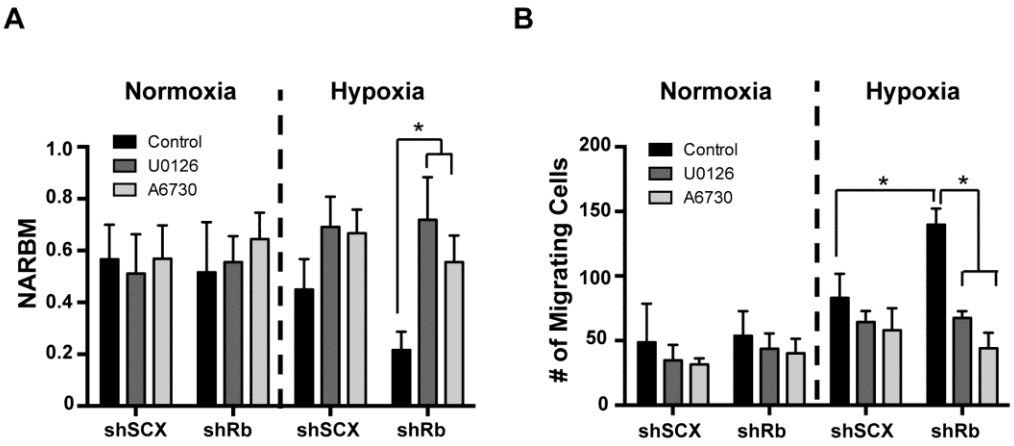

Figure 5.5. Rb-deficient breast cancer cells exposed to hypoxia exhibit AKT- and ERK1/2-dependent changes in cell mechanical properties and migration.

(A) MCF7 cells expressing Rb (shSCX) or lacking Rb (shRb) were treated with 4 days of hypoxia or left at normoxia and treated with or without 10 μM U0126 or 2 μM A6730. Variation in NARBM (Normalized Amplitude of Resultant Bead Movement) of shRb and shSCX MCF7 cells measured through manipulations with an oscillating optical tweezer. Values are presented as means + S.D. *p<0.05. **(B)**Total number of migrating MCF7 cells either expressing Rb (shSCX) or lacking Rb (shRb) and treated as above. Values are presented as means + S.D. *p<0.05.

5.4. Discussion

Hypoxia via the HIF1 complex activates genetic programs regulating key physiological functions in a coordinated fashion [126], and has been implicated in the biochemical alterations underlying cell invasion and metastasis. In addition, loss-of-function of Rb or genetic ablation of *RB1* has been implicated in advanced stages of brain cancers [305,306], lung cancer and breast cancer [294]. Furthermore, the loss of Rb and the activation of HIF1-regulated genes such as increased VEGF expression, microvascular hyperplasia and metastasis are traits that are common to progression in many solid tumors [205]. We showed previously that siRNA-mediated knockdown of Rb protein dysregulates HIF1-mediated transcription and increases cell invasion in MCF7 breast cancer cells [327]. We also determined that hypoxia in conjunction with Rb-loss promotes a more invasive and neuroendocrine phenotype in prostate cancer cells [388]. However, we were interested in further investigating the physiological connection between Rb function and hypoxia-inducible gene expression, especially HIF1-regulated transcriptional programs involved in breast cancer cell transformation.

We wanted to determine if Rb regulated HIF1 transcriptional programs that have been implicated in tumor progression and metastasis in breast cancer. Towards these ends, we interrogated the MCF7 transcriptome from cells deprived of Rb using retrovirally expressed short-hairpin RNAs under normoxic and hypoxic conditions. A large number of known HIF1 target genes were sensitive to loss of Rb (Figure 5.1, Table 5-1). Indeed, many established HIF1 target genes had significantly increased mRNA accumulation in response to loss of Rb only under hypoxic conditions including VEGF, CXCR4 and PDGFB, among others (Table 5-1). These and other genes that are sensitive to loss of Rb in a hypoxia-dependent fashion are possible candidates for direct regulation by the HIF-TRIP230-Rb transcriptional complex.

Gene ontology analysis of the sorted data suggests that loss of Rb selectively regulates a specific set of hypoxia-inducible gene programs. The gene lists created represent programs that regulate cellular movement, and cell development as well as cellular biochemistry that likely underlies the former two processes. The two networks identified with the highest gene ontology scores both mediate cellular movement (Figure 5.2A and B). Furthermore, the top molecular and cellular functions that many of the genes fall into regulated cellular movement, development, morphology and cell-to-cell signalling, all consistent with EMT and increased metastatic potential.

Loss of cellular adhesion is another hallmark of hypoxia-inducible transformation of cancer cells [398]. MUC1 [399], NOD2 [400], and DPP4 [401] contribute to a loss of cell adhesion. Over-expression of ITGA5 promotes metastasis [402], while PDGF-BB supports cell migration [403]. Paradoxically, MTUS1 has been identified as a potential tumor suppressor gene in breast and other carcinomas by virtue of its anti-mitotic potential [404], however a deletion variant of MTUS1 is associated with poor prognosis in breast cancer patients [405] and it is unknown whether MCF7 cells harbour this variant. Regardless, loss of Rb up-regulates multiple pro-metastatic factors.

While none of the down-regulated genes (Supplementary Information, Table 5-2) identified in our screens appear in the top functional networks identified by GO analysis, several promote cell adhesion. TGM2 [406], and SCG5 help maintain the extra-cellular matrix and SPRY4 inhibits prostate cancer cell motility [407], fibroblast cell invasion and

EMT [408,409]. A loss or breakdown in these activities will compromise the integrity of the extra-cellular matrix and facilitate the motility of transformed cells. Additionally, TGM2 and SCG5 are epigenetically silenced in breast cancer [410] and medulloblastomas [411], respectively. Thus, the Rb-HIF1 regulatory control of these transcriptional programs is essential for the suppression of tumour transformation and tumour cell motility and the loss of Rb culminates in a *perfect storm* of factors that drive tumour transformation/EMT, invasion and metastasis. Taken together, these data support our previous findings [327,388] and suggest that Rb mediates its repressor function via a direct interaction with TRIP230.

The identification of CXCR4, NDRG1, SIPR4 and STC1 in our microarray analysis upon depletion of Rb and hypoxia treatments in MCF7 cells led us to investigate the effects of Rb loss on actin reorganization and the migratory phenotype of MCF7 cells. CXCR4 expression is likely to be a key effector of the migratory phenotype [309,310]. CXCR4 promotes many key steps in epithelial to mesenchymal transition (EMT) and metastasis including detachment from neighboring cells, extra-vasation, metastatic colonization, angiogenesis and proliferation [311]. Additionally, CXCR4 is highly expressed and well characterized in metastatic breast cancer models [412] and mediates hypoxia-inducible invasion through ERK signaling in chondrosarcoma cells [413]. Under normoxic conditions, MCF7 cells maintain an epithelial and non-migratory phenotype regardless of Rb status. Upon Rb-depletion, hypoxia treatment triggered actin reorganization and migration (Figure 5.6A and B). Inhibitors of AKT1/2 and MEK1/2 activation blocked hypoxia-inducible actin reorganization in Rb-depleted cells, suggesting that ERK1/2 and AKT1/2 signalling have cooperative functions in metastatic breast cancer cell transformation after functional ablation of Rb. To our knowledge, this is the first study to report this phenomenon. Our data suggests that Rb attenuates HIF1 function to ensure the appropriate levels of HIF1-target gene expression. Thus, we propose that loss of Rb or breakdown of this pathway primes cancer cells for metastatic transformation by allowing for the over-expression of pro-metastatic factors.

5.5. Materials and Methods

5.5.1. Reagents

RGD peptide, U0126 and A6730 were purchased from Sigma-Aldrich (ON, Canada). The microbeads were purchased from Bangs Laboratory (ON, Canada).

5.5.2. Cell Culture

MCF7 and MDA-MB-231 cells (ATCC) were maintained in Dulbecco's Modified Eagle's Medium (DMEM; BioWhittaker, Lonza) with 10% fetal bovine serum (FBS; HyClone, Perbio, Thermo Fisher Scientific Inc.) supplemented with 100 units/ml potassium penicillin-100 μg/ml streptomycin sulphate (BioWhittaker, Lonza), and 4.5 g/L glucose and 4.5 g/L L-glutamine at 37°C, 20% O_2, and 5% CO_2.

5.5.3. Real-Time PCR

Real-time PCR (RT-PCR) experiments were performed as described previously [327]. Breifly, shRNA MCF7 or MDA-MB-231 cells were incubated under hypoxic conditions (1% O_2) for 24 h in a humidified CO_2 incubator. The mRNA levels of CXCR4, RB1, and 36B4 were determined using quantitative real-time PCR. The primer pairs for PLOD2, RB1 NDRG1 and 36B4 were described previously [284,388]. Total RNA was isolated using TRI reagent (Sigma, Cat. No. T9424-200ML) according to the manufacturer's protocol. Reverse transcription was performed using High Capacity cDNA Reverse Transcription Kit (Applied Biosystems, Part No.4368814) according to the manufacturer's protocol. A total of 2 – 4 μg of RNA was used in a 20 μL reaction amplified by cycling between 25°C for 5 min, 37°C for 120 min, and 85°C for 5 min (Veriti 96 Well Thermal Cycler, Applied Biosystems). From each experiment, a sample that was both Rb-depleted and pre-conditioned with hypoxia was used to generate a relative standard curve in which the sample was diluted 1:10 in five serial dilutions resulting in dilutions of 1:10, 1:100, 1:1,000, 1:10,000, and 1:100,000 whereas the samples were diluted 1:30; the analysis was done using StepOnePlus System (Applied Biosystems).

5.5.4. Immunoblotting

Protein analysis was performed by immunoblotting as described previously [86]. Briefly, MCF7 cells were incubated under hypoxic conditions (1% O_2) for 2-7 days. Cells were harvested and the protein concentration estimated by the Bradford assay. Equal amounts of proteins from the samples were resolved on a SDS-acrylamide gel then transferred to polyvinylidene fluoride (PVDF) membrane. Membranes were probes with anti-Rb (rabbit polyclonal IgG; Santa Cruz Biotechnology, Inc., SC-7905), anti-NDRG1 (rabbit polyclonal IgG; Santa Cruz Biotechnology, Inc., SC-7905), anti-S1PR4 (mouse monoclonal IgG, Sigma-Aldrich, SAB1406707) or anti-α-tubulin antibodies (mouse monoclonal IgG; Santa Cruz Biotechnology, Inc., SC-8035). The detection was done using horseradish peroxidase conjugated anti-mouse or anti-rabbit IgG (GE Healthcare,) and ECL detection kit (GE Healthcare).

5.5.5. Short-hairpin RNAs interference

MCF7 and MDA-MB-231 cells were stably infected with short-hairpin RNAs (shRNA) according to the method described by Wang et al [384]. The pQCXIPgfp vector was obtained from Dr. Oliver Hankinson (UC, Los Angeles). Oligonucleotides encoding short-hairpin RNAs directed to RB1 were annealed and cloned into the pQCXIPgfp vector 3-prime of the mouse U6 promoter. The RB1 forward and reverse primers were; RB1-CDS/13-14-F – TTTGGGATCTCAGCGATAGAAACTTCAAGAGAGTTTGTATCGCTGTGATCCTTTTT, and; RB1-CDS/13-14-R - AATTAAAAAGGATCACAGCGATACAAACTCTCTTGAAGTTTCTATCGCTGAGATCC

Human embryonic kidney 293T cells were transfected with the shRNA vectors and the pCL10A1 packaging vector using Lipofectamine 2000 (Invitrogen) and maintained in DMEM supplemented with 10% FBS and 1% penicillin/streptomycin. Twenty-four h after transfection, media was replaced and viral supernatants were collected 24 h later. MCF7 cells were seeded into 6-well plates (2x105 cells/well) and spin infections were performed using 2 ml of viral supernatant and centrifugation at 2500 rpm for 90 min at 30° C. Twenty-for h post-infections media was supplemented with 3

μg/ml puromycin. Infection was monitored by immunoflourescence of GFP and knock-down was determined by immunoblotting.

5.5.6. Gene Expression Array Analysis

Gene expression microarray analysis was performed at the Laboratory for Advanced Genome Analysis (Vancouver Prostate Centre, Vancouver, Canada). Messenger RNA from MCF7 cells stably expressing either shRb or the short-hairpin scrambled RNA (scx) was isolated using TRI reagent (Sigma) according to the manufacturer's protocol. Total RNA was quantified using a NanoDrop ND-1000 UV-VIS spectrophotometer to measure A260/280 and A260/230 ratios. We performed quality control checks of total RNA using an Agilent 2100 Bioanalyzer. One hundred ng of total RNA was converted to cRNA using T7 RNA polymerase in the presence of cyanine 3 (Cy3)-labeled CTP using an Agilent One-Color Microarray-Based Gene Expression Analysis Low Input Quick Amp Labeling v6.0 kit. Experiments were performed in triplicate and cRNAs were hybridized to Agilent GE Human Whole Genome 4x44Kv2 microarrays (Design ID 026652).

Arrays were scanned with an Agilent DNA Microarray Scanner at a 3□m resolution and data was processed using Agilent Feature Extraction 10.10 software. Green processed signal was quantile normalized with Agilent GeneSpring 11.5.1. To find significantly regulated genes, fold changes between the *RB1* shRNA and the scrambled (SCX) shRNA control groups and p-values gained from t-test between the same groups were calculated with a Benjamini-Hochberg multiple testing correction. The t-tests were performed on log transformed normalized data and the variances were not assumed to be equal between sample groups. Up- and down-regulated genes with P values < 0.05 and fold difference ≥1.5 compared to the control or to the hypoxia scrambled control group were selected for further analysis. Heat maps were created using the Hierarchical clustering program from the GenePattern website (http://genepattern.broadinstitute.org).

5.5.7. Oscillating Optical Tweezer Mechanical Charaterization

The stiffness of MCF7 cells was measured using an oscillating optical tweezer (OT) as described previously [397]. Briefly, the tripeptide Arg-Gly-Asp (RGD)-coated microbeads bound to the cell surface were trapped by the laser tweezer and then moved back and forth via oscillating laser trap with various frequencies of 0.1, 1, 10 Hz. As the beads moved sinusoidally, the cell develops internal stress and resistance to the bead motion that depends on the cell's mechanical properties. The resultant bead displacement in response to the force applied by the tweezer was measured optically and the bead motion equation was used to calculate the cell shear modulus and viscosity in the frequency domain.

Data Analysis

In order to analyze the experimental data and calculate the changes in cell mechanical properties, a bead motion equation was used as described previously [397]. The cell relaxation time was calculated by measuring fluctuations in the position of trapped beads linked to the cell cytoskeleton. By analyzing the normalized position auto-correlation function of trapped bead signal fluctuations in time domain, relaxation time was determined. The trapped bead motion equation can be described by:

$$x^{'} + (1/\tau_0)x = \xi(t)$$

$$\tau_0 = \frac{(\gamma + \beta)}{k_1}$$

$$\gamma = 6\pi a \eta_{med}$$

$$\beta = r_{cont}\eta_{cell}$$

where η_{med} and η_{cell} are the viscosity coefficients of the surrounding medium and the cell structure, and k_1 is the laser stiffness coefficient, and τ_0 is the relaxation time. Integrating both sides of the above equation with respect to time, we arrived at:

$$x(t) = e^{-t/\tau_0} \int_{-\infty}^{t} \frac{1}{(\gamma + \beta)} \xi(\tau^{'}) e^{\frac{\tau^{'}}{\tau_0}} d\tau^{'}$$

Calculating the normalized position autocorrelation function, and using the properties of $\xi(t)$ we arrived at:

$$< \xi_i(t) > = 0$$

$$< \xi_i(t)\xi_j(t^{'}) >= 2\gamma\beta k_B T\delta(t - t^{'})$$

$$< x_i(t)x_i(t+\tau) >= e^{\frac{-\tau}{\tau_0}}$$

Thus, by performing autocorrelation analysis on bead fluctuations and fitting the experimental results to the exponential function, we can determine the cell relaxation time.

5.5.8. Migration Assay

Control scrambled or shRb MCF7 cells were treated with hypoxia (1% O_2) or maintained at normoxic conditions and treated with either vehicle or drug (10 μM U0126, or 2 μM A6730) for 96 h. After 96 h, cells were washed, trypsinized, counted on a Haemocytometer and then seeded on ThinCerts (Greiner Bio-One) with 8.0 μm pore size at $1X10^4$ cells per cell culture insert. The cells were maintained in serum-free DMEM with L-glutamine in the upper chamber whereas the lower chamber contained DMEM media with L-glutamine and 50% FBS. Cells were treated as stated above for a further 96 h and then total migrating cells were counted using an Olympus CKX41 light microscope.

5.5.9. Statistical analysis

All Data are represented as means ± standard deviation (SD), and for statistical analysis we used an ANOVA test for comparing more than two groups of samples' mean. $P<0.05$ was considered as statistically significant.

5.6. Supplementary Information

Table 5.2. List of up-regulated genes identified in the MCF7-shRNA microarray used in the GO analysis.

Gene Name	ID Number	Associated Pathway	Fold Induction (vs shSCX-Norm)		
			shRb-Norm	shSCX-Hyp	shRb-Hyp
SEMA5B	NM_001031702		2.6819	12.192	45.9407
ASB2	NM_016150		1.665	23.8445	34.7281
NDRG1	NM_006096	MET	1.8595	20.7463	34.488
SPAG4	NM_003116	MET	2.2649	9.4096	15.369
PLAC8	NM_016619	EMT	4.1006	3.9889	14.6663
FGD5	NM_152536		1.2365	3.4061	14.6056
S1PR4	NM_003775		2.4918	5.804	14.001
STC1	NM_003155	MET	1.7672	8.5651	13.8954
VTCN1	NM_024626	MET	4.061	4.8074	13.1332
FAM13A	NM_014883		1.5326	6.8521	12.6826
LRP4	NM_002334		0.8321	7.7775	12.1727
LDLRAD1	NM_001010978		1.7046	3.7053	11.5997
PADI1	NM_013358		4.3484	1.5704	11.2928
EPHA3	NM_005233	ANGIO/MET	3.5866	1.9329	10.6874
GAL3ST1	NM_004861		1.0588	3.3125	10.4002
TLE6	NM_001143986		3.6094	5.383	9.7791
LOXL2	NM_002318	EMT/MET	2.2852	4.5204	9.5369
UCA1	NR_015379		5.1983	1.8198	9.3181
WNT11	NM_004626	MET	4.2943	1.7271	8.6906
HOXA13	NM_000522		2.329	4.0701	8.0788
SCNN1G	NM_001039		1.4687	3.1485	7.9785
PTGS1	NM_000962	MET	4.613	1.6494	7.9169
HEY1	NM_001040708		1.1653	4.0239	7.5989
EGLN3	NM_022073		1.144	5.3624	7.2161
EFCAB3	NM_001144933		1.8567	4.0265	7.0963
CPXM2	NM_198148		2.0749	1.3417	6.978
TARP	NM_001003799		4.0711	1.0458	6.8714
PCP4L1	NM_001102566		2.1561	4.7972	6.6552
KIAA1199	NM_018689	EMT/MET	3.1993	1.4493	6.6384

Gene Name	ID Number	Associated Pathway	Fold Induction (vs shSCX-Norm)		
			shRb-Norm	shSCX-Hyp	shRb-Hyp
HK2	NM_000189		1.5134	3.8237	5.7508
SCNN1B	NM_000336		0.9725	1.6127	5.6789
LEPREL1	NM_018192		3.2269	1.6239	5.67
PAM	NM_000919		1.8663	4.1069	5.4283
CSRP2	NM_001321		1.5306	2.774	5.4259
DPP4	NM_001935	MET	1.937	3.1657	5.2573
PTPRH	NM_002842		2.4397	2.4199	5.2459
MDGA2	NM_001113498		2.4756	1.596	4.9975
FAM105A	NM_019018		2.6705	1.6219	4.8526
HCG4	NR_002139		1.0056	3.3803	4.764
FAM26F	NM_001010919		1.0912	3.6116	4.7274
PAG1	NM_018440	MET	1.0571	3.1666	4.6211
MUC1	NM_002456	MET	2.5799	1.9335	4.5387
TNFAIP8	NM_014350	MET	2.3231	2.0515	4.4647
PCDH7	NM_002589	MET	2.8444	1.2074	4.4452
TH	NM_199292		1.5694	1.5108	4.4419
KCTD12	NM_138444		1.3874	3.3596	4.3913
DNAH7	NM_018897		1.5275	1.1218	4.3651
PGM5	NM_021965		2.8558	1.0753	4.3581
MMAB	NM_052845		1.4071	2.507	4.1558
CXCR4	NM_001008540	MET	0.9313	2.8015	3.7357
BMPER	NM_133468	EMT	1.7714	1.8844	2.9419
VEGFC	NM_005429	ANGIO	1.1541	1.7151	2.5788
NOD2	NM_022162	MET	1.4739	1.4085	2.2522
PDGFB	NM_002608	MET	1.2460	1.6411	2.1481

Table 5.3. List of down-regulated genes identified in the MCF7-shRNA microarray

Gene Name	ID Number	Actual Fold Repression (vs shSCX-N)		
		shRb-N	shSCX-H	shRb-H
SPANXA1	NM_013453	13.6027	2.0888	27.1677
SCG5	NM_003020	9.1948	2.0533	26.9354
PLAC1	NM_021796	11.6600	2.9946	21.1190
CSF3	NM_000759	11.3107	1.9915	17.6488
KRT23	NM_015515	7.4222	1.8907	16.1761
ATP8A2	NM_016529	4.5767	2.5873	11.2376
SPANXB2	NM_145664	6.4251	1.8725	10.3385
PCDH11Y	NM_032973	5.9627	0.6347	10.0006
ATP8A2	NM_016529	4.8717	1.6014	8.5669
ANKFN1	NM_153228	4.7831	2.7295	8.0971
PLUNC	NM_130852	4.7067	1.3556	7.4023
KLK7	NM_005046	3.9284	3.0449	7.2774
RBM24	NM_153020	1.9015	3.7043	6.0877
GUCY1B3	NM_000857	2.8484	2.6880	5.3289
PHF21B	NM_138415	2.6890	1.3772	5.2881
RDH12	NM_152443	2.9952	1.1319	5.0906
MARK1	NM_018650	1.3871	1.9403	4.9432
OSTalpha	NM_152672	2.7360	1.4800	4.9372
KRT4	NM_002272	2.3539	2.2994	4.7574
RPS6KL1	NM_031464	1.8111	1.7332	4.7093
CACNG1	NM_000727	2.3270	1.9075	4.6698
ZDHHC22	NM_174976	2.7026	1.3002	4.5231
KCNMA1	NM_002247	1.7745	1.0978	4.3308
BFSP2	NM_003571	2.4121	1.5846	4.2756
NFIA	NM_001134673	1.8873	1.0931	4.2339
H2BFXP	NR_003238	1.3687	2.4694	4.0783
SLC24A3	NM_020689	2.0832	1.7148	3.9980

Gene Name	ID Number	Actual Fold Repression (vs shSCX-N)		
		shRb-N	shSCX-H	shRb-H
GIMAP2	NM_015660	2.5125	1.1420	3.8355
OVOL2	NM_021220	1.5042	1.8924	3.6386
IRF2	NM_002199	2.0929	1.9656	3.5976
TAF9B	NM_015975	1.2663	2.2646	3.5620
ZNF385B	NM_152520	1.9410	1.3492	3.5537
TAF7L	NM_024885	1.8573	2.0791	3.5518
LAMA4	NM_001105209	1.9850	1.5422	3.5496
SECTM1	NM_003004	1.8662	1.3726	3.4147
STAT4	NM_003151	1.2449	1.7344	3.3856
SPRY4	NM_030964	1.8788	1.6637	3.3422
TGM2	NM_198951	1.0475	1.8359	3.2500
SHC3	NM_016848	1.3116	1.3749	3.2443
HLF	NM_002126	1.3677	1.8209	3.1743
PDLIM3	NM_014476	2.0539	2.0544	3.1280
CALB2	NM_001740	1.4428	1.0995	3.1226
EGR4	NM_001965	1.8877	1.6876	3.1219
SOBP	NM_018013	1.9826	1.2792	3.0508
CPEB1	NM_030594	1.2872	1.9788	3.0360
GALNT5	NM_014568	1.7247	1.8264	3.0222
EPHA8	NM_001006943	1.2708	1.3104	3.0203
KCNAB3	NM_004732	1.4641	1.0575	3.0132
PCDH11X	NM_014522	1.4975	0.9077	2.9754
CCNA1	NM_003914	1.5694	1.4168	2.9502
NLRC5	NM_032206	1.3812	1.3660	2.9235
LRFN4	NM_024036	1.8066	1.1766	2.7726
GPR68	NM_003485	1.6858	1.3447	2.7435
ADORA1	NM_000674	0.9010	0.7098	2.6844
PAQR3	NM_001040202	1.2385	1.3784	2.6797

Gene Name	ID Number	Actual Fold Repression (vs shSCX-N)		
		shRb-N	shSCX-H	shRb-H
IL27RA	NM_004843	1.5084	1.3077	2.6767
NEK10	NM_199347	1.4418	1.6547	2.6432
NANOG	NM_024865	1.2439	1.7340	2.6396
PRDM16	NM_022114	1.7008	1.2826	2.6213
LRRC52	NM_001005214	1.7408	1.0204	2.6185
BTC	NM_001729	1.6622	1.2941	2.5672
KIF7	NM_198525	1.6635	1.1251	2.5639
THBS4	NM_003248	1.4767	1.4208	2.5008
LYSMD2	NM_153374	1.5664	1.3877	2.4907
PPARGC1B	NM_133263	1.0593	1.4997	2.4556
MICALCL	NM_032867	0.7531	1.2830	2.4074
BMP8B	NM_001720	1.0633	1.4737	2.4062
LOH3CR2A	NR_024065	1.2926	1.3931	2.3736
WDR4	NM_033661	1.4433	1.3511	2.3537
CLIP2	NM_003388	1.0671	1.2378	2.3406
URB2	NM_014777	1.4037	1.2986	2.3157
ASPHD2	NM_020437	1.2231	1.0106	2.2231
LMCD1	NM_014583	1.4531	1.3186	2.2192
ZNF684	NM_152373	1.0844	1.2350	2.1675
PKP1	NM_000299	1.2899	1.2085	2.1478
LRRC14B	NM_001080478	0.8893	1.0576	2.1460
ST8SIA4	NM_005668	1.3758	1.3479	2.1221
FOXS1	NM_004118	0.4076	1.3597	2.1043
MYH3	NM_002470	1.2156	1.0697	2.0731
MRPL12	NM_002949	1.2903	1.1708	2.0494

.

Chapter 6. Conclusions and Future Directions

The penultimate goal of this work and as stated in chapter 1 of this thesis, was to delineate the molecular mechanisms employed by ARNT to control transcription in response to multiple environmental stimuli. To achieve this general objective, I studied two dynamics of ARNT transcriptional control 1) AHR/ARNT and disruption of ER-regulated transcription and 2) the role of the ARNT-TRIP230-Rb transcriptional complex in HIF1-regulated signaling. The first paradigm involved the testing of siRNAs to ARNT and AHR and investigating the impacts of ARNT knockdown on AHR-mediated transrepression of estrogen signaling. The second paradigm investigated the role of the ARNT-TRIP230-Rb complex in HIF1-regulated transcription. I used siRNAs to Rb to determine the transcriptional consequences of Rb-loss in cells under hypoxic stress. The latter paradigm also included the development of stable cell lines using shRNA technology and delineating the components of the ARNT-TRIP230-Rb complex through Rb-ablation. Additionally, we examined the HIF1-mediated gene regulatory networks impacted by Rb-depletion in prostate and breast cancer models using microarray technology and gene ontology analysis. It is hoped that these experiments will allow for a number of future experiments that may provide further insights of the role of Rb in HIF1-mediated signalling and cancer cell evolution. The following four sections of this chapter will review each of the papers and suggest what questions still remain and the potential for future research opportunities.

6.1. Chapter 2: Conclusions and Future Directions

In chapter 2 of this thesis, we used siRNAs to knockdown ARNT and AHR protein levels and described AHR transcription factor function at E2-inducible genes in both MCF7 and ECC-1 cells. Therein, it was shown that AHR-knockdown led to loss of dioxin-induced transrepression at ER-target genes but that ARNT-knockdown had no effect on TCDD-induced transrepression, suggesting that TCDD-induced disruption of

ER-signaling is dependent on AHR but not on ARNT. Unexpectedly, we also showed that ARNT acts as a coactivator in MCF7 cells and as a corepressor in ECC1 cells at E2-inducible genes, suggesting cell-line specific roles for ARNT as a transcriptional modifier.

Since the publication, the role of AHR and ARNT in ER-regulated transcription has been investigated further and expanded upon. Ahmed and colleagues [414] used zinc-finger nucleases to knockout AHR and ARNT protein expression and supported our findings that ARNT is indeed a coactivator of ER-regulated transcription in MCF7 cells. However, they also found that knockout of either AHR or ARNT abolished TCDD-mediated repression of E2-induced pS2 and GREB1 transcription, suggesting that both ARNT and AHR are required for TCDD-induced transrepression at ER-regulated genes. Undoubtedly, gene knockout techniques are far superior to siRNA-mediated knockdown as it is nearly impossible to completely ablate protein expression with siRNAs. Thus, it is possible that residual ARNT protein in our knockdown studies contributed to the observed TCDD-dependent inhibition of ER-regulated transcription and that a functional AHR/ARNT heterodimer is required for transrepression functions. Nevertheless, our data still refutes the notion that it is competition for ARNT/coactivators that leads to TCDD-induced disruption of ER-signaling since ARNT knockdown exacerbates ER-dependent transcription in ECC-1 cells and because TCDD still dampens the expression of E2-inducible targets in ECC-1 cells with depleted ARNT protein. Hence, a key question becomes what other corepressors or factors are involved in TCDD-dependent disruption of ER transcription factor function?

It has been well documented that nuclear receptor corepressor 1 (NCOR1) silencing mediator of retinoic acid and thyroid hormone receptor (SMRT/NCOR2), switch independent 3 (Sin3) and histone deacetylase (HDAC) corepressor complexes inhibit nuclear receptor transcription factor functions [415]. Additionally, ligand-induced activation facilitates the exchange of these corepressor complexes with coactivator complexes harbouring acetyltransferase and chromatin remodeling capabilities [415]. However, this theory represents mechanisms of repression at a nuclear receptor's own cognate response element and not the molecular mechanisms employed by the bHLH-PAS transcription factors. Although studies investigating the roles of NCOR1 and SMRT

in bHLH-PAS transcription factor functions are lacking, they remain attractive candidates as corepressors involved in AHR-mediated transrepression of ER-signaling for a few reasons; 1) NCOR1 and SMRT are crucial corepressors required for the transrepression functions of many of the nuclear receptors with immune system functions [292] suggesting that they may be involved in a similar capacity in other models of transrepression; 2) a physical interaction exists between AHR and SMRT and SMRT inhibits AHR-mediated transcriptional activities [278,416]; and 3) I have shown through chromatin immunoprecipitation that NCOR1 is significantly enriched at the pS2 promoter after combinatorial treatments with TCDD and E2 (Appendix A, Figure A1), suggesting that activated AHR may recruit NCOR1 to the pS2 promoter to repress ER-regulated transcription factor function. Taken together, this implies that NCOR1 and SMRT could facilitate the transrepression functions of AHR/ARNT in ER-dependent signaling. To further define the roles of NCOR1 and SMRT, future research efforts should focus on targeted disruption of NCOR1 and/or SMRT (si/shRNA, CRISPR, etc.) and the resultant transcriptional ramifications at ER-regulated genes with E2 and TCDD treatments. This will not only further characterize AHR-mediated transrepression functions but may potentially identify chemotherapeutic targets for ER-positive cancers.

6.2. Chapter 3: Conclusions and Future Directions

In Chapter 3 of this thesis, we set out to determine the role of Rb and TRIP230 in HIF-mediated transcription factor functions. We used siRNA mediated knockdown of Rb in MCF7 and LNCaP cells to determine the functional consequences of Rb-ablation in cells under hypoxic stress. We demonstrated that a combination of hypoxia and Rb-depletion led to concomitant increases in mRNA and protein for canonical HIF1-regulated genes. Additionally, we characterized the molecular interactions between ARNT, TRIP230 and Rb and further delineated the role of hyperphosphorylated Rb as a negative regulator of TRIP230 coactivator function. Finally, we showed that Rb-loss in conjunction with hypoxia led to significantly higher rates of cell invasion in MCF7 breast cancer cells and that our observations likely occurred independent of E2F-regulated mechanisms.

Two important questions arose from this work. The first of which was what are the broader implications of Rb-loss and hypoxia in the context of disease progression or cancer cell transformation? This question was answered in detail in chapters 4 and 5 of this thesis. The second question was does our molecular model of the ARNT-TRIP230-Rb transcriptional complex accurately represent what is happening clinically? Recapitulating results in gene knockout models using CRISPR-CAS9 would greatly strengthen our arguments that Rb is required for the appropriate expression of HIF1-regulated genes. As mentioned in the chapter 2 conclusions, siRNA has its pitfalls as knockdown does not completely silence Rb expression and there may be off-target effects occurring through the chemical treatments or through interactions with the siRNA to miRNAs or related RNA sequences. If Rb knockout through direct DNA editing phenocopies the siRNA results then that strongly supports our working hypothesis as harsh chemical treatments and low levels of functional Rb protein are no longer an issue. On the otherhand, we verified the transcriptional responses with two separate siRNAs as well as through reporter assays using a TRIP230 deletion mutant incapable of interacting with Rb thereby strengthening our observations that loss of Rb permits full coactivator potential of TRIP230 at HIF1-regulated genes. Moreover, loss of copy number or deletion of Rb rather than point mutations or frameshift mutations represent the majority of loss of function alterations occurring in clinical samples from patients whose cancers transform to a more aggressive phenotype [202,417]. Thus, using siRNA technology to deplete functional Rb in early stage cancer cell lines most accurately reflects the conditions observed in clinical examples. The molecular characterization of transcription factor function and the phenotypic consequences of Rb-loss and hypoxia in cell-based systems is only a starting point and the most accurate models require complete biological systems. However, *in vivo* experiments are intended for future research and are discussed further below.

Additional avenues of future research that could come from this chapter include determining the roles of putative corepressors identified in our chromatin immunoprecipitation assays in HIF1-mediated transcription. We discussed the potential for HDACs in activated HIF1 transcription factor function, however ChIP assays also identified SIN3A and SIN3B at the VEGF promoter and EPO enhancer after hypoxia treatments. Despite its known roles as a transcriptional corepressor, SIN3A is a potent

coactivator required for AHR transcription factor functions [418], suggesting it may play a similar role in activated HIF1 functions. Thus, further delineating the roles of canonical corepressors in activated transcription may provide further insight to genome-wide transcriptional regulation and provide future targets for cell- or tissue-specific chemotherapy.

6.3. Chapter 4: Conclusions and Future Directions

In chapter 4 of this thesis, we investigated the role that Rb plays in HIF1-mediated transcription by examining prostate cancer cells that expressed either a shRNA to a scrambled negative control RNA or a shRNA to Rb. Transformed LNCaP cells were either treated with hypoxia or left at normoxia and then microarray analysis was completed to determine the genetic programs controlled by the Rb-HIF1 complex. We found that Rb-ablation exacerbates HIF1-regulated gene programs involved in metastatic transformation and neuroendocrine differentiation. Additionally, factors identified in the microarray analysis mirrored the transcriptional profiles at the protein level. Finally. Rb-loss and hypoxia sensitized prostate cancer cells to kisspeptin-10, a potent KISS1R agonist, suggesting therapeutic complications in men with advanced stages of prostate cancer.

Collectively, this work represents the first in depth analysis of the loss of Rb function and the consequences to HIF1-mediated metastatic transformation. However, many questions remain that require further investigation. Firstly, gene ontology identified AKT, ERK1/2 and NFKB as key signaling nodes that control metastatic transformation and neuroendocrine differentiation. Future research efforts should directly target AKT, NFKB and ERK1/2 with chemical inhibitors to determine if we can block invasion and/or neuroendocrine differentiation after Rb-loss and hypoxia treatments. Additionally, receptors identified by the microarray that are upstream activators of ERK/AKT/NFKB, such as KISS1R [419] and CXCR4 [413], can be pharmaceutically inhibited to determine if receptor antagonism phenocopies inhibition of signaling nodes. These experiments may identify new chemotherapies for advanced stages of prostate cancer. Finally, using Rb-ablated cells in mouse models to see if we can recapitulate the array data would be of extreme interest. Sharma et al. [202] depleted Rb expression in LNCaP cells and

showed that mouse xenografts with Rb-loss had significant growth advantages and displayed characteristics of CRPC when compared to control xenografts. They suggested that CRPC progression after Rb-ablation was due to an E2F-mediated increase in AR activity. However, intratumour oxygen status was not determined and neuroendocrine markers were not investigated. Thus, determining these clinical parameters may also help identify the molecular mechanisms governing CRPC or NED progression.

6.4. Chapter 5: Conclusions and Future Directions

In chapter 5 of this thesis, we investigated the role of Rb in HIF1-regulated transcription by examining breast cancer cells that expressed either a shRNA to a scrambled negative control RNA or a shRNA to Rb. Methodologically, this chapter was very similar to chapter 4, however, here we investigated breast cancer models and discovered that loss of Rb and hypoxia led to aberrant expression of hypoxia-inducible gene programs involved in metastasis and cellular transformation. Furthermore, we showed that Rb-loss and hypoxia led to increased actin reorganization and cell migration and that blocking AKT and ERK1/2 signaling pathways significantly impeded actin reorganization and migration in hypoxic cells with depleted Rb.

Moving forward, it is imperative that we move into mouse models. We determined that Rb loss and hypoxia upregulated S1PR4, NDRG1 and CXCR4 expression. Orthotopic tumour implants of shSCX and shRb breast cancer cell lines in female NOD-SCID mice and then subsequent tissue analysis for metastases and expression of identified array genes may yield impactful results. For example, S1PR4 is a putative marker for breast cancer metastasis [420] and is over-represented in brain cancers. Thus, examining mouse brains for metastatic nodes after orthotopic implants and staining for S1PR4 expression may lead to valuable mechanistic insight on breast cancers that metastasize to the brain. Furthermore, injecting shRNA cells via tail vein and then determining if metastatic foci in the lungs increases in response to Rb-loss would significantly strengthen our hypothesis that loss of Rb function leads to acquisition of a metastatic phenotype. Furthermore, we showed that pharmacological inhibition of ERK1/2 and AKT could block hypoxia inducible actin reorganization and cell migration in

Rb-depleted cells. Thus, using U0126 and A6730 and the shRNA cell lines in mouse xenograft studies to determine if we can significantly inhibit tumour progression or metastasis in Rb-depleted xenografts would strongly support the microarray data Finally, targeting identified array genes with known roles in metastasis or EMT, such as NDRG1, STC1 and CXCR4 with chemical inhibitors or siRNAs to see if we can block invasion and metastasis is also important as these targets may be candidates for future treatments in advanced stages of breast cancer.

References

1. Watson JD, Crick FH (1953) Molecular structure of nucleic acids; a structure for deoxyribose nucleic acid. Nature 171: 737-738.

2. Crick FH, Barnett L, Brenner S, Watts-Tobin RJ (1961) General nature of the genetic code for proteins. Nature 192: 1227-1232.

3. Jacob F, Monod J (1961) Genetic regulatory mechanisms in the synthesis of proteins. J Mol Biol 3: 318-356.

4. Weil PA, Luse DS, Segall J, Roeder RG (1979) Selective and accurate initiation of transcription at the Ad2 major late promotor in a soluble system dependent on purified RNA polymerase II and DNA. Cell 18: 469-484.

5. Matsui T, Segall J, Weil PA, Roeder RG (1980) Multiple factors required for accurate initiation of transcription by purified RNA polymerase II. J Biol Chem 255: 11992-11996.

6. Banerji J, Rusconi S, Schaffner W (1981) Expression of a beta-globin gene is enhanced by remote SV40 DNA sequences. Cell 27: 299-308.

7. Johnson PF, McKnight SL (1989) Eukaryotic transcriptional regulatory proteins. Annu Rev Biochem 58: 799-839.

8. Kim YJ, Bjorklund S, Li Y, Sayre MH, Kornberg RD (1994) A multiprotein mediator of transcriptional activation and its interaction with the C-terminal repeat domain of RNA polymerase II. Cell 77: 599-608.

9. Flanagan PM, Kelleher RJ, 3rd, Sayre MH, Tschochner H, Kornberg RD (1991) A mediator required for activation of RNA polymerase II transcription in vitro. Nature 350: 436-438.

10. Kelleher RJ, 3rd, Flanagan PM, Kornberg RD (1990) A novel mediator between activator proteins and the RNA polymerase II transcription apparatus. Cell 61: 1209-1215.

11. Konopka RJ, Benzer S (1971) Clock mutants of Drosophila melanogaster. Proc Natl Acad Sci U S A 68: 2112-2116.

12. Bargiello TA, Young MW (1984) Molecular genetics of a biological clock in Drosophila. Proc Natl Acad Sci U S A 81: 2142-2146.

13. Zehring WA, Wheeler DA, Reddy P, Konopka RJ, Kyriacou CP, et al. (1984) P-element transformation with period locus DNA restores rhythmicity to mutant, arrhythmic Drosophila melanogaster. Cell 39: 369-376.

14. Reddy P, Zehring WA, Wheeler DA, Pirrotta V, Hadfield C, et al. (1984) Molecular analysis of the period locus in Drosophila melanogaster and identification of a transcript involved in biological rhythms. Cell 38: 701-710.

15. Crews ST, Thomas JB, Goodman CS (1988) The Drosophila single-minded gene encodes a nuclear protein with sequence similarity to the per gene product. Cell 52: 143-151.

16. Hoffman EC, Reyes H, Chu FF, Sander F, Conley LH, et al. (1991) Cloning of a factor required for activity of the Ah (dioxin) receptor. Science 252: 954-958.

17. Nambu JR, Lewis JO, Wharton KA, Jr., Crews ST (1991) The Drosophila single-minded gene encodes a helix-loop-helix protein that acts as a master regulator of CNS midline development. Cell 67: 1157-1167.

18. McIntosh BE, Hogenesch JB, Bradfield CA (2010) Mammalian Per-Arnt-Sim proteins in environmental adaptation. Annu Rev Physiol 72: 625-645.

19. Huang ZJ, Edery I, Rosbash M (1993) PAS is a dimerization domain common to Drosophila period and several transcription factors. Nature 364: 259-262.

20. Perdew GH, Bradfield CA (1996) Mapping the 90 kDa heat shock protein binding region of the Ah receptor. Biochem Mol Biol Int 39: 589-593.

21. Murre C, McCaw PS, Baltimore D (1989) A new DNA binding and dimerization motif in immunoglobulin enhancer binding, daughterless, MyoD, and myc proteins. Cell 56: 777-783.

22. Lassar AB, Buskin JN, Lockshon D, Davis RL, Apone S, et al. (1989) MyoD is a sequence-specific DNA binding protein requiring a region of myc homology to bind to the muscle creatine kinase enhancer. Cell 58: 823-831.

23. Crews ST (1998) Control of cell lineage-specific development and transcription by bHLH-PAS proteins. Genes Dev 12: 607-620.

24. Ikeda M, Nomura M (1997) cDNA cloning and tissue-specific expression of a novel basic helix-loop-helix/PAS protein (BMAL1) and identification of alternatively spliced variants with alternative translation initiation site usage. Biochem Biophys Res Commun 233: 258-264.

25. Hogenesch JB, Gu YZ, Jain S, Bradfield CA (1998) The basic-helix-loop-helix-PAS orphan MOP3 forms transcriptionally active complexes with circadian and hypoxia factors. Proc Natl Acad Sci U S A 95: 5474-5479.

26. Takahata S, Sogawa K, Kobayashi A, Ema M, Mimura J, et al. (1998) Transcriptionally active heterodimer formation of an Arnt-like PAS protein, Arnt3, with HIF-1a, HLF, and clock. Biochem Biophys Res Commun 248: 789-794.

27. Ikeda M, Yu W, Hirai M, Ebisawa T, Honma S, et al. (2000) cDNA cloning of a novel bHLH-PAS transcription factor superfamily gene, BMAL2: its

mRNA expression, subcellular distribution, and chromosomal localization. Biochem Biophys Res Commun 275: 493-502.

28. Hogenesch JB, Gu YZ, Moran SM, Shimomura K, Radcliffe LA, et al. (2000) The basic helix-loop-helix-PAS protein MOP9 is a brain-specific heterodimeric partner of circadian and hypoxia factors. J Neurosci 20: RC83.

29. Maemura K, de la Monte SM, Chin MT, Layne MD, Hsieh CM, et al. (2000) CLIF, a novel cycle-like factor, regulates the circadian oscillation of plasminogen activator inhibitor-1 gene expression. J Biol Chem 275: 36847-36851.

30. Wang GL, Jiang BH, Rue EA, Semenza GL (1995) Hypoxia-inducible factor 1 is a basic-helix-loop-helix-PAS heterodimer regulated by cellular O2 tension. Proc Natl Acad Sci U S A 92: 5510-5514.

31. Gekakis N, Staknis D, Nguyen HB, Davis FC, Wilsbacher LD, et al. (1998) Role of the CLOCK protein in the mammalian circadian mechanism. Science 280: 1564-1569.

32. Probst MR, Fan CM, Tessier-Lavigne M, Hankinson O (1997) Two murine homologs of the Drosophila single-minded protein that interact with the mouse aryl hydrocarbon receptor nuclear translocator protein. J Biol Chem 272: 4451-4457.

33. Michaud JL, DeRossi C, May NR, Holdener BC, Fan CM (2000) ARNT2 acts as the dimerization partner of SIM1 for the development of the hypothalamus. Mech Dev 90: 253-261.

34. Teh CH, Lam KK, Loh CC, Loo JM, Yan T, et al. (2006) Neuronal PAS domain protein 1 is a transcriptional repressor and requires arylhydrocarbon nuclear translocator for its nuclear localization. J Biol Chem 281: 34617-34629.

35. Pieper AA, Wu X, Han TW, Estill SJ, Dang Q, et al. (2005) The neuronal PAS domain protein 3 transcription factor controls FGF-mediated adult hippocampal neurogenesis in mice. Proc Natl Acad Sci U S A 102: 14052-14057.

36. Ooe N, Saito K, Mikami N, Nakatuka I, Kaneko H (2004) Identification of a novel basic helix-loop-helix-PAS factor, NXF, reveals a Sim2 competitive, positive regulatory role in dendritic-cytoskeleton modulator drebrin gene expression. Mol Cell Biol 24: 608-616.

37. Dioum EM, Rutter J, Tuckerman JR, Gonzalez G, Gilles-Gonzalez MA, et al. (2002) NPAS2: a gas-responsive transcription factor. Science 298: 2385-2387.

38. Labrecque MP, Prefontaine GG, Beischlag TV (2013) The aryl hydrocarbon receptor nuclear translocator (ARNT) family of proteins: transcriptional modifiers with multi-functional protein interfaces. Curr Mol Med 13: 1047-1065.

39. Burbach KM, Poland A, Bradfield CA (1992) Cloning of the Ah-receptor cDNA reveals a distinctive ligand-activated transcription factor. Proc Natl Acad Sci U S A 89: 8185-8189.

40. Fernandez-Salguero PM, Hilbert DM, Rudikoff S, Ward JM, Gonzalez FJ (1996) Aryl-hydrocarbon receptor-deficient mice are resistant to 2,3,7,8-tetrachlorodibenzo-p-dioxin-induced toxicity. Toxicol Appl Pharmacol 140: 173-179.

41. Hankinson O (1995) The aryl hydrocarbon receptor complex. Annu Rev Pharmacol Toxicol 35: 307-340.

42. Beischlag TV, Luis Morales J, Hollingshead BD, Perdew GH (2008) The aryl hydrocarbon receptor complex and the control of gene expression. Crit Rev Eukaryot Gene Expr 18: 207-250.

43. Opitz CA, Litzenburger UM, Sahm F, Ott M, Tritschler I, et al. (2011) An endogenous tumour-promoting ligand of the human aryl hydrocarbon receptor. Nature 478: 197-203.

44. Carver LA, Bradfield CA (1997) Ligand-dependent interaction of the aryl hydrocarbon receptor with a novel immunophilin homolog in vivo. J Biol Chem 272: 11452-11456.

45. Kazlauskas A, Poellinger L, Pongratz I (1999) Evidence that the co-chaperone p23 regulates ligand responsiveness of the dioxin (Aryl hydrocarbon) receptor. J Biol Chem 274: 13519-13524.

46. Ma Q, Whitlock JP, Jr. (1997) A novel cytoplasmic protein that interacts with the Ah receptor, contains tetratricopeptide repeat motifs, and augments the transcriptional response to 2,3,7,8-tetrachlorodibenzo-p-dioxin. J Biol Chem 272: 8878-8884.

47. Pongratz I, Mason GG, Poellinger L (1992) Dual roles of the 90-kDa heat shock protein hsp90 in modulating functional activities of the dioxin receptor. Evidence that the dioxin receptor functionally belongs to a subclass of nuclear receptors which require hsp90 both for ligand binding activity and repression of intrinsic DNA binding activity. J Biol Chem 267: 13728-13734.

48. Pollenz RS, Sattler CA, Poland A (1994) The aryl hydrocarbon receptor and aryl hydrocarbon receptor nuclear translocator protein show distinct subcellular localizations in Hepa 1c1c7 cells by immunofluorescence microscopy. Mol Pharmacol 45: 428-438.

49. Beischlag TV, Wang S, Rose DW, Torchia J, Reisz-Porszasz S, et al. (2002) Recruitment of the NCoA/SRC-1/p160 family of transcriptional coactivators by the aryl hydrocarbon receptor/aryl hydrocarbon receptor nuclear translocator complex. Mol Cell Biol 22: 4319-4333.

50. Reisz-Porszasz S, Probst MR, Fukunaga BN, Hankinson O (1994) Identification of functional domains of the aryl hydrocarbon receptor nuclear translocator protein (ARNT). Mol Cell Biol 14: 6075-6086.

51. Pongratz I, Antonsson C, Whitelaw ML, Poellinger L (1998) Role of the PAS domain in regulation of dimerization and DNA binding specificity of the dioxin receptor. Molecular and cellular biology 18: 4079-4088.

52. McGuire J, Okamoto K, Whitelaw ML, Tanaka H, Poellinger L (2001) Definition of a dioxin receptor mutant that is a constitutive activator of transcription: delineation of overlapping repression and ligand binding functions within the PAS domain. J Biol Chem 276: 41841-41849.

53. Kohle C, Hassepass I, Bock-Hennig BS, Walter Bock K, Poellinger L, et al. (2002) Conditional expression of a constitutively active aryl hydrocarbon receptor in MCF-7 human breast cancer cells. Arch Biochem Biophys 402: 172-179.

54. Hirose K, Morita M, Ema M, Mimura J, Hamada H, et al. (1996) cDNA cloning and tissue-specific expression of a novel basic helix-loop-helix/PAS factor (Arnt2) with close sequence similarity to the aryl hydrocarbon receptor nuclear translocator (Arnt). Mol Cell Biol 16: 1706-1713.

55. Dougherty EJ, Pollenz RS (2008) Analysis of Ah receptor-ARNT and Ah receptor-ARNT2 complexes in vitro and in cell culture. Toxicol Sci 103: 191-206.

56. Swedenborg E, Ruegg J, Makela S, Pongratz I (2009) Endocrine disruptive chemicals: mechanisms of action and involvement in metabolic disorders. J Mol Endocrinol 43: 1-10.

57. Mangelsdorf DJ, Thummel C, Beato M, Herrlich P, Schutz G, et al. (1995) The nuclear receptor superfamily: the second decade. Cell 83: 835-839.

58. Evans RM, Mangelsdorf DJ (2014) Nuclear Receptors, RXR, and the Big Bang. Cell 157: 255-266.

59. Green S, Walter P, Kumar V, Krust A, Bornert JM, et al. (1986) Human oestrogen receptor cDNA: sequence, expression and homology to v-erb-A. Nature 320: 134-139.

60. Hollenberg SM, Weinberger C, Ong ES, Cerelli G, Oro A, et al. (1985) Primary structure and expression of a functional human glucocorticoid receptor cDNA. Nature 318: 635-641.

61. Tsai MJ, O'Malley BW (1994) Molecular mechanisms of action of steroid/thyroid receptor superfamily members. Annu Rev Biochem 63: 451-486.

62. Barettino D, Vivanco Ruiz MM, Stunnenberg HG (1994) Characterization of the ligand-dependent transactivation domain of thyroid hormone receptor. EMBO J 13: 3039-3049.

63. Heery DM, Kalkhoven E, Hoare S, Parker MG (1997) A signature motif in transcriptional co-activators mediates binding to nuclear receptors. Nature 387: 733-736.

64. Warnmark A, Treuter E, Wright AP, Gustafsson JA (2003) Activation functions 1 and 2 of nuclear receptors: molecular strategies for transcriptional activation. Mol Endocrinol 17: 1901-1909.

65. Webb P, Nguyen P, Shinsako J, Anderson C, Feng W, et al. (1998) Estrogen receptor activation function 1 works by binding p160 coactivator proteins. Mol Endocrinol 12: 1605-1618.

66. Gibson DA, Saunders PT (2012) Estrogen dependent signaling in reproductive tissues - a role for estrogen receptors and estrogen related receptors. Mol Cell Endocrinol 348: 361-372.

67. Picard D (2006) Chaperoning steroid hormone action. Trends Endocrinol Metab 17: 229-235.

68. Wu Y, Koenig RJ (2000) Gene regulation by thyroid hormone. Trends Endocrinol Metab 11: 207-211.

69. Cole TJ, Blendy JA, Monaghan AP, Krieglstein K, Schmid W, et al. (1995) Targeted disruption of the glucocorticoid receptor gene blocks adrenergic chromaffin cell development and severely retards lung maturation. Genes Dev 9: 1608-1621.

70. Reichardt HM, Kaestner KH, Tuckermann J, Kretz O, Wessely O, et al. (1998) DNA binding of the glucocorticoid receptor is not essential for survival. Cell 93: 531-541.

71. Krishnan V, Porter W, Santostefano M, Wang X, Safe S (1995) Molecular mechanism of inhibition of estrogen-induced cathepsin D gene expression by 2,3,7,8-tetrachlorodibenzo-p-dioxin (TCDD) in MCF-7 cells. Mol Cell Biol 15: 6710-6719.

72. Ohtake F, Takeyama K, Matsumoto T, Kitagawa H, Yamamoto Y, et al. (2003) Modulation of oestrogen receptor signalling by association with the activated dioxin receptor. Nature 423: 545-550.

73. Beischlag TV, Perdew GH (2005) ER alpha-AHR-ARNT protein-protein interactions mediate estradiol-dependent transrepression of dioxin-inducible gene transcription. J Biol Chem 280: 21607-21611.

74. Zacharewski TR, Bondy KL, McDonell P, Wu ZF (1994) Antiestrogenic effect of 2,3,7,8-tetrachlorodibenzo-p-dioxin on 17 beta-estradiol-induced pS2 expression. Cancer Res 54: 2707-2713.

75. Krishnan V, Safe S (1993) Polychlorinated biphenyls (PCBs), dibenzo-p-dioxins (PCDDs), and dibenzofurans (PCDFs) as antiestrogens in MCF-7 human breast cancer cells: quantitative structure-activity relationships. Toxicol Appl Pharmacol 120: 55-61.

76. Wang F, Samudio I, Safe S (2001) Transcriptional activation of cathepsin D gene expression by 17beta-estradiol: mechanism of aryl hydrocarbon receptor-mediated inhibition. Mol Cell Endocrinol 172: 91-103.

77. Duan R, Porter W, Samudio I, Vyhlidal C, Kladde M, et al. (1999) Transcriptional activation of c-fos protooncogene by 17beta-estradiol: mechanism of aryl hydrocarbon receptor-mediated inhibition. Mol Endocrinol 13: 1511-1521.

78. Coumoul X, Diry M, Robillot C, Barouki R (2001) Differential regulation of cytochrome P450 1A1 and 1B1 by a combination of dioxin and pesticides in the breast tumor cell line MCF-7. Cancer Res 61: 3942-3948.

79. Reen RK, Cadwallader A, Perdew GH (2002) The subdomains of the transactivation domain of the aryl hydrocarbon receptor (AhR) inhibit AhR and estrogen receptor transcriptional activity. Arch Biochem Biophys 408: 93-102.

80. Spink DC, Lincoln DW, 2nd, Dickerman HW, Gierthy JF (1990) 2,3,7,8-Tetrachlorodibenzo-p-dioxin causes an extensive alteration of 17 beta-estradiol metabolism in MCF-7 breast tumor cells. Proc Natl Acad Sci U S A 87: 6917-6921.

81. Wormke M, Stoner M, Saville B, Walker K, Abdelrahim M, et al. (2003) The aryl hydrocarbon receptor mediates degradation of estrogen receptor alpha through activation of proteasomes. Mol Cell Biol 23: 1843-1855.

82. Ohtake F, Baba A, Takada I, Okada M, Iwasaki K, et al. (2007) Dioxin receptor is a ligand-dependent E3 ubiquitin ligase. Nature 446: 562-566.

83. Shipley JM, Waxman DJ (2006) Aryl hydrocarbon receptor-independent activation of estrogen receptor-dependent transcription by 3-methylcholanthrene. Toxicol Appl Pharmacol 213: 87-97.

84. Brunnberg S, Pettersson K, Rydin E, Matthews J, Hanberg A, et al. (2003) The basic helix-loop-helix-PAS protein ARNT functions as a potent coactivator of estrogen receptor-dependent transcription. Proc Natl Acad Sci U S A 100: 6517-6522.

85. Matthews J, Wihlen B, Thomsen J, Gustafsson JA (2005) Aryl hydrocarbon receptor-mediated transcription: ligand-dependent recruitment of estrogen receptor alpha to 2,3,7,8-tetrachlorodibenzo-p-dioxin-responsive promoters. Mol Cell Biol 25: 5317-5328.

86. Labrecque MP, Takhar MK, Hollingshead BD, Prefontaine GG, Perdew GH, et al. (2012) Distinct roles for aryl hydrocarbon receptor nuclear translocator and ah receptor in estrogen-mediated signaling in human cancer cell lines. PLoS One 7: e29545.

87. Wihlen B, Ahmed S, Inzunza J, Matthews J (2009) Estrogen receptor subtype- and promoter-specific modulation of aryl hydrocarbon receptor-dependent transcription. Mol Cancer Res 7: 977-986.

88. Perdew GH, Hollingshead BD, Dinatale BC, Morales JL, Labrecque MP, et al. (2010) Estrogen receptor expression is required for low-dose resveratrol-mediated repression of aryl hydrocarbon receptor activity. J Pharmacol Exp Ther 335: 273-283.

89. Jang M, Cai L, Udeani GO, Slowing KV, Thomas CF, et al. (1997) Cancer chemopreventive activity of resveratrol, a natural product derived from grapes. Science 275: 218-220.

90. Macpherson L, Matthews J (2010) Inhibition of aryl hydrocarbon receptor-dependent transcription by resveratrol or kaempferol is independent of

estrogen receptor alpha expression in human breast cancer cells. Cancer Lett 299: 119-129.

91. Ruegg J, Swedenborg E, Wahlstrom D, Escande A, Balaguer P, et al. (2008) The transcription factor aryl hydrocarbon receptor nuclear translocator functions as an estrogen receptor beta-selective coactivator, and its recruitment to alternative pathways mediates antiestrogenic effects of dioxin. Mol Endocrinol 22: 304-316.

92. Clark WH (1991) Tumour progression and the nature of cancer. Br J Cancer 64: 631-644.

93. Vogelstein B, Kinzler KW (2004) Cancer genes and the pathways they control. Nat Med 10: 789-799.

94. Hanahan D, Weinberg RA (2000) The hallmarks of cancer. Cell 100: 57-70.

95. Fresno Vara JA, Casado E, de Castro J, Cejas P, Belda-Iniesta C, et al. (2004) PI3K/Akt signalling pathway and cancer. Cancer Treat Rev 30: 193-204.

96. Vaux DL, Cory S, Adams JM (1988) Bcl-2 gene promotes haemopoietic cell survival and cooperates with c-myc to immortalize pre-B cells. Nature 335: 440-442.

97. Fodde R, Brabletz T (2007) Wnt/beta-catenin signaling in cancer stemness and malignant behavior. Curr Opin Cell Biol 19: 150-158.

98. Polakis P (2007) The many ways of Wnt in cancer. Curr Opin Genet Dev 17: 45-51.

99. Kastan MB, Onyekwere O, Sidransky D, Vogelstein B, Craig RW (1991) Participation of p53 protein in the cellular response to DNA damage. Cancer Res 51: 6304-6311.

100. Weinberg RA (1995) The retinoblastoma protein and cell cycle control. Cell 81: 323-330.

101. Kondo K, Klco J, Nakamura E, Lechpammer M, Kaelin WG, Jr. (2002) Inhibition of HIF is necessary for tumor suppression by the von Hippel-Lindau protein. Cancer Cell 1: 237-246.

102. Knudson AG, Jr. (1971) Mutation and cancer: statistical study of retinoblastoma. Proc Natl Acad Sci U S A 68: 820-823.

103. Srivastava S, Zou ZQ, Pirollo K, Blattner W, Chang EH (1990) Germ-line transmission of a mutated p53 gene in a cancer-prone family with Li-Fraumeni syndrome. Nature 348: 747-749.

104. Vogelstein B, Fearon ER, Hamilton SR, Kern SE, Preisinger AC, et al. (1988) Genetic alterations during colorectal-tumor development. N Engl J Med 319: 525-532.

105. Hanahan D, Weinberg RA (2011) Hallmarks of cancer: the next generation. Cell 144: 646-674.

106. Heppner GH (1984) Tumor heterogeneity. Cancer Res 44: 2259-2265.

107. Fidler IJ, Kripke ML (1977) Metastasis results from preexisting variant cells within a malignant tumor. Science 197: 893-895.

108. Mani SA, Guo W, Liao MJ, Eaton EN, Ayyanan A, et al. (2008) The epithelial-mesenchymal transition generates cells with properties of stem cells. Cell 133: 704-715.

109. Reya T, Morrison SJ, Clarke MF, Weissman IL (2001) Stem cells, cancer, and cancer stem cells. Nature 414: 105-111.

110. Greaves M, Maley CC (2012) Clonal evolution in cancer. Nature 481: 306-313.

111. Ono M (2008) Molecular links between tumor angiogenesis and inflammation: inflammatory stimuli of macrophages and cancer cells as targets for therapeutic strategy. Cancer Sci 99: 1501-1506.

112. Carreau A, El Hafny-Rahbi B, Matejuk A, Grillon C, Kieda C (2011) Why is the partial oxygen pressure of human tissues a crucial parameter? Small molecules and hypoxia. J Cell Mol Med 15: 1239-1253.

113. Spencer JA, Ferraro F, Roussakis E, Klein A, Wu J, et al. (2014) Direct measurement of local oxygen concentration in the bone marrow of live animals. Nature 508: 269-273.

114. Vaupel P, Mayer A, Briest S, Hockel M (2003) Oxygenation gain factor: a novel parameter characterizing the association between hemoglobin level and the oxygenation status of breast cancers. Cancer Res 63: 7634-7637.

115. McKeown SR (2014) Defining normoxia, physoxia and hypoxia in tumours-implications for treatment response. Br J Radiol 87: 20130676.

116. Semenza GL (2009) Regulation of oxygen homeostasis by hypoxia-inducible factor 1. Physiology (Bethesda) 24: 97-106.

117. Bayer C, Vaupel P (2012) Acute versus chronic hypoxia in tumors: Controversial data concerning time frames and biological consequences. Strahlenther Onkol 188: 616-627.

118. Dewhirst MW, Cao Y, Moeller B (2008) Cycling hypoxia and free radicals regulate angiogenesis and radiotherapy response. Nat Rev Cancer 8: 425-437.

119. Bartels K, Grenz A, Eltzschig HK (2013) Hypoxia and inflammation are two sides of the same coin. Proc Natl Acad Sci U S A 110: 18351-18352.

120. Movsas B, Chapman JD, Hanlon AL, Horwitz EM, Pinover WH, et al. (2001) Hypoxia in human prostate carcinoma: an Eppendorf PO2 study. Am J Clin Oncol 24: 458-461.

121. Vaupel P, Hockel M, Mayer A (2007) Detection and characterization of tumor hypoxia using pO2 histography. Antioxid Redox Signal 9: 1221-1235.

122. Jiang BH, Semenza GL, Bauer C, Marti HH (1996) Hypoxia-inducible factor 1 levels vary exponentially over a physiologically relevant range of O2 tension. Am J Physiol 271: C1172-1180.

123. Tian H, McKnight SL, Russell DW (1997) Endothelial PAS domain protein 1 (EPAS1), a transcription factor selectively expressed in endothelial cells. Genes Dev 11: 72-82.

124. Gu YZ, Moran SM, Hogenesch JB, Wartman L, Bradfield CA (1998) Molecular characterization and chromosomal localization of a third alpha-class hypoxia inducible factor subunit, HIF3alpha. Gene Expr 7: 205-213.

125. Hogenesch JB, Chan WK, Jackiw VH, Brown RC, Gu YZ, et al. (1997) Characterization of a subset of the basic-helix-loop-helix-PAS superfamily that interacts with components of the dioxin signaling pathway. J Biol Chem 272: 8581-8593.

126. Hirota K, Semenza GL (2006) Regulation of angiogenesis by hypoxia-inducible factor 1. Crit Rev Oncol Hematol 59: 15-26.

127. Bruick RK, McKnight SL (2001) A conserved family of prolyl-4-hydroxylases that modify HIF. Science 294: 1337-1340.

128. Ivan M, Haberberger T, Gervasi DC, Michelson KS, Gunzler V, et al. (2002) Biochemical purification and pharmacological inhibition of a mammalian prolyl hydroxylase acting on hypoxia-inducible factor. Proc Natl Acad Sci U S A 99: 13459-13464.

129. Epstein AC, Gleadle JM, McNeill LA, Hewitson KS, O'Rourke J, et al. (2001) C. elegans EGL-9 and mammalian homologs define a family of dioxygenases that regulate HIF by prolyl hydroxylation. Cell 107: 43-54.

130. Lando D, Peet DJ, Gorman JJ, Whelan DA, Whitelaw ML, et al. (2002) FIH-1 is an asparaginyl hydroxylase enzyme that regulates the transcriptional activity of hypoxia-inducible factor. Genes Dev 16: 1466-1471.

131. Mahon PC, Hirota K, Semenza GL (2001) FIH-1: a novel protein that interacts with HIF-1alpha and VHL to mediate repression of HIF-1 transcriptional activity. Genes Dev 15: 2675-2686.

132. Maxwell PH, Wiesener MS, Chang GW, Clifford SC, Vaux EC, et al. (1999) The tumour suppressor protein VHL targets hypoxia-inducible factors for oxygen-dependent proteolysis. Nature 399: 271-275.

133. Kallio PJ, Wilson WJ, O'Brien S, Makino Y, Poellinger L (1999) Regulation of the hypoxia-inducible transcription factor 1alpha by the ubiquitin-proteasome pathway. J Biol Chem 274: 6519-6525.

134. Huang LE, Gu J, Schau M, Bunn HF (1998) Regulation of hypoxia-inducible factor 1alpha is mediated by an O2-dependent degradation domain via the ubiquitin-proteasome pathway. Proc Natl Acad Sci U S A 95: 7987-7992.

135. Salceda S, Caro J (1997) Hypoxia-inducible factor 1alpha (HIF-1alpha) protein is rapidly degraded by the ubiquitin-proteasome system under

normoxic conditions. Its stabilization by hypoxia depends on redox-induced changes. J Biol Chem 272: 22642-22647.

136. Lando D, Peet DJ, Whelan DA, Gorman JJ, Whitelaw ML (2002) Asparagine hydroxylation of the HIF transactivation domain a hypoxic switch. Science 295: 858-861.

137. O'Rourke JF, Tian YM, Ratcliffe PJ, Pugh CW (1999) Oxygen-regulated and transactivating domains in endothelial PAS protein 1: comparison with hypoxia-inducible factor-1alpha. J Biol Chem 274: 2060-2071.

138. Maynard MA, Evans AJ, Hosomi T, Hara S, Jewett MA, et al. (2005) Human HIF-3alpha4 is a dominant-negative regulator of HIF-1 and is down-regulated in renal cell carcinoma. FASEB J 19: 1396-1406.

139. Vaupel P, Kelleher DK, Hockel M (2001) Oxygen status of malignant tumors: pathogenesis of hypoxia and significance for tumor therapy. Semin Oncol 28: 29-35.

140. Zhong H, De Marzo AM, Laughner E, Lim M, Hilton DA, et al. (1999) Overexpression of hypoxia-inducible factor 1alpha in common human cancers and their metastases. Cancer Res 59: 5830-5835.

141. Keith B, Adelman DM, Simon MC (2001) Targeted mutation of the murine arylhydrocarbon receptor nuclear translocator 2 (Arnt2) gene reveals partial redundancy with Arnt. Proc Natl Acad Sci U S A 98: 6692-6697.

142. Chavez JC, Baranova O, Lin J, Pichiule P (2006) The transcriptional activator hypoxia inducible factor 2 (HIF-2/EPAS-1) regulates the oxygen-dependent expression of erythropoietin in cortical astrocytes. J Neurosci 26: 9471-9481.

143. Maltepe E, Keith B, Arsham AM, Brorson JR, Simon MC (2000) The role of ARNT2 in tumor angiogenesis and the neural response to hypoxia. Biochem Biophys Res Commun 273: 231-238.

144. Card PB, Erbel PJ, Gardner KH (2005) Structural basis of ARNT PAS-B dimerization: use of a common beta-sheet interface for hetero- and homodimerization. J Mol Biol 353: 664-677.

145. Erbel PJ, Card PB, Karakuzu O, Bruick RK, Gardner KH (2003) Structural basis for PAS domain heterodimerization in the basic helix--loop--helix-PAS transcription factor hypoxia-inducible factor. Proc Natl Acad Sci U S A 100: 15504-15509.

146. Semenza GL, Wang GL (1992) A nuclear factor induced by hypoxia via de novo protein synthesis binds to the human erythropoietin gene enhancer at a site required for transcriptional activation. Mol Cell Biol 12: 5447-5454.

147. Semenza GL, Nejfelt MK, Chi SM, Antonarakis SE (1991) Hypoxia-inducible nuclear factors bind to an enhancer element located 3' to the human erythropoietin gene. Proc Natl Acad Sci U S A 88: 5680-5684.

148. Forsythe JA, Jiang BH, Iyer NV, Agani F, Leung SW, et al. (1996) Activation of vascular endothelial growth factor gene transcription by hypoxia-inducible factor 1. Mol Cell Biol 16: 4604-4613.

149. Chang KH, Chen Y, Chen TT, Chou WH, Chen PL, et al. (1997) A thyroid hormone receptor coactivator negatively regulated by the retinoblastoma protein. Proc Natl Acad Sci U S A 94: 9040-9045.

150. Beischlag TV, Taylor RT, Rose DW, Yoon D, Chen Y, et al. (2004) Recruitment of thyroid hormone receptor/retinoblastoma-interacting protein 230 by the aryl hydrocarbon receptor nuclear translocator is required for the transcriptional response to both dioxin and hypoxia. J Biol Chem 279: 54620-54628.

151. McInerney EM, Rose DW, Flynn SE, Westin S, Mullen TM, et al. (1998) Determinants of coactivator LXXLL motif specificity in nuclear receptor transcriptional activation. Genes Dev 12: 3357-3368.

152. Rios RM, Tassin AM, Celati C, Antony C, Boissier MC, et al. (1994) A peripheral protein associated with the cis-Golgi network redistributes in the intermediate compartment upon brefeldin A treatment. J Cell Biol 125: 997-1013.

153. Chen Y, Chen PL, Chen CF, Sharp ZD, Lee WH (1999) Thyroid hormone, T3-dependent phosphorylation and translocation of Trip230 from the Golgi complex to the nucleus. Proc Natl Acad Sci U S A 96: 4443-4448.

154. Infante C, Ramos-Morales F, Fedriani C, Bornens M, Rios RM (1999) GMAP-210, A cis-Golgi network-associated protein, is a minus end microtubule-binding protein. J Cell Biol 145: 83-98.

155. Partch CL, Card PB, Amezcua CA, Gardner KH (2009) Molecular basis of coiled coil coactivator recruitment by the aryl hydrocarbon receptor nuclear translocator (ARNT). J Biol Chem 284: 15184-15192.

156. Friend SH, Bernards R, Rogelj S, Weinberg RA, Rapaport JM, et al. (1986) A human DNA segment with properties of the gene that predisposes to retinoblastoma and osteosarcoma. Nature 323: 643-646.

157. Zhu L, van den Heuvel S, Helin K, Fattaey A, Ewen M, et al. (1993) Inhibition of cell proliferation by p107, a relative of the retinoblastoma protein. Genes Dev 7: 1111-1125.

158. Classon M, Salama S, Gorka C, Mulloy R, Braun P, et al. (2000) Combinatorial roles for pRB, p107, and p130 in E2F-mediated cell cycle control. Proc Natl Acad Sci U S A 97: 10820-10825.

159. Smith EJ, Leone G, DeGregori J, Jakoi L, Nevins JR (1996) The accumulation of an E2F-p130 transcriptional repressor distinguishes a G0 cell state from a G1 cell state. Mol Cell Biol 16: 6965-6976.

160. Wirt SE, Sage J (2010) p107 in the public eye: an Rb understudy and more. Cell Div 5: 9.

161. Giacinti C, Giordano A (2006) RB and cell cycle progression. Oncogene 25: 5220-5227.

162. Dyson N (1998) The regulation of E2F by pRB-family proteins. Genes Dev 12: 2245-2262.

163. Lee JO, Russo AA, Pavletich NP (1998) Structure of the retinoblastoma tumour-suppressor pocket domain bound to a peptide from HPV E7. Nature 391: 859-865.

164. Balog ER, Burke JR, Hura GL, Rubin SM (2011) Crystal structure of the unliganded retinoblastoma protein pocket domain. Proteins 79: 2010-2014.

165. Xiao B, Spencer J, Clements A, Ali-Khan N, Mittnacht S, et al. (2003) Crystal structure of the retinoblastoma tumor suppressor protein bound to E2F and the molecular basis of its regulation. Proc Natl Acad Sci U S A 100: 2363-2368.

166. Hassler M, Singh S, Yue WW, Luczynski M, Lakbir R, et al. (2007) Crystal structure of the retinoblastoma protein N domain provides insight into tumor suppression, ligand interaction, and holoprotein architecture. Mol Cell 28: 371-385.

167. Ahlander J, Chen XB, Bosco G (2008) The N-terminal domain of the Drosophila retinoblastoma protein Rbf1 interacts with ORC and associates with chromatin in an E2F independent manner. PLoS One 3: e2831.

168. Rubin SM, Gall AL, Zheng N, Pavletich NP (2005) Structure of the Rb C-terminal domain bound to E2F1-DP1: a mechanism for phosphorylation-induced E2F release. Cell 123: 1093-1106.

169. Rubin SM (2013) Deciphering the retinoblastoma protein phosphorylation code. Trends Biochem Sci 38: 12-19.

170. Hochegger H, Takeda S, Hunt T (2008) Cyclin-dependent kinases and cell-cycle transitions: does one fit all? Nat Rev Mol Cell Biol 9: 910-916.

171. Berthet C, Aleem E, Coppola V, Tessarollo L, Kaldis P (2003) Cdk2 knockout mice are viable. Curr Biol 13: 1775-1785.

172. Rane SG, Dubus P, Mettus RV, Galbreath EJ, Boden G, et al. (1999) Loss of Cdk4 expression causes insulin-deficient diabetes and Cdk4 activation results in beta-islet cell hyperplasia. Nat Genet 22: 44-52.

173. Ye X, Zhu C, Harper JW (2001) A premature-termination mutation in the Mus musculus cyclin-dependent kinase 3 gene. Proc Natl Acad Sci U S A 98: 1682-1686.

174. Hu MG, Deshpande A, Enos M, Mao D, Hinds EA, et al. (2009) A requirement for cyclin-dependent kinase 6 in thymocyte development and tumorigenesis. Cancer Res 69: 810-818.

175. Adhikari D, Zheng W, Shen Y, Gorre N, Ning Y, et al. (2012) Cdk1, but not Cdk2, is the sole Cdk that is essential and sufficient to drive resumption of meiosis in mouse oocytes. Hum Mol Genet 21: 2476-2484.

176. Santamaria D, Barriere C, Cerqueira A, Hunt S, Tardy C, et al. (2007) Cdk1 is sufficient to drive the mammalian cell cycle. Nature 448: 811-815.

177. Kozar K, Ciemerych MA, Rebel VI, Shigematsu H, Zagozdzon A, et al. (2004) Mouse development and cell proliferation in the absence of D-cyclins. Cell 118: 477-491.

178. Brandeis M, Rosewell I, Carrington M, Crompton T, Jacobs MA, et al. (1998) Cyclin B2-null mice develop normally and are fertile whereas cyclin B1-null mice die in utero. Proc Natl Acad Sci U S A 95: 4344-4349.

179. Balmanno K, Cook SJ (1999) Sustained MAP kinase activation is required for the expression of cyclin D1, p21Cip1 and a subset of AP-1 proteins in CCL39 cells. Oncogene 18: 3085-3097.

180. Densham RM, Todd DE, Balmanno K, Cook SJ (2008) ERK1/2 and p38 cooperate to delay progression through G1 by promoting cyclin D1 protein turnover. Cell Signal 20: 1986-1994.

181. Clurman BE, Sheaff RJ, Thress K, Groudine M, Roberts JM (1996) Turnover of cyclin E by the ubiquitin-proteasome pathway is regulated by cdk2 binding and cyclin phosphorylation. Genes Dev 10: 1979-1990.

182. Connell-Crowley L, Harper JW, Goodrich DW (1997) Cyclin D1/Cdk4 regulates retinoblastoma protein-mediated cell cycle arrest by site-specific phosphorylation. Mol Biol Cell 8: 287-301.

183. Lundberg AS, Weinberg RA (1998) Functional inactivation of the retinoblastoma protein requires sequential modification by at least two distinct cyclin-cdk complexes. Mol Cell Biol 18: 753-761.

184. Cobrinik D (2005) Pocket proteins and cell cycle control. Oncogene 24: 2796-2809.

185. Chellappan SP, Hiebert S, Mudryj M, Horowitz JM, Nevins JR (1991) The E2F transcription factor is a cellular target for the RB protein. Cell 65: 1053-1061.

186. Nevins JR, Chellappan SP, Mudryj M, Hiebert S, Devoto S, et al. (1991) E2F transcription factor is a target for the RB protein and the cyclin A protein. Cold Spring Harb Symp Quant Biol 56: 157-162.

187. Dick FA, Rubin SM (2013) Molecular mechanisms underlying RB protein function. Nat Rev Mol Cell Biol 14: 297-306.

188. Lees JA, Buchkovich KJ, Marshak DR, Anderson CW, Harlow E (1991) The retinoblastoma protein is phosphorylated on multiple sites by human cdc2. EMBO J 10: 4279-4290.

189. Burke JR, Deshong AJ, Pelton JG, Rubin SM (2010) Phosphorylation-induced conformational changes in the retinoblastoma protein inhibit E2F transactivation domain binding. J Biol Chem 285: 16286-16293.

190. Kitagawa M, Higashi H, Jung HK, Suzuki-Takahashi I, Ikeda M, et al. (1996) The consensus motif for phosphorylation by cyclin D1-Cdk4 is different from that for phosphorylation by cyclin A/E-Cdk2. EMBO J 15: 7060-7069.

191. Harbour JW, Luo RX, Dei Santi A, Postigo AA, Dean DC (1999) Cdk phosphorylation triggers sequential intramolecular interactions that progressively block Rb functions as cells move through G1. Cell 98: 859-869.

192. Knudsen ES, Knudsen KE (2008) Tailoring to RB: tumour suppressor status and therapeutic response. Nat Rev Cancer 8: 714-724.

193. Pediconi N, Ianari A, Costanzo A, Belloni L, Gallo R, et al. (2003) Differential regulation of E2F1 apoptotic target genes in response to DNA damage. Nat Cell Biol 5: 552-558.

194. Qin XQ, Livingston DM, Kaelin WG, Jr., Adams PD (1994) Deregulated transcription factor E2F-1 expression leads to S-phase entry and p53-mediated apoptosis. Proc Natl Acad Sci U S A 91: 10918-10922.

195. Bates S, Phillips AC, Clark PA, Stott F, Peters G, et al. (1998) p14ARF links the tumour suppressors RB and p53. Nature 395: 124-125.

196. Hsieh JK, Fredersdorf S, Kouzarides T, Martin K, Lu X (1997) E2F1-induced apoptosis requires DNA binding but not transactivation and is inhibited by the retinoblastoma protein through direct interaction. Genes Dev 11: 1840-1852.

197. Ianari A, Natale T, Calo E, Ferretti E, Alesse E, et al. (2009) Proapoptotic function of the retinoblastoma tumor suppressor protein. Cancer Cell 15: 184-194.

198. Hilgendorf KI, Leshchiner ES, Nedelcu S, Maynard MA, Calo E, et al. (2013) The retinoblastoma protein induces apoptosis directly at the mitochondria. Genes Dev 27: 1003-1015.

199. Fulda S, Debatin KM (2006) Extrinsic versus intrinsic apoptosis pathways in anticancer chemotherapy. Oncogene 25: 4798-4811.

200. Cook R, Zoumpoulidou G, Luczynski MT, Rieger S, Moquet J, et al. (2015) Direct involvement of retinoblastoma family proteins in DNA repair by non-homologous end-joining. Cell Rep 10: 2006-2018.

201. Herschkowitz JI, He X, Fan C, Perou CM (2008) The functional loss of the retinoblastoma tumour suppressor is a common event in basal-like and luminal B breast carcinomas. Breast Cancer Res 10: R75.

202. Sharma A, Yeow WS, Ertel A, Coleman I, Clegg N, et al. (2010) The retinoblastoma tumor suppressor controls androgen signaling and human prostate cancer progression. J Clin Invest 120: 4478-4492.

203. Nevins JR (2001) The Rb/E2F pathway and cancer. Hum Mol Genet 10: 699-703.

204. Sun H, Wang Y, Chinnam M, Zhang X, Hayward SW, et al. (2011) E2f binding-deficient Rb1 protein suppresses prostate tumor progression in vivo. Proc Natl Acad Sci U S A 108: 704-709.

205. Brat DJ, Castellano-Sanchez A, Kaur B, Van Meir EG (2002) Genetic and biologic progression in astrocytomas and their relation to angiogenic dysregulation. Adv Anat Pathol 9: 24-36.

206. Gabellini C, Del Bufalo D, Zupi G (2006) Involvement of RB gene family in tumor angiogenesis. Oncogene 25: 5326-5332.

207. Canadian Cancer Society's Advisory Committee on Cancer Satistics (2015) Canadian Cancer Statistics 2015. Toronto, ON: Canadian Cancer Society.

208. Humphrey PA (2012) Histological variants of prostatic carcinoma and their significance. Histopathology 60: 59-74.

209. Cancer Genome Atlas Research N (2015) The Molecular Taxonomy of Primary Prostate Cancer. Cell 163: 1011-1025.

210. Yang Q, Fung KM, Day WV, Kropp BP, Lin HK (2005) Androgen receptor signaling is required for androgen-sensitive human prostate cancer cell proliferation and survival. Cancer Cell Int 5: 8.

211. Heinlein CA, Chang C (2004) Androgen receptor in prostate cancer. Endocr Rev 25: 276-308.

212. Abrahamsson PA (1996) Neuroendocrine differentiation and hormone-refractory prostate cancer. Prostate Suppl 6: 3-8.

213. di Sant'Agnese PA (1992) Neuroendocrine differentiation in carcinoma of the prostate. Diagnostic, prognostic, and therapeutic implications. Cancer 70: 254-268.

214. Grigore AD, Ben-Jacob E, Farach-Carson MC (2015) Prostate cancer and neuroendocrine differentiation: more neuronal, less endocrine? Front Oncol 5: 37.

215. Bonkhoff H, Stein U, Remberger K (1993) Androgen receptor status in endocrine-paracrine cell types of the normal, hyperplastic, and neoplastic human prostate. Virchows Arch A Pathol Anat Histopathol 423: 291-294.

216. Bonkhoff H (2001) Neuroendocrine differentiation in human prostate cancer. Morphogenesis, proliferation and androgen receptor status. Ann Oncol 12 Suppl 2: S141-144.

217. McVary KT, McKenna KE, Lee C (1998) Prostate innervation. Prostate Suppl 8: 2-13.

218. Sun Y, Niu J, Huang J (2009) Neuroendocrine differentiation in prostate cancer. Am J Transl Res 1: 148-162.

219. Aparicio A, Logothetis CJ, Maity SN (2011) Understanding the lethal variant of prostate cancer: power of examining extremes. Cancer Discov 1: 466-468.

220. Yuan TC, Veeramani S, Lin MF (2007) Neuroendocrine-like prostate cancer cells: neuroendocrine transdifferentiation of prostate adenocarcinoma cells. Endocr Relat Cancer 14: 531-547.

221. Beltran H, Tomlins S, Aparicio A, Arora V, Rickman D, et al. (2014) Aggressive variants of castration-resistant prostate cancer. Clin Cancer Res 20: 2846-2850.

222. Ito T, Yamamoto S, Ohno Y, Namiki K, Aizawa T, et al. (2001) Up-regulation of neuroendocrine differentiation in prostate cancer after androgen deprivation therapy, degree and androgen independence. Oncol Rep 8: 1221-1224.

223. Huang J, Yao JL, di Sant'Agnese PA, Yang Q, Bourne PA, et al. (2006) Immunohistochemical characterization of neuroendocrine cells in prostate cancer. Prostate 66: 1399-1406.

224. Sauer CG, Roemer A, Grobholz R (2006) Genetic analysis of neuroendocrine tumor cells in prostatic carcinoma. Prostate 66: 227-234.

225. Shen R, Dorai T, Szaboles M, Katz AE, Olsson CA, et al. (1997) Transdifferentiation of cultured human prostate cancer cells to a neuroendocrine cell phenotype in a hormone-depleted medium. Urol Oncol 3: 67-75.

226. Zelivianski S, Verni M, Moore C, Kondrikov D, Taylor R, et al. (2001) Multipathways for transdifferentiation of human prostate cancer cells into neuroendocrine-like phenotype. Biochim Biophys Acta 1539: 28-43.

227. Yuan TC, Veeramani S, Lin FF, Kondrikou D, Zelivianski S, et al. (2006) Androgen deprivation induces human prostate epithelial neuroendocrine differentiation of androgen-sensitive LNCaP cells. Endocr Relat Cancer 13: 151-167.

228. Lin D, Wyatt AW, Xue H, Wang Y, Dong X, et al. (2014) High fidelity patient-derived xenografts for accelerating prostate cancer discovery and drug development. Cancer Res 74: 1272-1283.

229. Karantanos T, Corn PG, Thompson TC (2013) Prostate cancer progression after androgen deprivation therapy: mechanisms of castrate resistance and novel therapeutic approaches. Oncogene 32: 5501-5511.

230. Wang HT, Yao YH, Li BG, Tang Y, Chang JW, et al. (2014) Neuroendocrine Prostate Cancer (NEPC) progressing from conventional prostatic adenocarcinoma: factors associated with time to development of NEPC and survival from NEPC diagnosis-a systematic review and pooled analysis. J Clin Oncol 32: 3383-3390.

231. Scher HI, Sawyers CL (2005) Biology of progressive, castration-resistant prostate cancer: directed therapies targeting the androgen-receptor signaling axis. J Clin Oncol 23: 8253-8261.

232. Tagawa ST (2014) Neuroendocrine prostate cancer after hormonal therapy: knowing is half the battle. J Clin Oncol 32: 3360-3364.

233. Tomlins SA, Rhodes DR, Perner S, Dhanasekaran SM, Mehra R, et al. (2005) Recurrent fusion of TMPRSS2 and ETS transcription factor genes in prostate cancer. Science 310: 644-648.

234. Williamson SR, Zhang S, Yao JL, Huang J, Lopez-Beltran A, et al. (2011) ERG-TMPRSS2 rearrangement is shared by concurrent prostatic adenocarcinoma and prostatic small cell carcinoma and absent in small cell carcinoma of the urinary bladder: evidence supporting monoclonal origin. Mod Pathol 24: 1120-1127.

235. van Steenbrugge GJ, van Uffelen CJ, Bolt J, Schroder FH (1991) The human prostatic cancer cell line LNCaP and its derived sublines: an in vitro model for the study of androgen sensitivity. J Steroid Biochem Mol Biol 40: 207-214.

236. Burchardt T, Burchardt M, Chen MW, Cao Y, de la Taille A, et al. (1999) Transdifferentiation of prostate cancer cells to a neuroendocrine cell phenotype in vitro and in vivo. J Urol 162: 1800-1805.

237. Macleod KF The RB tumor suppressor: a gatekeeper to hormone independence in prostate cancer? J Clin Invest 120: 4179-4182.

238. Tricoli JV, Gumerlock PH, Yao JL, Chi SG, D'Souza SA, et al. (1996) Alterations of the retinoblastoma gene in human prostate adenocarcinoma. Genes Chromosomes Cancer 15: 108-114.

239. Tan HL, Sood A, Rahimi HA, Wang W, Gupta N, et al. (2014) Rb loss is characteristic of prostatic small cell neuroendocrine carcinoma. Clin Cancer Res 20: 890-903.

240. Parisi T, Bronson RT, Lees JA (2015) Inactivation of the retinoblastoma gene yields a mouse model of malignant colorectal cancer. Oncogene.

241. Zhou Z, Flesken-Nikitin A, Corney DC, Wang W, Goodrich DW, et al. (2006) Synergy of p53 and Rb deficiency in a conditional mouse model for metastatic prostate cancer. Cancer Res 66: 7889-7898.

242. Chiaverotti T, Couto SS, Donjacour A, Mao JH, Nagase H, et al. (2008) Dissociation of epithelial and neuroendocrine carcinoma lineages in the transgenic adenocarcinoma of mouse prostate model of prostate cancer. Am J Pathol 172: 236-246.

243. Sorlie T, Tibshirani R, Parker J, Hastie T, Marron JS, et al. (2003) Repeated observation of breast tumor subtypes in independent gene expression data sets. Proc Natl Acad Sci U S A 100: 8418-8423.

244. Foulkes WD, Stefansson IM, Chappuis PO, Begin LR, Goffin JR, et al. (2003) Germline BRCA1 mutations and a basal epithelial phenotype in breast cancer. J Natl Cancer Inst 95: 1482-1485.

245. Saal LH, Gruvberger-Saal SK, Persson C, Lovgren K, Jumppanen M, et al. (2008) Recurrent gross mutations of the PTEN tumor suppressor gene in breast cancers with deficient DSB repair. Nat Genet 40: 102-107.

246. Turner NC, Reis-Filho JS, Russell AM, Springall RJ, Ryder K, et al. (2007) BRCA1 dysfunction in sporadic basal-like breast cancer. Oncogene 26: 2126-2132.

247. Ertel A, Dean JL, Rui H, Liu C, Witkiewicz AK, et al. (2010) RB-pathway disruption in breast cancer: differential association with disease subtypes,

disease-specific prognosis and therapeutic response. Cell Cycle 9: 4153-4163.

248. Nik-Zainal S, Davies H, Staaf J, Ramakrishna M, Glodzik D, et al. (2016) Landscape of somatic mutations in 560 breast cancer whole-genome sequences. Nature 534: 47-54.

249. Sasich LD, Sukkari SR (2012) The US FDAs withdrawal of the breast cancer indication for Avastin (bevacizumab). Saudi Pharm J 20: 381-385.

250. Gilkes DM, Bajpai S, Wong CC, Chaturvedi P, Hubbi ME, et al. Procollagen lysyl hydroxylase 2 is essential for hypoxia-induced breast cancer metastasis. Mol Cancer Res 11: 456-466.

251. Liu YL, Yu JM, Song XR, Wang XW, Xing LG, et al. (2006) Regulation of the chemokine receptor CXCR4 and metastasis by hypoxia-inducible factor in non small cell lung cancer cell lines. Cancer Biol Ther 5: 1320-1326.

252. Elizondo G, Fernandez-Salguero P, Sheikh MS, Kim GY, Fornace AJ, et al. (2000) Altered cell cycle control at the G(2)/M phases in aryl hydrocarbon receptor-null embryo fibroblast. Mol Pharmacol 57: 1056-1063.

253. Fernandez-Salguero P, Pineau T, Hilbert DM, McPhail T, Lee SS, et al. (1995) Immune system impairment and hepatic fibrosis in mice lacking the dioxin-binding Ah receptor. Science 268: 722-726.

254. Alexander DL, Ganem LG, Fernandez-Salguero P, Gonzalez F, Jefcoate CR (1998) Aryl-hydrocarbon receptor is an inhibitory regulator of lipid synthesis and of commitment to adipogenesis. J Cell Sci 111 (Pt 22): 3311-3322.

255. Kimura A, Naka T, Nohara K, Fujii-Kuriyama Y, Kishimoto T (2008) Aryl hydrocarbon receptor regulates Stat1 activation and participates in the development of Th17 cells. Proc Natl Acad Sci U S A 105: 9721-9726.

256. Hollingshead BD, Beischlag TV, Dinatale BC, Ramadoss P, Perdew GH (2008) Inflammatory signaling and aryl hydrocarbon receptor mediate synergistic induction of interleukin 6 in MCF-7 cells. Cancer Res 68: 3609-3617.

257. Kumar MB, Perdew GH (1999) Nuclear receptor coactivator SRC-1 interacts with the Q-rich subdomain of the AhR and modulates its transactivation potential. Gene Expr 8: 273-286.

258. Kim JH, Stallcup MR (2004) Role of the coiled-coil coactivator (CoCoA) in aryl hydrocarbon receptor-mediated transcription. J Biol Chem 279: 49842-49848.

259. Chen YH, Beischlag TV, Kim JH, Perdew GH, Stallcup MR (2006) Role of GAC63 in transcriptional activation mediated by the aryl hydrocarbon receptor. J Biol Chem 281: 12242-12247.

260. Kollara A, Brown TJ (2006) Functional interaction of nuclear receptor coactivator 4 with aryl hydrocarbon receptor. Biochem Biophys Res Commun 346: 526-534.

261. Matthews J, Wihlen B, Thomsen J, Gustafsson JA (2005) Aryl Hydrocarbon Receptor-Mediated Transcription: Ligand-Dependent Recruitment of Estrogen Receptor {alpha} to 2,3,7,8-Tetrachlorodibenzo- p-Dioxin-Responsive Promoters. Mol Cell Biol 25: 5317-5328.

262. Tian Y, Ke S, Denison MS, Rabson AB, Gallo MA (1999) Ah receptor and NF-kappaB interactions, a potential mechanism for dioxin toxicity. J Biol Chem 274: 510-515.

263. Mangelsdorf DJ, Thummel C, Beato M, Herrlich P, Schutz G, et al. (1995) The nuclear receptor superfamily: the second decade. Cell 83: 835-839.

264. Acconcia F, Kumar R (2006) Signaling regulation of genomic and nongenomic functions of estrogen receptors. Cancer Lett 238: 1-14.

265. Biegel L, Safe S (1990) Effects of 2,3,7,8-tetrachlorodibenzo-p-dioxin (TCDD) on cell growth and the secretion of the estrogen-induced 34-, 52- and 160-kDa proteins in human breast cancer cells. J Steroid Biochem Mol Biol 37: 725-732.

266. Kharat I, Saatcioglu F (1996) Antiestrogenic effects of 2,3,7,8-tetrachlorodibenzo-p-dioxin are mediated by direct transcriptional interference with the liganded estrogen receptor. Cross-talk between aryl hydrocarbon- and estrogen-mediated signaling. J Biol Chem 271: 10533-10537.

267. Safe S, Wormke M, Samudio I (2000) Mechanisms of inhibitory aryl hydrocarbon receptor-estrogen receptor crosstalk in human breast cancer cells. J Mammary Gland Biol Neoplasia 5: 295-306.

268. Castro-Rivera E, Wormke M, Safe S (1999) Estrogen and aryl hydrocarbon responsiveness of ECC-1 endometrial cancer cells. Mol Cell Endocrinol 150: 11-21.

269. Ricci MS, Toscano DG, Toscano WA, Jr. (1999) ECC-1 human endometrial cells as a model system to study dioxin disruption of steroid hormone function. In Vitro Cell Dev Biol Anim 35: 183-189.

270. Murray IA, Krishnegowda G, DiNatale BC, Flaveny C, Chiaro C, et al. (2010) Development of a selective modulator of aryl hydrocarbon (Ah) receptor activity that exhibits anti-inflammatory properties. Chem Res Toxicol 23: 955-966.

271. Murray IA, Flaveny CA, Chiaro CR, Sharma AK, Tanos RS, et al. (2011) Suppression of cytokine-mediated complement factor gene expression through selective activation of the Ah receptor with 3',4'-dimethoxy-alpha-naphthoflavone. Mol Pharmacol 79: 508-519.

272. Vendrell JA, Magnino F, Danis E, Duchesne MJ, Pinloche S, et al. (2004) Estrogen regulation in human breast cancer cells of new downstream gene targets involved in estrogen metabolism, cell proliferation and cell transformation. J Mol Endocrinol 32: 397-414.

273. Astroff B, Rowlands C, Dickerson R, Safe S (1990) 2,3,7,8-Tetrachlorodibenzo-p-dioxin inhibition of 17 beta-estradiol-induced

increases in rat uterine epidermal growth factor receptor binding activity and gene expression. Mol Cell Endocrinol 72: 247-252.

274. Astroff B, Safe S (1988) Comparative antiestrogenic activities of 2,3,7,8-tetrachlorodibenzo-p-dioxin and 6-methyl-1,3,8-trichlorodibenzofuran in the female rat. Toxicol Appl Pharmacol 95: 435-443.

275. Gallo MA, Hesse EJ, Macdonald GJ, Umbreit TH (1986) Interactive effects of estradiol and 2,3,7,8-tetrachlorodibenzo-p-dioxin on hepatic cytochrome P-450 and mouse uterus. Toxicol Lett 32: 123-132.

276. Reyes H, Reisz-Porszasz S, Hankinson O (1992) Identification of the Ah receptor nuclear translocator protein (Arnt) as a component of the DNA binding form of the Ah receptor. Science 256: 1193-1195.

277. Partch CL, Gardner KH (2011) Coactivators necessary for transcriptional output of the hypoxia inducible factor, HIF, are directly recruited by ARNT PAS-B. Proc Natl Acad Sci U S A 108: 7739-7744.

278. Nguyen TA, Hoivik D, Lee JE, Safe S (1999) Interactions of nuclear receptor coactivator/corepressor proteins with the aryl hydrocarbon receptor complex. Arch Biochem Biophys 367: 250-257.

279. Arany Z, Huang LE, Eckner R, Bhattacharya S, Jiang C, et al. (1996) An essential role for p300/CBP in the cellular response to hypoxia. Proc Natl Acad Sci U S A 93: 12969-12973.

280. Boitano AE, Wang J, Romeo R, Bouchez LC, Parker AE, et al. (2010) Aryl hydrocarbon receptor antagonists promote the expansion of human hematopoietic stem cells. Science 329: 1345-1348.

281. DiNatale BC, Schroeder JC, Francey LJ, Kusnadi A, Perdew GH (2010) Mechanistic insights into the events that lead to synergistic induction of interleukin 6 transcription upon activation of the aryl hydrocarbon receptor and inflammatory signaling. J Biol Chem 285: 24388-24397.

282. Hestermann EV, Brown M (2003) Agonist and chemopreventative ligands induce differential transcriptional cofactor recruitment by aryl hydrocarbon receptor. Mol Cell Biol 23: 7920-7925.

283. Labrecque MP, Prefontaine GG, Beischlag TV (2013) The Aryl Hydrocarbon Receptor Nuclear Translocator (ARNT) Family of Proteins: Transcriptional Modifiers with Multi-Functional Protein Interfaces. Current molecular medicine 13: 1047-1065.

284. Wang F, Zhang R, Beischlag TV, Muchardt C, Yaniv M, et al. (2004) Roles of Brahma and Brahma/SWI2-related gene 1 in hypoxic induction of the erythropoietin gene. J Biol Chem 279: 46733-46741.

285. Staller P, Sulitkova J, Lisztwan J, Moch H, Oakeley EJ, et al. (2003) Chemokine receptor CXCR4 downregulated by von Hippel-Lindau tumour suppressor pVHL. Nature 425: 307-311.

286. Gilkes DM, Bajpai S, Wong CC, Chaturvedi P, Hubbi ME, et al. (2013) Procollagen lysyl hydroxylase 2 is essential for hypoxia-induced breast cancer metastasis. Molecular cancer research : MCR 11: 456-466.

287. Eisinger-Mathason TS, Simon MC (2010) HIF-1alpha partners with FoxA2, a neuroendocrine-specific transcription factor, to promote tumorigenesis. Cancer Cell 18: 3-4.

288. Simon MC, Keith B (2008) The role of oxygen availability in embryonic development and stem cell function. Nat Rev Mol Cell Biol 9: 285-296.

289. Gordan JD, Lal P, Dondeti VR, Letrero R, Parekh KN, et al. (2008) HIF-alpha effects on c-Myc distinguish two subtypes of sporadic VHL-deficient clear cell renal carcinoma. Cancer Cell 14: 435-446.

290. Lee JH, Suk J, Park J, Kim SB, Kwak SS, et al. (2009) Notch signal activates hypoxia pathway through HES1-dependent SRC/signal transducers and activators of transcription 3 pathway. Mol Cancer Res 7: 1663-1671.

291. Qi J, Nakayama K, Cardiff RD, Borowsky AD, Kaul K, et al. (2010) Siah2-dependent concerted activity of HIF and FoxA2 regulates formation of neuroendocrine phenotype and neuroendocrine prostate tumors. Cancer Cell 18: 23-38.

292. Lee JW, Choi HS, Gyuris J, Brent R, Moore DD (1995) Two classes of proteins dependent on either the presence or absence of thyroid hormone for interaction with the thyroid hormone receptor. Mol Endocrinol 9: 243-254.

293. Jung SY, Malovannaya A, Wei J, O'Malley BW, Qin J (2005) Proteomic analysis of steady-state nuclear hormone receptor coactivator complexes. Mol Endocrinol 19: 2451-2465.

294. Scambia G, Lovergine S, Masciullo V (2006) RB family members as predictive and prognostic factors in human cancer. Oncogene 25: 5302-5308.

295. Simin K, Wu H, Lu L, Pinkel D, Albertson D, et al. (2004) pRb inactivation in mammary cells reveals common mechanisms for tumor initiation and progression in divergent epithelia. PLoS Biol 2: E22.

296. Yokota J, Nishioka M, Tani M, Kohno T (2003) Genetic alterations responsible for metastatic phenotypes of lung cancer cells. Clin Exp Metastasis 20: 189-193.

297. Du W, Pogoriler J (2006) Retinoblastoma family genes. Oncogene 25: 5190-5200.

298. Grandinetti KB, David G (2008) Sin3B: an essential regulator of chromatin modifications at E2F target promoters during cell cycle withdrawal. Cell Cycle 7: 1550-1554.

299. Lai A, Kennedy BK, Barbie DA, Bertos NR, Yang XJ, et al. (2001) RBP1 recruits the mSIN3-histone deacetylase complex to the pocket of retinoblastoma tumor suppressor family proteins found in limited discrete regions of the nucleus at growth arrest. Mol Cell Biol 21: 2918-2932.

300. Lai A, Lee JM, Yang WM, DeCaprio JA, Kaelin WG, Jr., et al. (1999) RBP1 recruits both histone deacetylase-dependent and -independent repression activities to retinoblastoma family proteins. Mol Cell Biol 19: 6632-6641.

301. Dick FA, Rubin SM (2013) Molecular mechanisms underlying RB protein function. Nature reviews Molecular cell biology 14: 297-306.

302. Zia MK, Rmali KA, Watkins G, Mansel RE, Jiang WG (2007) The expression of the von Hippel-Lindau gene product and its impact on invasiveness of human breast cancer cells. Int J Mol Med 20: 605-611.

303. Elferink CJ, Ge NL, Levine A (2001) Maximal aryl hydrocarbon receptor activity depends on an interaction with the retinoblastoma protein. Mol Pharmacol 59: 664-673.

304. Partch CL, Card PB, Amezcua CA, Gardner KH (2009) Molecular basis of coiled coil coactivator recruitment by the aryl hydrocarbon receptor nuclear translocator (ARNT). The Journal of biological chemistry 284: 15184-15192.

305. Nishikawa R, Furnari FB, Lin H, Arap W, Berger MS, et al. (1995) Loss of P16INK4 expression is frequent in high grade gliomas. Cancer Res 55: 1941-1945.

306. Schmidt EE, Ichimura K, Reifenberger G, Collins VP (1994) CDKN2 (p16/MTS1) gene deletion or CDK4 amplification occurs in the majority of glioblastomas. Cancer Res 54: 6321-6324.

307. Bookstein R, Rio P, Madreperla SA, Hong F, Allred C, et al. (1990) Promoter deletion and loss of retinoblastoma gene expression in human prostate carcinoma. Proceedings of the National Academy of Sciences of the United States of America 87: 7762-7766.

308. Tricoli JV, Gumerlock PH, Yao JL, Chi SG, D'Souza SA, et al. (1996) Alterations of the retinoblastoma gene in human prostate adenocarcinoma. Genes, chromosomes & cancer 15: 108-114.

309. Bachelder RE, Wendt MA, Mercurio AM (2002) Vascular endothelial growth factor promotes breast carcinoma invasion in an autocrine manner by regulating the chemokine receptor CXCR4. Cancer research 62: 7203-7206.

310. Helbig G, Christopherson KW, 2nd, Bhat-Nakshatri P, Kumar S, Kishimoto H, et al. (2003) NF-kappaB promotes breast cancer cell migration and metastasis by inducing the expression of the chemokine receptor CXCR4. The Journal of biological chemistry 278: 21631-21638.

311. Sun X, Cheng G, Hao M, Zheng J, Zhou X, et al. (2010) CXCL12 / CXCR4 / CXCR7 chemokine axis and cancer progression. Cancer Metastasis Rev 29: 709-722.

312. Gilkes DM, Chaturvedi P, Bajpai S, Wong CC, Wei H, et al. (2013) Collagen prolyl hydroxylases are essential for breast cancer metastasis. Cancer research 73: 3285-3296.

313. Gilkes DM, Bajpai S, Chaturvedi P, Wirtz D, Semenza GL (2013) Hypoxia-inducible factor 1 (HIF-1) promotes extracellular matrix remodeling under hypoxic conditions by inducing P4HA1, P4HA2, and PLOD2 expression in fibroblasts. The Journal of biological chemistry 288: 10819-10829.

314. Jeon HW, Lee YM (2010) Inhibition of histone deacetylase attenuates hypoxia-induced migration and invasion of cancer cells via the restoration of RECK expression. Mol Cancer Ther 9: 1361-1370.

315. Kato H, Tamamizu-Kato S, Shibasaki F (2004) Histone deacetylase 7 associates with hypoxia-inducible factor 1alpha and increases transcriptional activity. J Biol Chem 279: 41966-41974.

316. Qian DZ, Kachhap SK, Collis SJ, Verheul HM, Carducci MA, et al. (2006) Class II histone deacetylases are associated with VHL-independent regulation of hypoxia-inducible factor 1 alpha. Cancer Res 66: 8814-8821.

317. Rubin SM (2013) Deciphering the retinoblastoma protein phosphorylation code. Trends in biochemical sciences 38: 12-19.

318. Langer R, Conn H, Vacanti J, Haudenschild C, Folkman J (1980) Control of tumor growth in animals by infusion of an angiogenesis inhibitor. Proc Natl Acad Sci U S A 77: 4331-4335.

319. Traina TA (2009) Bevacizumab in the treatment of metastatic breast cancer. Oncology (Williston Park) 23: 327-332.

320. Honey K (2009) Good and bad news for an antiangiogenic. Journal of Clinical Investigation Investigation 119: 1400.

321. Ebos JM, Lee CR, Cruz-Munoz W, Bjarnason GA, Christensen JG, et al. (2009) Accelerated metastasis after short-term treatment with a potent inhibitor of tumor angiogenesis. Cancer Cell 15: 232-239.

322. Imai T, Horiuchi A, Wang C, Oka K, Ohira S, et al. (2003) Hypoxia attenuates the expression of E-cadherin via up-regulation of SNAIL in ovarian carcinoma cells. Am J Pathol 163: 1437-1447.

323. Prefontaine GG, Lemieux ME, Giffin W, Schild-Poulter C, Pope L, et al. (1998) Recruitment of octamer transcription factors to DNA by glucocorticoid receptor. Mol Cell Biol 18: 3416-3430.

324. Chen C, Pore N, Behrooz A, Ismail-Beigi F, Maity A (2001) Regulation of glut1 mRNA by hypoxia-inducible factor-1. Interaction between H-ras and hypoxia. J Biol Chem 276: 9519-9525.

325. Zagzag D, Lukyanov Y, Lan L, Ali MA, Esencay M, et al. (2006) Hypoxia-inducible factor 1 and VEGF upregulate CXCR4 in glioblastoma: implications for angiogenesis and glioma cell invasion. Lab Invest 86: 1221-1232.

326. Gilkes DM, Bajpai S, Chaturvedi P, Wirtz D, Semenza GL (2013) Hypoxia-inducible factor 1 (HIF-1) promotes extracellular matrix remodeling under hypoxic conditions by inducing P4HA1, P4HA2, and PLOD2 expression in fibroblasts. J Biol Chem 288: 10819-10829.

327. Labrecque MP, Takhar MK, Jagdeo JM, Tam KJ, Chiu C, et al. (2014) A TRIP230-retinoblastoma protein complex regulates hypoxia-inducible factor-1alpha-mediated transcription and cancer cell invasion. PLoS One 9: e99214.

328. Theodorescu D, Broder SR, Boyd JC, Mills SE, Frierson HF, Jr. (1997) p53, bcl-2 and retinoblastoma proteins as long-term prognostic markers in localized carcinoma of the prostate. J Urol 158: 131-137.

329. Ghafar MA, Anastasiadis AG, Chen MW, Burchardt M, Olsson LE, et al. (2003) Acute hypoxia increases the aggressive characteristics and survival properties of prostate cancer cells. Prostate 54: 58-67.

330. Yamasaki M, Nomura T, Sato F, Mimata H (2013) Chronic hypoxia induces androgen-independent and invasive behavior in LNCaP human prostate cancer cells. Urol Oncol 31: 1124-1131.

331. Fiorentino FP, Marchesi I, Giordano A (2013) On the role of retinoblastoma family proteins in the establishment and maintenance of the epigenetic landscape. J Cell Physiol 228: 276-284.

332. Nielsen SJ, Schneider R, Bauer UM, Bannister AJ, Morrison A, et al. (2001) Rb targets histone H3 methylation and HP1 to promoters. Nature 412: 561-565.

333. Brehm A, Miska EA, McCance DJ, Reid JL, Bannister AJ, et al. (1998) Retinoblastoma protein recruits histone deacetylase to repress transcription. Nature 391: 597-601.

334. Robertson KD, Ait-Si-Ali S, Yokochi T, Wade PA, Jones PL, et al. (2000) DNMT1 forms a complex with Rb, E2F1 and HDAC1 and represses transcription from E2F-responsive promoters. Nat Genet 25: 338-342.

335. Massah S, Hollebakken R, Labrecque MP, Kolybaba AM, Beischlag TV, et al. (2014) Epigenetic characterization of the growth hormone gene identifies SmcHD1 as a regulator of autosomal gene clusters. PLoS One 9: e97535.

336. Fullwood MJ, Liu MH, Pan YF, Liu J, Xu H, et al. (2009) An oestrogen-receptor-alpha-bound human chromatin interactome. Nature 462: 58-64.

337. Handoko L, Xu H, Li G, Ngan CY, Chew E, et al. (2011) CTCF-mediated functional chromatin interactome in pluripotent cells. Nat Genet 43: 630-638.

338. Nichols DE, Nichols CD (2008) Serotonin receptors. Chem Rev 108: 1614-1641.

339. Acevedo N, Saaf A, Soderhall C, Melen E, Mandelin J, et al. Interaction between retinoid acid receptor-related orphan receptor alpha (RORA) and neuropeptide S receptor 1 (NPSR1) in asthma. PLoS One 8: e60111.

340. Noel SD, Kaiser UB G protein-coupled receptors involved in GnRH regulation: molecular insights from human disease. Mol Cell Endocrinol 346: 91-101.

341. Inagaki H, Eimoto T, Haimoto H, Hosoda S, Kato K (1993) Aldolase C in neuroendocrine tumors: an immunohistochemical study. Virchows Arch B Cell Pathol Incl Mol Pathol 64: 297-302.

342. Clegg N, Ferguson C, True LD, Arnold H, Moorman A, et al. (2003) Molecular characterization of prostatic small-cell neuroendocrine carcinoma. Prostate 55: 55-64.

343. Tian L, Zhou J, Casimiro MC, Liang B, Ojeifo JO, et al. (2009) Activating peroxisome proliferator-activated receptor gamma mutant promotes tumor growth in vivo by enhancing angiogenesis. Cancer Res 69: 9236-9244.

344. Nishio S, Ushijima K, Tsuda N, Takemoto S, Kawano K, et al. (2008) Cap43/NDRG1/Drg-1 is a molecular target for angiogenesis and a prognostic indicator in cervical adenocarcinoma. Cancer Lett 264: 36-43.

345. Pena C, Cespedes MV, Lindh MB, Kiflemariam S, Mezheyeuski A, et al. STC1 expression by cancer-associated fibroblasts drives metastasis of colorectal cancer. Cancer Res 73: 1287-1297.

346. Cangul H (2004) Hypoxia upregulates the expression of the NDRG1 gene leading to its overexpression in various human cancers. BMC Genet 5: 27.

347. Law AY, Ching LY, Lai KP, Wong CK (2010) Identification and characterization of the hypoxia-responsive element in human stanniocalcin-1 gene. Mol Cell Endocrinol 314: 118-127.

348. Li H, Ge C, Zhao F, Yan M, Hu C, et al. (2011) Hypoxia-inducible factor 1 alpha-activated angiopoietin-like protein 4 contributes to tumor metastasis via vascular cell adhesion molecule-1/integrin beta1 signaling in human hepatocellular carcinoma. Hepatology 54: 910-919.

349. Miki N, Ikuta M, Matsui T (2004) Hypoxia-induced activation of the retinoic acid receptor-related orphan receptor alpha4 gene by an interaction between hypoxia-inducible factor-1 and Sp1. J Biol Chem 279: 15025-15031.

350. Minchenko OH, Opentanova IL, Ogura T, Minchenko DO, Komisarenko SV, et al. (2005) Expression and hypoxia-responsiveness of 6-phosphofructo-2-kinase/fructose-2,6-bisphosphatase 4 in mammary gland malignant cell lines. Acta Biochim Pol 52: 881-888.

351. Mole DR, Blancher C, Copley RR, Pollard PJ, Gleadle JM, et al. (2009) Genome-wide association of hypoxia-inducible factor (HIF)-1alpha and HIF-2alpha DNA binding with expression profiling of hypoxia-inducible transcripts. J Biol Chem 284: 16767-16775.

352. Schioppa T, Uranchimeg B, Saccani A, Biswas SK, Doni A, et al. (2003) Regulation of the chemokine receptor CXCR4 by hypoxia. J Exp Med 198: 1391-1402.

353. Schodel J, Oikonomopoulos S, Ragoussis J, Pugh CW, Ratcliffe PJ, et al. (2011) High-resolution genome-wide mapping of HIF-binding sites by ChIP-seq. Blood 117: e207-217.

354. Ullah MS, Davies AJ, Halestrap AP (2006) The plasma membrane lactate transporter MCT4, but not MCT1, is up-regulated by hypoxia through a HIF-1alpha-dependent mechanism. J Biol Chem 281: 9030-9037.

355. Wang Q, Li LH, Gao GD, Wang G, Qu L, et al. (2013) HIF-1alpha up-regulates NDRG1 expression through binding to NDRG1 promoter, leading to proliferation of lung cancer A549 cells. Mol Biol Rep 40: 3723-3729.

356. Wang V, Davis DA, Haque M, Huang LE, Yarchoan R (2005) Differential gene up-regulation by hypoxia-inducible factor-1alpha and hypoxia-inducible factor-2alpha in HEK293T cells. Cancer Res 65: 3299-3306.

357. Wykoff CC, Beasley NJ, Watson PH, Turner KJ, Pastorek J, et al. (2000) Hypoxia-inducible expression of tumor-associated carbonic anhydrases. Cancer Res 60: 7075-7083.

358. Mathelier A, Zhao X, Zhang AW, Parcy F, Worsley-Hunt R, et al. (2014) JASPAR 2014: an extensively expanded and updated open-access database of transcription factor binding profiles. Nucleic Acids Res 42: D142-147.

359. Sandelin A, Alkema W, Engstrom P, Wasserman WW, Lenhard B (2004) JASPAR: an open-access database for eukaryotic transcription factor binding profiles. Nucleic Acids Res 32: D91-94.

360. Horoszewicz JS, Leong SS, Kawinski E, Karr JP, Rosenthal H, et al. (1983) LNCaP model of human prostatic carcinoma. Cancer Res 43: 1809-1818.

361. Cho SG, Wang Y, Rodriguez M, Tan K, Zhang W, et al. (2011) Haploinsufficiency in the prometastasis Kiss1 receptor Gpr54 delays breast tumor initiation, progression, and lung metastasis. Cancer Res 71: 6535-6546.

362. Dupre DJ, Hammad MM, Holland P, Wertman J (2012) Role of chaperones in G protein coupled receptor signaling complex assembly. Subcell Biochem 63: 23-42.

363. Tao YX, Conn PM (2014) Chaperoning G protein-coupled receptors: from cell biology to therapeutics. Endocr Rev 35: 602-647.

364. Liao D, Corle C, Seagroves TN, Johnson RS (2007) Hypoxia-inducible factor-1alpha is a key regulator of metastasis in a transgenic model of cancer initiation and progression. Cancer Res 67: 563-572.

365. Geradts J, Kratzke RA, Crush-Stanton S, Wen SF, Lincoln CE (1996) Wild-type and mutant retinoblastoma protein in paraffin sections. Mod Pathol 9: 339-347.

366. Geradts J, Wilson PA (1996) High frequency of aberrant p16(INK4A) expression in human breast cancer. Am J Pathol 149: 15-20.

367. Xia X, Lemieux ME, Li W, Carroll JS, Brown M, et al. (2009) Integrative analysis of HIF binding and transactivation reveals its role in maintaining histone methylation homeostasis. Proc Natl Acad Sci U S A 106: 4260-4265.

368. Beltran H, Rickman DS, Park K, Chae SS, Sboner A, et al. (2011) Molecular characterization of neuroendocrine prostate cancer and identification of new drug targets. Cancer Discov 1: 487-495.

369. Abdul M, Anezinis PE, Logothetis CJ, Hoosein NM (1994) Growth inhibition of human prostatic carcinoma cell lines by serotonin antagonists. Anticancer Res 14: 1215-1220.

370. Ohtaki T, Shintani Y, Honda S, Matsumoto H, Hori A, et al. (2001) Metastasis suppressor gene KiSS-1 encodes peptide ligand of a G-protein-coupled receptor. Nature 411: 613-617.

371. Messager S, Chatzidaki EE, Ma D, Hendrick AG, Zahn D, et al. (2005) Kisspeptin directly stimulates gonadotropin-releasing hormone release via G protein-coupled receptor 54. Proc Natl Acad Sci U S A 102: 1761-1766.

372. Matsui H, Tanaka A, Yokoyama K, Takatsu Y, Ishikawa K, et al. (2012) Chronic administration of the metastin/kisspeptin analog KISS1-305 or the investigational agent TAK-448 suppresses hypothalamic pituitary gonadal function and depletes plasma testosterone in adult male rats. Endocrinology 153: 5297-5308.

373. Seminara SB, Dipietro MJ, Ramaswamy S, Crowley WF, Jr., Plant TM (2006) Continuous human metastin 45-54 infusion desensitizes G protein-coupled receptor 54-induced gonadotropin-releasing hormone release monitored indirectly in the juvenile male Rhesus monkey (Macaca mulatta): a finding with therapeutic implications. Endocrinology 147: 2122-2126.

374. MacLean DB, Matsui H, Suri A, Neuwirth R, Colombel M (2014) Sustained exposure to the investigational Kisspeptin analog, TAK-448, down-regulates testosterone into the castration range in healthy males and in patients with prostate cancer: results from two phase 1 studies. J Clin Endocrinol Metab 99: E1445-1453.

375. Zajac M, Law J, Cvetkovic DD, Pampillo M, McColl L, et al. (2011) GPR54 (KISS1R) transactivates EGFR to promote breast cancer cell invasiveness. PLoS One 6: e21599.

376. Wang H, Jones J, Turner T, He QP, Hardy S, et al. (2012) Clinical and biological significance of KISS1 expression in prostate cancer. Am J Pathol 180: 1170-1178.

377. Huang S, Pettaway CA, Uehara H, Bucana CD, Fidler IJ (2001) Blockade of NF-kappaB activity in human prostate cancer cells is associated with suppression of angiogenesis, invasion, and metastasis. Oncogene 20: 4188-4197.

378. Ismail HA, Lessard L, Mes-Masson AM, Saad F (2004) Expression of NF-kappaB in prostate cancer lymph node metastases. Prostate 58: 308-313.

379. Jin R, Yi Y, Yull FE, Blackwell TS, Clark PE, et al. (2014) NF-kappaB gene signature predicts prostate cancer progression. Cancer Res 74: 2763-2772.

380. Murillo H, Huang H, Schmidt LJ, Smith DI, Tindall DJ (2001) Role of PI3K signaling in survival and progression of LNCaP prostate cancer cells to the androgen refractory state. Endocrinology 142: 4795-4805.

381. Reddy KB, Nabha SM, Atanaskova N (2003) Role of MAP kinase in tumor progression and invasion. Cancer Metastasis Rev 22: 395-403.

382. Bachelder RE, Wendt MA, Mercurio AM (2002) Vascular endothelial growth factor promotes breast carcinoma invasion in an autocrine manner by regulating the chemokine receptor CXCR4. Cancer Res 62: 7203-7206.

383. Ranasinghe WK, Xiao L, Kovac S, Chang M, Michiels C, et al. (2013) The role of hypoxia-inducible factor 1alpha in determining the properties of castrate-resistant prostate cancers. PLoS One 8: e54251.

384. Wang F, Zhang R, Wu X, Hankinson O (2010) Roles of coactivators in hypoxic induction of the erythropoietin gene. PLoS One 5: e10002.

385. Edgar R, Domrachev M, Lash AE (2002) Gene Expression Omnibus: NCBI gene expression and hybridization array data repository. Nucleic Acids Res 30: 207-210.

386. Roodink I, Leenders WP (2010) Targeted therapies of cancer: angiogenesis inhibition seems not enough. Cancer Lett 299: 1-10.

387. Semenza GL (2008) Hypoxia-inducible factor 1 and cancer pathogenesis. IUBMB Life 60: 591-597.

388. Labrecque MP, Takhar MK, Nason R, Santacruz S, Tam KJ, et al. (2016) The retinoblastoma protein regulates hypoxia-inducible genetic programs, tumor cell invasiveness and neuroendocrine differentiation in prostate cancer cells. Oncotarget.

389. Li EY, Huang WY, Chang YC, Tsai MH, Chuang EY, et al. (2016) Aryl Hydrocarbon Receptor Activates NDRG1 Transcription under Hypoxia in Breast Cancer Cells. Sci Rep 6: 20808.

390. Knaup KX, Monti J, Hackenbeck T, Jobst-Schwan T, Klanke B, et al. (2014) Hypoxia regulates the sperm associated antigen 4 (SPAG4) via HIF, which is expressed in renal clear cell carcinoma and promotes migration and invasion in vitro. Mol Carcinog 53: 970-978.

391. Long JS, Fujiwara Y, Edwards J, Tannahill CL, Tigyi G, et al. (2010) Sphingosine 1-phosphate receptor 4 uses HER2 (ERBB2) to regulate extracellular signal regulated kinase-1/2 in MDA-MB-453 breast cancer cells. J Biol Chem 285: 35957-35966.

392. Chang AC, Doherty J, Huschtscha LI, Redvers R, Restall C, et al. (2015) STC1 expression is associated with tumor growth and metastasis in breast cancer. Clin Exp Metastasis 32: 15-27.

393. Li C, Ma H, Wang Y, Cao Z, Graves-Deal R, et al. (2014) Excess PLAC8 promotes an unconventional ERK2-dependent EMT in colon cancer. J Clin Invest 124: 2172-2187.

394. Chakraborty S, Lakshmanan M, Swa HL, Chen J, Zhang X, et al. (2015) An oncogenic role of Agrin in regulating focal adhesion integrity in hepatocellular carcinoma. Nat Commun 6: 6184.

395. Canesin G, Cuevas EP, Santos V, Lopez-Menendez C, Moreno-Bueno G, et al. (2015) Lysyl oxidase-like 2 (LOXL2) and E47 EMT factor: novel partners in E-cadherin repression and early metastasis colonization. Oncogene 34: 951-964.

396. Shafie SM, Grantham FH (1981) Role of hormones in the growth and regression of human breast cancer cells (MCF-7) transplanted into athymic nude mice. J Natl Cancer Inst 67: 51-56.

397. Khakshour S, Beischlag TV, Sparrey C, Park EJ (2015) Probing mechanical properties of Jurkat cells under the effect of ART using oscillating optical tweezers. PLoS One 10: e0126548.

398. Hasan NM, Adams GE, Joiner MC, Marshall JF, Hart IR (1998) Hypoxia facilitates tumour cell detachment by reducing expression of surface adhesion molecules and adhesion to extracellular matrices without loss of cell viability. Br J Cancer 77: 1799-1805.

399. Wesseling J, van der Valk SW, Vos HL, Sonnenberg A, Hilkens J (1995) Episialin (MUC1) overexpression inhibits integrin-mediated cell adhesion to extracellular matrix components. J Cell Biol 129: 255-265.

400. Rosenstiel P, Sina C, End C, Renner M, Lyer S, et al. (2007) Regulation of DMBT1 via NOD2 and TLR4 in intestinal epithelial cells modulates bacterial recognition and invasion. J Immunol 178: 8203-8211.

401. Yu DM, Wang XM, McCaughan GW, Gorrell MD (2006) Extraenzymatic functions of the dipeptidyl peptidase IV-related proteins DP8 and DP9 in cell adhesion, migration and apoptosis. FEBS J 273: 2447-2460.

402. Valastyan S, Chang A, Benaich N, Reinhardt F, Weinberg RA (2010) Concurrent suppression of integrin alpha5, radixin, and RhoA phenocopies the effects of miR-31 on metastasis. Cancer Res 70: 5147-5154.

403. Engebraaten O, Bjerkvig R, Pedersen PH, Laerum OD (1993) Effects of EGF, bFGF, NGF and PDGF(bb) on cell proliferative, migratory and invasive capacities of human brain-tumour biopsies in vitro. Int J Cancer 53: 209-214.

404. Rodrigues-Ferreira S, Di Tommaso A, Dimitrov A, Cazaubon S, Gruel N, et al. (2009) 8p22 MTUS1 gene product ATIP3 is a novel anti-mitotic protein underexpressed in invasive breast carcinoma of poor prognosis. PLoS One 4: e7239.

405. Frank B, Bermejo JL, Hemminki K, Sutter C, Wappenschmidt B, et al. (2007) Copy number variant in the candidate tumor suppressor gene MTUS1 and familial breast cancer risk. Carcinogenesis 28: 1442-1445.

406. Zemskov EA, Janiak A, Hang J, Waghray A, Belkin AM (2006) The role of tissue transglutaminase in cell-matrix interactions. Front Biosci 11: 1057-1076.

407. Wang J, Thompson B, Ren C, Ittmann M, Kwabi-Addo B (2006) Sprouty4, a suppressor of tumor cell motility, is down regulated by DNA methylation in human prostate cancer. Prostate 66: 613-624.

408. Taniguchi K, Ishizaki T, Ayada T, Sugiyama Y, Wakabayashi Y, et al. (2009) Sprouty4 deficiency potentiates Ras-independent angiogenic signals and tumor growth. Cancer Sci 100: 1648-1654.

409. Tennis MA, Van Scoyk MM, Freeman SV, Vandervest KM, Nemenoff RA, et al. (2010) Sprouty-4 inhibits transformed cell growth, migration and invasion, and epithelial-mesenchymal transition, and is regulated by Wnt7A through PPARgamma in non-small cell lung cancer. Mol Cancer Res 8: 833-843.

410. Ai L, Kim WJ, Demircan B, Dyer LM, Bray KJ, et al. (2008) The transglutaminase 2 gene (TGM2), a potential molecular marker for chemotherapeutic drug sensitivity, is epigenetically silenced in breast cancer. Carcinogenesis 29: 510-518.

411. Waha A, Koch A, Hartmann W, Milde U, Felsberg J, et al. (2007) SGNE1/7B2 is epigenetically altered and transcriptionally downregulated in human medulloblastomas. Oncogene 26: 5662-5668.

412. Muller A, Homey B, Soto H, Ge N, Catron D, et al. (2001) Involvement of chemokine receptors in breast cancer metastasis. Nature 410: 50-56.

413. Sun X, Wei L, Chen Q, Terek RM (2010) CXCR4/SDF1 mediate hypoxia induced chondrosarcoma cell invasion through ERK signaling and increased MMP1 expression. Mol Cancer 9: 17.

414. Ahmed S, Wang A, Celius T, Matthews J (2014) Zinc finger nuclease-mediated knockout of AHR or ARNT in human breast cancer cells abolishes basal and ligand-dependent regulation of CYP1B1 and differentially affects estrogen receptor alpha transactivation. Toxicol Sci 138: 89-103.

415. McKenna NJ, O'Malley BW (2002) Combinatorial control of gene expression by nuclear receptors and coregulators. Cell 108: 465-474.

416. Fallone F, Villard PH, Seree E, Rimet O, Nguyen QB, et al. (2004) Retinoids repress Ah receptor CYP1A1 induction pathway through the SMRT corepressor. Biochem Biophys Res Commun 322: 551-556.

417. Niederst MJ, Sequist LV, Poirier JT, Mermel CH, Lockerman EL, et al. (2015) RB loss in resistant EGFR mutant lung adenocarcinomas that transform to small-cell lung cancer. Nat Commun 6: 6377.

418. Solaimani P, Wang F, Hankinson O (2014) SIN3A, generally regarded as a transcriptional repressor, is required for induction of gene transcription by the aryl hydrocarbon receptor. J Biol Chem 289: 33655-33662.

419. Goertzen CG, Dragan M, Turley E, Babwah AV, Bhattacharya M (2016) KISS1R signaling promotes invadopodia formation in human breast cancer cell via beta-arrestin2/ERK. Cell Signal 28: 165-176.

420. Pyne S, Edwards J, Ohotski J, Pyne NJ (2012) Sphingosine 1-phosphate receptors and sphingosine kinase 1: novel biomarkers for clinical prognosis in breast, prostate, and hematological cancers. Front Oncol 2: 168.

Appendix A.

NCOR1 is enriched at the pS2 promoter after treatment with TCDD and E2

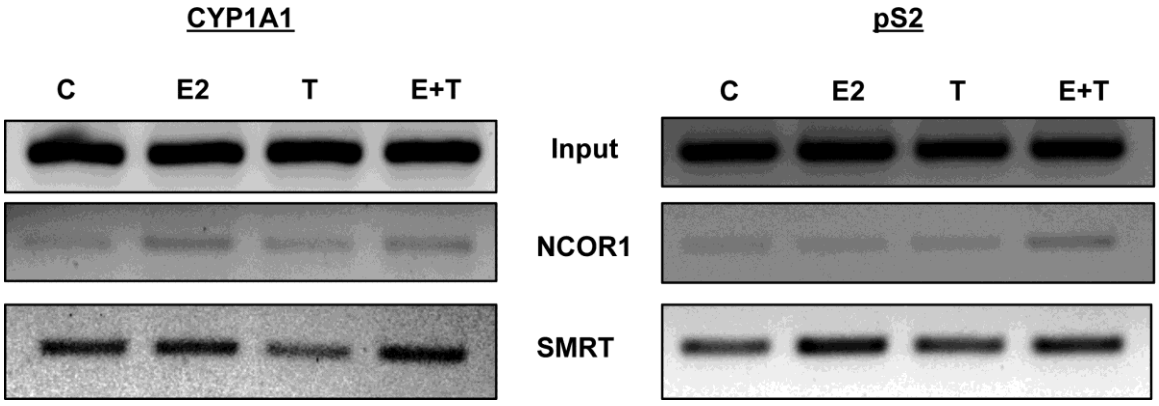

Figure A1. NCOR1 is enriched at the pS2 promoter after treatment with TCDD and E2.

Chromatin immunoprecipitation assays of the *CYP1A1* enhancer and *pS2* promoter regions in ECC-1 cells using antibodies targeting NCOR1 and SMRT .Cells were treated for 45 min with either DMSO, E2 (10 nM), TCDD (2 nM) or a combination of E2 and TCDD.